Design and Implementation of HTS Technology for Cellular Base Stations:

An Investigation into Improving Cellular Communication

A thesis presented in partial fulfilment of the requirements for the degree of

Doctor of Philosophy
in
Electrical Engineering
at
Massey University, Palmerston North, New Zealand
and
James Cook University, Townsville, Australia

Adrian Knack

2006

ABSTRACT

When placed between the antenna and receiver electronics of a cellular base transceiver station, a Cryogenic Receiver Front End (CRFE), consisting of a High Temperature Superconducting (HTS) filter and modern Low Noise Amplifier (LNA), can significantly improve the base stations' coverage and capacity. Due to CRFEs being hurried to the telecommunications industry in a competitive market, the development of CRFEs and their performance have been classified. This left it to be pondered whether HTS filters could really have been beneficial or if they were always just of academic interest. It is the main objective of this thesis to ***investigate if and under what circumstances high temperature RF-superconductivity can prove to be an important technological contribution to current and future wireless communications***.

This dissertation presents the analysis of an existing CRFE developed by Cryoelectra GmbH and its performance characteristics measured in a field trial held in rural China. With the aid of a CDMA Uplink Model developed by the author, the data was analysed and several novel engineering improvements were made to create an advanced CRFE which was economical to deploy. The analysis of results from a field trial in Beijing city using the CDMA Uplink Model led to the exploration of alternative filter technologies which could achieve similar results to the HTS filter technology. This culminated in the development of dielectric resonators filters which could be used as an alternative and as a supplement to the HTS filters used in the CRFE. The design of two novel dielectric resonator duplexers and two advanced multi-operator combiner antenna sharing solutions followed the successful implementation of a high performance dielectric resonator filter.

The performed investigation and development described in this thesis suggest that HTS filter technology for terrestrial wireless communications can be beneficial in current cellular networks, but due to its high cost is economical for use only under certain conditions. However, HTS filter technology may be of great importance in the design and implementation of spectrum friendly wireless communications systems in the future.

ACKNOWLEDGEMENTS

CONTENTS

FIGURES

TABLES

CHAPTER 1

INTRODUCTION

In 1986 two researchers at the IBM Research Laboratory in Rüschlikon, Switzerland, Alex Müller and Georg Bednorz created a ceramic compound that exhibited the transition superconductivity at a temperature of 30K [1], which was at that time the highest known critical temperature (T_c) of a superconductor. This was the first record of high temperature superconductivity, which was made more significant by the fact that previously researches had not considered ceramic materials for superconductivity experiments because ceramics are normally associated with insulators. This incredible discovery was awarded the Nobel Prize one year later 1987. Also in 1987 research into the new superconducting ceramics led a research team at the University of Alabama-Huntsville to develop a new and quite structurally different molecule by substituting Yttrium for Lanthanum in the Müller and Bednorz molecule to create $YBa_2Cu_3O_{7-\delta}$ (YBCO) [2]. This new material exhibited superconductivity at temperatures up to 92K, which could be reached using liquid nitrogen, a commonly available and inexpensive coolant [3].

Early exploratory measurements of the Radio Frequency (RF) Joule losses in polycrystalline YBCO samples [4] and the encouraging experimental results on the RF surface resistance of epitaxially grown YBCO thin films on Strontium Titanate ($SrTiO_3$) substrates [5, 6] indicated the possibility of the application of HTS materials in microwave systems. The early availability of high quality, commercially produced YBCO coated sapphire wafers [7] nourished this expectation. About five years after the discovery of high temperature superconductivity planar superconducting microwave band pass filters appeared to be one of the first and challenging applications of HTS technology in the fast growing area of wireless communication.

At the same time researchers discovered HTS technology and began to think about the first applications, the personal wireless communications industry was beginning to boom. The first analogue mobile phone service (AMPS), a cellular system, had been deployed in Tokyo in 1979 [8]. This system proved to be very successful and subsequently grew in popularity around the world, eventually necessitating the need for the development of more spectrally efficient digital systems to cope with increasing demand. Global System for Mobile (GSM) communications and Code Division Multiple Access (CDMA) were developed in the late 1980s when the AMPS system was approaching its user capacity in heavily populated areas. Today these systems are known as 2nd Generation (2G) systems. By the late 1990s the 2G systems had evolved to include data services in so called 2.5G systems. Wide band variations of these GSM and CDMA systems that incorporate fast data services and multimedia capabilities, known as 3rd Generation (3G) systems, are currently being deployed around the world and offer the latest in communications technology.

The popularity and affordability of mobile phones has increased since their inception. Today over 1.5 billion people around the world (1/4 of the world's population) [9] own a mobile phone and in the foreseeable future service providers will once again be presented with network capacities shortages like the AMPS system experienced in the late 1980s. Several options exist to increase the capacity and quality of service, the most obvious of which is to increase the density of base stations in a given area. But the presence of these structures and the associated antennas is not popular with the general public. Another solution would be to use highly selective filters of low insertion loss and cryogenic low noise amplifiers (LNA) of high dynamic range to ensure that only the signals from a chosen service provider's customers are received and not noise from competitor channels, other wireless services or white noise [10].

In order to provide the highest quality communications services and efficient use of the allocated bandwidth, cellular base stations require highly selective, low insertion loss, band pass filters in the front end of their receivers. When coupled with a LNA of high dynamic range, this Filter-LNA combination (FLNA) in such a base station receiver front end can reduce adjacent channel interference and ensure an increase in the signal-to-noise ratio (SNR). Due to the improved SNR base stations can potentially improve their coverage; eliminating areas with poor reception, black spots, and increase capacity without requiring an increase in the antenna height or number of base stations [11-13]. The low loss nature of the new HTS materials meant planar band pass filters fabricated from YBCO thin film wafers combined with cooled low noise amplifiers (LNA) were considered to be attractive as cryogenic receiver front ends (CRFE) for wireless base stations in cellular communication systems all around the world.

When it became clear that these HTS filters could be reliably fabricated the subject of application became of high economic interest due to the large wireless communications market. A number of commercial companies formed with an aim to develop filter applications and capture this market. The outcome of industry commercialisation was that the new applications and their implementation became confidential. Of the major companies that formed, Superconducting Core Technologies, Superconductor Technologies Inc. (STI), Conductus Inc. and Illinois Superconductor Corporation, the most successful commercial application of CRFE was demonstrated by STI with the installation of about 5000 systems up to September 2005, predominantly in the United States of America [14]. However, due to difficulties in implantation, production, reliability and cost, the new technology has not been widely adopted by the market. As a result many of these companies which formed during the initial hype have now abandoned their work leaving it to be pondered whether HTS filters could really have been used or if they were always just of academic interest. It is the main objective of this thesis *to investigate if and under what circumstances high temperature RF-superconductivity can prove to be an important technological contribution to future wireless communication*.

This thesis begins by describing the basic principles of wireless communication, followed by an introduction to RF superconductivity and discussion on HTS filter design. After this introduction, fundamental elements and the design of a CRFE (manufactured by Cryoelectra, version D6) are

described. This includes detailed information on a HTS filter designed at Tsinghua University and an excellent Cryolectra LNA.

Subsequently the author's work is presented, beginning with his primary contribution to the field, namely a CDMA uplink model. This model primarily allows for the calculation of base station coverage versus capacity (number of users per sector) for different front end setups and environments. The developed model is one of the first of its kind to be published and has been used to examine field trials of the D6 CRFE, discriminating between the improvement caused by the LNA and that caused by the HTS filter. The results of this examination led to the author to develop a series of improvements to create an advanced CRFE in an effort to optimise the performance cost ratio and bring the technology closer to the market. One of the advanced CRFE (D7) has been trialled successfully in Beijing, China. Ultimately two novel room temperatures hardware concepts for base station front ends which can achieve similar performance to the CRFE at significantly reduced expense are proposed. The investigation concludes by looking at the developed CRFE and concepts proposed with the consideration that for any new technology to be successful it must be an improvement over existing technology or be economically beneficial, preferably both.

A chapter by chapter summary of this thesis is given below.

Chapter 2 discusses wireless communications technology and theory which is used in today's cellular systems. Understanding this is a vital component to making correct design decisions in the development of the CRFE. The chapter begins by explaining the essentials of wireless communications technology; the mobile communications environment, the cellular concept, diversity, fading and the radio frequency spectrum. The current 2nd and 3rd generation mobile phone services are describe in the last section of this chapter.

Chapter 3 briefly describes the fundamentals of microwave filter designs using lumped elements to model distributed element filters such as cavities, metallic, dielectric resonator and planar filters. It also shows how the geometrical factor and losses in the resonator affect its unloaded Q-factor.

Chapter 4 of this thesis outlines the important material properties and physics theories surrounding RF superconductivity and describes why RF filters generated so much excitement as one of the most promising applications of HTS technology. The chapter concludes with some basic planar filter theory and several examples of HTS filters.

Chapter 5 gives an introduction into the conventional base stations and explains why HTS planar filters appear attractive to be used in CRFE. Additionally the current state of the art technology that was used in the first demonstrator CRFE developed by Cryoelectra named D6 is explained. This chapter concludes with the analysis of the March 24th 2004 field trial carried out at Wunongchang, China, performed using D6.

Chapter 6 presents a CDMA coverage capacity uplink model which was created by the author to examine and explain the results which were obtained in the field trials. This chapter explains the development of the model and analysis of several theoretical situations in order to determine which individual properties of the CRFE are responsible for increasing the coverage and capacity of the base station under different conditions. Finally the need for specific field trials in order to obtain conclusive data is identified.

Chapter 7 describes the improvements made by the author to the old D6 CRFE to create several new advanced CRFE with enhanced performance. Advances in several of the core components make the CRFEs faster to produce and less expensive, while enhancements to the usability of the systems make them easier to operate and modifications to the layout increased the deployment options. The chapter is concludes by presenting the five base station field trials held in the city of Beijing, China. The trials prompted questions as to the nature of the improvements and incited further investigation into other filter technology which might be able to provide similar results at substantially reduced costs.

Chapter 8 present the authors designs of dielectric resonator filters and a couple of novel dielectric resonator duplexers for use in the *ultimate* base station. The conceptual design for an advanced Multi-operator Combiner using dielectric resonators filters and HTS filters is also given.

The conclusions to the thesis are presented in Chapter 9, which includes a discussion of future work in the area of CRFE and other possible implementations of HTS filters.

CHAPTER 2

WIRELESS COMMUNICATION TECHNOLOGY

The first telephone was invented by Alexander Graham Bell in 1876. No one at that time fully envisaged the immense impact this invention would have on the lives of people around the world. For the first time in history people could communicate in real time without being face-to-face over very large distances. In the years since the wire line phone has evolved into what is known today as the cellular or mobile phone. Unlike the wire line system, which uses cables (copper or optical fibre) to transmit signals from one point to another, the cellular system utilises signals propagating through the air between mobile phones and cellular base stations. The base stations are then responsible for connecting calls to their final destination, either directly via the standard wire line phone network or using both the wire line network and another cellular base station. Like the original telephone which brought real time voice communications into peoples homes and businesses, the cellular phone revolution has also had a huge impact on the way people live and work by providing them with communications, and more recently data and video services, anywhere, anytime.

2.1 ESSENTIALS OF WIRELESS COMMUNICATION

As mentioned above, in wireless (or radio) communication an electromagnetic signal is transmitted through free space (air) rather than via a wire. Transmission of signals through the air presents a unique set of challenges which includes the necessity to use antennas for both transmission (Tx) and reception (Rx). These antennas are responsible for transforming electromagnetic waves in free space to time varying voltages and currents in electrical circuits and vice versa. The antenna design is usually independent of its intended purpose (Tx or Rx) and is defined by parameters such as frequency, beamwidth, bandwidth, gain and polarisation.

Information in wireless telecommunications in not transmitted in its raw form, but rather it is processed. A transducer converts the original signal (eg. voice) to an electromagnetic signal which is used to modulate a carrier signal. A carrier signal is usually a simple sinusoidal signal at a much higher frequency than the original signal (typical audio frequencies cover 8 kHz – 22 kHz). Carrier signals are used primarily for two reasons; the first is to reduce the wavelength of the signal for transmission and reception and the second is to allow for simultaneous use of the same channel by multiplexing.

The optimum antenna size is one half or one quarter the wavelength of the Tx or Rx signals, which means that for a 10kHz audio signal an antenna of at least 7.5km would have been required. In contrast by using a carrier signal at 800MHz, such as in 1st and 2nd generation cellular phones, the antenna size is reduced to 76.2mm. With the invention of high relative permittivity (ε_r) dielectrics it became possible to build very broadband antennas [15, 16] even smaller than one quater the wavelength of the carrier, which is very important for miniaturised antennas for mobile handsets. For this reason the use of a carrier is not

significant from the point of view of antenna size but rather due to the ability to filter noise and interference from the signals.

The second and now most important reason for the use of a carrier signal is that it allows for simultaneous use of the same channel by multiplexing. Cellular networks primarily use Code Division Multiple Access (CDMA) or Time Division Multiple Access (TDMA – which is the basis the GSM system) to allow multiple phone conversations over a common channel. Allowing for multiple users inside each channel is very important as the radio spectrum is a limited natural resource, and the demands on it are increasing. The limitation on the use of higher frequencies for radio networks is their susceptibility to environmental propagation loss (explained in the next section). Descriptions of CDMA and TDMA systems are given in Sections 2.2 and 2.3.

2.1.1   THE MOBILE ENVIRONMENT

Atmospheric propagation losses increase significantly at high frequencies as shown in Figure 2.1. Losses above 10GHz are caused by moisture in the atmosphere. Peaks occur at 20GHz, due to signal absorption of water vapour, and at 60GHz, due to signal absorption by oxygen molecules. Therefore the mobile phone spectrum has been implemented at frequencies around 800MHz and 1800MHz to 2200MHz where gaseous absorption is minimised and the wavelength is already short.
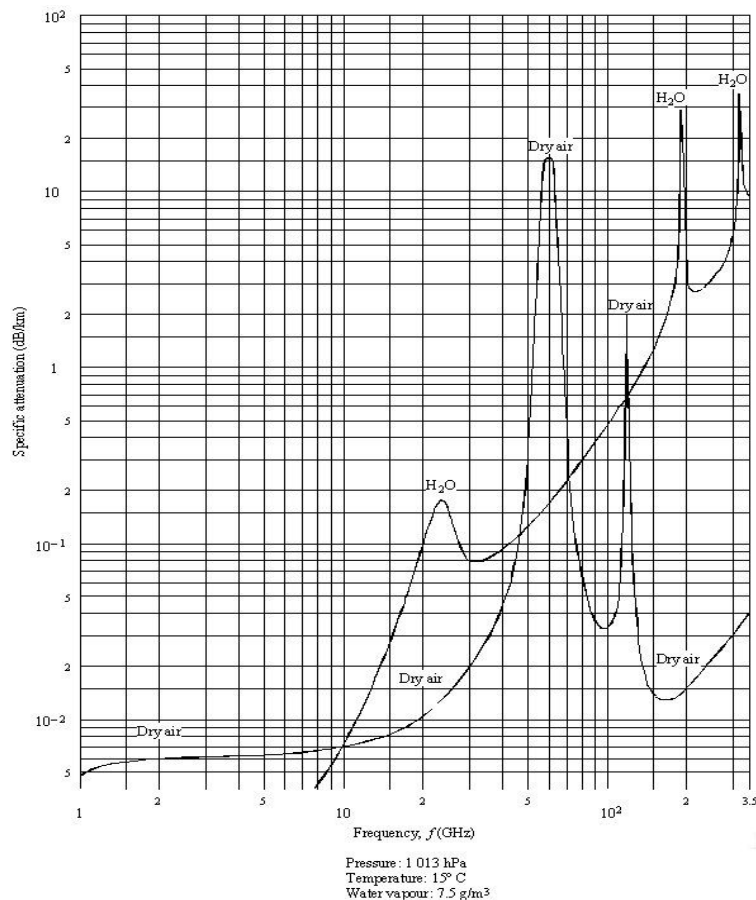
Figure 2.1. Specific Absorption of RF Signals due to Atmospheric Gases vs. Frequency [8]

Because base station antennas and mobile antennas are located close to the Earth's surface, the propagating radio waves are susceptible to natural variation in the terrain, human made structures and electromagnetic industrial noise. As a mobile station moves, the received signal can become stronger or weaker depending on the mobile station's position and the location of hills or buildings. Additionally ground reflected waves can be received from the base station antenna as well as the direct wave. These reflected waves cause a d^4 propagation loss, which is significantly higher than the d^2 propagation loss through free space, where d is the distance between transmit and receive antenna.

Inside cities human made structures, such as buildings and bridges, cause the signals to be reflected back and forth before reaching the mobile unit, causing signal fading as the mobile unit moves. This multi-path fading causes the average carrier power of the receiving signal to be reduced and therefore degrades voice quality and data rates.

Another problem in urban environments is the electromagnetic noise generated from human made sources such as vehicles, powerlines, industrial equipment and other wireless series. The noise floor is higher in urban areas than suburban areas or open areas, and in general decreases at higher frequencies. One 8 cylinder engine at 3000rpm can generate 200 spikes per second, each spike in the time domain spreads its energy across a wide band in the frequency domain. Hence increased traffic density in urban areas contributes to the higher noise floor in these areas. The noise from 100 vehicles per hour is 32dB above the thermal noise floor at 100MHz, but at 1GHz, 1000 vehicles per hour will only cause a 5dB increase in the noise above the thermal noise floor [8]. Therefore, working in the 800MHz – 2.2GHz region minimises the atmospheric losses and human made noise therefore maximising the systems capacity.

Loss minimisation is particularly important in the case of the uplink (from mobile units to base stations) since the transmit power is much lower than the signals from base stations. Consequently it is important that base stations have very sensitive receivers in order to receive the weakest signal possible, thereby increasing call quality and maximising base station coverage.

2.1.2   THE CELLULAR CONCEPT

The concept of using a hexagonal shape to approximate the coverage of the cellular radio network came about in the early development of Analogue Mobile Phone Service (AMPS). It was desirable to geographically depict an area totally covered by the radio network without any gaps or overlapping lines. The solution therefore was to use a hexagon rather than a circle (Figure 2.2).
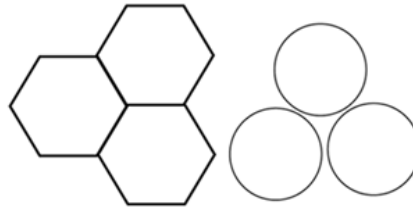
Figure 2.2. Map Coverage Using Hexagonal and Circular Cells

Obviously other shapes could achieve the same goal so why was the hexagon shape chosen? To answer this question it must first be understood that a "cell site" or the base station location is not at the centre of the "cell" or geographical area. In fact each cell site lies at the edge of several cells (Figure 2.3). A reason for the selection of a hexagon was to do with frequency planning and vehicle traffic. Using three sectored sites and a frequency reuse pattern of seven network planners could service all areas and make the most efficient use of the available channels as no adjacent cells would ever use the same channel as illustrated in Figure 2.4.
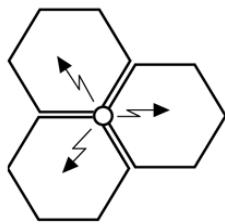
Figure 2.3. A Cell Site lie at the Edge of Several Cells [17]
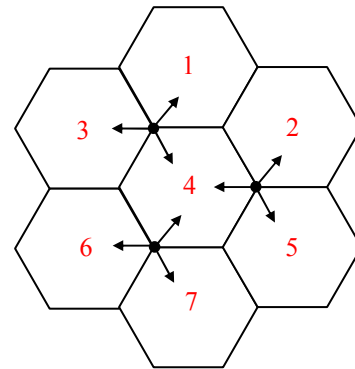
Figure 2.4. Cell Geography Showing Cell Site Antenna Direction and Channel Reuse for AMPS

If sites with the same channels are located too closely together, the signals from the adjacent cell cause interference. Because cellular systems were first planned to be used in city areas and modern cities are based on a grid pattern, network planners needed a solution which would best serve those streets. If four sectors were used (in a square pattern) the cell borders would be at along the streets (if the antenna was directed away from the street) or the sector would point along the street (if the antenna was directed along the street). Either case would cause the mobile units to handoff to the adjacent cell site continuously due to signal fluctuations, creating a ping-pong effect. A large number of handoffs place a very large load on the system and reduce its capacity significantly. The solution to the problem of continuous handoffs was to service the streets using a single dominant sector in the hexagonal pattern. The complete mathematical analysis of this situation of this situation was done by Dr. William Lee at the inception of the AMPS network and been published in many of his works including [8, 18].

2.1.3 MULTIPATH SIGNAL FADING AND DIVERSITY ANTENNAS

Because the earth is not flat and objects (natural and man made) adorn its surface, RF signals do not always travel directly between transmitters and receivers. In a mobile wireless communication systems, such as the cellular phone network, a RF signal may travel between a transmitter and receiver over multiple reflective paths. This phenomenon is known as *multipath* propagation. Multipath signals can experience reflection, diffraction and scattering. Reflection takes place when the propagating signal impinges on a relatively smooth surface much larger than the signal wavelength. Diffraction happens when the RF signal encounters a large (compared to the wavelength of the signal) dense object, causing secondary waves to be produced behind the obstruction. In the case where there is no line-of-sight between the transmitter and the receiver, diffraction is the phenomenon that allows the transmitted signal to reach its destination. Scattering occurs when the signal is incident on a rough surface or one of dimensions is close to or smaller than the signal wavelength, causing the reflected signal to spread out in all directions. *Multipath fading* is the name given when multipath signals affected by these phenomenon cause fluctuations in the received signal's amplitudes, phase and angle of arrival.

Prominent terrain, such as hills, forests and buildings, may *shadow* receivers from transmitters. The average signal power attenuation or path loss due to motion over large areas is known as large scale fading. Small scale (Rayleigh fading) refers to changes in signal amplitude and phase that can be experienced in the spatial separation between receivers and transmitters. This form of fading has two primary mechanisms; time spreading of the signal, or signal dispersion, and time variant behaviour of the channel. The time variant behaviour occurs because of the motion between the transmitter and receiver causing propagation path changes. This type of fading is also known as Rayleigh fading, because, if no line-of-sight path exists between transmit and receive antenna, then the link is formed via multiple reflective paths. The envelope of the received signal formed by the reflective signals is statistically determined by a Rayleigh probability density function [8, 19]. Roaming mobile radio signals will experience both types of fading and the receiver must still be able to process the received data for a successful link.

In multipath conditions there is the possibility that all the propagated signals from a transmitter will nullify each other creating a fade where the incident signal strength is lower than the mean level in the surrounding area [20]. While the precise location of a fade is random, on average they are separated by approximately half the wavelength of the signal. For voice services the problem is manageable. For example a person standing still while talking; if the person notices a diminished voice quality or volume from the other party the person tends to move a small amount to where the voice quality improves. In the example of a moving vehicle, the time when bad fading is experienced is relatively short due to the vehicle's movement. However for data services the problem of multipath fading can cause a significant decrease in data throughput due to the stepping down of data rates to maintain an acceptable bit error rate.

By using two or more separate receive antenna the effects of multipath fading can be significantly reduced. Typically such a system is only implemented at the cellular base station where one antenna is the

main antenna, which is used for both transmit and receive signals through a duplexer (refer to Figure 5.4), and the other antenna is a diversity antenna, which is receive only. So as to prevent both antenna seeing a deep fade at the same time the antennas are separated by several wavelengths. While this setup has been using at base stations since the inception of the original AMPS network [8] discussion has recently taken place about using a similar system on 3G mobile phone handsets [20].

2.1.4 RADIO FREQUENCY SPECTRUM, DEMAND AND CAPACITY

Different types of radiation, such as visible light, radio waves, X-rays, etc. are referred to as the electromagnetic spectrum. For the reasons mentioned in the Section 2.1.1 only frequencies up to about 10 GHz are useful for communications systems. In particular mobile communications frequencies currently used are between 400MHz and 2.5GHz in order to take advantage of large bandwidths and minimal propagation losses. Because of the limited useful frequency range, the electromagnetic spectrum is regarded as a limited natural resource and therefore needs to be managed efficiently if it is to provide a sufficient medium for communications now and in the future. In wireless communications radio interference and neighbouring channels limit the usability of the spectrum.

When the digital cellular phone spectrum was allocated in the USA, the major driving market factors were [8],

1. Good coverage
2. Good voice quality
3. No dropped calls
4. Low cost
5. Small handsets

These factors and the existing spectrum allocations led to the selection of the 800MHz allocation for cellular communications. Subsequently 1800-1900MHz and 2100-2200MHz frequency bands were allocated when data applications became available and the capacity of the original allocation was being reached.

High data rate applications, such as video, picture messaging and internet require wider frequency bandwidth than traditional voice applications. The voice quality, data rate and system performance are inversely propositional to the system capacity (number of simultaneous users). Therefore in order to maintain the quality of service and add high speed data transfer capability while maintaining customer numbers, the spectrum needs to be used more efficiently. This can be achieved in several ways; improving the sensitivity of the front end of a base station by incorporating low loss filters, cooled high gain amplifiers and tower mounting of the front end could effectively reduce the minimum allowable signal level by improving the signal to noise ratio (SNR), which will allow more concurrent users in a system. Filters with very small transition regions (steep skirts) can effectively reduce the size of the guard bands (unused gap between channels to prevent co-channel interference) and the effects of strong out-of-band interferers which cause inter-modulation distortion inside the passband (due to non-linear elements

such as mixers and amplifiers). Eliminating inter-modulation distortion is an important aspect in maximising the performance of a radio network. As such improving the linearity of the amplifier and mixers is vital in achieving this goal.

2.2   2ND GENERATION CELLULAR SYSTEMS

The first generation analogue mobile phone system (AMPS) proved to be very successful and subsequently grew in popularity around the world, eventually necessitating the need for the development of more spectrally efficient digital systems to cope with increasing demand. The second generation of cellular phones developed during the 1980's to facilitate the rapid growth of the cellular communications market. A group, referred to as the Groupe Spécial Mobile (GSM), was formed at the 1982 Conference of European Posts and Telegraphs with the aim to develop a pan-European public land mobile system, now commonly known as Global System for Mobile Communications (GSM) [21]. In February 1989 the CDMA (code division multiple access) system for cellular was introduced. Theoretically CDMA provided 10 times the capacity of the original AMPS system. The successful demonstration by Qualcomm on the 3rd on November 1989 paved the way for CDMA to be adopted as the 2nd generation standard in the USA after a relatively short 5 year development period (GSM took closer to 10 years) [8]. The GSM and CDMA systems are briefly described below.

2.2.1   GLOBAL SYSTEM FOR MOBILE COMMUNICATIONS (GSM)

The criteria set down by the developers of the GSM standard were the following:

- Good subjective speech quality
- Low terminal and service cost
- Support for international roaming
- Ability to support handheld terminals
- Spectral efficiency
- ISDN compatibility
- Support for a range of new services and facilities

These features are taken for granted today and the new services which were added to the original analogue system have been highly successful. The most successful is probably the Short Message Service (SMS); SMS is a bidirectional service for short alphanumeric messages between two subscribers with a message receipt being sent to the sender. SMS has also been used in broadcast mode for traffic updates and network updates when one enters a new country for the first time. GSM users can also send and receive data at 9600bps from normal telephone data services. Other features of the GSM standard included several forms of call forwarding, call barring, caller identification, call waiting and multiparty conversations.

To achieve these results significant network architecture and radio link development was done. The GSM network architecture consists of mobile handsets and the base station subsystems, which controls the radio link with the mobile stations and the network subsystem. This network subsystem performs the

switching of calls between mobile users and between mobile and fixed network users. The focus of this work is on the front end of the base station subsystem and requires understanding the radio link aspects. As such this is the focus of the discussion in the remainder of this section.

In most parts of the world GSM-900 and GSM-1800 are used. GSM-900 uses 890-915MHz for the uplink (Mobile to Base Station) and 935-960MHz for the downlink. GSM-1800 uses 1710-1785MHz for the uplink and 1805-1880MHz for the downlink. GSM-850, GSM-1900, GSM-400 and variations of GSM-900 are also used in various regions in the world [22].

GSM uses a combination of Time and Frequency Division Multiple Access (TDMA/FDMA). The FDMA part divides the maximum 25MHz bandwidth of the GSM channel into 124 carrier frequencies spaced 200kHz apart. A TDMA scheme is then used to further divide the carrier frequencies in time. Eight *burst periods*, which lasts 15/26ms each, make up a *TDMA frame* to form a basic logic unit (Figure 2.5). One physical channel (an active subscriber) is one burst period per TDMA frame [21]. The frames are serviced in a round robin fashion and because the rotation is so fast users are unaware of the time slots.
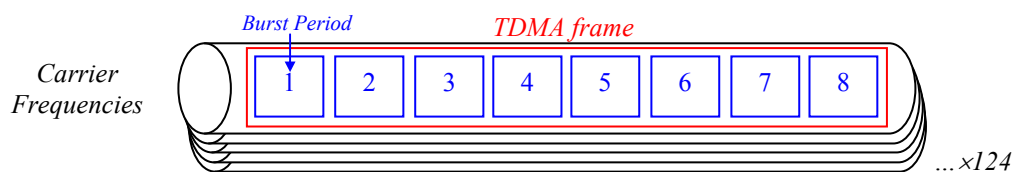
Figure 2.5. Diagram Representing a 25MHz Bandwidth GSM Channel showing 124 Carrier Frequencies (FDMA) and the TDMA frame and burst periods (TDMA)

Because GSM is a digital system, speech has to be digitised before it is transmitted. This is done using a Regular Pulse Excited - Linear Predictive Coder (RPE-LPC) with a Long Term Predictor loop. Convolutional encoding and block interleaving are used to protect the encoded speech or data signals transmitted to the receiver such that they are received correctly despite interference and fading issues [21].

Slow frequency hopping, where the mobile and base stations transmit each TDMA frame on a different carrier frequency, takes advantage of the frequency dependency of the location of signal nulls to alleviate problems with multipath fading. Additionally Co-channel interference is normalised across all the active channels. Discontinuous transmission (DTX), where the transmitter is turned off during silent periods, which account for more than 60% of a typical conversation, is also used to reduce co-channel interference in GSM systems [8, 21, 23].

Another important interference control mechanism implemented in GSM is that of power control. Power control allows mobile units to operate at a minimum power level required to maintain a successful link with a base station. The mobile unit measures the SNR based on the Bit Error Ratio and relays the information to the base station. The base station then decides if the power of the mobile unit requires

changing. This functionality forms the basis of drive tests, which are used to measure the performance of base stations. While important to GSM for controlling co-channel interference, the power control plays a far more important role in controlling CDMA systems [8, 17, 21].

2.2.2   CODE DIVISION MULTIPLE ACCESS (CDMA)

Because the CDMA cellular service began development 7 years later than the GSM service, it included all the features of the GSM service (discussed in the previous section). However the radio link for the CDMA system is very different to its FDMA/TDMA counterpart. The CDMA system employs what is referred to as a wideband spread spectrum technique to carry digitised voice and data transmissions. Each connected mobile phone in a channel is assigned a unique digital code know as a *Walsh* code. The code is assigned as a unique pseudorandom noise code generated by the digital radio. This allows the digital signal to be spread over the entire channel along with signals from other mobiles all using the same channel (Figure 2.6). The digital signal of the selected transmission can be decoded at the receiver (which knows the corresponding Walsh code), while all other CDMA signals will appear to be noise. There is a maximum of sixty-four pseudorandom Walsh codes per 1.25MHz carrier in the CDMA modulation scheme. Theoretically there can be nine 1.25MHz carriers per cell, although up to eleven have been used successfully. Typically twenty-two to forty voice calls can be handled simultaneously, however twelve to fourteen are the average for most carriers today. The cell reuse factor of CDMA is usually one, rather than the seven used for the old AMPS system, meaning a more efficient use of the spectrum [17, 24, 25].

1.25MHz CDMA Channel

Walsh Coded CDMA Signals
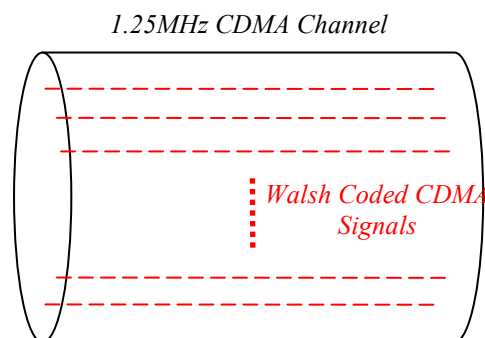
Figure 2.6. Diagram Representing a 1.25MHz CDMA Channel Showing MultipleWalsh Coded CDMA Signal

Like GSM, the CDMA base stations use power control to limit the power of the mobile units. It is very important that all CDMA signals arrive at a base station with roughly the same power level so that they can be properly decoded. Power control is required to maintain the system capacity so that close mobiles do not "drown out" the signals from more distant mobiles. The CDMA system can be thought of like a room full of people talking to one another at the same time. If everyone talks very loudly then nobody can hear the person they are speaking to. If however everyone only speaks as loud as required to be heard by their partner then everyone can continue speaking successfully. While in AMPS and GSM systems power control is a performance benefit, for CDMA power control is a critical function in order for the system to operate successfully [25].

2.3   3RD GENERATION CELLULAR SYSTEMS

In recent years the new 3G cellular network and phones has been the focus of much attention. The revolution is that mobile communications is moving from the voice only delivery to a multimedia capable system, combining camera, video camera, computer, media player and radio into handsets. The 3G also brings together high-speed radio and IP-based services like those available from an internet connected PC. The packet based IP system allows users to be permanently online and gives access to Mobile Internet services including personalised portals, new entertainment, commerce and unified messaging. High speed data, superior quality voice and video communication and other location-based services can be available with the user only paying for sending and receiving data [26]. Like with 2G, the world doesn't have a unified 3G standard but rather several 3G standards developed from their 2G counterparts. These are briefly described below.

GPRS, General Packet Radio Service is an enhancement of the GSM network that introduces packet data transmission, allowing for a permanent connection to online services and the internet with cost incurred for time of use. GPRS can be viewed as a 2.5G service since only packet data nodes have been added to the existing 2G network, but is typically classed as 3G.

EDGE, Enhanced Data Rates for Global Evolution enables GSM operators to offer 3G services over their existing frequencies. This required a complete upgrade of the GSM system to a full IP and multimedia network. Data speeds of up to 384kbps are available using this system.

WCDMA, Wideband CDMA or **UMTS** (Universal Mobile Telecommunications System), as it is known in Europe and Japan, is a 3G wideband CDMA service that provides very high speed data rates (up to 2Mbps) and a highly efficient use of the frequency spectrum. At this data rate access to several voice, video and data services is available simultaneously.

The **cdma2000** system was built around the framework of the original cdmaOne system (the American 2G CDMA system) and allows current CDMA operators a path to deploying 3G in their existing networks. Fully 3G services are offered with cdma2000, including a packet data rate of up to 2Mbps.

Improvements in chip rate, channel and pilot structure, power control mechanisms, diversity techniques, handoff efficiency and base station synchronisation have significantly enhanced 3G systems since the inception of their 2G counterparts in the early 1990s. However there is a problem with the proposed UMTS (or WCDMA) systems caused by the specification requirement for channels to fit into a 5MHz bandwidth with more than 35dB isolation between adjacent services. A solution to fulfil this requirement is for the UMTS system to use modern, highly selective filters in the receive side of the front end of the base stations [27].

Spacing of UMTS Frequency Bands

UMTS Rx or Tx: **9.9** – User block; **5** – Carrier spacing; **4.2** – Carrier BW; **0.75** – Carrier guard BW; **9.15**– User useful BW;
-30 dB – Required isolation; Min. Steepness=15dB/0.375MHz= 40 dB/MHz
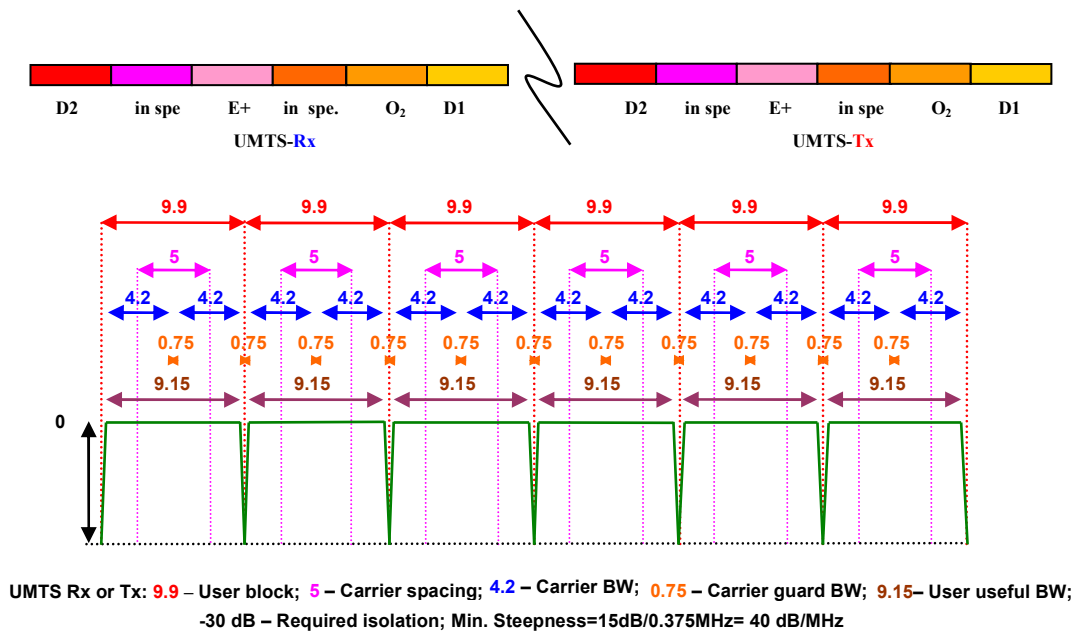
Figure 2.7. European UMTS Frequency Allocations

In Europe UMTS providers are allocated a 9.9MHz user block containing 2 carriers or channels (Figure 2.7). Each carrier has a 4.2MHz bandwidth and carriers are spaced 5MHz apart. Transmit and receive channels should have 80dB isolation at the base station. Individual channels are required to have an isolation of 30dB which requires filters with a minimum steepness of 40dB/MHz [28]. As is described in the next chapter HTS filters, which can yield an almost ideal filter using HTS thin films on a suitable substrate [29-33], are said to be very well suited to this task.

Before discussing the suitability of different filter technologies it is important to understand some of the fundamentals of filter technology. This as well as some practical examples of different filter technologies is the focus of the next chapter.

CHAPTER 3

FUNDAMENTALS OF FILTER TECHNOLOGY

The task of a filter in wireless subsystems is to reduce the bandwidth of the spectrum received by an antenna to the useful frequency range. A bandpass filter can be represented as a chain of coupled resonant circuits. There are several types of resonant circuits which can be manufactured, most commonly used in microwave communications are cavity filter designs. Theoretically cavity filters, metallic filters, dielectric filters and HTS planar filters can all be used in cellular base transceiver stations and each type have certain advantages and disadvantages. While the unloaded quality factor (Q_0) of individual resonators of a filter is an excellent indicator of its performance, practical matters related to implementation are also important. Understanding both of these factors is essential in selecting the correct filter type to achieve a higher performance and a practical receiver front end.

3.1 FILTER BASICS

RF Filters have two figures of merit which describe the performance of the filter. The first metric is the steepness of the transition region of the transfer characteristic, which is proportional to the number of resonators and transmission zeros. The second metric is the unloaded quality factor, Q_0, which describes the insertion loss and rounding of the band edges. A higher unloaded Q indicates lower losses and less rounding, a more ideal response.

An ideal resonator can be represented by an LC circuit (Figure 3.1). A filter is made from coupled resonators and the coupling between resonators can be electrical, as in Figure 3.2, or magnetic. In practice, excluding lumped element filters, the coupling is a mixture of both electric and magnetic types. This is generally the case at the high frequencies used in wireless communications.
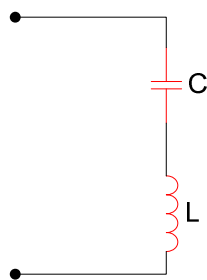
Figure 3.1. Ideal LC Resonator   **Figure 3.2. Ideal Filter with Electrical Couplings**
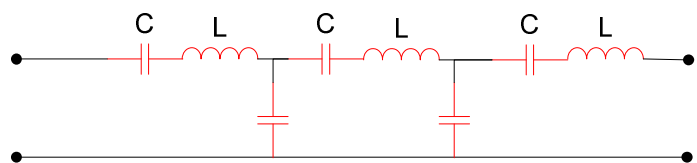
Increasing the number of resonators in most filter designs is quite simple and improves the steepness of the response in the transition region. Transmission zeros, created by adding a cross coupling between non-adjacent resonators [30], can also be used to increase the steepness of the transition region. However, as more resonators are added and cross couplings are included, tuning and trimming of the filter response

becomes more difficult. Furthermore resonators can not be added indefinitely. Each resonator has a finite Q_0, determined by the losses in the resonator (equation (3.1)). As more resonators are added more losses are introduced into the filter causing the insertion loss to increase and the rounding of the band edges to become more pronounced (Figure 3.3). Therefore the figure of merit of primary concern is the finite unloaded quality factor of the resonator, described by a well known equation;

$$Q_0 = \omega_0 \frac{\text{mean energy stored}}{\text{mean energy dissipated}} = \frac{\omega_0 W}{P} \tag{3.1}$$
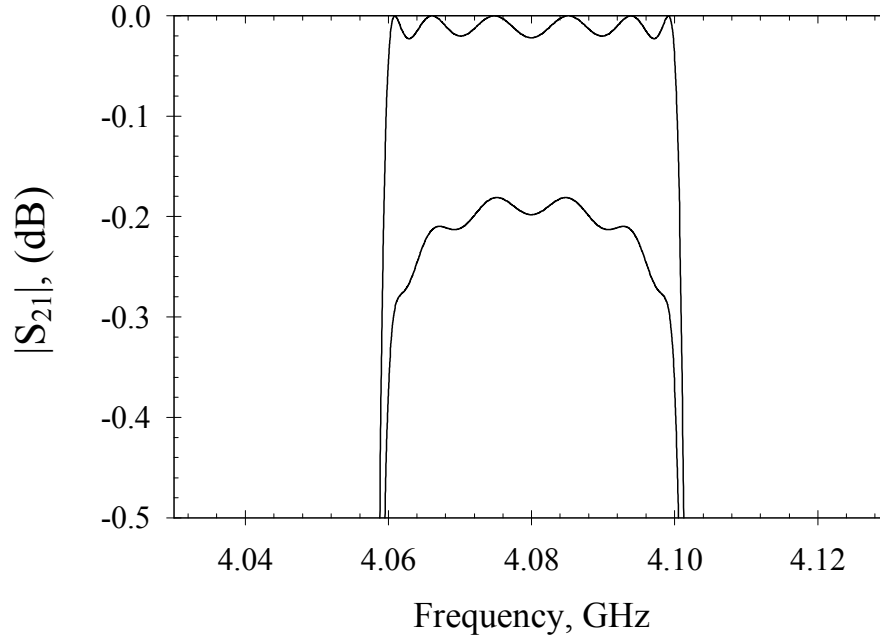
Figure 3.3. Transfer Characteristics of a lossless filter and a filter with a finite Q_0 of 20000

Distributed resonant structures are subject to three basic loss mechanisms, conductive losses, P_{cond}, in the metal surfaces which have a current flowing, losses in the dielectric, P_{diel}, which is proportional to the $\tan \delta$ of the dielectric used, and the radiation losses to the housing, P_{rad}. Considering these loss mechanisms one can derive from eq. (3.1) an equation for $1/Q_0$,

$$\frac{1}{Q_0} = \frac{P_{cond}}{\omega_0 W} + \frac{P_{diel}}{\omega_0 W} + \frac{P_{rad}}{\omega_0 W} \tag{3.2}$$

Therefore the unloaded quality factor is given by,

$$\frac{1}{Q_0} = \frac{1}{Q_{0,cond}} + \frac{1}{Q_{0,diel}} + \frac{1}{Q_{0,rad}} \tag{3.3}$$

As described in the next chapter the application of superconducting technology can significantly increase $Q_{0,cond}$. The best superconducting resonator is therefore a cavity resonator where both P_{diel} and P_{rad} are equal to zero.

3.2 CAVITY FILTERS

To minimise the losses in the resonator the most ideal structure is that of a cavity with a maximum of EM field volume and a minimum of RF surface. In a cavity, because the entire field is enclosed by metallic walls, there are no radiation losses. Assuming there is a vacuum in the cavity, the dielectric losses are zero. The only losses to be considered are the conductive losses in the cavity walls and Q_0 is given by $Q_{0,cond}$, where P_{cond} is the surface losses in the metallic wall given by [34],

$$P_{cond} = \frac{1}{2} Rs H_s^2 \tag{3.4}$$

Therefore,

$$Q_0 = \frac{\omega_0}{Rs} \cdot \frac{\int_V \left| \vec{H}(\vec{r}) \right|^2 dV}{\int_{Sc} \left| \vec{H}(\vec{r}) \right|^2 dS} \tag{3.5}$$

which can be simplified to the geometric factor, G, divided by the surface resistance, Rs,

$$Q_0 = G / Rs \tag{3.6}$$

where the geometrical factor is given by [35],

$$G = \frac{2\pi}{\lambda_0} \cdot v_p \cdot \frac{\int_V \left| \vec{H}(\vec{r}) \right|^2 dV}{\int_{Sc} \left| \vec{H}(\vec{r}) \right|^2 dS} \tag{3.7}$$

v_p is the phase velocity in free space which is approximately equal to the speed of light, c, and λ_0 is the free space wavelength, $\lambda_0 = c / f_0$.

Generally speaking a higher quality factor requires a large geometrical factor and low surface resistance. Typically the geometrical factor increases with an increasing ratio of volume to surface.

The surface resistance is given by the frequency and the conductivity of the metallic wall of the resonator [36],

$$Rs = \frac{1}{\sigma\delta} \tag{3.8}$$

Where σ is the conductivity of the metal (e.g. for copper @ room temperature $\sigma = 5.7 \times 10^7/(\Omega \cdot m)$) and δ is the skin depth which is given by,

$$\delta = \left(\frac{2}{\mu\sigma\omega} \right)^{\frac{1}{2}} \tag{3.9}$$

where μ is the magnetic permeability of the wall.

Since all the losses are determined by the walls of the cavity a low loss material should be used. Typically gold, silver or copper is used, but because at high frequencies the skin depth is small, the entire cavity need not be made of these materials and plating is sufficient. (For example the skin depth of copper at 2GHz is approximately 1.48μm)
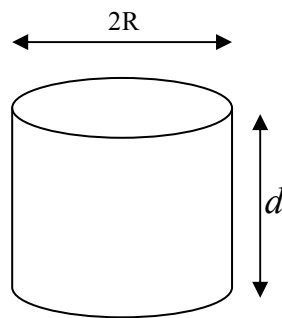
Figure 3.4. A Pillbox Cavity
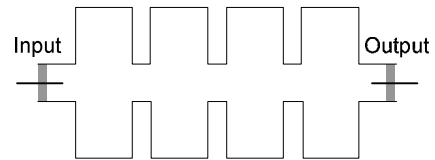
Figure 3.5. Pillbox Cavity Filter

Figure 3.6. Photograph of Pillbox Cavity Filters at Mt. Stuart, Townsville

Pillbox cavities (Figure 3.4) operating in the TM_{010} mode are typically coupled electrically as shown in Figure 3.5 and Figure 3.6 to give a Chebyshev filter response. For this structure the resonant frequency of the TM_{010} mode is given by,

$$\omega_{010} = \frac{2.405c}{R} \qquad (3.10)$$

and is independent of the cavity length [34]. The geometrical factor in ohms is given by [34],

$$G = \frac{453\dfrac{d}{R}}{1+\dfrac{d}{R}} \qquad (3.11)$$

A 2GHz copper pillbox cavity has a Q_0 of approximately 22500 at room temperature. Microwave pillbox cavities typically exhibit Q_0 values of several thousands when made from traditional materials such as copper [37]. If a superconducting niobium operating at 2K is used, the surface resistance is in the order of nΩ, Q_0 values are of the order of 10^{10} [34, 38]. A structure which exhibits such high unloaded quality factors are the accelerating cavities used for particle accelerators (Figure 3.7 & Figure 3.8). Both copper and niobium, are typically found in linear accelerator structures [38, 39]. HTS materials however are unsuitable for making cavities due to their layered crystallographic structure and related anisotropy of their conductivity.
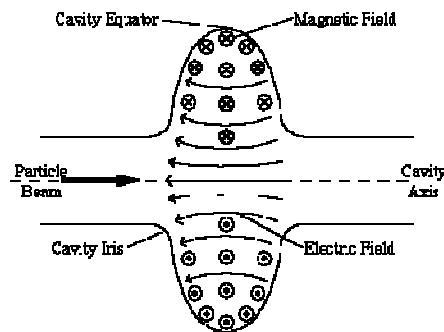
Figure 3.7. Schematic of an RF Cavity for Particle Accelerators Showing EM Field Lines [39]

Figure 3.8. 9 Cell as Used in the TESLA Test Facility [39]

Unfortunately pillbox cavities are too bulky and using niobium cavities for communications filters is not feasible in practice due to their size, the cost of manufacturing and the cost of cooling with liquid helium in a cryostat. As such, smaller filter designs are used in communications and cavities.

Combline resonators or coaxial resonators, are the filters typically used in today's wireless communication. Coaxial resonators are typically a quarter-wavelength coaxial stub inserted into an air filled cavity (Figure 3.9). The diameter of the cavity is about 3 times the diameter of the coaxial line, in order to minimise losses in the walls, and therefore the filter is typically quite large, although smaller than a pillbox cavity. Coupling is achieved by opening an iris between the adjacent resonators to allow the electromagnetic fields to couple. Coupling between two non-adjacent resonators in a quadruplet creates

symmetrical transmission zeros for a quasi-elliptic response. Metallic tuning rods above each resonator can be used for adjusting the resonant frequency and a metallic trim rod in the iris can be used to open/close the iris and weaken/strengthen the coupling.
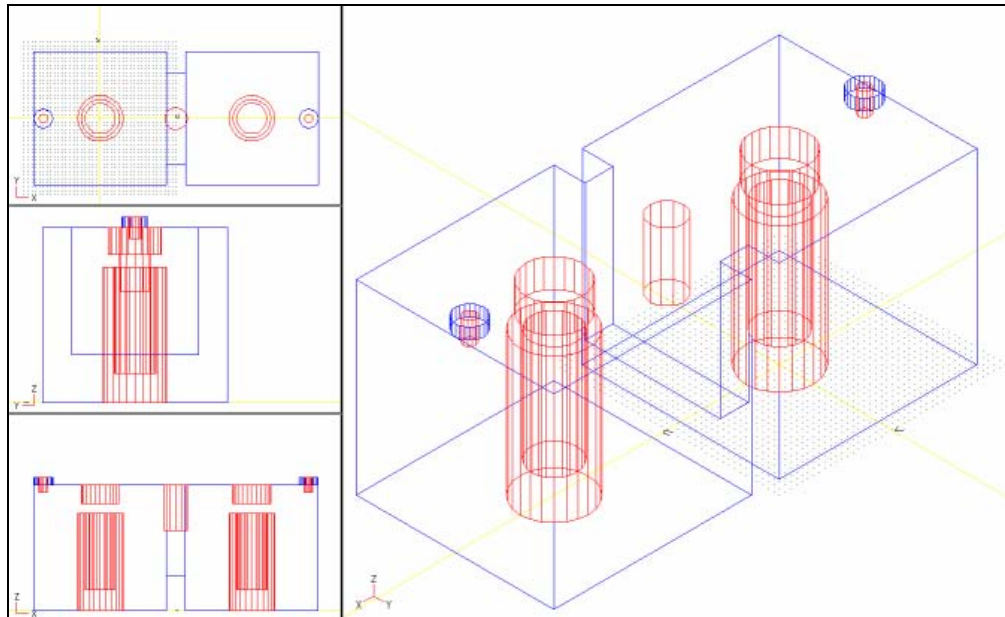
Figure 3.9. Coupled Coaxial Resonators

The loss mechanism in coaxial resonators is that of the conductive losses in the walls of the housing and the coaxial stub which is very similar to the situation with the cavity. From equation (3.7) for the geometrical factor, it can be seen that for a coaxial resonator the volume (the numerator) is decreased compared to what it was for a cavity and the surface area (the denominator) is increased compared to the cavity, therefore G is decreased. Assuming the same conductive material is used for both the cavity and coaxial resonators the unloaded Q is decreased by a factor of 3 to 10 [35], but the overall size of the coaxial resonator is significantly smaller. Typical Q-factors of coaxial resonators are in the vicinity of 5000.

Combline Resonator filters use a coaxial stub inserted into a larger coaxial stub to create a capacitive element (Figure 3.10). While this reduces performance slightly (Q-factor ~ 4000) it further reduces the size of the resulting filter. As with coaxial filters, combline filters couple electromagnetically and can be trimmed, for example, by using a metallic trim rod inserted into the iris between the resonators (not shown in Figure 3.10). Tuning is achieved using a metallic plunger inserted into the lid above the resonator. A major benefit of the combline filter is that it can be designed so that the interplay of distributed and lumped elements can be used to eliminate the higher order passbands.
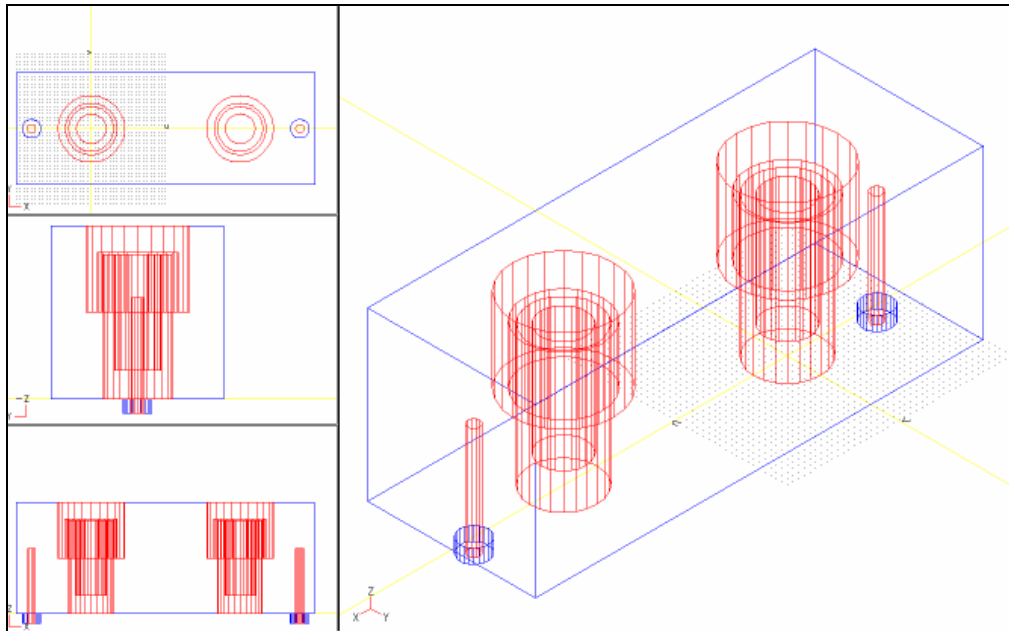
Figure 3.10. Coupled Combline Resonators

3.3 DIELECTRIC RESONATOR FILTERS

Low loss (*tan* δ < 0.0001) temperature stable (α ≈ 0ppm/°C) dielectric materials with relatively high permittivity (ε_r > 37) have been used to develop dielectric resonators (DR) [40]. By placing a dielectric puck inside a cavity the electromagnetic field is concentrated in the dielectric. Therefore DR filters exhibit less conductive losses in the housing at RF frequencies than cavity filters and cavities, and can be made more compact in size [41]. However, the losses in the dielectric must be taken into account.
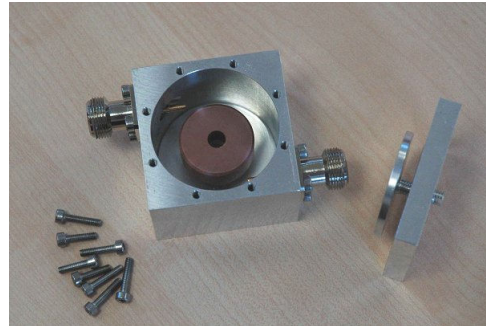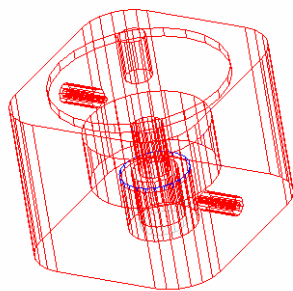
Figure 3.11. Dielectric Resonator Developed in Chapter 8 (Left: CAD, Right: Manufactured)

The unloaded Q of a dielectric resonator is calculated by summing the unloaded Q factors of the dielectric and the conductive losses. The housing is calculated in two parts, the walls and the lid/base, assuming that the dielectric puck is placed directly in the centre of the housing. Therefore the equation describing Q_0 of the dielectric resonator is [42, 43],

$$\frac{1}{Q_0} = \frac{Rs}{G} + p_e \tan \delta \qquad (3.12)$$

Where G is the geometrical factor of the metallic cavity, p_e is the electrical energy filling factor and $\tan\delta$ is the loss tangent of dielectric puck. Typical unloaded Q-factors of dielectric resonators in the range of 1GHz to 3GHz are between 10000 and 40000.

Due to their high Q and compact size, microwave band pass dielectric resonator cavity filters have been used in satellite communications since the early 1980's [44]. Terrestrially, in order to cope with the increasing demand for capacity in restricted spectral bandwidth, channel spacing in 3rd generation cellular communications has been reduced, requiring improved filter steepness while maintaining low insertion losses and an acceptable group delay characteristic [45]. High Q_0 and power handling capabilities of dielectric resonators make them suitable for use in DR duplexers, which can be used to replace the metallic duplexers on the main antenna. The duplexer serves as pre-selection filtering for the receiver side and to clean up spurious signals before transmission on the transmit side. It is the author's opinion that DR filters can serve as an economical intermediary step between conventional cavity filters and currently expensive HTS filters. Based on this conjecture, it became clear that when coupled with a CRFE the partnership would provide the best possible base station front end performance. Additionally DR filters exhibit high enough Q-factors (>20000) that it is feasible to design filters for use in both transmit and receive filtering for a multi-operator combiner without the use of signal splitter-combiners. It is entirely feasible to design a DR filter that is tuneable for each channel in the UMTS receive (1920 – 1980MHz) or transmit (2110 – 2170MHz) bands that using the same dielectric puck (different pucks are used for receive and transmit bands) and filter cavity (common to both bands). These ideas are discussed further in Chapter 8.

3.3.1 COUPLING, TUNING AND TRIMMING

In order to limit losses from the conductive enclosure, the cavity diameter is usually greater than 1.5 times the dielectric puck diameter, and the height of the cavity is about 3 times the thickness of the dielectric puck [44] (Figure 3.12). Tuning can be achieved by introducing a metallic plunger into the lid of the cavity. Using the plunger effectively decreases the size of the cavity and increases the resonant frequency of the resonator. The side effect of this deformation is a decrease the Q-factor of the resonator, due to increasing losses in the cavity walls. A dielectric plunger narrower than the size of the hole in the dielectric puck can be used to tune the resonant frequency lower. The losses introduced by this tuning method are considerably less; however the cost of dielectric tuning screws has to be weighed against the benefits.
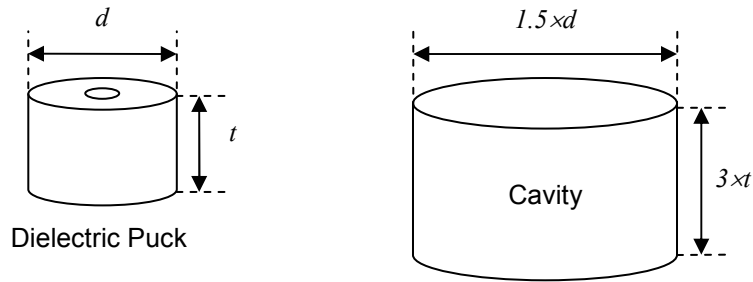
Figure 3.12. Diagram of a Dielectric Puck and Cavity

As mentioned earlier single resonators must be coupled together in order to produce a filter response. Typically this is achieved by opening an iris between the adjacent cavities. The iris relies on magnetic coupling and should open in a parallel direction to the magnetic field where it is a maximum. For a filter structure consisting of $TE_{01\sigma}$ mode cavity resonators the iris opens along the z direction (Figure 3.13). Closing the iris by adjusting the height weakens the coupling. Typically this is realised using an adjustable trim rod placed in the lid of the housing. The width of the iris should not be too wide in order to keep the coupled $TM_{01\sigma}$ mode away from the $TE_{01\sigma}$ mode [44].
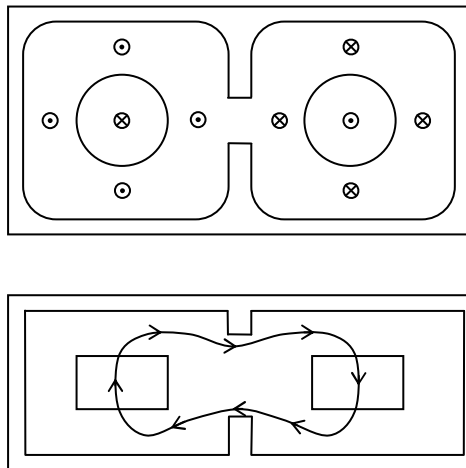
Figure 3.13. Top: Magnetic Mode Fields from Top View of Coupled Cavities; Bottom: Side view of Magnetic Fields between Two Coupled Cavities

In order to realise a quasi-elliptic frequency response with symmetric transmission zeros a negative coupling is required between non-adjacent cells in a quadruplet (Figure 3.14). Because the adjacent cells are coupled magnetically this can be regarded as positive coupling. The term positive coupling refers to the sign of the coupling coefficient when two resonators are coupled. The value for the coupling coefficient is given by equation (3.13), where f_1 and f_2 denote the frequencies of each of the resonators.

$$K = \frac{f_2 - f_1}{\left(\dfrac{f_2 + f_1}{2}\right)}$$

(3.13)

When the coupling between the resonators change from being predominantly magnetically (positively coupled in this case) to predominately electrically coupled f_1 becomes greater than f_2 and the sign of the coupling coefficient becomes negative, hence the term negative coupling. Therefore to provide a negative coupling the non-adjacent cells must be electrically coupled. This can be realised by using a metallic antenna passed through and isolated from the wall between the non-adjacent resonators. The antenna couples to the electric field around the puck creating an electrical coupling between the two resonators. Adjustments in the length (provided it is shorter than $\frac{1}{4}\lambda$) and orientation can increase or decrease the strength of the electrical coupling. A similar antenna setup can also be used to couple the ports to the first and last resonators.
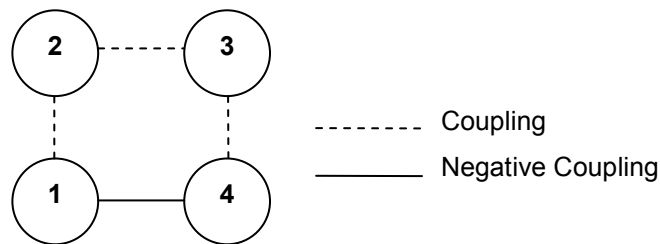
Figure 3.14. Quadruplet Structure Using a Negative Cross-Coupling to Obtain a Quasi-Elliptic Response

3.4 PLANAR FILTERS

Planar filters comprised of microstrip resonators, an example of which is shown in Figure 3.15, have conductive strips on the top surface of the dielectric substrates, which on the other side have conductive ground planes. All three loss mechanisms (conductive, dielectric and radiation) are exhibited in this architecture. To decrease radiation loss planar filters are normally housed in a metallic box. The propagation of electromagnetic fields emitted by the "open structure" of the microstrip is affected by the housing causing the Q-factor of the filter to decrease.
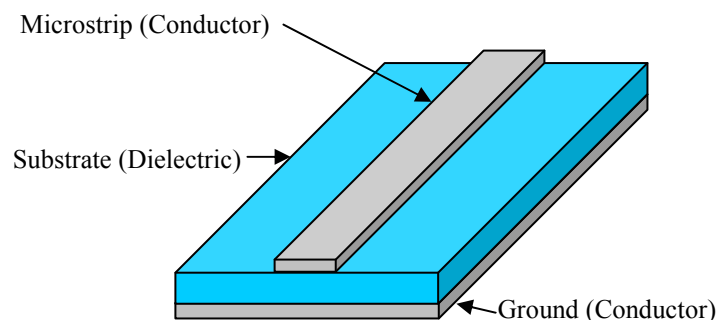
Figure 3.15. Half Wavelength Microstrip Resonator

Planar filters rely on electric and/or magnetic couplings between resonators to transfer the signal. Because the volume of the microstrip is very small in comparison with the surface area, the geometrical factor is also very small [46] (recall equation (3.7)). It is possible to slightly increase the geometrical factor by widening the microstrip, trading off between surface area and unloaded quality factor. In the lumped

element model all the loss mechanisms (conductive in the microstrip, dielectric in the substrate and radiation) need to be accounted for. For a resonator made of a normal metal (such as cooper) the conductive losses dominate and Q_0 of several hundred are common. Using a superconductor for the microstrip and ground greatly reduces the conductive losses, however radiation losses become more prominent and cannot be ignored. In practice Q_0 in excess of 50000 are common (depending on temperature) although initial designs based on conventional filter theory did not perform as well as expected due to the increased influence of phenomena such as coupling losses and radiation effects. The consequence was that new design procedures and more advanced simulators were required to accurately model superconducting planar resonator designs.

Table 3.1. Q_0 values and Size Various Filter Designs

Resonator	Typical Q_0	Size
Pill Box Cavity (Copper)	5000 – 10000	Large
Pill Box Cavity (Niobium @ 2K)	~ 10^{10}	Large
Coaxial (Copper)	~ 5000	Medium
Combline (Copper)	~ 4000	Medium
Dielectric Resonator	10000 – 40000	Medium
Stripline (Copper)	100 – 500	Small
Microstripline (Copper)	~ 200	Very Small
Microstripline (YBCO @ < 92K)	50000 – 500000	Very Small

Another design issue coming about due to the low loss nature of superconducting materials is the ability to miniaturise the resonators while maintaining low insertion loss and high out-of-band rejection. Miniaturisation of resonators causes a reduction in the geometrical factor due to increased currents near the bends due to current crowding. Such a loss is unacceptable when the geometrical factor is already small and the conductive losses are relatively large. However when the losses are extremely small, as in the superconducting case, such a loss is acceptable. It has been the focus of much research to design miniaturised resonators of high Q-factor and small size in order to produce the smallest possible HTS filter which still yields an almost ideal frequency response [31-33, 47-50]. However, it can be concluded, based on current commercial filter designs, that very small HTS filters do not serve any practical purpose given the size of the vacuum and cooling equipment required to support them. Furthermore, realisation, tuning and trimming of these filters is usually significantly more difficult than less compact designs, making them unsuitable for mass production due to the time and cost involved tuning and trimming each filter (which would outweigh the cost saving benefits of using less substrate). Minimising the number of resonators required to achieve the specified frequency response will also minimise tuning and trimming times. Designers also have an option of incorporating cross-couplings to produce transmission zeros near the band edges. These transmission zeros produce a quasi-elliptic filter response, meaning that fewer poles (resonators) are required to achieve a specified out-of-band rejection at the expense of a more uniform group delay. Cross couplings however, should be used judicially, because they introduce additional dependencies on the adjacent resonators, which can make trimming more difficult. Keeping this in mind, it is the goal of the designer to design a resonator and subsequently a filter that achieves the required frequency response with as few resonators as possible and which is easily tuned and trimmed. It should also use the HTS substrate economically given the cost of the raw materials. This may be the

reason that the two groups currently producing cryogenic receiver front ends (CRFEs) have not published competing miniaturised designs [51].

The specifics of filter design are complicated and rely very much on the designers experience and tradeoffs between design parameters. One good source of filter design theory is Matthei, Young and Jones [52]. A review specifically for HTS filters is also available [30].

3.4.1 PACKAGING, TRIMMING AND TUNING

HTS filters must be packaged inside a metallic box in order to perform correctly. If it is not packaged or the filter is not grounded to the box sufficiently then microwave interference will degrade the frequency characteristic of the filter. Typically the filter chip is glued to a carrier of equal thermal expansion coefficient and attached to the housing using conductive two part glue which requires pressure and heating in order to make a good permanent contact. SMA connectors are attached to the ports of the filter and the housing is screwed shut.

Dielectric tuning screws are used to tune (shift in frequency) and trim (obtain good matching in the passband). These screws are placed in the roof of the housing above the ends of the resonators. In this way they affect the electric field (or capacitive coupling), which reaches a maximum at the end of the resonators, therefore allowing the designer to fine tune the filter's response.

3.4.2 HTS FILTER DESIGNS

When considering filters for 3G communication applications the primary focus is on achieving filters with very steep transition regions and low insertion loss. Because of the low loss nature of HTS materials, creating filters with very low insertion loss and passband ripple is a simple task, even with miniaturised designs. Typically the focus is on achieving very steep transition regions, which means designers have tended to start with Chebyshev filter approximations rather than Butterworth or Bessel approximations.

An early request of Japan's NTT DoCoMo was for a filter design with extremely steep skirts in order to remove the interference generated from a neighbouring wireless service. This was the first market request for a high temperature superconducting filter triggered by the claims of very high selectivity and sensitivity of HTS filters. By the year 2000 CryoDevice (Japan) and Cryoelectra (Germany) had both demonstrated UMTS band pass filters which met the DoCoMo requirements (20MHz bandwidth, 80 dB/MHz skirt steepness in the transition region). The CryoDevice design was a 32 pole Chebyshev filter using a J shaped resonators on a $4560mm^2$ YBCO coated MgO substrate. The Cryoelectra device used a novel elliptical filter architecture. Seventeen poles were used to obtain the same steepness as the CryoDevice design by using dual mode resonators on a $1400mm^2$ YBCO coated Sapphire substrate. In 2002 Conductus demonstrated a 22 pole filter, utilising 5 quadruplet cross couplings. This quasi-elliptic filter gave 10 symmetric transmission zeros at finite frequencies and produced a skirt steepness of 260 dB/MHz on a $2027mm^2$ YBCO coated MgO substrate. All of these filters are examined in the next three sections.

Without considering the possibility of realisation, lumped element models of each of the three filter types were created to show the theoretically achievable steepness (Figure 3.16). All the filters have a bandwidth of 20MHz and are designed for use in the UMTS band (1920 – 1980 MHz) and out-of-band rejection of 85 dB. Realised filters are also shown by points on the graph. It can be seen that both the Chebyshev and Quasi-elliptic filter approach their theoretical limits. The Elliptic design, particularly at higher orders, deviates from the ideal limit. This problem is most likely due to parasitic coupling but further research into this field by Cryoelectra has been limited due to the available computing power [53].
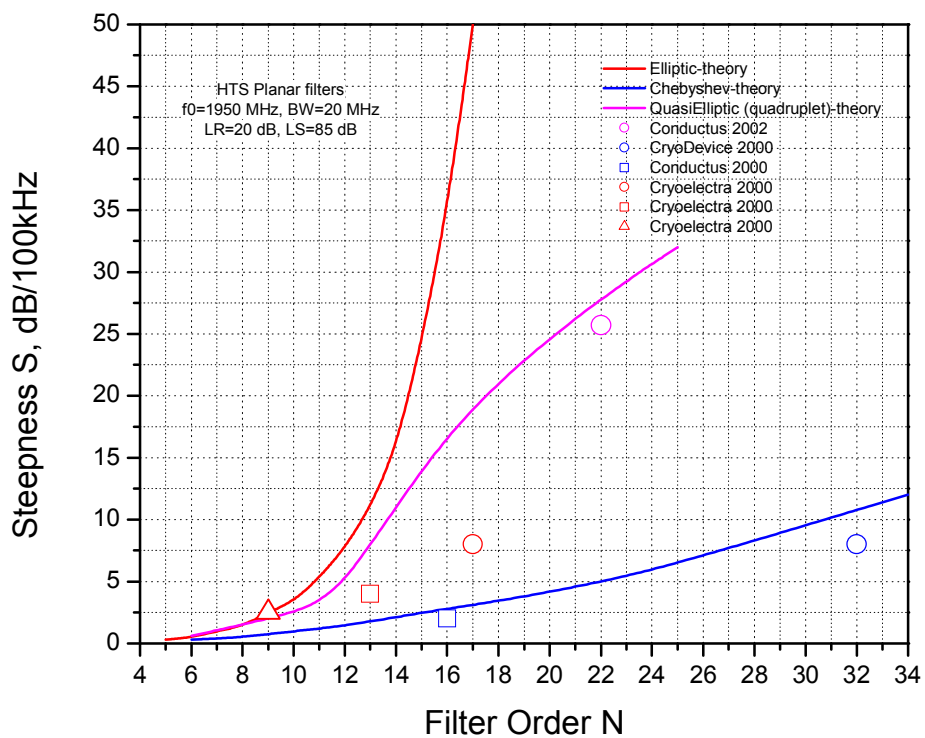
Figure 3.16 - Theoretically achievable skirt steepness for different filter architecture depending on the filter order [53]

3.4.2.1   32 POLE CHEBYSHEV FILTER [31]

Like all the filters discussed in this section, this filter was designed for use in the UMTS band. It has a bandwidth of 20 MHz and uses J-shaped resonators made from an arc and two lines (Figure 3.17). The J-shaped resonators are arranged in a circular pattern to maximise the number of resonators on the 3 inch YBCO coated MgO wafer to create the filter (Figure 3.18). The coupling between resonators is determined by the length of the straight line on either side of the arc and the centre angle (θ) between adjacent resonators. It was found that for certain combinations of line length the coupling could be adjusted positively or negatively between resonators by modifying θ. This allowed the designer to

implement controllable cross couplings between non-adjacent resonators which would introduce transmission zeros at the band edges.
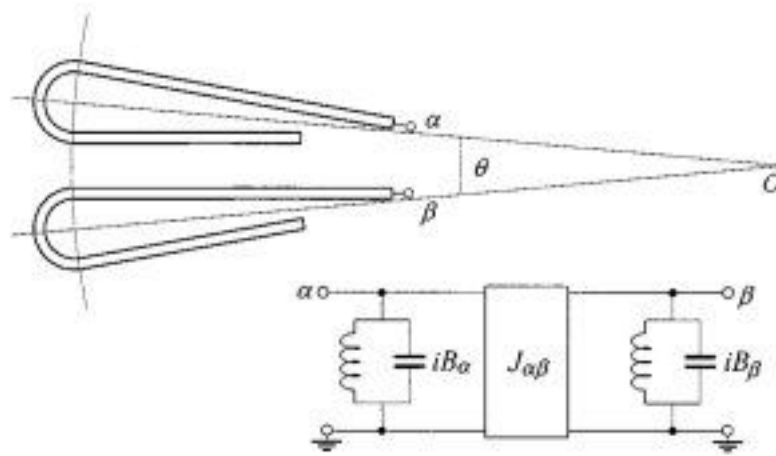
Figure 3.17 - Layout of Coupling between two J-Shaped Resonators and the Equivalent Circuit [31]
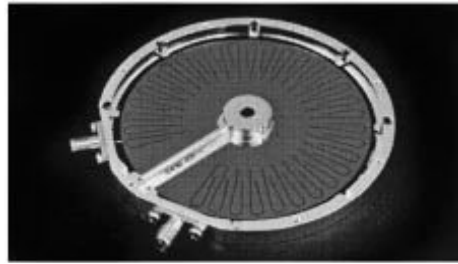
Figure 3.18 - 32 Pole Chebyshev Filter [31]

The paper in which this filter was presented also described a new permanent tuning method based on measuring each resonators resonant frequency and doping them with a film of dielectric material, in this case with CeO_2. This method has advantages over conventional tuning screws in that it is permanent and more accurate for filters with a large numbers of resonators and cross-couplings.

3.4.2.2   22 POLE QUASI-ELLIPTIC FILTER [32, 33]

This filter was published by G. Tsuzuki, S. Ye and S. Berkowitz at Conductus in 2002 and demonstrated the highest skirt steepness of any HTS filter produced so far. This filter utilised a quadruplet cross-coupling technique (Figure 3.20) to produce symmetric transmission zeros at the band edges and a novel clip resonator. The filter was fabricated on a 2 inch YBCO coated MgO wafer, which is less expensive and less prone to defects than the 3 inch wafer used in the Chebyshev design discussed previously. It should be noted that the Tsuzuki does not discuss how the tuning and trimming of this design was performed or the time that was required in either of the referenced publications.
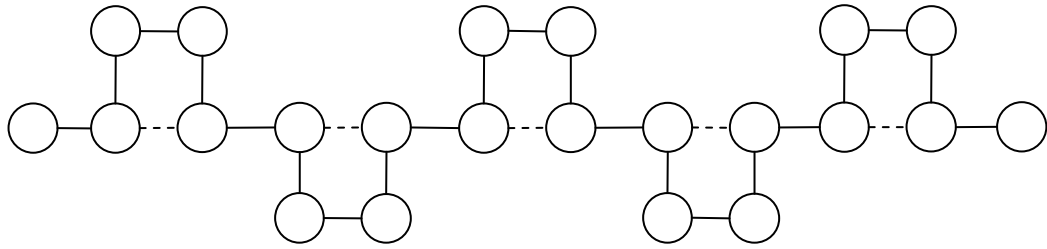
Figure 3.19 - Quadruplet Structure used to Place 10 Transmission Zeros (dotted lines represent cross couplings) [30]
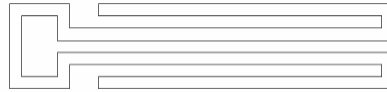
Figure 3.20 - Topology of Clip Resonator [32]

3.4.2.3   17 POLE ELLIPTIC FILTER

This filter is based on a dual mode resonator designed by H. Chaloupka [54], shown in Figure 3.21. The exceptional characteristic of this resonator is that it has two poles and two finite transmission zeros, which can be adjusted without strongly affecting the placement of the poles. The simulated and measured frequency responses of this HTS resonator are shown in Figure 3.22. The two poles and two transmission zeros can be seen clearly [29].
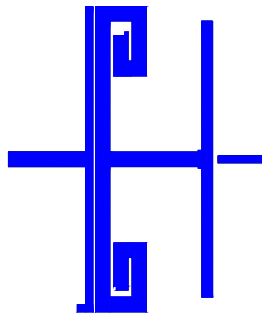
Figure 3.21 - Dual mode resonator with input and output ports
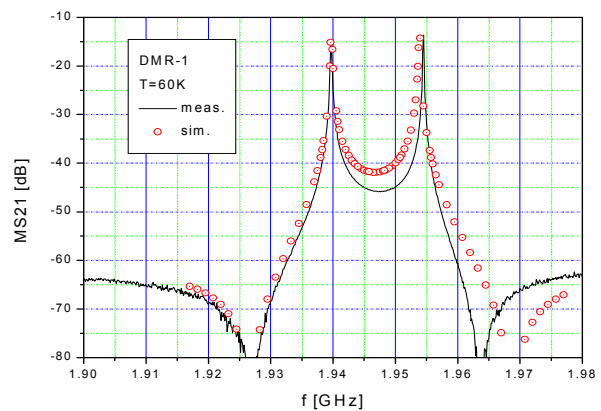
Figure 3.22 - Simulated and measured characteristic of dual mode resonator

There are two possibilities for realising the filter using this dual mode resonator, a symmetrical layout, where dual identical resonators (i.e. two resonators with the same resonant frequencies) are placed either side of an H-shaped resonator or an asymmetric layout where each individual resonator has its own resonant frequencies. Only the asymmetric design will produce a truly elliptic response as the symmetric design will produce only one pair of transmission zeros for each pair of identical resonators either side of the H-shaped resonator (although these are double transmission zeros and will appear to have a deeper notch).

The seventeen pole filter was designed based on the experiences of designing 5, 9 and 13 pole filters, all using the same symmetric layout of dual mode resonators with a centre H-shaped resonator [51]. The decision to use the symmetrical design was based on limited computing power available at the time. With the symmetrical design both halves of the filter would act the same way and could be combined mathematically using a lumped element model rather than doing a full EM simulation. The process was more complicated than this simple explanation but not relevant in the context of this review.

The filter was manufactured on a 1400mm^2 YBCO coated Sapphire (Al$_2$O$_3$) substrate and produced skirt steepness comparable to that of the 32 pole Chebyshev design (approx. 85dB/MHz) and greater than 85dB out-of-band attenuation. Although this filter was difficult to trim correctly, it remains interesting being the only elliptical filter design with such a large number of poles. Other elliptical designs make use of dual mode patch resonators such as those describe in [55] and are usually of low orders.

3.5   FINAL COMMENTS ON FILTER TECHNOLOGY

This chapter has looked very briefly at some of the concepts of HTS filter design and several examples. As the design of HTS filters is not a major goal of this work more specific filter design theory has not been included. Pioneering filter design work has been published primarily by university groups worldwide, some of the most notable include Prof. M. Lancaster's group at the University of Birmingham [56], Prof. H. Chaloupka's group at University of Wuppertal [54, 57-59] and Tsuzuki [31, 32]. The microwave filter design principles penned in Matthaei, Young and Jones's book "Microwave Filters, Impedance-Matching Networks, and Coupling Structures" in 1980 [52] remains the basis for modern microwave HTS filter design theory. Reference [30] also has a detailed description of HTS filter design and more examples.

The simple architecture of a Chebyshev filter, in which only the resonant frequencies of the individual resonators can be controlled, does not require extensive tuning or trimming, unlike the sophisticated elliptical and quasi-elliptical designs. Because this tuning and trimming process is time consuming it makes mass production of sophisticated designs very difficult. Furthermore not all base stations will require filters with extremely sharp skirts, only the improved insertion loss will be required in many circumstances. Hence it seems appropriate that anyone developing cryogenic front ends should have an easily mass producible Chebyshev design which ideally would not require tuning, at the expense of a filter design which approximates the ideal brick wall response.

Dielectric resonator filters exhibit performance close to that of current HTS filter designs, while costing little more than conventional metallic filters and being significantly smaller. Additionally the exceptional tuneable range means that this technology should not be ignored when trying to decide *if high temperature RF-superconductivity can prove to be an important technological contribution to future wireless communication*. Therefore DR filter technology can be thought of as possibly the 2nd generation of microwave filter technology in wireless communication.

HTS filters; the 3rd generation of microwave filter technology in wireless communication, while offering undisputedly the best performance for low power applications such as CRFE come at a high cost and are difficult to understand. Indeed there is currently no sufficient explanation of the physics behind the HTS phenomena available today, but some simple explanations based on existing theories can be used to understand the application of this technology to filter theory and this is what is discussed in the next chapter.

CHAPTER 4

FUNDAMENTALS OF RF SUPERCONDUCTIVITY

Chapter 2 identified that providing high quality communications services requires highly selective and very sensitive band pass filters are required in the receive side of the base transceiver stations. High selectivity and low insertion loss demand filters with extremely high Q factors, which is achieved through the minimisation of RF losses in the filter. To realise this goal two new technologies have come to the forefront, dielectrics and high temperature superconductors. While dielectrics have been used in filters for satellite communications since the 1980s [44] and appear to be the natural progression of filters for terrestrial communications, HTS filters may be the next step, or the third generation in filter evolution. To understand why HTS filters have the opportunity to fulfil this evolutionary role it is important to understand some of the fundamentals of superconductivity and how they relate to filter design. The following section is a review of these fundamentals.

The unloaded quality factor of the resonators forming a bandpass filter is an important figure of merit for the filter. In a cavity resonator it is related to the surface resistance of the material of the cavity walls and given by equation (3.6) to be G/Rs with G being only determined by the cavity geometry and the mode excited in the resonator. Cooling a cavity resonator made of a superconducting material like niobium, for example, will result in a reduction of the surface resistance as the conductivity, σ, of the material increases (see eq. (3.8) and (3.9)). As soon as the temperature of the cavity walls is cooled below the critical temperature, Tc, a dramatic reduction of the surface resistance Rs and a corresponding increase of Q_0 can be observed.

4.1 THE SUPERCONDUCTING STATE AND THE LONDON TWO FLUID MODEL

In 1911, only three years after helium was first liquefied, H. K. Onnes found that mercury lost its DC resistivity at a temperature of 4.15K [10, 36] as shown in Figure 4.1. Many elemental metals, such as Lead, Lanthanum, Mercury, Tin, Aluminium, Zinc, Titanium, Uranium and Platinum, were later found to exhibit this new phenomenon, known as superconductivity, below a certain critical temperature, T_c. In 1933 Meissner and Ochsenfeld observed that when a superconductor was immersed in a magnetic field that was below the critical magnetic field, the magnetic field was expelled from superconductor, such that the superconductor was exhibiting perfect diamagnetism. This was found to be true not only when the superconductor was in the superconducting state and the field was applied, but also when the superconductor was first placed in the field and then cooled below its transition temperature. Superconductivity therefore demonstrated to be a new thermodynamic state of matter. In 1957, Bardeen, Cooper and Schrieffer were able to explain the microscopic mechanism behind the superconductivity phenomena [60] in what is now known as the BCS theory. A description of this theory is beyond the

scope of this thesis but elements of it are useful in justification of the two-fluid model of a superconductor introduced by H. London already in 1934 after the discovery of the Meissner effect. The two-fluid model is useful for understanding the basic properties of superconductors in an RF field, which is the case for the RF-filters under consideration in this thesis. In his two-fluid model H. London introduced two fluids; one formed by the normal conduction electrons and the other by so called superconducting electrons.
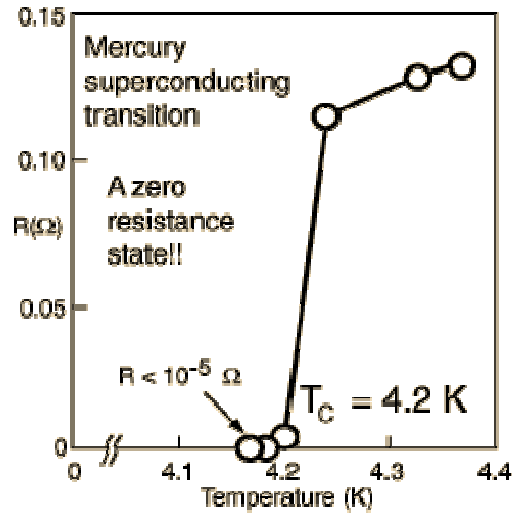
Figure 4.1. Graph of Mercury's Transition to the Superconducting State [61]

The BCS theory described that, in metal, interactions of conduction electrons with vibrations of atoms in the crystal lattice resulted in a very small net attraction between electrons. As a result the conduction electrons[1] could form electron pairs, referred to as Cooper pairs. These Cooper pairs are the particles which H. London referred to as superconducting electrons. The binding energy per electron of a Cooper pair, $\Delta(T)$, is temperature dependent and very weak. At temperature of 0K the binding energy is found by BSC theory to be,

$$\Delta(0) = \alpha k T_c \tag{4.1}$$

Where k is the Boltzmann constant and BCS theory determined α to be 1.762 [53].

Above the critical temperature there are no Cooper pairs, all the electrons are normal conducting electrons, hence the material is no longer in the superconducting state. At absolute zero all conduction electrons are paired. At finite temperatures the thermal energy can ionise Cooper pairs back into two normal electrons. It has been shown using Quantum statistics that the probability of a Cooper pair being broken up is given by the ratio of the densities of normal electrons (n_e) and Cooper pairs (n_c) [36],

---

[1] A more precise characterisation of the free electrons in a conductor would be to call them quasi particles. They are moving in the electromagnetic of the many atoms of the lattice forming a solid body and interact with the lattice vibrations. The term conduction electron can be misunderstood as describing a free electron.

$$\frac{n_e}{n_c} \approx e^{-\frac{\Delta(T)}{kT}}$$

(4.2)

At temperatures below half of the critical temperature ($\frac{1}{2}T_c$), the number of Cooper pairs, n_c, and the binding energy, Δ, are very close to their values at absolute zero (n_0 and $\Delta(0)$). Hence the two fluids in London's model are the superfluid of the Cooper pairs of density n_0 and the normal fluid of conduction electrons of density $n_e(T)$ where,

$$n_e(T) = 2n_0 e^{-\alpha\frac{T_c}{T}}$$

(4.3)

for T < T$_c$/2

An intuitive explanation as to why the Cooper pair fluid can carry an electric current without any losses was given by R.P. Feynman [62]. Cooper pairs can be seen as Bose particles and when there are many Bosons in a given state there is a large probability that all the other Bosons will enter the same state. At temperatures below T_c/2 nearly all the Cooper pairs will be locked down at the lowest energy in the same state. The probability to enter this state is a factor of $\sqrt{n_0}$ higher than the probability to enter into any state of higher energy. Because every atom in a conductor delivers at least one electron, n_0 is comparable to the density of atoms, which is about 6×10^{23} per mol. Therefore, because n_0 is very large, the Cooper pairs are moving at the same quantum energy level and hence it is impossible to transfer energy to the lattice. As a consequence the Cooper pairs flow through the lattice without losses. For a superconducting RF filter, reducing the temperature of operation increases the number of Cooper pairs in the material and therefore minimises the loss of energy to the crystal lattice, hence reducing the insertion loss and maximising the unloaded quality factor.

4.2 OTHER SUPERCONDUCTIVITY LIMITING PHENOMENA

4.2.1 IONISATION OF COOPER PAIRS BY RADIATION

Cooper pairs can be ionised by electromagnetic radiation if the frequency is high enough. This means that superconductivity has a finite useful frequency range and power handling capabilities. The energy of the photons required to ionise Cooper pairs in a superconductor is given by,

$$h\nu = 2\Delta(T)$$

(4.4)

where $h\nu$ is the photon energy and $T \leq T_c$.

Cooper pairs may be considered, for the purposes of explanation, as a bound state with the distance between the electrons given by the coherence length, ξ. In actual fact Cooper pairs are ordered states in momentum space with the two electrons having opposite but equal momentum and opposite spins. But by considering Cooper pairs as bound state it is possible to explain the requirements for a pure mono-

crystalline superconductor. If the critical temperature, T_c, of the superconductor is high, then a larger binding energy is required to bind the conduction electrons into Cooper pairs. A larger binding energy results in a shorter coherence length (the electrons in the Cooper pair are closer together). Should these close electrons encounter an imperfection in the crystal lattice they are likely to be ionised back into normal conduction electrons due to the increase of current in this region causing there kinetic energy to increase beyond that of the binding energy, as explained in Section 4.2.3. Lower binding energies mean a longer coherence length and therefore a reduced probability that both electrons will meet the imperfections in the crystal lattice causing them to be ionised.

4.2.2 CRITICAL MAGNETIC FIELD

Superconductivity can be destroyed by a sufficiently strong magnetic field [53]. This so called critical value of the field for type one superconductors is denoted by $H_c(T)$ and exhibits a temperature dependence given by [36],

$$H_c(T) = H_c(0)\left(1 - \left(\frac{T}{T_c}\right)^2\right) \tag{4.5}$$

As mentioned earlier Meissner and Ochsenfeld [63] found that a superconductor which is cooled to below T_c in an uniform external field smaller than H_c completely expels the magnetic field. The interior of the superconductor is screened by currents which flow in a very thin skin layer on the surface. The external magnetic field exponentially decays in the surface layer and its decay length is referred to as the London penetration depth, λ.

In the London two-fluid model it is shown that this penetration is given by [64];

$$\lambda = \sqrt{\frac{m}{(2e)^2 n_c \mu_0}} \tag{4.6}$$

Where m is the effective mass of the Cooper pairs, e is the charge and n_c is the superconducting carrier density as given in equation (4.2).

4.2.3 CRITICAL CURRENT DENSITY IN A SUPERCONDUCTOR

The density of a super current flowing (j_{sc}) in the penetration depth of an external field (the shielding current) may be written as [53];

$$j_{sc} = 2en_c v_c \tag{4.7}$$

Where $2e$ is the charge of a Cooper Pair, v_c is its velocity. Increasing j_{sc} means increasing v_c and thereby the kinetic energy of the Cooper Pairs. The maximum kinetic energy of a Cooper Pair should not exceed its binding energy otherwise it will ionise into conduction electrons and increase the losses in the superconductor. The losses increase significantly in a non-linear fashion with increased power [65]. Hence there is a limiting current density, which, once exceeded, will cause the superconducting material

stop superconducting. This is an important consideration is selecting the line widths of a planar HTS filter design and the reason that is it difficult to design HTS filters to filter the high powers transmit signal a base station.

4.2.4 RF SURFACE RESISTANCE OF SUPERCONDUCTORS

In contrast to the zero resistivity for DC electric currents in superconducting materials, there are losses if the superconductor is exposed to a high frequency field. Using the two fluid model these losses can be explained as follows. The time varying magnetic surface field, $H_s \cos \omega t$, penetrates into the superconductor and induces an electric field in the London penetration depth. According to Faraday's law of induction this field is proportional to the time derivative of the magnetic field and the amplitude of this field is proportional to ωH_s. The electric field accelerates the Cooper pairs which transport part of the surface current without losses. Because of the inertia of the paired electrons the electric field inside the superconductor is not shunted to zero, therefore it accelerates the normal electrons which interact with the lattice and produce losses according to the anomalous skin effect. The power dissipated in a superconducting resonator per unit area P_s can therefore be expressed as [53],

$$P_s \sim n_e(T)(\omega H_S)^2 \tag{4.8}$$

And using equation (4.3),

$$P_s \sim n_0 \omega^2 e^{-\alpha \frac{T_c}{T}} H_s^2 \tag{4.9}$$

for, $T < \dfrac{T_c}{2}$.

Taking equation (4.9) over the surface area, A, of the resonator,

$$R_s^t = A\omega^2 e^{-\alpha \frac{T_c}{T}} + R_{res} \tag{4.10}$$

The temperature dependent part of equation agrees well with results obtained from the BCS theory. The residual resistance R_{res} describes losses created by normal conducting surface. The quadratic dependence of the surface resistance on frequency is characteristic for the metallic as well as for the oxide superconductors.

The microwave impedance of superconducting materials can also be defined in the same way as for conventional conductors, namely as a ratio of electric and magnetic field on the surface of the macterial;

$$Z_S = \frac{E_x}{H_y}\bigg|_{z=0} = \sqrt{\frac{j\mu\omega}{\sigma}} = R_s + jX_s \tag{4.11}$$

where $\sigma = \sigma_1 - i\sigma_2$ where σ_1 and σ_2 are the conductivities of normal and superconducting electron pairs respectively (the conductivity of metals is exclusively real). The surface resistance of the superconductor

is strongly dependent of temperature and frequency as shown in Figure 4.2, which depicts the surface resistance at 10GHz of Yttrium Barium Copper Oxide reducing with temperature, and Figure 4.3.
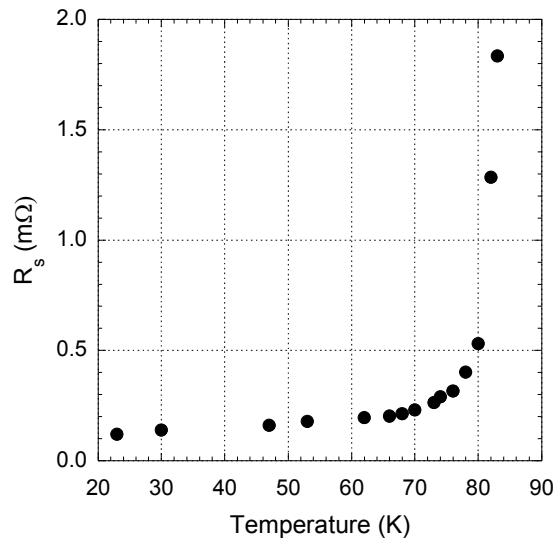
Figure 4.2. Surface Resistance of YBCO Thin Film on LaAlO3 Substrate at 10GHz [66]

The graph in Figure 4.3 shows the surface resistance as a function of frequency for niobium at 7.7K compared to the theory calculated using equation (4.10), shown by the dashed line, and the measured surface resistance for copper. Since the development of HTS, measurements of YBCO at 77K have also been added by different groups shown by numbered circles and squares. Because the T_c for YBCO is 92K (and for niobium it is 9.2K) the ratio of Tc/T remains the same, meaning that the YBCO should follow the same surface resistance to frequency dependence, which it has been shown experimentally to do.
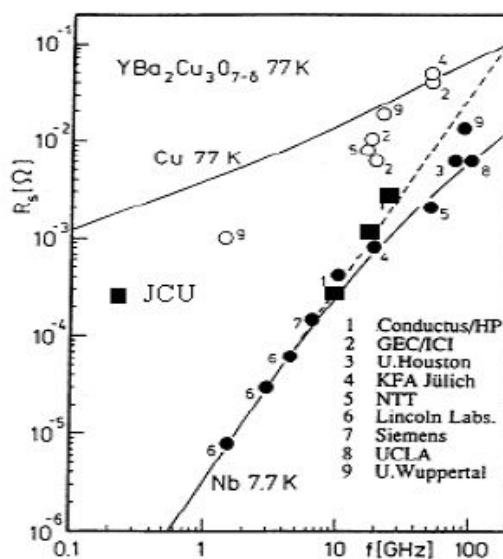
Figure 4.3. Surface Resistance as a Function of Frequency for YBCO Thin Films and Copper at 77K and Bulk Niobium (Nb) at 7.7K [10]

Another phenomenon which has a significant impact on the surface resistance of a HTS material is the nonlinearity of the material itself. This generates harmonics by the transfer of energy from the input signal which increase the surface resistance. Although this effect is present at currents smaller than the critical current it is much more significant above it (Figure 4.4).
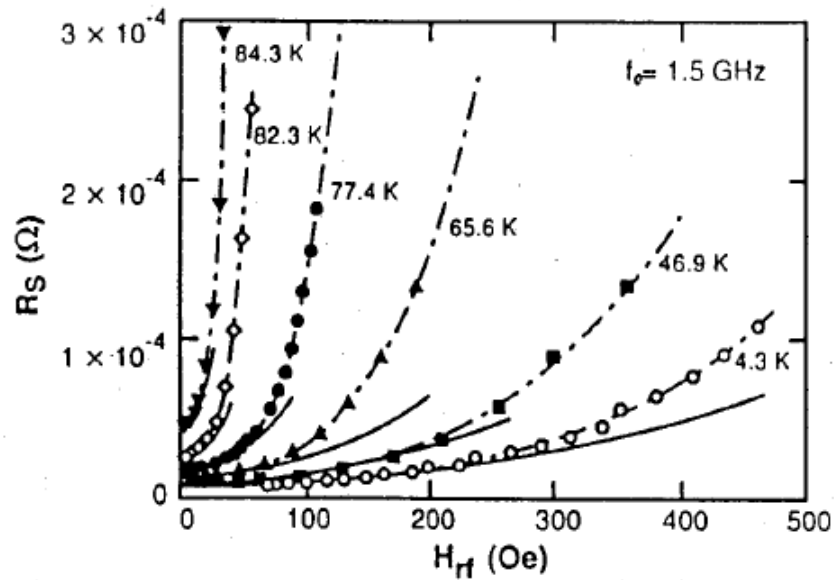
Figure 4.4. Rs vs Hrf at f0 = 1.5GHz on YBa2Cu3O7-x stripline resonator for different temperatures.

Another consequence of nonlinearity is the creation of intermodulation distortion (IMD). When a signal with two frequencies, f_1 and f_2, which are fairly close together, is applied to a nonlinear element, harmonics are created, of which the 3rd order harmonics at $2f_1 - f_2$ and $2f_2 - f_1$ are dominant and close to the fundamental frequency [67]. The effect of the IMD is dependent on input power as is shown in Figure 4.5; as the input power is increased the IMD increases in a roughly linearly way at the rate of 3:1 as it does for metals. The fundament frequency output power increases linearly at a rate of 1:1 with the input power and is eventually dominated at high powers by the IMD. The nonlinear effects deteriorate the performance of linear devices based on HTS technology including filters, particularly on the transmission side which requires high input power [68]. A detail discussion of nonlinear effects can be found in several publications, examples being [69], [70], [71], [72], [73] and [74].
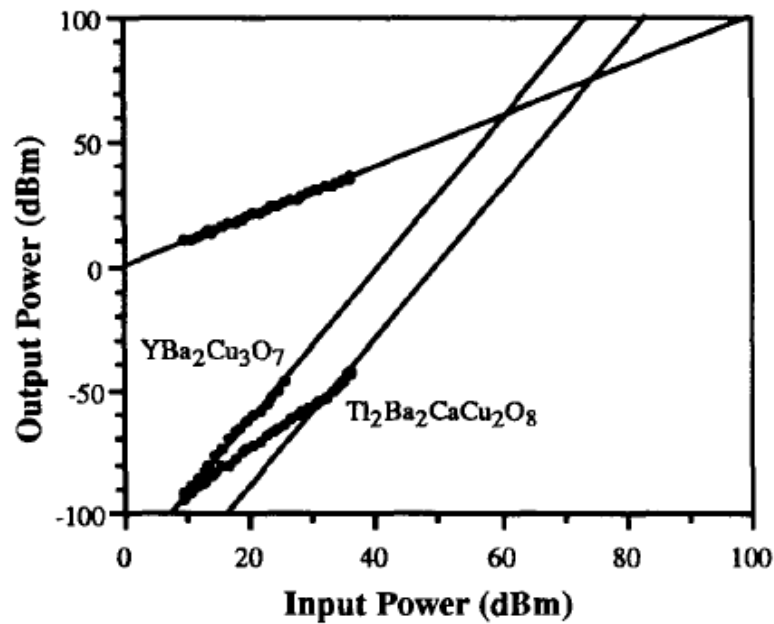
Figure 4.5. Comparison of Input Power versus Output Power at 1.3 GHz for a TI$_2$Ba$_2$CaCu$_2$O$_8$ Film at 80K and a YBa$_2$Cu$_3$O$_7$ Film at 70K [69]

None of the current superconductivity theories completely describe the electromagnetic properties of the "new" high T_c ceramic superconductors. Fortunately the important properties of these HTS materials are much the same as for low temperature superconductors and their very low surface resistance and the ability to cool them using inexpensive and readily available liquid nitrogen made them ideal for use in designing planar resonators and filters with very high Q factors. These filters combined with a low noise amplifier of high dynamic range create what is known as a Cryogenic Receiver Front End. The next chapter introduces the Cryogenic Receiver Front End, the potential advantages it holds over existing technology and the components which are necessary for its operation.

CHAPTER 5

CRYOGENIC RECEIVER FRONT ENDS FOR

WIRELESS BASE STATIONS

Even in the late 1980's, just after the discovery of HTS, the wireless telecommunications industry was exceptionally large and growing at a phenomenal rate. This prompted the formation of four major companies in the USA with the goal to bring HTS filters for wireless communications to the market. It was not until 1996 that the first system utilising HTS filters made it to the market place, it was named Reach^{TM} 1900 and built by Superconductor Core Technologies. Reach^{TM} 1900 was reported to show 6dB improvement in receiver sensitivity and increase cell coverage by approximately 80%. Other systems were rushed to the market not long after. Superconductor Technologies Inc. (STI) introduced SuperFilter^{TM}, Conductus built ClearSite® and Illinois Superconductor Corporation released Spectrum Master^{TM}. These systems were followed later by more advanced systems but despite the initial hype the market for HTS filters in wireless communications was stifled by high equipment costs and lack of clearly defined results, which resulted in the closure of all of the above companies except for STI.

Figure 5.1. STIs' SuperLink^{TM} Rx 850
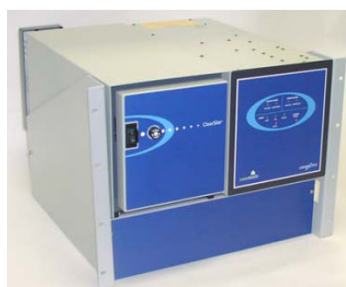
Figure 5.2. Conductus' ClearSite® 2300

Figure 5.3. ISCOs' OMNI

Today there are millions of cellular **b**ase **t**ransceiver **s**tations (BTS), approximately 5000 of which are said to contain superconducting or cooled elements between the antenna and the receiver electronics. The name given to these special elements by the industry is "Cryogenic Receiver Front End" (CRFE), a somewhat vague name in line with the secrecy that surrounds the hardware contained within the CRFE. Since High Temperature Superconducting materials found an application in wireless communication systems and predictions were made about the potential market worth being between US$280,000 and US$350,000 per base station over the lifetime of the installation [75], detailed information on CRFE designs stopped being published. Hence it became a matter of guessing rather than scientific proof as to the validity of the reported improvements resulting from the use of CRFE in existing BTS. Moreover it was not clear whether the improvements were due to superconducting technology or simply the improvements made in other components, such as cabling, low noise amplifiers or receiver electronics.

Widely varying reports on the quantitative improvements in performance of base station with CRFE installed had noise figures reduced by between 6dB and 2dB [75] and handset transmit power reduced by 2 to 7 times , which prevented reliable discussion on the true nature of the improvements HTS technology could offer.

This chapter contains a description of what a CRFE is and how it is retrofitted to conventional base stations. A detailed description of the CRFE developed by Cryoelectra and field tested at Wunongchang in China is given in the second part of this chapter. This CRFE formed the basis for building and testing of a more advanced CRFE (Chapter 7) in the scope of this thesis and answering the research question *if and under what circumstances high temperature RF-superconductivity can prove to be an important technological contribution to future wireless communication*.

5.1 BASE STATION RECEIVERS AND CRFES

A typical cellular base transceiver station may be considered as a cascade of three components; the antenna, the pre-selection filter and the base station electronics (Figure 5.4). A duplexer between the main antenna and base station electronics allows the main antenna to be used for both transmit and receive signals, while the diversity antenna is used for received signals only, as explained in Chapter 2.1.3. Pre-selection filtering (Chapter 3) is used to attenuate signals outside the channel bandwidth to protect the LNA in the base station electronics. The electronics are typically a separate piece of equipment from the antenna and pre-selection filter giving service providers the flexibility to determine their own setup based on the coverage and capacity requirements in a given region.
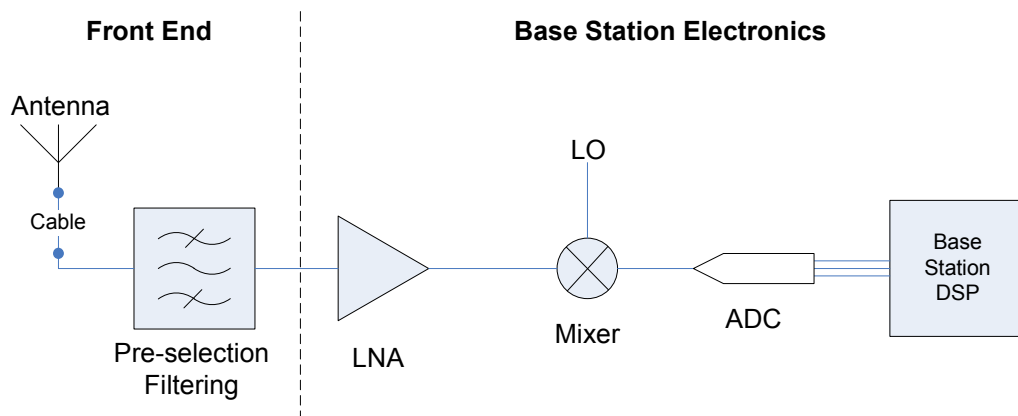
Figure 5.4. Schematic Diagram of the Receive Side of a Conventional Base Station

The base station electronics, which is available from manufacturers such as Xilinx, Ericsson and Toshiba, typically have the layout as shown in Figure 5.5. The electronics contain an amplifying section, followed by digital filtering, baseband processing and a network interface unit, all of which is controlled by a processor on the main control board [76-78].
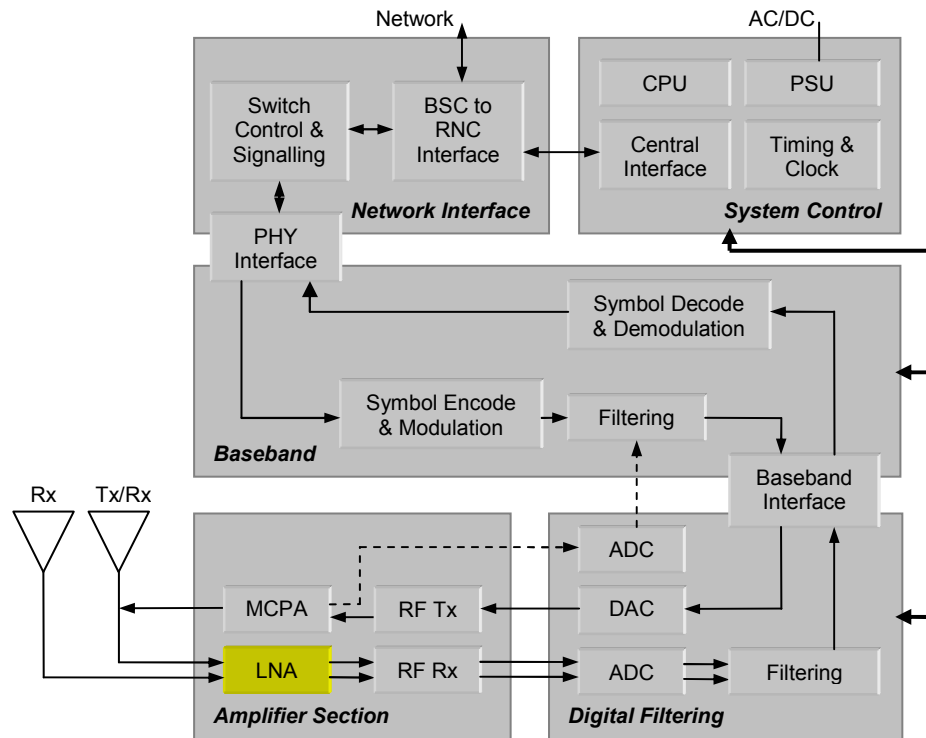
Figure 5.5. Simplified Base Station Block Diagram

The combination of a pre-selection filter and low noise amplifier is known as the "analogue front end", "system front end" or just "front end". The figure of merit for front ends is their Noise Figure. The Noise Figure of the front end comprises of the noise of the antenna, the cables, the pre-selection filter and the LNA. As mentioned in the Introduction, in order to provide high quality communications services and efficient use of the allocated bandwidth, cellular base stations require highly selective, low insertion loss, band pass filters in the front end of their receivers. When combined with a LNA of high dynamic range, this Filter-LNA combination (FLNA) can reduce the noise figure and the adjacent channel interference seen by the base station receiver, therefore increasing the signal-to-noise ratio (SNR). Due to the improved SNR, base stations can potentially improve their coverage, thus reducing areas with poor reception and black spots, and increase service capacity without requiring an increase in antenna height or the number of base stations [11-13]. The reduction of adjacent channel interference due to the highly selective filtering allows for more efficient spectrum usage, which in CDMA systems, where users are all allocated the same frequency segment, will increase the capacity. The popular GSM system, because it is based on a Time Division Multiple Access (TDMA) system (where users are allocated a time segment), will not benefit from the increase in capacity, except in the case where inter-modulation distortion is completely destroying channels.

High selectivity and very low insertion loss demand filters with extremely high Q-factors. Superconducting thin films deposited on low loss substrates can produce miniaturised planar filters with extremely high Q-factors suitable for wireless communications, which exceed the performance, in terms of Q and physical dimensions, of the relatively large conventional metallic cavities most commonly used today [79].

The draw back of the HTS filter technology is the necessity of cooling the superconducting thin films to below the critical temperature, T_c (89K for YBCO thin films). The cryogenic coolers used to achieve this task virtually remove any size advantage over metallic cavities; however the cooler does allows for the cooling of the LNA that immediately follows the HTS filter, which further reduces the system's Noise Figure. This combination of cryogenic cooler, HTS filter and LNA is commonly referred to a Cryogenic Receiver Front End (CRFE) or Cryogenic Front End (CFE) as shown in Figure 5.6.

Receiving antenna

-200°C

To receiver

Cable leading from the top of the mast to the input of the receiver front end

Cryogenic low noise amplifier
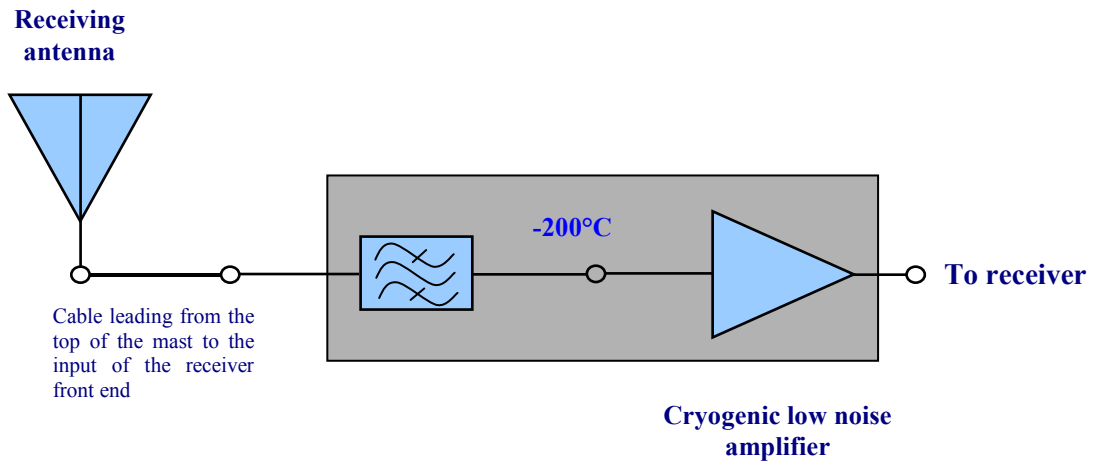
Figure 5.6. Block Diagram of the Cryogenic Receiver Front End (CRFE)

Currently CRFEs used in conventional base stations are "intruders". The CRFE are inserted between the antenna and electronic systems of the BTS and have not as yet been accepted by the companies supplying the network operators to replace the original pre-selection filter (Figure 5.4) and the LNA (marked in yellow in Figure 5.5). Additionally an attenuator is needed to reduce the gain of the signal from the CRFE LNA such that it does not saturate the amplifier in the conventional base station electronics. The result is that additional noise is introduced into the system from the redundant room temperature components and the attenuator, although it is cooled with the rest of the CRFE to minimise its noise figure. An "intruder" setup is shown in Figure 5.7. A bypass around the CRFE to the conventional filter is typically used in the case of a cooler failure causing the HTS filter to exceed its T_C and no longer be superconducting.
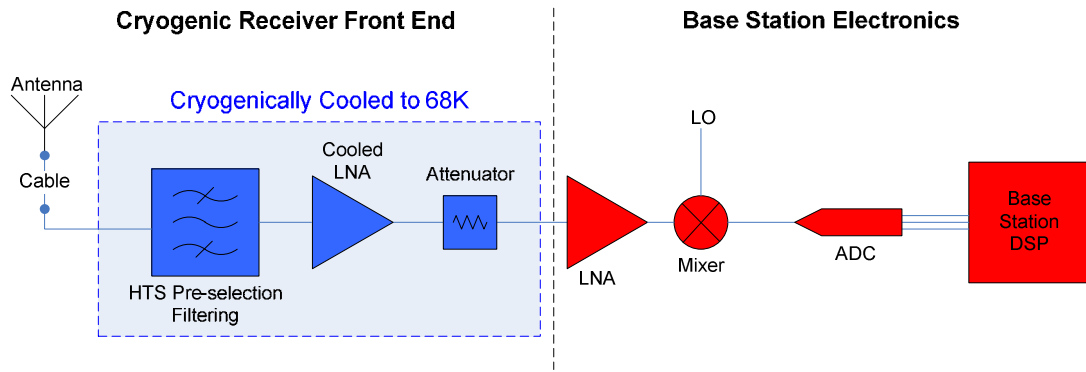
Figure 5.7. Schematic Diagram of CRFE in a Base Station - Blue objects are cooled under vacuum to 68K, Red objects are room temperature

The noise introduced by the redundant components does not significantly affect the overall performance of a base station fitted with a CRFE. This is due to the gain of the cooled LNA reducing the total Noise Figure of the receiver proven for the performance of the base station is characterised in terms of the effective noise factor of each of it components below. The noise figure of the HTS filter is dependent on the insertion loss $1/G_1$ (where $G_1 \leq 1$), and the operating temperature T relative to room temperature T_0 as shown in Equation (5.1) [12]:

$$F_1 = 1 + \frac{1 - G_1}{G_1}\left(\frac{T}{T_0}\right) \tag{5.1}$$

The total noise factor of the base station is given by the cascade formula [12]:

$$F_O = F_1 + \frac{F_2 - 1}{G_1} + \frac{F_3 - 1}{G_1 G_2} + \frac{F_4 - 1}{G_1 G_2 G_3} \tag{5.2}$$

where F_1 is the noise factor of the HTS filter, F_2 is the noise factor of the cooled LNA with a gain of G_2, F_3 is the noise factor of the cooled attenuator which protects the receiver electronics, G_3 is the gain of the attenuator and F_4 is the noise factor of the rest of the receive electronics, including the redundant pre-amplifier. Hence due to the gain of the cooled LNA the redundant components contribution to the overall system noise is limited.

The CRFE "intruder" system setup also generates a group delay from the increased steepness in the transition band of the filter. This delay, if beyond the threshold of the base station electronics, cannot be corrected and will therefore reduce the effective useful bandwidth of the receiver. In an integrated system it would be simple enough to modify the base station electronics to cope with the added delay, but in an "intruder" setup this is not possible. Fortunately due to the significant size of the guard bands in current cellular systems and the distance to any out-of-band interferer this problem is not usually significant.

5.2   CRFE DEMONSTRATOR 6 BY CRYOELECTRA

A collaboration between Cryoelectra GmbH and Tsinghua University resulted in the development of a CRFE referred to as Demonstrator D6. This system has been installed in Wunongchang base station in China's Tang Shan province in March of 2004 and tested. The successful test proved that it was possible to use HTS filters and LNA combinations in the front end of an existing base station to improve the quality of received signals but it alone didn't answer *if and under what circumstances high temperature RF-superconductivity can prove to be an important technological contribution to future wireless communication*.

The author of this thesis was given the opportunity to examine the D6 system and the test results. The opportunity extended to the development of an improved CRFE in order to verify the hypothesis of this PhD thesis. The next part of this chapter describes the author's understanding of the essential technical components of the cryogenic receiver front end used in the field test at Wunongchang learnt during the initial phase of this PhD work.

5.2.1   D6 SYSTEM OVERVIEW

The CRFE used in the field trials at Wunongchang base station in China (Chapter 5.3) dubbed "demonstrator D6" is a 3 RF channel ground based system. The basic components D6 are; the RF components, the supporting vacuum and cryogenic equipment, and the control systems as shown in Figure 5.8. The control systems are shown in black, vacuum equipment in purple, cryogenics in blue and RF in red. Dashed lines indicate items which were only required for setup and initialisation of the system.
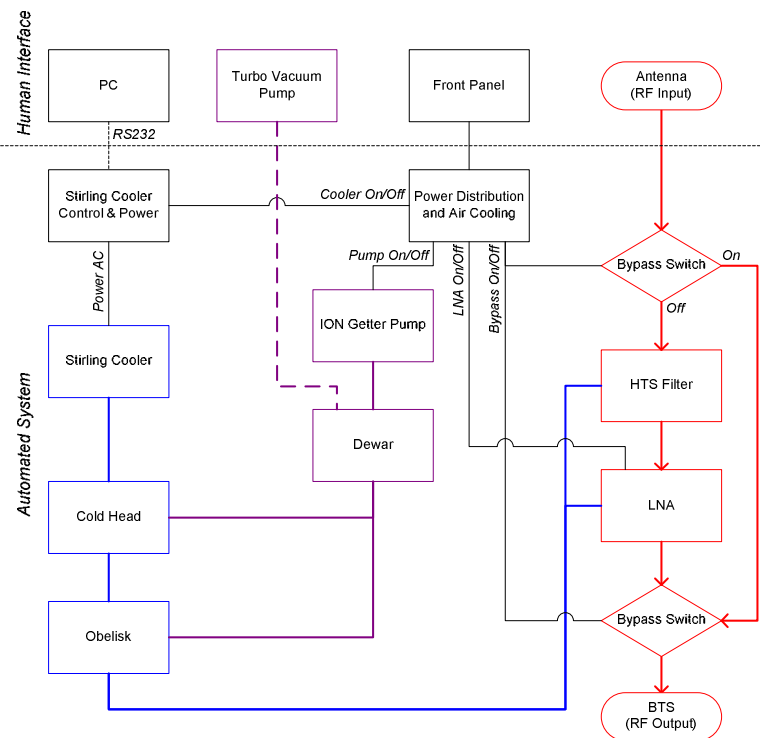
Figure 5.8. Block Diagram of Demonstrator D6 CRFE

The RF equipment is the most fundamental part of the CRFE and deals with the RF signals received by the base station, all the other components are used to support the operation. The Vacuum and Cryogenic equipment is used to maintain a suitable operating temperature for the HTS filter and LNA. The front panel and the power distribution board are used to control operation of the CRFE and a PC is used for the setup and monitoring of operational parameters for Stirling cooler. The concepts for the design of each of these components are described in the rest of this chapter. Observations have also been made about possible areas of improvement to this CRFE for future commercial products. The realisation of the improvements made by the author and the results are presented in Chapter 7.

5.2.2 THE HTS FILTER

The superconducting filter used in D6 (see Figure 5.9) was designed in at Tsinghua University, China. The design featured 16 half-wavelength meander line resonators. Every second resonator in the filter has been flipped along the vertical axis in order to reduce the coupling strength between adjacent resonators and cross couplings between non-adjacent resonators. These measures improved the quality of the manufactured filter and reduced the time required for tuning and trimming. The filter was etched using a YBCO film on a 0.435mm thick Sapphire substrate (of dielectric constant 9.95) manufactured by Theva.
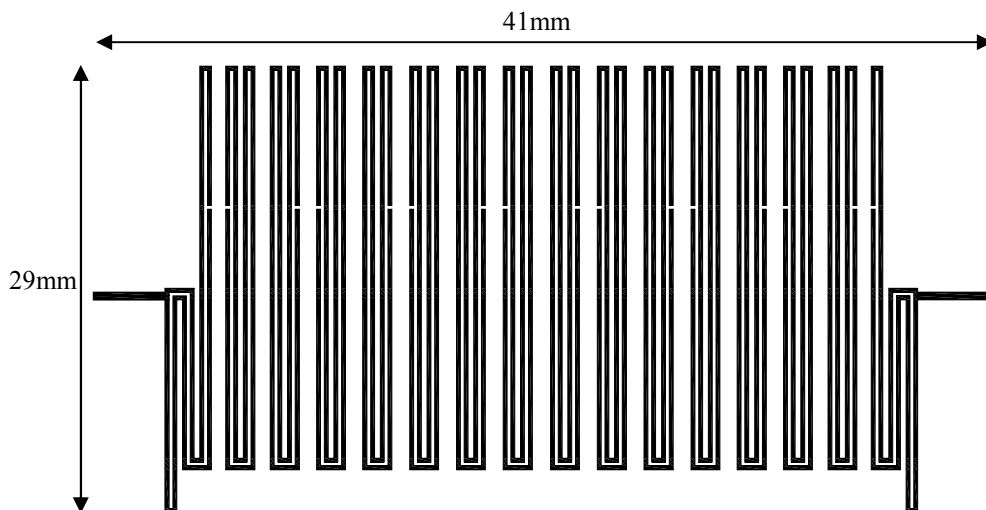
Figure 5.9. Tsinghua's 16 Pole HTS Filter Design

The filter had close to -20dB matching for the simulated response, which equated to 1% reflected power. Better matching means less reflected power, therefore less losses due to the filters presence and a higher percentage of the incoming power being transmitted, a very important factor for the sensitivity of the front end. Typically the simulated response should be at least 3dB better matched than the required matching in the manufactured filter due to inaccuracies in the manufacturing process. In HTS filters it is typical for the manufactured filter to have 5dB worse than the simulation, therefore an acceptable manufactured filter should have minimally -15dB matching. This is approximately the same as for STI's manufactured HTS filters of VSWR of 1.5:1 or -14dB matching [80]. -15dB matching was achieved for this filter design when manufactured and Q-factors of over 70000 were typical.

The HTS filter was packaged inside an aluminium box, as is common for RF electronics, in order to perform correctly. Typically the filter chip is glued to a carrier of equal thermal expansion coefficient and attached to the housing using conductive two part glue which requires pressure and heating in order to make a good permanent contact. An equal or very similar thermal expansion coefficient for the carrier is vital so that the filter does not become detached in the process of cooling the filter to cryogenic temperatures due to different rates of expansion. SMA connectors were inserted into the box at each end bonding wire is ultrasonically bonded (Figure 5.10 & Figure 5.11) between the SMA pin and the gold contacts left on the surface of the HTS filter. Silver loaded two component epoxy adhesive was used to strengthen the bonds at each port. The lid of the housing was then bolted shut using 6 bolts. A small hole was left in the lid of the housing (Figure 5.12) to allow air to be evacuated when then system is put under vacuum. Without this hole air would slowly escape from the inside of the box and spoil the vacuum over the operational life of the system.
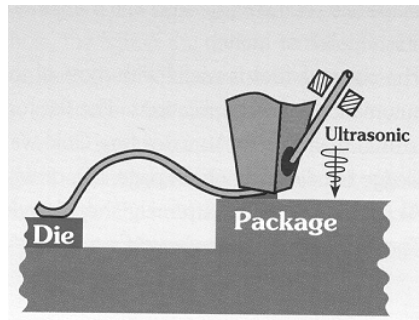
Figure 5.10. Schematic of the Principle of Ultrasonic Wedge Bonding used to Bond the Filter Ports to SMA Connectors
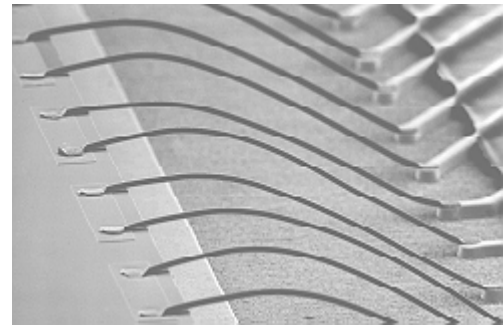
Figure 5.11. Example of Ultrasonic Wedge Bonding (Picture is not of the Filter Bonds)

Figure 5.12. Filter Housing with Small Air Hole in the Top Left Hand Corner

Dielectric tuning screws were used to tune (shift in frequency) and trim (obtain good matching in the passband) the filters frequency response. These screws were placed in the roof of the housing above the ends of the resonators (Figure 5.14). In this way they affect the electric field (or capacitive coupling), which is a maximum at the end of the resonators, therefore allowing the designer to fine tune the filter's response.

Because the HTS filter only becomes conductive and transmits a filtered signal at cryogenic temperatures, the tuning/trimming process must take place at this temperature. In order to do this a special Dewar with

tuning rods (Figure 5.13) was used to cool the filter to the 68K operating temperature. Using an HP8720C network analyser to see the filter characteristic an operator trimmed the filters response to achieve the desired -15dB matching across the passband by adjusting each individual tuning screw. Before these measurements took place however the network analyser was calibrated using a full two port calibration at room temperature. The test cables inside the Dewar were not calibrated out, as they were similar in length to the stainless steel cables forming part of D6 (described in Chapter 5.2.4).
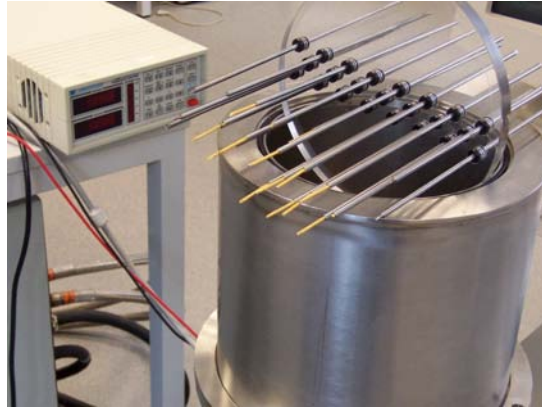
Figure 5.13. Tuning Dewar

Because the HTS filter was coupled with a LNA (Figure 5.14), the tuning and trimming of the filter took place while connected to the LNA in order to account for any mismatch between these components. The entire process was very time consuming for the filter LNA combinations used in D6 taking five to eight hours to complete. The measured frequency responses for the 3 filter-LNA combinations tested Wunongchang in D6 are shown in Figure 5.15.
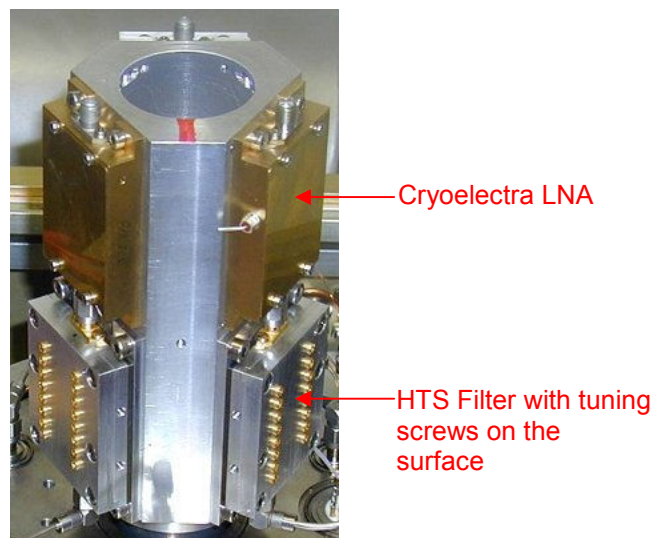
Figure 5.14. D6's 3Channel Obelisk with Filter-LNA Combinations Mounted

Channel 0

Channel 1

Channel R
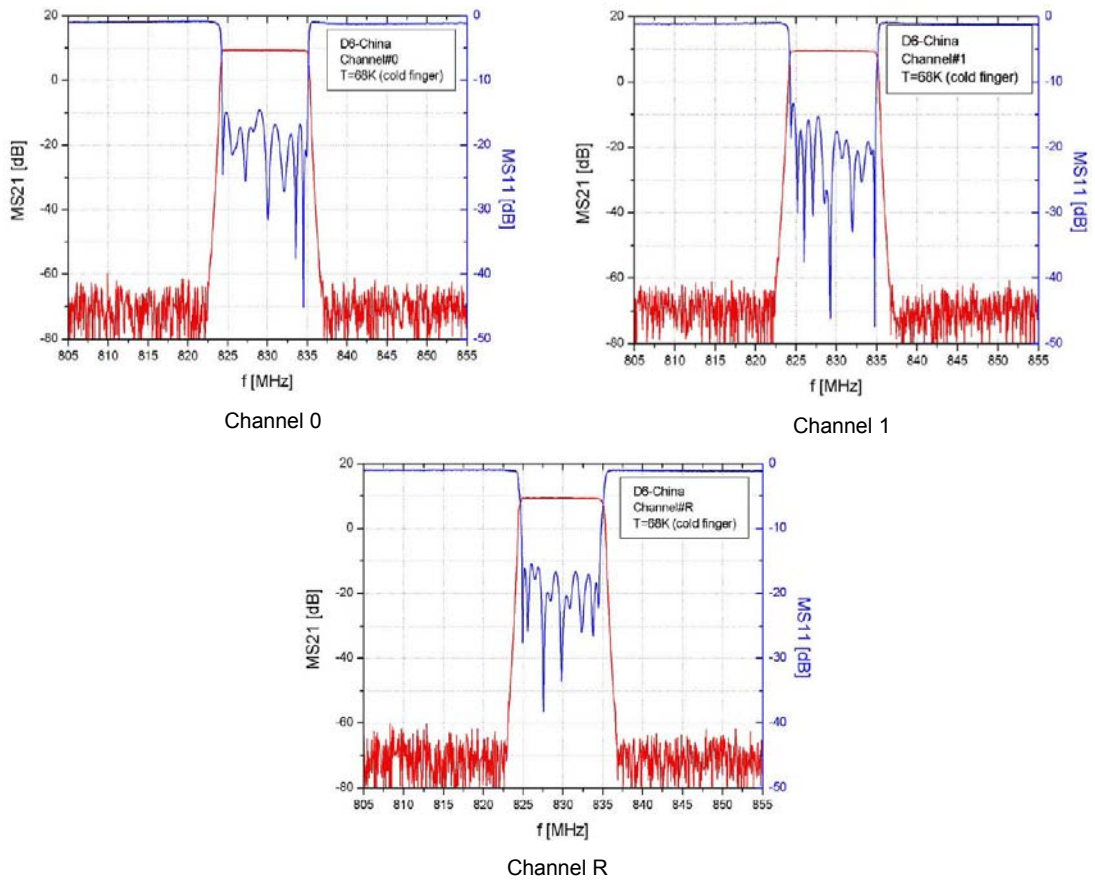
Figure 5.15. Frequency Responses for 3 Filter-LNA Combinations in D6

5.2.3 A LINEAR LOW NOISE AMPLIFIER FOR WIRELESS COMMS.

As mentioned earlier the CRFE consist of a Filter-LNA (FLNA) combination. An amplifier is used to increase the amplitude of the RF signals received at the antenna, thereby improving the SNR and dynamic range of the system. This is necessary as high frequency cellular radio signals (800MHz – 950MHz or 1900 – 2100MHz) are mixed with a local oscillator to obtain the intermediate frequency [8] and mixers generally introduce a relatively high level of noise. Therefore it is important that the received RF signal has minimal attenuation from the filtering process (Chapter 5.2.2) and is amplified such that the noise introduced by the mixer and other electronic elements is not significant enough to inhibit the decoding of the signal.

In order to improve the range and quality of communications a receiver must respond to signals between the minimum detectable signal (*MDS*) and the maximum acceptable signal (*MAS*) that still causes acceptable levels of inter-modulation (IM) distortion. The dynamic range of the system is given by the difference in power between the *MDS* and the *MAS* which could be as large as 120dB. The *MDS* is given by,

$$MDS \text{ [dBm]} = -174 + 10\log BW + NF$$

where *NF* is the noise figure of the system, -174 dBm is the thermal noise power per Hz at 290K (room temperature of the antenna) and *BW* is the bandwidth of the system. In practice Linear Dynamic Range (LDR) and more commonly Spurious Free Dynamic Range (SFDR) are used to describe a LNA. The LDR is defined as a distance (in dB) between the MDS and IP1. The spurious free dynamic range (SFDR) can be approximated as a distance (in dB) between MDS and the Pin at which the amplifier generates OIP = MDS.

These parameters, bandwidth (determined by the preselection filter), gain (given by the LNA), dynamic range (primarily determined by the LNA) and the noise figure (determined primarily by the LNA and the preselection filter) fully characterise the Cryogenic Front End.

The LNA designed by Cryoelectra and manufactured for the Demonstrator D6 CRFE used a Gallium Arsenide pseudomorphic high electron mobility transistor and dual matching networks decoupled and re-coupled by two 3dB 90° hybrid couplers [81]. The Cryoelectra LNA was packaged in a brass housing weighing 151g and is shown in Figure 5.16.
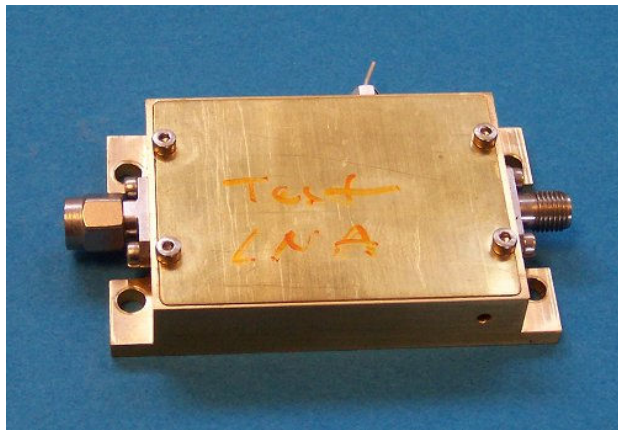
Figure 5.16. Cryoelectra LNA in Brass Housing

The Cryoelectra LNA exhibited a gain of 15.2dB and a noise figure of 0.8dB at ambient temperature with a supply voltage of 5V. Figure 5.17 shows the measured power output P_{out} of the amplifier as a function of the input power at ambient temperature. P1, the point where the amplifiers response varies by 1dB from the ideal linear response, is reached when the input power IP1 = 6.4dBm and the output power OP1 = 20.4dBm. The OIP3 was measured to be +35 dBm at Pin, which approximately corresponds to the upper edge of the SFDR [82]. The full specifications of the LNA are given in Table 5.1.
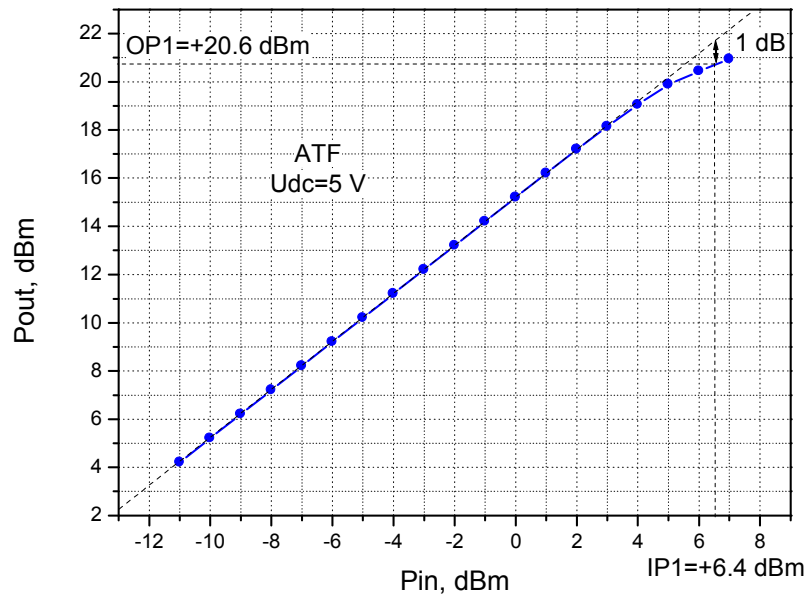
Figure 5.17. Experimental OP1 Measurements of the Cryoelectra LNA at $U_{dc} = 5V$

Table 5.1. Cryoelectra LNA specification

RF Frequency Range, MHz	1900 to 2000
Gain, dB	14 to 16
Gain Variation, dB	± 0.5 (max)
Noise Figure @ 290 K, dB	0.9 (max)
Noise Figure @ 77 K, dB	0.2 (max)
VSWR, Input	1.28:1
VSWR, Output	1.28:1
Impedance, Ω	50
DC Voltage, V @ DC Current, mA	5 @ 120
Output IP3, dBm	+35
Operating Temperature, K	50 to 300
Connectors	SMA

A comparison between the Cryoelectra LNA with a commercial MITEQ LNA done in 2004 indicated the superior dynamic range of the Cryoelectra LNA. The MITEQ LNA was characterised at ambient temperature by an operating voltage of 3V, a gain of 16.2dB and a noise figure of 0.8dB. Figure 5.18 shows the P_{out} against the P_{in} characteristic of the MITEQ LNA at ambient temperature at an operating voltage of 3V. The OIP3 was measured to be +22.7 dBm at Pin, which approximately corresponds to the upper edge of the SFDR. The IP1 = -3dBm and the OP1 = 12.1dBm [82].
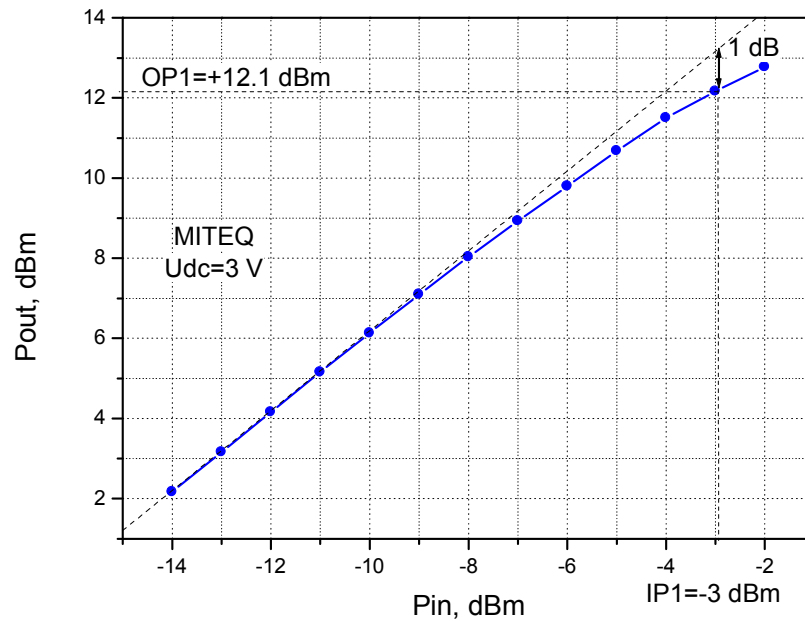
Figure 5.18. OP1-Measurement of a MITEQ LNA

Comparing both LNAs at U_{dc}= +3.5V the OP1 of the Cryoelectra LNA was measured to be +20.6dBm compared to +12.1 dBm of the MITEQ LNA (Figure 5.19). The OIP3 of the Cryoelectra LNA was measured to be +35dBm compared to +22.7dBm of the MITEQ LNA. This results in the spurious free dynamic range (SFDR) of the Cryoelectra LNA being,

$$SFDR = OIP3 - MDS$$

$$= +35dBm - (-174 + 10 \log(2\pi \times 100MHz) + 30.8)dBm$$

$$= 35dBm - (-55.22)dBm$$

$$= 90.22dBm$$

and the SFDR of the MITEQ LNA being SFDR = 22.7dBm – (-55.22)dBm = 77.92dBm.

The Cryoelectra LNA had a sharper transition from the linear to the nonlinear behaviour, suggesting a bigger distance (in dB) between the P1 and IP3 points. For the Cryoelectra LNA the linear range was, OIP3 – OP1 = 35dBm – 20.6dBm = 14.4dB while for the MITEQ LNA the linear range was 10.6dB, 3.8dB worse than for the Cryoelectra amplifier.
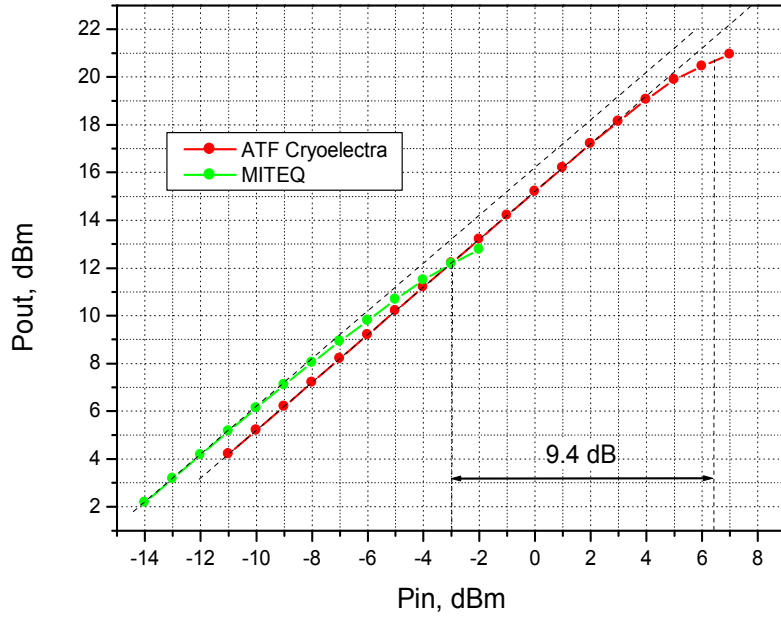
Figure 5.19. Measured Characteristic of OP1 at 3.5V

At the temperature of 50K, both LNAs exhibited an increase in the linear range by about 1.5dB as compared to room temperature and at the same time a decrease in the IP1 values by about 1.5 – 2dB. The main result of the operation of both LNAs at cryogenic temperatures was that their noise figure was reduced to less than 0.2dB compared to 0.8dB at room temperature. This led to an equal improvement in the sensitivity (*MDS*) of both LNAs.

5.2.4 SUPPORTING EQUIPMENT

In order to obtain and maintain the required 68K operating temperature for the filter and LNA specialised cooling, vacuum and electronic control and monitoring equipment is required. Additionally Filter-LNA mounting, signal feed though and bypass circuitry all needed consideration.

5.2.4.1 COOLING

In order to reduce the temperature of HTS filters to below the critical temperature (T_c) of the superconducting material a cryocooler is used. The cooler chosen for the developed CRFE is known as a Stirling Cooler. This cooler can achieve the desired 68K operating temperature with only air cooling of the heat sinks at hot end of the heat transfer at an experimentally calculated cooling efficiency of close to 3%. The efficiency was determined by operating the cooler at the intended operating temperature and measuring the operating power $P_{c(\text{initial})}$. Introducing a heat source of known input power to the system increased the operating power of the cooler to $P_{c(\text{final})}$. The efficiency of the cooler was given by the input power divided by the change in operating power (Equation (5.3)). Improving the cooling of the hot end of the heat transfer increases the efficiency of the cooler.

$$Efficiency = \frac{P_{INPUT}}{\Delta P_c} \tag{5.3}$$

Minimising heat transfer mechanisms to the system led to a reduction in the operating power of the cooler required to maintain a temperature below the T_c of the filters. In a normal system heat transfer via convection though liquids or gases may account for 60% to 70% of the total heat transferred. In the cryogenic receiver front end, because the cold components are operated in a vacuum, these mechanisms are minimised [83-85]. Conduction through solids is limited to the cold head and the stainless steel RF cables at the inputs and outputs which connect to feed throughs on the base and lid of the Dewar. The remaining heat is transferred via infrared radiation. Figure 5.20 is a cross-sectional view of the vacuum chamber and depicts the source of the radiation. The outside walls of the vacuum chamber are at temperature T_1, 300K. The cold parts of the assembly (outlined in blue) are at temperature T_0 which was set to approximately 68K.
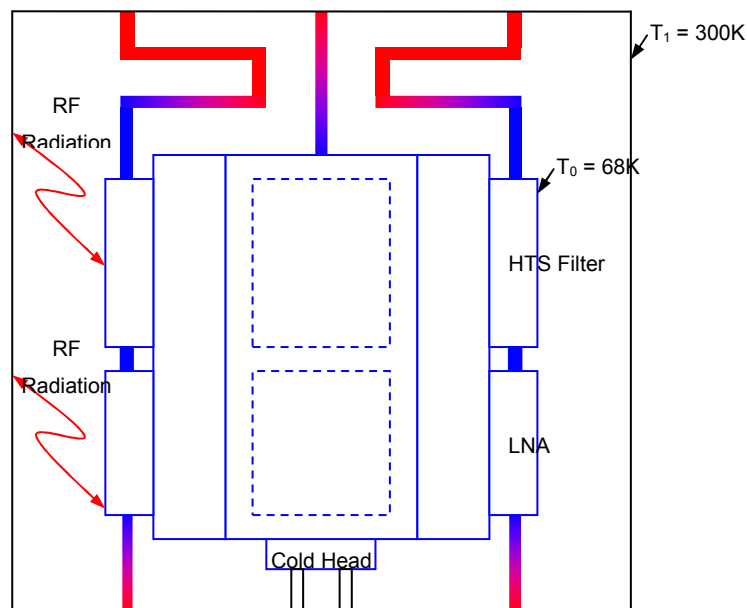
Figure 5.20 - Cross-Sectional View of the Interior of the Vacuum Chamber or Dewar

Semi-rigid Stainless Steel RF cables are connected to the input and output feed throughs in the Dewar to allow the signal to pass from the antenna along the cable through the walls of the Dewar to the filter-LNA combination and the out through the Dewar wall again and onto the receiver electronics. The side effect of these RF cables is that because they are touching the outside world, which is at 300K, they transfer heat to the cold parts, which are at 68K, thus increasing the cooler power required to maintain the operating temperature of the HTS filters. These cables are necessary so eliminating the heat input completely is impossible, but it can be minimised. The input cables must be relatively short in order to minimise the noise introduced before the signal is filtered and amplified, which is important for the sensitivity of the front end. The output cables can and should be long (Figure 5.22). After the signal is filtered and amplified the small amount of additional noise from the cable does not make a significant difference to the SNR.

To maximise the usefulness of the CRFE and offset the cost of the support equipment for the HTS filters, three filter-LNA combinations were mounted to an obelisk (Figure 5.21) on the cold head (Figure 5.22). This allowed for three channels, typically the main antenna from each sector, to be serviced by the one CRFE.
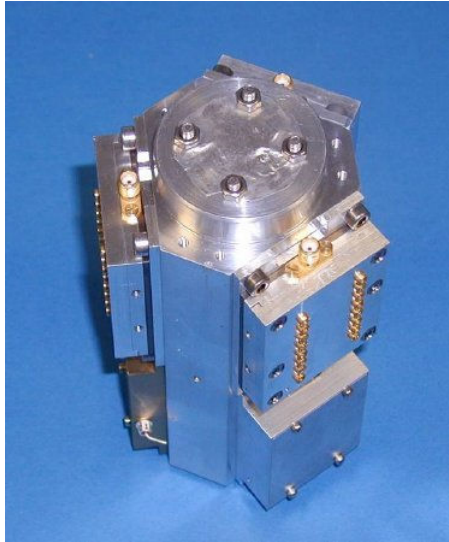
Figure 5.21. Bottom of 3 Channel Obelisk
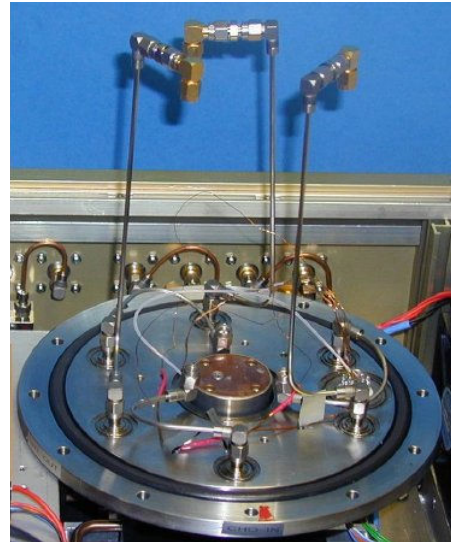
Figure 5.22. Open Dewar of D6 with RF Cables Connected to SMA Feed Throughs

5.2.4.2   VACUUM

In order to evacuate the gases a Turbo Molecular Vacuum Pump (TVP) (Figure 5.23) was used to obtain a vacuum of better than 10^{-6} mbar when the system is cold. By evacuating all the air from the Dewar two heat mechanisms, conduction via gases and convection no longer played a significant role in transferring heat from the outside to the cooled filter-LNA combinations.

Figure 5.23. Demonstrator D6 (left) Connected to a TVP (right) at Cryoelectra's Lab

Unfortunately over time, the well known phenomena of hydrogen escaping from the surface of the Dewar into the vacuum slowly spoiled the vacuum. Heat treating the surface of the Dewar causes the trapped molecules (typically water) to be excited and break free of their bonds to the metal surface. The freed electrons are then pumped free of the chamber using the TVP. This minimises the expulsion of gases from its surface of the Dewar but does not completely remove the problem. Hydrogen is still absorbed by the metal on the outside of the Dewar and passed through to the vacuum within. As such vacuum maintenance is an important part of the support system for cryogenics.

Using the TVP to maintain the vacuum was not an elegant solution and made the completed product larger (Figure 5.23). Smaller vacuum maintenance pumps, such as an ION getter pump (Figure 5.24), were better suited to the task. In high-vacuum conditions a surface can hold large quantities of gases compared to the amount of gas present in the space. Using a surface to capture gas this produces a pumping action either by physisorption or gettering, which refers to a chemical combination between the surface and the pumped gas [86]. To produce the pumping action the getter surface needs to be continually refreshed as it absorbs gases. By heating a new film can be deposited on the getter surface by evaporation or sublimation. The fresh surface then can capture surrounding gas molecules that strike the surface. The pump used with D6 has a pumping speed of 2 litres per second. It was connected with a specially designed high voltage power cord to the high voltage power supply inside of the chassis of CFE6. The ground connection of this cord was fixed with a screw at the magnet of the ion getter pump (Figure 5.25). The high voltage power supple required a 12V DC input and draws up to 1.5A.

Figure 5.24. ION Getter Pump

Figure 5.25. ION Getter Pump Connected to High Voltage Power Supply

Figure 5.26. High Voltage Power Supply for ION Getter Pump

5.2.4.3   ELECTRONICS

The supporting electronics for the front end was responsible for the control and monitoring of the cryocooler, system temperature monitoring, LNA control and bypass control as well as for power regulation and distribution. The power regulation and distribution board is shown in Figure 5.27 and the schematic in Figure 5.28. The board took a 48V DC supply and Traco Power regulators provided power to all of the components as described in Table 5.2.

Figure 5.27. D6 Prototype Power Regulation and Distribution Board
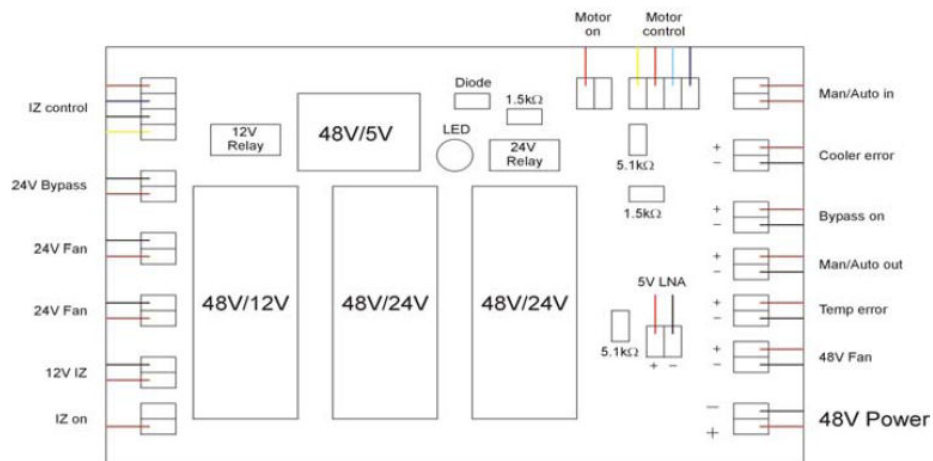
Figure 5.28. Schematic of D6 Prototype Power Regulation and Distribution Board

Table 5.2. Voltage Supplies and Connections for the Power Regulation and Distribution Board

Voltage	Max. Current	To Component
5 VDC	1000 mA	LNAs
12 VDC	1250 mA	High voltage power supply Control of the RF-Bypass
24 VDC	415 mA	RF-Bypass switches Chassis fans
48 VDC	Supply Dependent	Cyrocooler

The bypass control, for switching the RF signal to bypass the HTS filter and cooled LNA, was automatic when the system was operating and used the 12V and 24V relay on the power regulation and distribution board to switch the bypass on or off. Spinner BN 25 96 80 Low Loss RF Coaxial Relays were used to switch the signal between the bypass and the HTS filters. The RF relay was set to bypass mode when at 0V. This active low setup ensured that in the case of a power failure, which means the cryocooler was no longer cooling the HTS filters causing them to become resistive, the bypass would be active. The bypass could be manually switched using the three way switch on the front of the CRFE (Figure 5.29). Position 0 was off, I was manual on, II was automatic.

Figure 5.29. D6 Front Panel

The cryocooler in the D6 system was a Laybold Stirling cooler controlled using the Polar Drive C, which was a DC-AC inverter and controller (Figure 5.30). The Polar Drive C took a 48V DC input, 5 basic motor control signals and a PT100 input for temperature measurement of the cold head. It outputs a variable voltage AC signal for controlling the cryocooler's motor. The Polar Drive C was programmed using Laybold's Polarware (Figure 5.31) running on a control PC connected to the Polar Diver C via an RS232 cable. Polarware allowed the setting of the operating temperature at the cold head as well as several advanced settings for the cryocooler motor. The Polarware software was also used for data logging of the temperature and motor power.
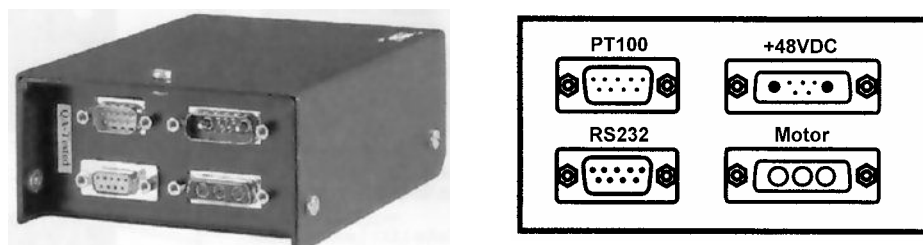
Figure 5.30. Polar Drive C (left) and Schematic of Inputs and Outputs (right)
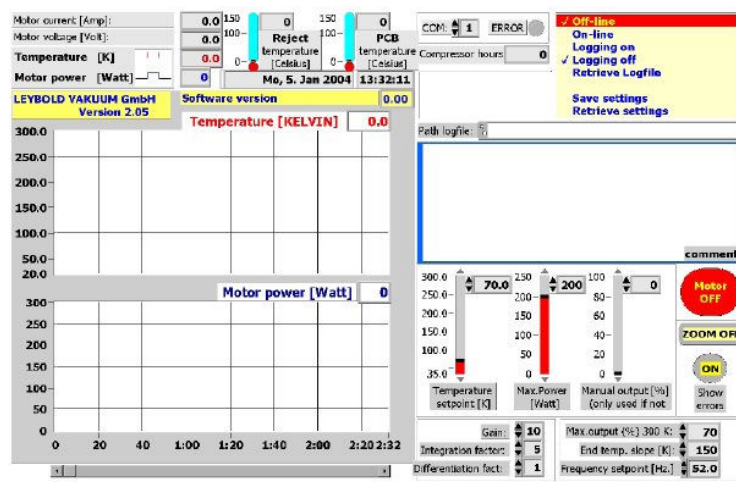
Figure 5.31. Polarware – Software to Control Cryocooler

Pictures of the CRFE D6 as a finish product are shown below. This system was sent to China for the first base station field test in March of 2004.

Figure 5.32. D6 Front View of Chassis
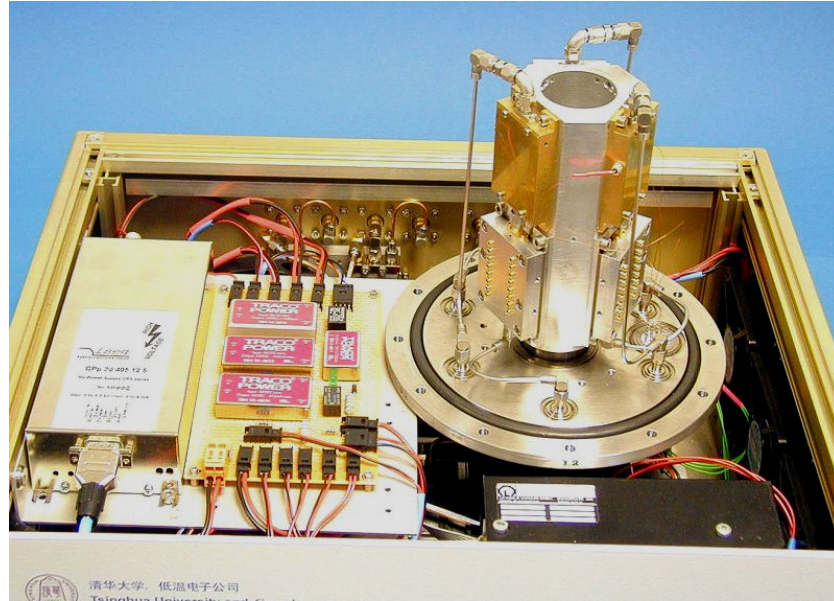
Figure 5.33. D6 Open Chassis and Open Dewar

5.3　THE WUNONGCHANG FIELD TRIAL

The field trials of the first CRFE developed by Cryoelectra and Tsinghua University were designed to study the effects of using HTS filters and cooled LNAs as front end components in existing cellular base transceiver stations. The results were expected to show a significant improvement in coverage and capacity of cellular CDMA system based upon the improved sensitivity and selectivity of the front end, and the results obtained in simulations using the CDMA Uplink Model.

The measured S_{21} response of the conventional metallic cavity filter-LNA combination resident in the Unicom base station towers is shown below in Figure 5.34. The useful channel bandwidth is between 825MHz and 837.5MHz but this cavity filter does not attenuate signals near the band edge to any significant degree. Therefore interference from adjacent CDMA channels is expected cause IM products which deteriorate the performance of the base station.

联通CDMA基站常规接收滤波器频率响应（MHz）
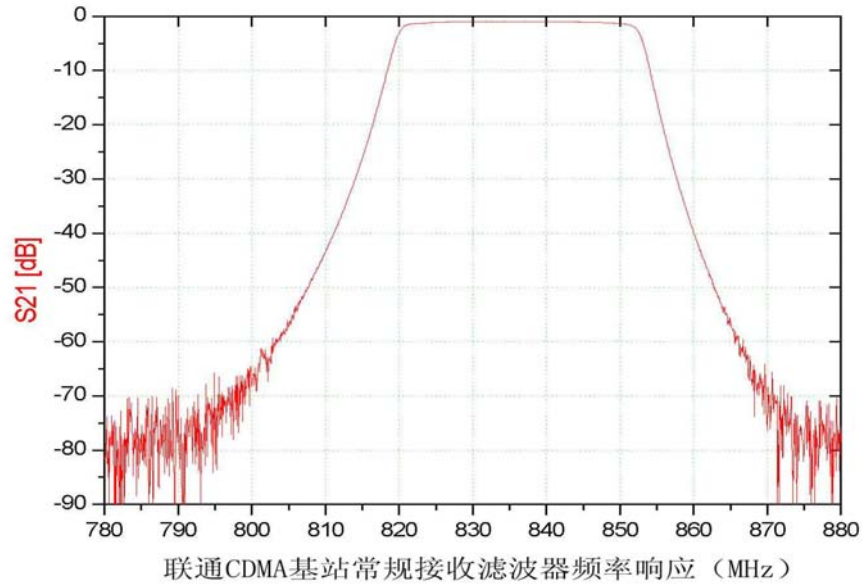
Figure 5.34. China Unicom CDMA Base Transceiver Station Measured Metallic Filter Response

Figure 5.35 shows the measured responses of the 16 pole HTS filter-LNA combination (black) used in the CRFE and the conventional cavity filter-LNA combination (red) of similar characteristic to the China Unicom pre-selection filter. The greatly improved selectivity and out-of-band attenuation offered by the HTS filter over its conventional metallic counterpart is visible in the graph. A reduction in out-of-band interference is expected to improve in the coverage and/or capacity of the BTS. The extent of the improvement is determined by the level of the interference affecting the base station.
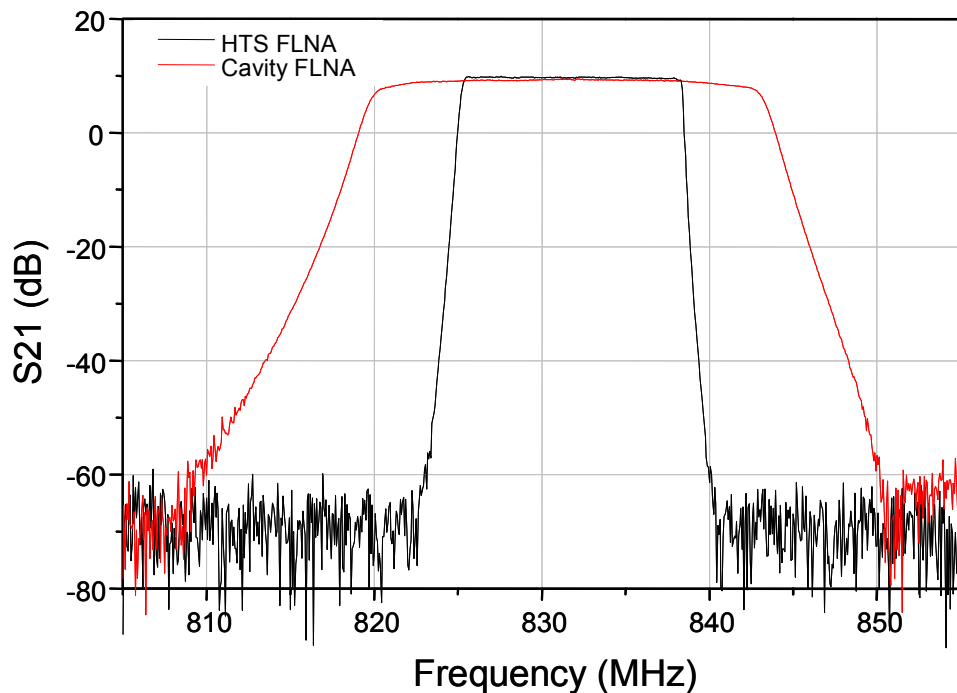
Figure 5.35. Measure S21 of the HTS Filter and Metallic Filter of the same Operational Bandwidth

As mentioned earlier the first field test of the Cryoelectra D6 Front End was conducted in March of 2004 at Wunongchang CDMA base station and the results were made available in July of the same year. The test conducted was a "drive test", in which the transmit power of the mobile station required for an active uplink to the base station was measured as the mobile station was moved along a predetermined route at a constant speed (25-30km/h). Measurements were performed before and after the addition of the CRFE on similar days at the same times to eliminate the effects from capacity loading. Details of the testing procedure used and the results of the tests are given in Appendix A.

The performance tests showed that the addition of the CRFE to Wuningchang base station reduced the average transmit power from 1.305dB to -1.809dB, which equated to a 3.114dB improvement in the sensitivity of the receiver and suggested an increase in coverage of over 105%. Alternatively the capacity of the CDMA system could be increased while maintaining the current coverage. In fact China Unicom continues to use the CRFE in their base station today accumulating over 2.5 years of continual usage proving both the performance and the reliability of this system.

Figure 5.36 - Wunongchang base station in China

Figure 5.37 - D6 operational in Wunongchang base station

The purpose of this field trial of CRFE Demonstrator D6 was to test if the CRFE and its components would survive transport to China from Germany, be operable by people other than the designers and if these succeeded then to obtain test results. All the components survived the journey and were able to be reassembled with the help of the provided user manual. The user manual allowed for the successful setup and running of the system for the field trials which yielded a 3.114dB or approximately 2 times reduction in the handset transmit power.

China Unicom requested that the system stay in the Wunongchang base station after the field trials were completed meaning that from a technical perspective the technology was attractive to network operators. This request also allowed a prolonged reliability test of the system, which has now been in use since March 2004. In conclusion this field trail showed that HTS enabled front end technology could be employed in the field reliably and provide significant performance advantages over the existing technology.

CHAPTER 6

CDMA UPLINK MODEL

Service providers and base station manufacturers who wish to evaluate HTS technology in terms of system capacity, coverage and quality of service do not have tools to perform this task. Simplified single and multiple base station models with arbitrary numbers of users described in [8] and [23] do not take into account receiver nonlinearities, which result in inter-modulation (IM) distortions in the passband in the presence of close out-of-band interferers. Models presented in [12] and [87] have been developed to examine a specific case and are not suitable for a general analysis of cellular system performance of under differing conditions of noise, interference and hardware configurations. Hence a model has been developed in the course of this work, referred to as the CDMA Uplink Model, to examine possible advantages of CRFE technology in cellular CDMA base stations. The CDMA model may be easily expanded to be used for GSM and UMTS services. Rather than using the general propagation loss model the author of this thesis has used in the CDMA uplink model, a more detailed propagation loss model could also be used to fully evaluate specific areas of interest more closely and include multi-path propagation of signals.

The CDMA Uplink Model has been created to better evaluate the performance of CDMA base stations with a cryogenic receiver front end. The model caters for different environmental noise, interference, positioning and hardware conditions and was deliberately created to analyse the field tests results returned from demonstrator D6 and the advanced CRFE.

6.1 CDMA UPLINK MODEL DEVELOPMENT

In developing the CDMA Uplink Model the following assumptions were made in respect to the CDMA wireless systems to ensure the model was applicable to most CDMA systems:

1. A CDMA network consists of many mobile subscribers who communicate with base stations serving as gateways to connect calls to the public phone system.
2. In a multiple cell system the power of a mobile unit is determined by a base station the unit connects to. A choice of a station by the mobile unit is not dependent on the distance between a caller and a base station but rather on the maximum pilot power of the base stations from which the subscriber receives signals.
3. The capacity limiting factor of CDMA networks is the uplink, namely the total interference (i.e. same cell interference, other cell interference and interference from non-CDMA sources).
4. All components that can be used to optimize coverage capacity performance (including antenna beam widths and orientations), other than Front End components, are assumed to be static unless stated otherwise.

5. Factors affecting voice quality include interference from adjacent cells and nonlinearities in the receiver system. The signal strength at the receiver depends on the path losses to the base station of interest and is inversely proportional to the interference from other users [12, 23]. Furthermore nonlinearities of the receiver components, such as LNAs, duplexers, mixers etc. induce IM products at their output. Because only the LNA and not the duplexers, mixers etc. is replaced by the CRFE, only its IIP3 point is variable and the others are all assumed to be constant, meaning that the system IIP3 is dependent on the LNA. The third order IM products, which are located at frequencies $2f_1 - f_2$ and $2f_2 - f_1$ are the strongest and closest to the user band, (where f_1 is the receiver frequency and f_2 is the frequency of the out-of-band interferer) [23, 88].

Initially in this thesis a single base station operating on its own with an arbitrary number of users was considered with sectors being under the influence of background noise and discontinuous transmission. The CDMA uplink model was then expanded to include a multiple base stations, out-of-cell interference, inter-modulation distortion and propagation loss for various environmental conditions.

6.1.1   THE SINGLE BASE STATION CDMA UPLINK MODEL

Each subscriber in a CDMA network making a call occupies the entire allocated spectrum using a spread spectrum waveform. There are many specifications of CDMA but the specifics of the spread spectrum and modulation techniques have little bearing on the developed model. In a single cell with adaptive power control (see Chapter 2.2.2), the uplink signal received at the base station from each mobile unit is of the same amplitude, S. If there are N users within the cell, the base station must demodulate the desired signal of amplitude S from a composite waveform leaving $(N-1)$ interfering signals also of amplitude S. Hence the signal to noise ratio in this case is [23],

$$SNR = \frac{S}{(N-1)S} = \frac{1}{N-1} \qquad (6.1)$$

The bit energy-to-noise plus interference ratio,

$$E_b/(N_0 + I_0) \qquad (6.2)$$

is the important parameter to determine whether the uplink successfully sends voice or data to the base station. E_b is the received bit energy, N_0 and I_0 is the received noise and interference respectively. Bit energy-to-noise plus interference ratio, more commonly referred to as bit energy to noise density ratio, determines the probability that signal can be decoded reliably without a bit error given for a given bit error rate (BER). The required $E_b/(N_0 + I_0)$ ratio for a successful uplink was based on data in [89], with factors such as phase coherence, amplitude fading characteristics, power control techniques and the distribution of interfering signal considered. Given that for the single base station model, phase coherence is set and the distribution of interfering signals is taken care of by ideal power control techniques (which makes all interferers received to be of equal power, recall Chapter 2) the bit energy-to-noise ratio is dependant primarily on amplitude fading. The fading case occurs when the mobile unit is in motion and this is the situation catered for in the model (as it is the worst case scenario) by making $E_b/(N_0 + I_0)$ equal

to 7dB [18, 23]. A non-fading case exists when the mobile unit is stationary and requires a far lower bit energy-to-noise ratio, typically 4.5dB [18]. A full description of signal fading is given by Lee in [8, 18].

To calculate the bit energy to noise plus interference ratio from the received signal, the numerator, E_b, is given by the desired signal amplitude, S, divided by the information bit rate, R. The denominator, $N_0 + I_0$, can be described as the system noise, $(N - 1)S$, in the channel bandwidth, W. Hence the bit energy to noise plus interference ratio for a single base station can be described as;

$$\frac{E_b}{N_0 + I_0} = \frac{\frac{S}{R}}{\frac{(N-1)S}{W}} = \frac{W/R}{N-1} \tag{6.3}$$

In a typical CDMA system the channel bandwidth, W, is 1.2288 MHz and the information bit rate, R, for voice is 9.6kbps.

System noise, η, has also been included in the CDMA Uplink Model. This noise occurs within the channel bandwidth due to spurious interference (receiver noise) and thermal noise (background noise). Typically the thermal noise floor ranges from 150K in rural or suburban areas up to 300K in urban metropolitan areas [87]. For the CDMA Uplink model thermal noise values of 150K and 250K for typical suburban and urban environments, respectively, have been used. Introducing the system noise yields the a new equation for the signal to noise ratio,

$$SNR = \frac{S}{(N-1)S + \eta} \tag{6.4}$$

and the bit energy-to-noise plus interference ratio in the presence of system noise can be expressed as,

$$\frac{E_b}{N_0 + I_0} = \frac{W/R}{(N-1) + \eta/S} \tag{6.5}$$

Typically the term "processing gain", G_p, is used to describe the bandwidth, W, divided by the information bit rate, R. Therefore equation (6.5) becomes,

$$\frac{E_b}{N_0 + I_0} = \frac{G_p}{(N-1) + \eta/S} \tag{6.6}$$

In a practical CDMA network every cell is divided into a maximum of three sectors, each with its own pair of 120° effective beamwidth directional antennas. The effective noise seen in a sector is only one third of that for the base station with a single omni-directional antenna. The three sectors reduce the $(N - 1)$ term in the signal-to-noise ratio in a sector by a factor of 3 and effectively increases the number of users N by 3 times for a given signal amplitude, S. If N_s is the number of users in a sector, in a cell the

number of users is $N = 3N_s$. Hence the noise term, $(N-1)S$, for a single cell becomes $(N_s-1)S$ for a sector. The division of the cell into sectors is very common in cellular systems today and was also recommended in [18, 23] back in 1991 when the capacity of the new CDMA system was first being examined. Hence forth whenever capacity is mentioned it is refereeing to the capacity of a sector unless otherwise stated.

All CDMA mobile units are able to suppress transmission when no voice from either party is present. This is known as Discontinuous Transmission (DTX). Statistical studies have shown that either speaker is active only 35% to 40% of the time [23]. This phenomenon is described as the "voice activity factor", denoted α, and in the CDMA Uplink Model is assumed to be 37.5% or 3/8. On average for a single base station DTX will reduce the interference from other subscribers from $(N_s-1)S$ to $\alpha(N_s-1)S$, making the new equations for signal to noise ratio and bit energy-to-noise plus interference ratio to be,

$$SNR = \frac{S}{\alpha(N_s-1)S+\eta} \tag{6.7}$$

$$\frac{E_b}{N_0+I_0} = \frac{G_p}{\alpha(N_s-1)+\eta/S} \tag{6.8}$$

The short fall of the single base station CDMA Uplink Model is that it doesn't consider co-channel interference from neighbouring cells. This issue is explored next.

6.1.2 MULTIPLE BASE STATION CDMA UPLINK MODEL

As mentioned earlier, in a real multiple cell system the power of a mobile phone handset is determined by the base station it subscribes to. The base station a mobile unit connects to is not dependent on the distance from the base station but rather the maximum pilot power among the base stations from which the subscriber receives a signal. The interference level from adjacent cells is dependent on the attenuation in the path to the base station of interest and is inversely proportional to the attenuation from interfering users to their own base stations. With power control, the attenuation of the interfering users may vary depending on the interference present at their base station, which also affects the interference levels at the base station of interest. In practical CDMA systems the losses are proportional to other effects as well, the most important of which is shadowing. In order to model the shadowing phenomena accurately a ray trace model of a given service area is required. Because the CDMA Uplink Model has been designed for a general case, shadowing has not been specifically included and more general path loss algorithms have been used instead. However, it is possible to adapt the developed model to use the data from a ray trace model for specific cases using a ray trace path loss algorithm.

A generally accepted model for the path loss is attenuation, which is the product of the fourth power of distance, d, and a log-normal random variable, ε, whose standard deviation is 8dB [23]. If fast fading is assumed not to affect the average power level of the mobile phone handset, then, if d_0 is the distance to

the mobile unit of interest and d_m is the distance to an interfering unit in another cell (Figure 6.1), the interference can be described as [23],

$$I = \left(\frac{10^{\left(\varepsilon_0/10\right)}}{d_0^4}\right)\left(\frac{d_m^4}{10^{\left(\varepsilon_m/10\right)}}\right)S$$

$$I = S\left(\frac{d_m}{d_0}\right)^4 10^{(\varepsilon_0-\varepsilon_m)/10}$$

(6.9)

where ε_m and ε_0 are Gaussian random variables with a standard deviation of 8.
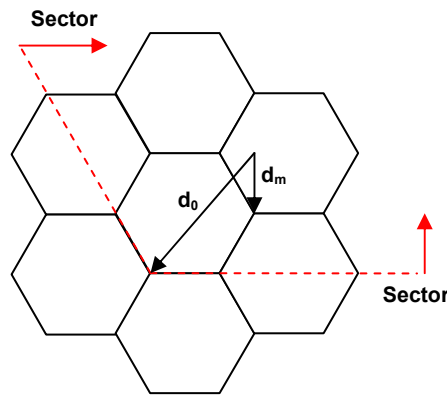
Figure 6.1. Cell Topology Showing Adjacent Cell Interference [8, 17]

The $\left(\dfrac{d_m}{d_0}\right)^4$ term is the attenuation caused by the distance and blocking of the base station of interest.

The second term $10^{(\varepsilon_0-\varepsilon_m)/10}$ is power control at the base station of interest compensating for the corresponding attenuation due to the out-of-cell interferers. Assuming a uniform density of subscribers and a normalised cell radius to unity Klien Gilhousen et al in [23] found statistically that the average interference added from out-of-cell interferers is given by,

$$I \le 0.247 N_s \times S$$

(6.10)

With a variance of

$$var(I) = 0.078 N_s \times S$$

(6.11)

Gilhousen's value for I of 2.47 was checked against a d^4 free space path loss by the author of this thesis to determine if the result was accurate for what the CDMA Uplink model was trying to achieve. It was assumed that users in the local cell were at an average distance of d from the base station and that users in the adjacent cells were at an average distance of $2d$ from the base station of interest. The users in the next farthest cells were at an average of $3.33d$ from the base station of interest (see Figure 6.2), the next at $4d$ and so forth.
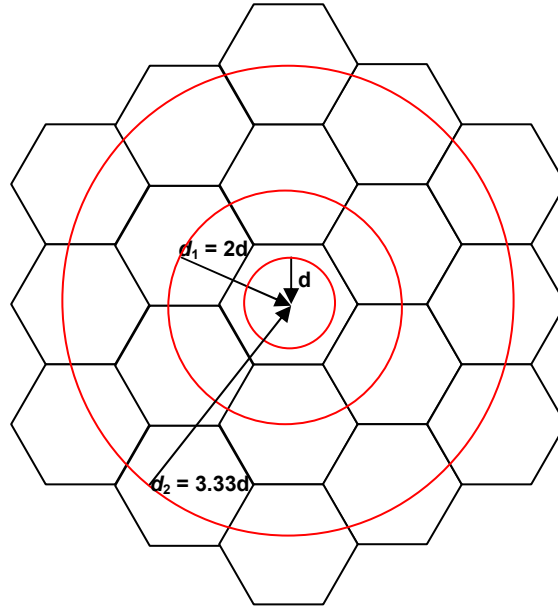
Figure 6.2. Average User Distance from Base Station of Interest (The Base Station is at the Centre of Each Cell in this Diagram for Simplification)

Assuming all the base stations receiving the same signal of amplitude S from their subscribers and a voice activity factor $\alpha = 0.375$ with perfect power control, the power seen at the base station of interest from the out-of-cell subscribers can be described as,

$$I = \alpha\left(X_{BTS@d_1} \times S \times N_s \times (d_1)^{-4} + X_{BTS@d_2} \times S \times N_s \times (d_2)^{-4} + ...\right) \tag{6.12}$$

Where $X_{BTS@dx}$ is the number of base stations in the range d_x where $x = 1, 2, 3, ...$ Therefore,

$$I = \alpha(6 \cdot S \cdot Ns \cdot (2d)^{-4} + 12 \cdot S \cdot Ns \cdot (3.33d)^{-4} + ...) \approx 0.25 S \cdot N_s \cdot d^4 \tag{6.13}$$

Assuming unity distance d to simulate the worst case scenario then equation (6.13) can be simplified to,

$$I \approx 0.25 N_s \cdot S \tag{6.14}$$

The result shows that Gilhousen's value for I is accurate for the CDMA Uplink model. Therefore, including the new term to take into account interference from adjacent cells into the signal-to-noise ratio equation for the multiple base stations, the equation for SNR in the CDMA uplink model becomes,

$$SNR = \frac{S}{\alpha(N_s - 1)S + \eta + I} = \frac{S}{\alpha(N_s - 1)S + \eta + 0.247 N_s \cdot S} \tag{6.15}$$

And therefore the bit energy to noise plus interference density ratio is,

$$\frac{E_b}{N_0 + I_0} = \frac{G_p}{\alpha(N_s - 1) + \left(\eta/S\right) + \left(I/S\right)} = \frac{G_p}{\alpha(N_s - 1) + \left(\eta/S\right) + 0.247 N_s} \tag{6.16}$$

Intermodulation distortion from a strong interferer signal located at a frequency close to the CDMA channel (such as was the case with NTT DoCoMo in Japan in the late 1990s) can significantly affect the performance of base stations and needed to be considered in the CDMA uplink model. The phenomenon is discussed in the next section.

6.1.3 INTERMODULATION DISTORTION

Nonlinearities of the receiver components, such as the low noise amplifier, induce inter-modulation (IM) products at their output. The third order IM products, which are located at frequencies $2f_1 - f_2$ and $2f_2 - f_1$ are the strongest and closest to the mobile phone user band, as illustrated in Figure 6.3, where f_1 is the receiver frequency and f_2 is the frequency of the out-of-band interferer.

Assuming that the transmissions of the two frequencies (f_1 desired and f_2 the interferer) occur at the same time in the same sector of the CDMA system, the power from the IM distortion is given by [88],

$$P_{IMD} = 3P_i - 2IIP3, \text{ [dB]} \tag{6.17}$$

where P_i is the out-of-band interferer power at the input of the receiver and IIP_3 is the input third-order intercept point of the receiver. P_{IMD} represents the power of the IM distortion as seen by the receiver and f_{IMD} is its frequency. f_{rx} is the receive band frequency range.
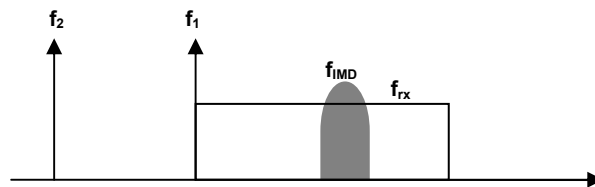
Figure 6.3. Inter-modulation Distortion [90]

The interferer power obtained at the receiver, P_i, can be described as,

$$P_i = P_s - L_A, \text{ [dB]} \tag{6.18}$$

where, L_A is the antenna isolation between the interferer and P_s, is the interfering signal transmit power.

Pre-selection filters in the front end of base station receiver are designed to attenuate out-of-band signals before they reach nonlinear parts of the receiver. Attenuating these out-of-band interferers effectively reduces the IM products created in the system by these signals meeting non-linear components, as illustrated in Figure 6.4. To take into account the effects of the preselection filter selectivity at the frequency of the interferer f_2, the formula for P_{IMD} in equation (6.17) is modified as follows, where $x = 2/3$ for third order IM products [88].

$$P_{IMD} = 3P_i - 2IIP_3 - \frac{L_F}{x} \qquad (6.19)$$

where L_F is the attenuation of the out-of-band interfering signal due to the pre-selection filter and is given by equation (6.20).

$$L_F = \Delta f \times L_s \qquad (6.20)$$

Δf is the difference between the filter cut-off frequency, f_1, and the interferer frequency, f_2, and L_s is the steepness of the pre-selection filter skirts in dB/MHz.
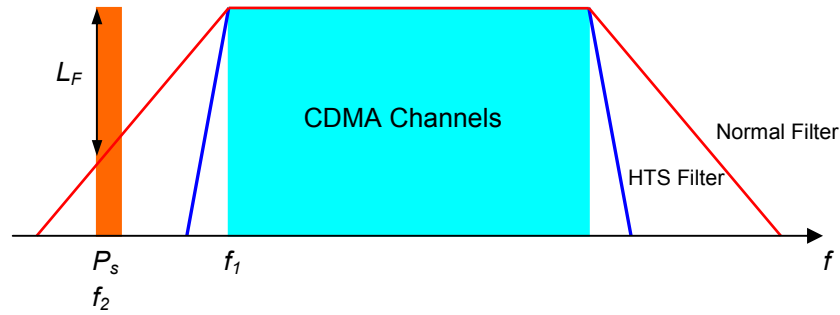
Figure 6.4. Effect of Pre-selection Filter on Out-of-Band Interferer

When an interferer is included in the multiple base stations CDMA Uplink Model the equation for signal-to-noise ratio can be described as,

$$SNR = \frac{S}{\alpha(N_s - 1)S + \eta + 0.247 N_s \cdot S + P_{IMD}} \qquad (6.21)$$

and the bit energy-to-noise ratio is given by,

$$\frac{E_b}{N_0 + I_0} = \frac{G_p}{\alpha(N_s - 1) + \left(\eta/S\right) + 0.247 N_s + \left(P_{IMD}/S\right)} \qquad (6.22)$$

6.1.4 FINAL CDMA UPLINK MODEL

Eq. (6.22), can be rearranged to find the required signal level, S, in order to maintain good quality communication between the base station and the mobile station for a set of parameters determined by the environment, namely

$$S = \frac{\eta + P_{IMD}}{\dfrac{G_p}{\left(\dfrac{E_b}{N_0 + I_0}\right)} - 0.247 N_s - \alpha(N_s - 1)} \qquad (6.23)$$

Assuming that P_{MS} denotes the transmit power level of the mobile handset, L is the propagation loss, G_{BS} is the gain of the antenna on the base station and G_{MS} is the mobile handset antenna gain one can express the signal received by the base station as,

$$S\,[\text{dB}] = P_{MS} + G_{MS} + G_{BS} - L \qquad (6.24)$$

The propagation losses for urban and suburban environments for equation (6.24) can be calculated using the empirical Okumura-Hata model for large cities [91]. Variations of this model can be used to calculate propagation losses in rural and open areas [88, 90, 91]. Because the Okumura-Hata model has only four parameters computations are easy. However the Okumura-Hata model neglects the terrain profile between the transmitter and receiver as well as reflection and shadowing. More complex and accurate models, particularly for urban environments, such as the Walfisch-Ikegami model and the WinProp Ray Tracing can be found in [92]. The drawback of these Ray Optical propagation models is that they require a geographical map of the urban environment and therefore lose generality. Furthermore shadowing was not taken into consideration in calculating the required uplink amplitude in equation (6.23) and consequently has not be included in the propagation loss calculations.

In urban environments the propagation loss was described by the Okumura-Hata model as,

$$L_{urban} = 69.55 + 26.16\log f - 13.82\log h_{eff} - a(h_{BS}) + \left(44.9 - 6.55\log h_{eff}\right)\log d \qquad (6.25)$$

where,

$$a(h_{BS}) = 3.2\left[\log\left(11.25 h_{BS}\right)\right]^2 - 4.97 \qquad (6.26)$$

In suburban areas,

$$L_{suburban} = 34.4 + 20\log f + \left(44.9 - 6.55\log h_{eff}\right)\log d \qquad (6.27)$$

In rural areas,

$$L_{rural} = L_{suburban} - 4.78\left(\log\frac{f}{28}\right)^2 - 5.4 \qquad (6.28)$$

In an open areas,

$$L_{open} = L_{suburban} - 4.78\left(\log f\right)^2 + 18.33\log f - 40.94 \qquad (6.29)$$

where h_{MS} and h_{BS} are the heights of the mobile station transmitter and base station receiver respectively in meters, h_{eff} is the effective height, $h_{eff} = |h_{BS} - h_{MS}|$, f is the channel frequency in MHz and d is the distance to the mobile subscriber from the base station in km. To ensure the maximum coverage and capacity it has been assumed that the mobile station transmits at a maximum power of $P_{MS} = 200\text{mW}$ or 23dBm.

6.2 PERFORMANCE SIMULATIONS OF BASE STATION FRONT ENDS

The CDMA Uplink Model developed in the course of this thesis and described in section 6.1 has been used to simulate the operation of base stations with differing receiver front ends in order to understand their influence on base station performance in terms of coverage and capacity. The primary components which are analysed are those that are most significant to the performance of the CRFE, namely the cooled LNA and the HTS filter. Both of these components are compared individually to conventional and hypothetical alternatives under varying conditions of noise (base on environment) and in the presence of a hypothetical out-of-band interferer to analysis of coverage vs. capacity in a single sector. Tower mounting of the base station front end has also been investigated to complete the analysis of currently available technology. Results of these simulations give a good indication of which aspects of CRFE are most important to base station performance. The link budget parameters used in the CDMA Uplink model are given in Table 6.1.

Table 6.1. Link Budget Parameters

Parameter	Symbol	Value
Bit Energy-to-Noise plus Interference Ratio	$E_b/(N_0 + I_0)$	7 [dB]
Standard Temperature	T_0	290 [K]
Antenna Noise Temperature (Suburban)	$T_{A(su)}$	150 [K]
Antenna Noise Temperature (Urban)	$T_{A(u)}$	250 [K]
Antenna Noise Figure (where T_A is either $T_{A(su)}$ or $T_{A(u)}$ depending on whether the antenna is situated in an suburban or urban area respectively)	N_A	= $10 \log(1 + T_A/T_0)$ [dB]
Receiver Noise Temperature	T_R	=$T_0(10^{N/10} - 1)$ [K]
Receiver Noise Figure	N_R	Measured for each system [dB]
System Noise Figure	η	= $N_A + N_R$ [dB]
Channel Bandwidth	W	1.2288 [MHz]
Data Rate	R	9.6 [kbps]
Processing Gain	G_p	= W/R
Voice Activity Factor	α	0.375
Number of Sectors		3
Number of Users per Sector	N_s	**Independent Variable**
Number of Users per Cell	N	$3N_s$
Boltzmann's Constant	k	1.38×10^{-23} [J/K]
Mobile Station Maximum Transmit Power	P_{MS}	200 [mW] = 23 [dBm]

Parameter	Symbol	Value
Mobile Station Antenna Gain	G_{MS}	1 [dB]
Base Station Antenna Gain	G_{BS}	1 [dB]
Out-of-Band Interferer Power	P_s	20 [W] = 13 [dB]
Isolation between Interferer and Receiver	L_A	40 [dB]
Preselection Filter Selectivity	L_F	Measured for each system [dB/MHz]
Interferer Power Received at Antenna	P_i	See equation (6.18) [dB]
LNA Third-order Intercept	IIP_3	Measured for each system [dBm]
Centre Frequency of Channel	$f1$	830 [MHz]
Centre Frequency of Interferer	$f2$	828 [MHz]
Power Intermodulation Distortion	P_{IMD}	See equation (6.19) [dB]
Height of Base Station	h_{BS}	[m]
Height of Mobile Station	h_{MS}	[m]
Effective Height	h_{eff}	= h_{BS} - h_{MS} [m]
Distance from Mobile Station to Base Station	D	**Dependent Variable, see equations** (6.30) – (6.34) [km]
Propagation Losses	L	See equations (6.25) – (6.29) [dB]
Received CDMA Signal Power	S	See equations (6.23) & (6.24) [mW]

The equations (6.23), (6.24) with the propagation loss given by equations (6.25) - (6.29), depending on the environment, can be rearranged to give an equation for the performance metric used to compare the base stations in this thesis; coverage, *d*, vs. capacity, N_s. The obtained equations for the maximum coverage radius, *d*, in kilometres for each of the different environments are shown in Equations (6.30) – (6.34).

Urban environment,

$$d = \frac{10^{\left(\frac{P_{MS}+G_{MS}+G_{BS}-\left(69.55+26.16\log f -13.82\log h_{eff} -a(h_{BS})\right)}{44.9-6.55\log h_{eff}}\right)}}{S^{\left(\frac{10}{44.9-6.55\log h_{eff}}\right)}} \tag{6.30}$$

where

$$a(h_{BS}) = 3.2[\log(11.25h_{BS})]^2 - 4.97 \tag{6.31}$$

Suburban environment,

$$d = \frac{10^{\left(\frac{P_{MS}+G_{MS}+G_{BS}-\left(33.4+20\log f\right)}{44.9-6.55\log h_{eff}}\right)}}{S^{\left(\frac{10}{44.9-6.55\log h_{eff}}\right)}}$$ (6.32)

Rural environment,

$$d = \frac{10^{\left(\frac{P_{MS}+G_{MS}+G_{BS}-\left(33.4+20\log f-4.78\left(\log\frac{f}{28}\right)^2-5.4\right)}{44.9-6.55\log h_{eff}}\right)}}{S^{\left(\frac{1}{44.9-6.55\log h_{eff}}\right)}}$$ (6.33)

Open environment,

$$d = \frac{10^{\left(\frac{P_{MS}+G_{MS}+G_{BS}-\left(33.4+20\log f-4.78(\log f)^2+18.33\log f-40.94\right)}{44.9-6.55\log h_{eff}}\right)}}{S^{\frac{1}{44.9-6.55\log h_{eff}}}}$$ (6.34)

6.2.1 PERFORMANCE SIMULATIONS IN THE PRESENCE OF NOISE AND INTERFERENCE

Simulation results of a CDMA base station utilising four different front ends with a centre frequency of 835MHz and useful bandwidth of 10MHz were performed to obtain the maximum coverage of the base station for a given number of users in a sector. The four systems analysed consisted of:

- a conventional Ground-based Front End,
- a conventional Tower-mounted Front End,
- a Ground-based CRFE, and
- a Tower-mounted CRFE.

For each system performance was computed in a presence of noise only as well as for noise plus interference with a hypothetical 20W narrow band interferer at 825MHz. 40dB isolation was assumed between the transmit antenna for the interfering signal and the CDMA receiver antenna.

Most important parameters used in the simulations of each base stations performance are given in Table 6.2. Tower-mounted conventional receivers were assumed to have a Noise Figure of 1.4dB, and Ground-based conventional systems to have 0.5dB more. The Noise Figure of HTS Filter-LNA combination was taken to be 0.8dB and the selectivity as 25dB/MHz [14]. The selectivity of conventional filter was assumed as 5.4dB/MHz [93]. An antenna Noise Temperature of 250K was chosen for urban environments [23] and the maximum transmit power of a mobile station of 200mW (23dBm) was assumed in the simulations.

The same system linearity was assumed for four systems, namely IP3 equal to 35dBm, which in fact could only be true when a modern low noise amplifier is used in all systems. This assumption means that the system IP3 is kept as a constant and therefore noise and interference can be focused on. However, in practice, modern amplifiers are not typically used in all conventional receiver front ends and systems will have different linearity. All other parameters are given in Table 6.1.

Table 6.2. Properties of Base Station Receiver Front Ends

	Ground-based Conventional Receiver	Tower Mounted Conventional Receiver	Ground-based CRFE	Tower Mounted CRFE
Noise Figure N_R [dB]	1.9	1.4	1.3	0.8
Selectivity L_F [dB/MHz]	5.4	5.4	25	25
System OIP3 [dBm]	+35	+35	+35	+35

Computed performance of four CDMA front ends in an urban environment in the presence of the receiver noise only is illustrated in Figure 6.5. For all receivers the coverage of the base station decreases with the increase in the number of users as expected.
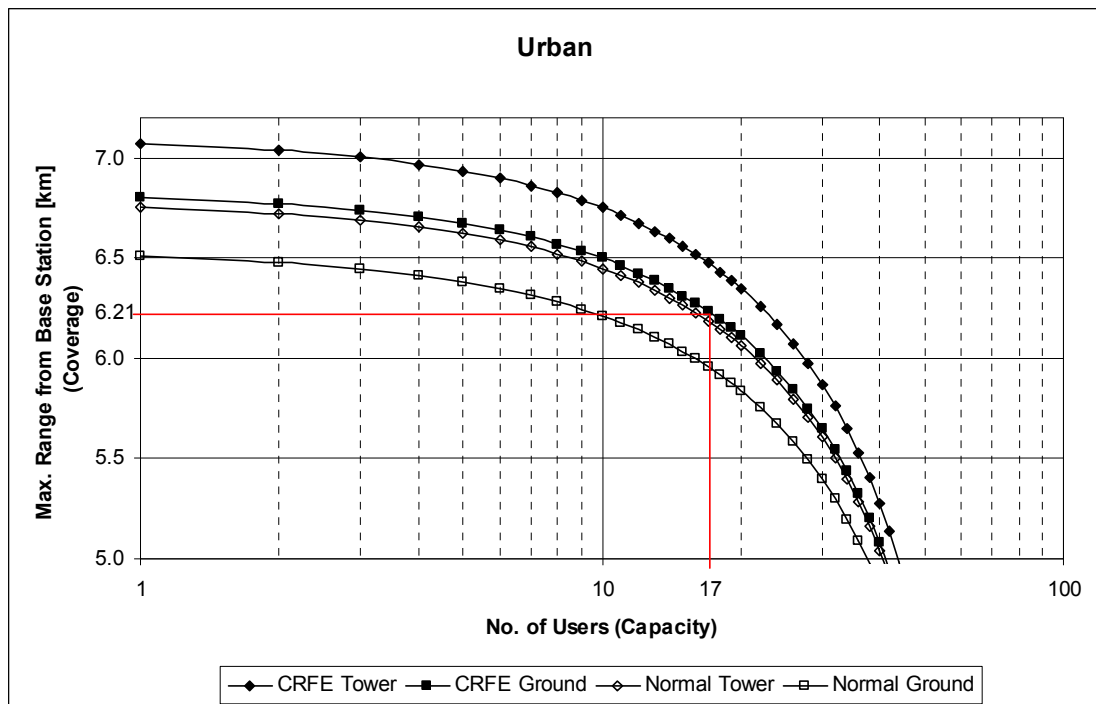
Figure 6.5. Computed Coverage vs. Capacity (per Sector) with Noise Only

The computed performance is shown to depend on the noise figure of the receiver front end. Hence there is an advantage in tower mounting of the receiver front end, which could reduce the system noise by 0.5dB and create a 4% improvement in coverage or 60% improvement in capacity.

The simulations have shown that the CRFE reduces the system noise by 0.7dB compared to conventional front ends, increasing the calculated maximum coverage for 10 users from 6.21km to 6.5km for a ground based receiver. This equates to a 5% improvement in coverage of the base station due to the reduced noise figure of the CRFE, which can be considered as a only a small improvement. Coverage improvements are most attractive for use in rural areas when there are few users or developing countries which are installing their first mobile communications systems. Most developed cities already have an extensive network of base station antennas. Extending the coverage in an existing network may lead to cells overlapping which can cause an increase in pilot signal pollution, therefore increasing the number of soft handoffs (make-before-break handoff) and therefore the total interference.

While the increase in coverage may be used to fill coverage gaps in this situation, by far the more attractive aspect of this technology is the increased capacity that CRFEs can provide while maintaining the same coverage. In the example of Figure 6.5 the number of users can be increased from 10 to 17 users while maintaining a 6.21km coverage radius when using a ground based CRFE rather than a conventional receiver front end.

The computed performance for the same four front ends when a 20W interferer is located 5MHz from the operational band edge (as illustrated in Figure 6.6) is presented in the Figure 6.7.
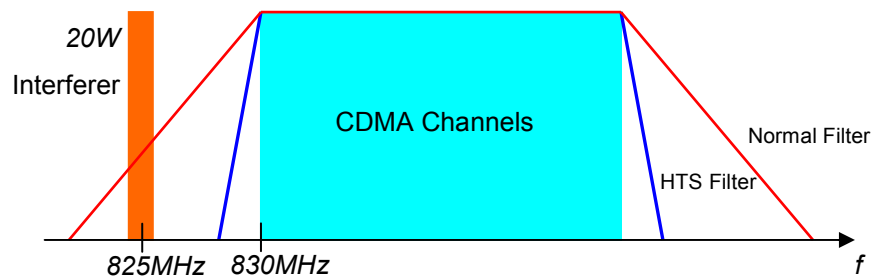
Figure 6.6. Schematic of 20W Out-of-Band Interferer, CDMA Channels and Filter Characteristics used in Simulations
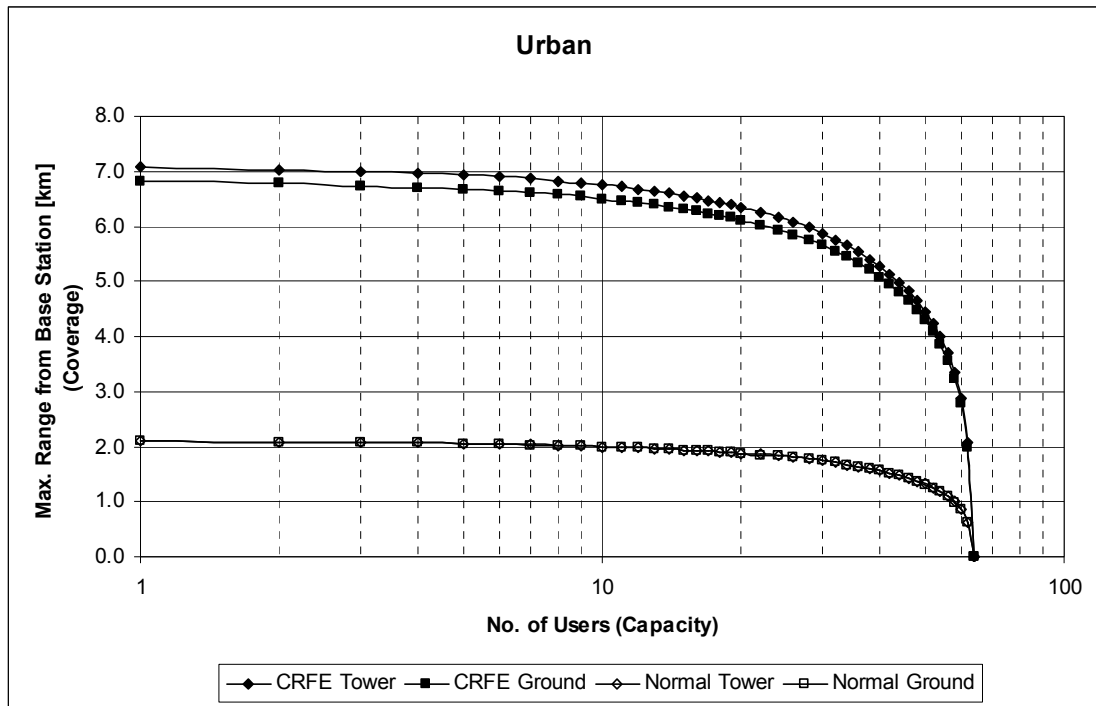
Figure 6.7. Computed Coverage vs. Capacity (per Sector) with Noise and a Narrowband Out-of-Band Interfernce of 20W @ 825MHz

In the presence of strong narrowband interference of 20W the Tower mounted and the Ground based conventional receivers have their range reduced from 6.21km for 10 users to approximately 2.1km. This is due to the non-linear effects of the amplifier and other non-linear components spreading the interfering signal into the CDMA channel of interest. The coverage of the CRFE is not affected and maintained the same 6.5km coverage as when there was no interference (Figure 6.5). This is due to the filter effectively suppressing the out-of-band interferer to a level such that the LNA is operating in its linear range, given by IP3 point. While situations of interferers close to the operating frequency are not very common today, heavy communications traffic can effectively utilise the higher selectivity of HTS filters to allow for more flexibility in spectrum allocation and cell site planning. Highly selective filters will be of particular benefit to 3G UMTS networks where they can be used to select an entire channel, effectively protecting it even from interference from other UMTS channels.

6.2.2   PERFORMANCE SIMULATIONS OF THE EFFECT OF SYSTEM IP3

Simulations using the developed CDMA Uplink model were performed for ground based systems with an IIP3 of 5dBm for the conventional front end, 10dBm for a hypothetical modern front end and 15dBm for the CRFE. The same selectivity of 5.4dB/MHz was assumed for all systems as shown in Table 6.3. A 20W interferer was assumed to be present at 825MHz with the same 40dB isolation between the antennas as in the previous example. All simulations done assume a conventional metallic filter with selectivity of 5.4dB/MHz. Computed results of Maximum range and Number of Users are displayed in Figure 6.8.

Table 6.3. Parameters of Investigated Base Station Receiver Front Ends

	Traditional Amplifier [94]	Theoretical Amplifier	Cooled Low Noise Amplifier [7]
Noise Figure NR [dB]	1.9	1.9	1.3
Selectivity LF [dB/MHz]	5.4	5.4	5.4
Amplifier IP3 [dBm]	+5	+10	+15
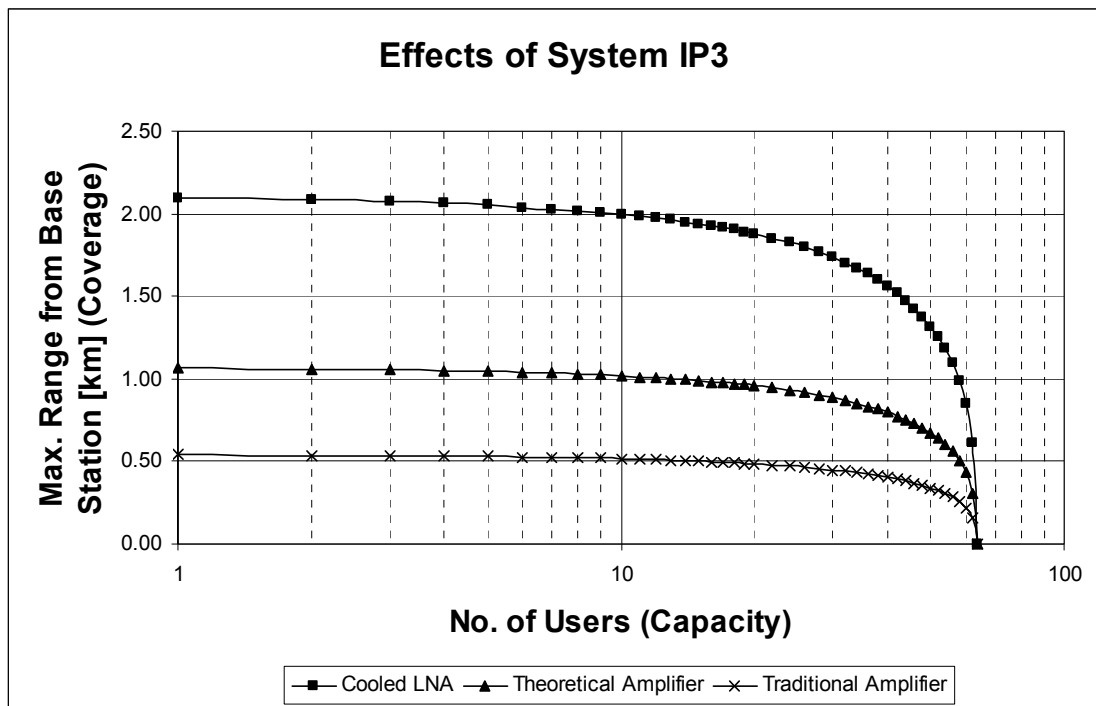
Figure 6.8. Computed Coverage vs. Capacity (per Sector) for Different System IP3 in the presence of interference of 20W

For a base station using a ground mounted receiver with an amplifier IIP3 point of +5dBm and a conventional filter of 5.4dB/MHz selectivity the coverage of the base station of only 0.54km was obtained. Improving the IIP3 point of the amplifier to +10dBm increases the coverage to 1.07km, giving almost a 100% improvement. Using a cooled LNA of the IIP3 of +15dBm yielded a 2.09km coverage radius. The results suggest that when there is an out-of-band interferer (which may produces IM products due to non-linear components) improving the linearity (IIP3) of the amplifier alone will reduce the impact the interferer has on coverage and capacity. Theoretically if the amplifier and rest of the system electronics were linear no filtering of out-of-band interference would be required.

The developed CDMA uplink model has demonstrated the importance of having a linear system, which is typically limited by the input IP3 point of the amplifier. Increasing the linear range of the amplifier has a significant effect on improving the coverage and capacity of the CDMA systems, particularly in high

traffic areas where out-of-band interference is prevalent. Replacing traditional amplifiers with more modern or cooled LNAs may be a good option for current installations of CDMA cellular base station receivers, in terms of performance and cost. Indeed if a perfectly linear system could be developed, intermodulation products would not be an issue and filtering would be unnecessary.

6.2.3   PERFORMANCE SIMULATIONS OF FILTER SELECTIVITY

This section presents the results obtained using the CDMA Uplink model where the filter steepness is the only variable affecting the performance of the base station. The LNA for all the investigated systems was assumed to have an IIP3 of 15dBm. Simulations were performed assuming the filter from Narda Components [93] of steepness of 5.4dB/MHz, a hypothetical filter with a steepness of 10dB/MHz and the Cryoelectra-Tsinghua University 16 pole HTS filter [14] with a steepness of 25dB/MHz. The noise in each scenario was assumed to be that of a conventional ground mounted front end (1.9dB). Two cases have been considered, the first with the familiar 20W interferer located at 825MHz and a second (more extreme case) where the interferer is placed at 828.5MHz only 1.5MHz from the operation band edge.

Table 6.4. Parameters of Filters used in Filter Selectivity Experiments

	Conventional Filter	Theoretical Filter	Cryoelectra-Tsinghua University Filter
Selectivity [dB/MHz]	5.4	10	25
Noise Figure NR [dB]	1.9	1.9	1.9
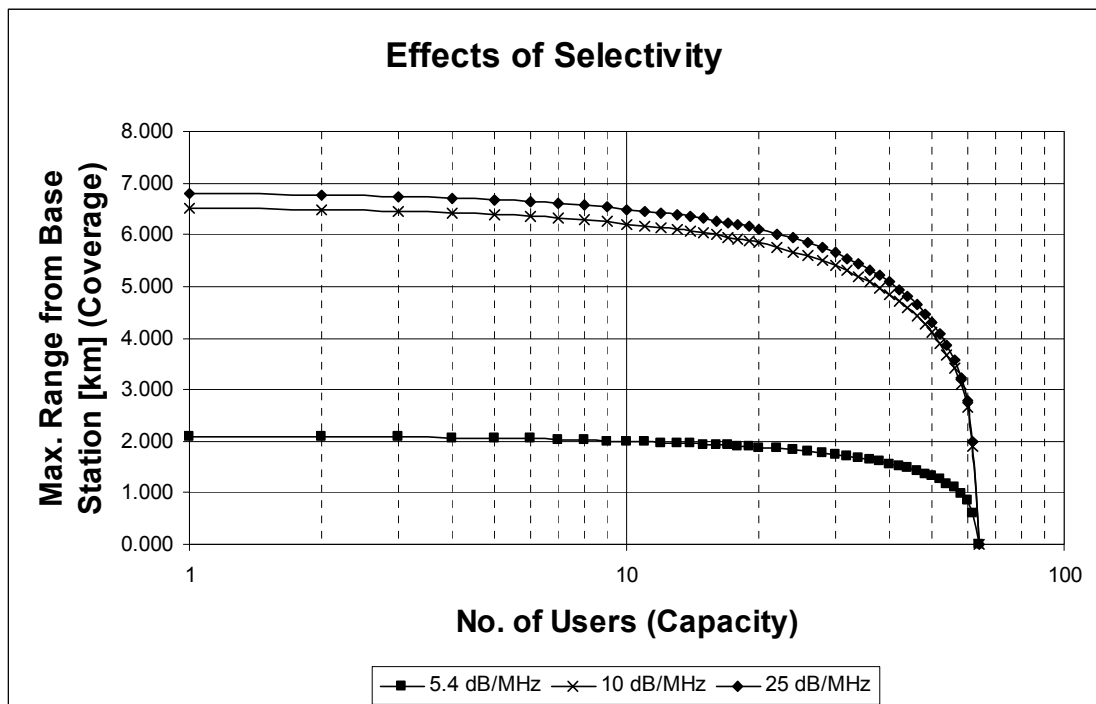
Figure 6.9. Computed Coverage vs. Capacity (per Sector) for Filters of Different Selectivity with Noise and a Narrowband Out-of-Band Interfernce of 20W @ 825MHz

Simulation results of the performance of the base stations pictured in Figure 6.9 show the receiver with the traditional filter of steepness of 5dB/MHz provided a 2km coverage radius when 10 users were connected simultaneously. Improving the filter steepness to 10dB/MHz resulted in a three times larger coverage radius with the same number of users. This improvement suggests that in the presence of an out of band interferer a filter with a steeper response, which attenuates out-of-band signals, improves the performance of a base station. Further improving the filter beyond the point where the out-of-band interferer is attenuated such that inter-modulation distortion is no longer generated in non-linear components has very little or no effect. Interestingly in the case described even a small improvement in the filter to 10dB/MHz can yield great results. Hence dielectric filter technology, which can produce filters with a steepness of up to 25dB/MHz (with only slightly higher insertion loss than HTS filters) and are significantly less expensive than a CRFE should, according to the above results, also be attractive as base station front end filters.

The simulations were repeated for an extreme case where there is a 20W interferer at 828.5MHz, very close to the 830MHz edge of the passband. This time a 5.4dB/MHz, 15dB/MHz, 20dB/MHz and 25dB/MHz filters were compared using the same setup parameters as in the previous simulation. This was to consider not only out-of-band signals generated from another source, but out-of-band signals generated by neighbouring CDMA channels (which can also cause IM products). Due to cellular site planning this is not typically an issue in today's mobile environment. But as user numbers increase and data services become more accessible, maximising the capacity of networks will become more important.
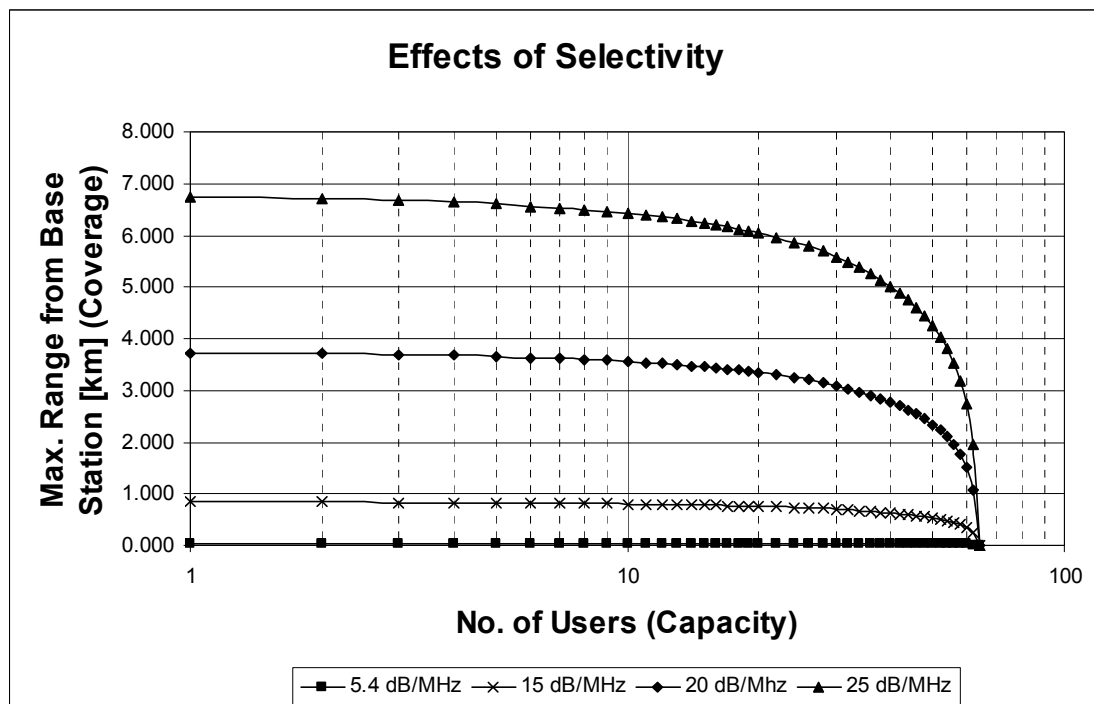
Figure 6.10. Computed Coverage vs. Capacity (per Sector) for Filters of Different Selectivity with Noise and a Narrowband Out-of-Band Interfernce of 20W @ 828.5MHz

The traditional filter in the presence of such a close strong out-of-band interferer provided almost no coverage (due to extreme interference from IM products) while the HTS filter with selectivity of 25dB/MHz increased coverage and capacity to almost the same levels as when the interferer was not present. This simulation result shows the potential importance of high selectivity filters to the future cellular communication industry.

6.2.4 PERFORMANCE SIMULATIONS IN DIFFERENT ENVIRONMENTS

The following simulations show the effects of a CRFE versus a traditional front end in urban, suburban, and rural environments. The front end specifications are assumed the same as those of the ground based receivers in Table 6.2. The thermal noise levels for each environment is described in Table 6.1 and the path loss algorithms are described by Equations (6.30) to (6.33) as in Chapter 6.1.4. Two cases are considered for each environment; the first when the base station is only in the presence of noise and the second when a 20W interferer is introduced at 825MHz (as in previous simulations).
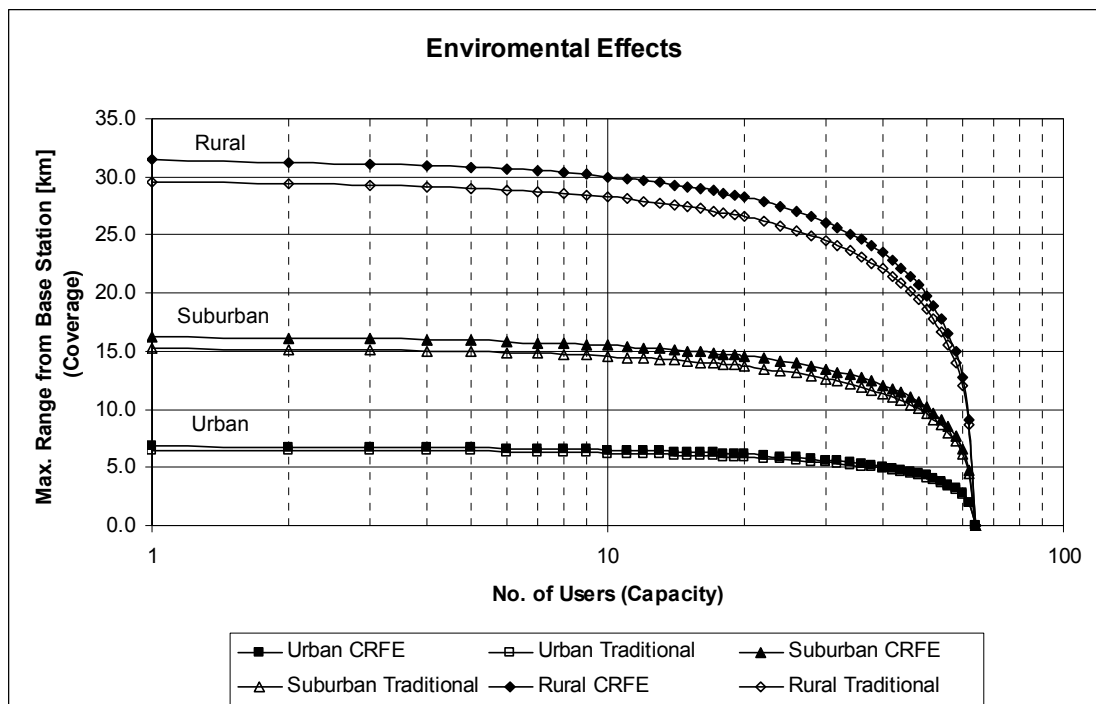
Figure 6.11. Computed Coverage vs. Capacity (per Sector) for Different Enviroments with Noise Only

As expected the influence of environment (which significantly affects the path loss experience by the signal) is strong when only noise is present. A base station situated in a rural environment can have a 5x larger coverage area than the same base station located in an urban environment. The simulated CRFE results under noise only conditions (represented by solid markers) show less than 10% improvement in coverage in all cases. The capacity improvement is a greater than 70%, however in rural areas it is unlikely that this is meaningful.
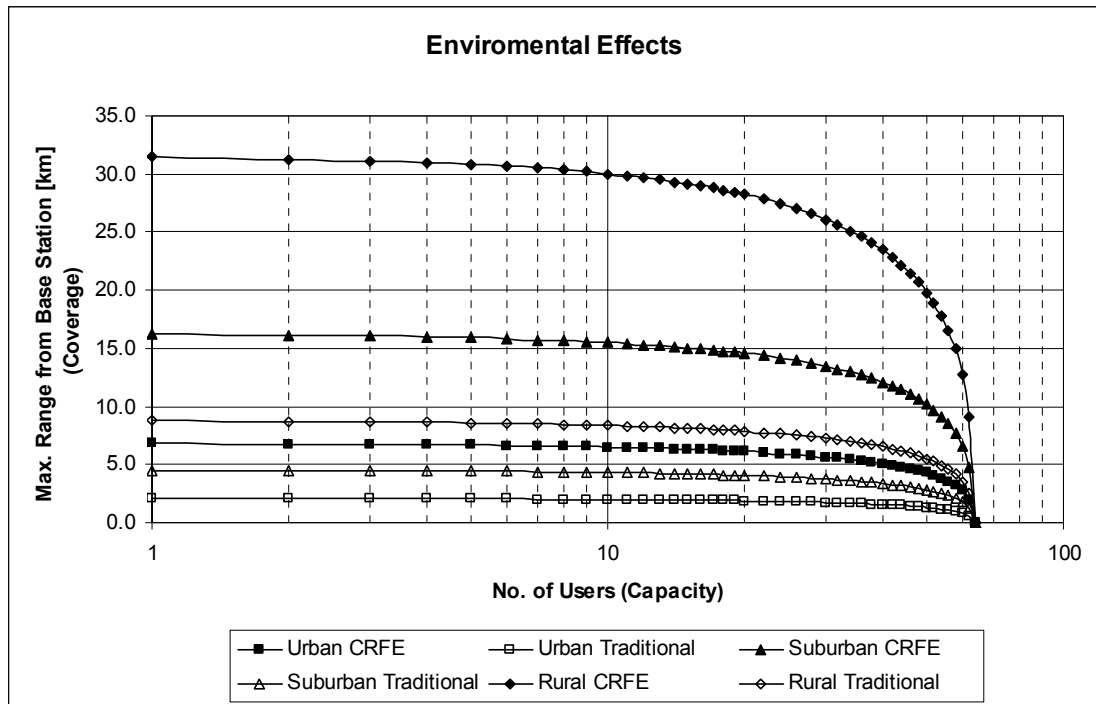
Figure 6.12. Computed Coverage vs. Capacity (per Sector) for Different Environments with Noise and a Narrowband Out-of-Band Interfernce of 20W @ 825MHz

Results of the simulations assuming the same base station front ends in the presence of interference are significantly different then those for the noise only situation. In all environments the traditional front end has experienced a 65% reduction in coverage compared to when there was no out-of-band interferer. The CRFE has experienced no significant decrease in coverage due to the improved selectivity of the HTS filter effectively suppressing the interferer. In each case it's the selectivity of the filter in the CRFE and the linearity of the LNA that reduces the effects of the IM distortion in the passband and therefore maintains the coverage levels.

6.3 INTERPRETATION OF THE SIMULATION RESULTS

The CDMA Uplink Model presented in this chapter has proved to be a useful tool for the performance analysis of CDMA base station receivers in systems where the downlink is not the limiting factor. The model can be used by base station manufacturers who wish to evaluate the performance of CDMA base station with novel front end solutions in terms of system capacity, coverage and quality of service in non-specific environments. The model incorporates the influence of IM distortion and interference effects and allowed for the analysis of conventional and CRFE enabled CDMA base stations operating under differing conditions and in different environments. The simulations performed in this chapter have clearly shown the effects on the performance of a base station under in the presence of noise and out-of-band interference using filters of with various levels of selectivity and amplifier of vairied dynamic range.

Cryogenic receiver front ends incorporating highly selective and low loss HTS filters and high dynamic range low noise amplifiers provide the receiver with improved sensitivity and selectivity when compared to conventional receiver front ends. The improvement in sensitivity is due to the reduction in the noise produced in the front end which will improve the receiver's ability to detect weak signals. The improvement in selectivity due to HTS filter technology increases the attenuation of out-of-band signals close to the receiver frequency.

Simulations performed using the developed CDMA Uplink model showed that in situations where there are no significant out-of-band signals close to the receiver frequency the simulations suggest that there is only a small improvement in coverage to be gained due to the reduced noise in the front end assuming the capacity of the system is unchanged. In the situation where out-of-band interferers are present the results of the addition of HTS technology become more apparent. The steepness in the skirts of the HTS filter can attenuate out-of-band interferes more than conventional filter technology, which results in the reduction or elimination of inter-modulation products appearing inside the channel.

In the alternate case where the coverage was kept constant and the capacity varied, the capacity of the CDMA network has been slightly increased by the improved sensitivity of the cryogenic receiver front end. As was found for the coverage investigation, it is the ability of the HTS filter to highly attenuate out-of-band signals which provided the significant improvement in the capacity of the system. This is because multiple mobile subscribers concurrently use the same channel and the removal of strong inter-modulation products in the channel will effectively increase the channels capacity by reducing the in channel noise. UMTS systems should also achieve capacity gains by implementing HTS technology into cryogenic receiver front ends as the system operates based on a CDMA signal. GSM networks however, will not see any significant increase in the capacity due to operating on a TDMA/FDMA signal. A small increase may be possible in the situation where additional channels, which were previously unusable due to 3rd order inter-modulation products, become available.

Additionally the simulations have shown that replacing existing amplifiers with LNAs of higher IP3 (more linear) and/or cooled LNAs (less noise) will also produce significant performance gains of the CDMA base station receivers. This is due to a reduction in IM distortion created by out-of-band interference and adjacent CDMA channel interference produced by neighbouring CDMA channels.

The simulation results presented in this chapter suggest that HTS filters combined with cooled LNA to produce CRFE are currently the best performing front end in terms of coverage and capacity, particularly in the situations where strong out-of-band interferes are present. While only CDMA systems are discussed in this chapter, similar results may be expected for UMTS, and GSM. However, it is unlikely, due to modern network planning and spectrum utilisation that strong out-of-band interferers such as those depicted in the simulations exist commonly. Therefore highly selective filters are not required today and lower order filters with low noise figures coupled with a modern LNA are potentially more significant to today's network operators than extremely high order almost ideal filters. Therefore it may be that CRFE

systems in many cases will not produce an improvement significant enough to offset the cost of implementing such a system in currently existing networks.

Understanding that noise and interference are the main obstacles in maximising coverage and capacity and that a cost effective solution for current day networks is desirable, it appears that dielectric filter technology combined with modern amplifiers could achieve a similar selectivity with slightly reduced sensitivity. Similar coverage and capacity as for CRFE could be provided at a significantly reduced cost because no vacuum or cooling equipment is required. Furthermore replacing the conventional duplexer with a dielectric duplexer would further reduce the noise figure of the front end and improve coverage and capacity of wireless base stations. The issue of DR Filters and Multiplexers is investigated further in Chapter 8.

While currently limited by its cost it is foreseeable that HTS technology will become more important in the future as more efficient use of the mobile radio frequency spectrum becomes more important and providers try to maximise the capacity of their systems to meet increasing demand.

6.4   ANALYSIS OF THE WUNONGCHANG FIELD TRIAL

Using the CDMA Uplink Model described in Chapter 6 it was possible to further examine the implications of the results from the Wunongchang field trials in terms of coverage and capacity. The drive tests showed the transmit power of the mobile station was decreased by an average of 3.1dBm while achieving the same signal to noise ratio at the base station using handset power control. The measured 3.1dBm reduction in required mobile handset transmission power suggests that when using the CRFE in just one sector of a BTS a mobile handset can achieve the same coverage as with a conventional front end using less than half the transmit power.

Using the CDMA Uplink model and assuming appropriate levels of noise, filter selectivity and amplifier specifications the minimum signal power, S, for a successful uplink could be calculated. Unfortunately the values used were only an educated guess as data sheets for the base station being tested were not made available. Hence by reducing P_{MS} in equation (6.24) by 3.1dBm while keeping the coverage radius, d, constant will give the new minimum signal power, S, required for a successful link;

$$S = (P_{MS} - 3.114) + G_{MS} + G_{BS} - L \qquad (6.35)$$

Once the new minimum signal power at the base station is known, to find the new maximum coverage with the CRFE installed, the transmit power of the mobile station was increased to its maximum (23dBm) and equation (6.33) is solved for the coverage in a rural environment, as

$$d = \frac{10^{\left(\dfrac{P_{MS}+G_{MS}+G_{BS}-\left(69.55+26.16\log f-13.82\log h_{eff}-a(h_{BS})-4.78\left(\log\dfrac{f}{28}\right)^2-5.4\right)}{44.9-6.55\log h_{eff}}\right)}}{S^{\left(\dfrac{10}{44.9-6.55\log h_{eff}}\right)}} \qquad (6.36)$$

where

$$a(h_{BS}) = [1.1\log(f)-0.7]h_{BS} - (1.56\log(f)-0.8) \qquad (6.37)$$

Using the CDMA Uplink model and assuming a 3.1dB decrease in required transmitter power as measured a 105% increase in the coverage of the base station at full power is calculated using the model. Unfortunately exact field data and system specifications at the time of the test were not available for modelling and therefore the simulation results are only indicative of what might be expected with the CRFE installed in this situation. Hence the specific reasons for the improvement are not fully clear as several components in the CRFE may individually or in combination be able to account for the result or the assumption of the parameters could be incorrect. In all likelihood the performance increase is predominantly due to the reduction of out-of-band interference, probably created by adjacent CDMA carriers. There is nothing to suggest that a strong out-of-band interferer in the rural environment (in which the field trial was performed) was present to have any significant effect on the system performance. Therefore the reduction in handset transmission power is primarily due to the modern LNA with its high dynamic range which increased linearity of the front end and resulted in a reduction of the IM caused by neighbouring CDMA channels. It is probable, based on the simulations and the existing knowledge of the base station that 1dB improvement results from a reduction in the system noise due to the cooled front end. As shown in Figure 6.13 the simulated results for the CRFE (depicted by black diamonds) and the experimental results (depicted by red triangles) are similar.
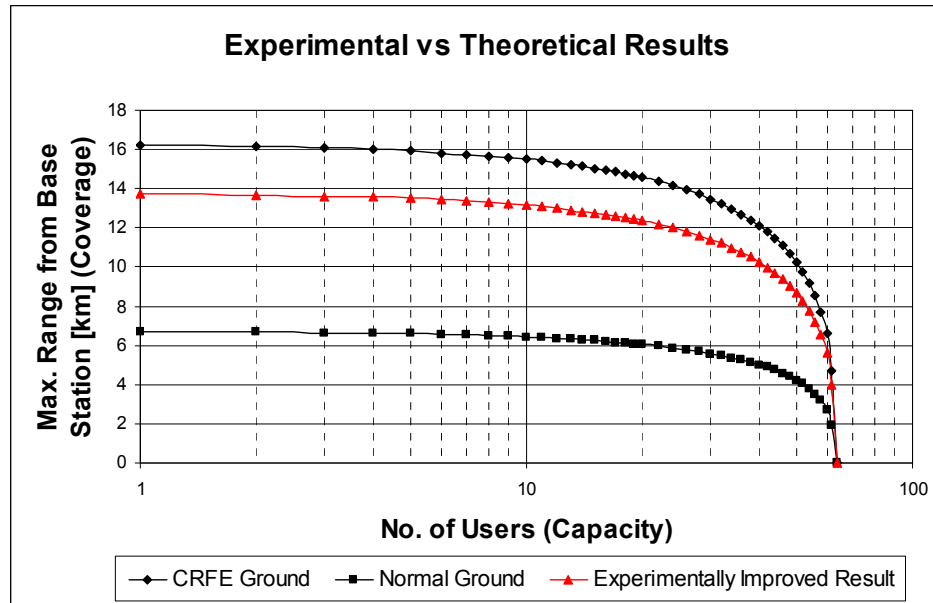
Figure 6.13. Experimental Results Compared to Simulated Results using the CDMA Uplink Model

The difference between the experiential results and the simulated results for the CRFE can be accounted for by several phenomena which the CDMA Uplink model doesn't take into consideration but are probably present in this situation and will degrade performance. It is probable that surrounding cells, which were all using conventional front ends, were producing higher levels of adjacent cell interference than in the test sector. The CDMA Uplink model assumes all cells have the same setup and therefore adjacent cells produce a level of interference based on that setup, which means in this situation that the surrounding cells would have been modelled as contributing less interference than they actually were. Additionally the improved coverage of the single sector when the CRFE was in use would have increased the overlap of sectors. Any handsets operating in the overlap area will make try to make a soft handoff to the base station which can accept it with the lowest uplink power. Since the overlap is increased more handsets will be trying to make handoffs and may even be switching between two base stations which can significantly increase the interference resulting in the experimentally measured coverage being smaller than the coverage projected using the CDMA Uplink model. To better understand the effects of the CRFE further field test have been undertaken in the next chapter with more CRFE enabled sectors to eliminate the effects of these phenomena.

CHAPTER 7

DEVELOPMENT OF AN ADVANCED CRFE

In the course of investigating *if and under what circumstances high temperature RF-superconductivity can prove to be an important technological contribution to future wireless communication* a series of engineering innovations and improvements have been developed by the author of this thesis to create an advanced CRFE in an effort to optimise the performance cost ratio and bring the technology closer to the market. The goal of the new system was to achieve the best possible technical performance while also improving its install flexibility, operator usability and minimising the cost of production. In the process a family of advanced CRFE were manufactured, one of which, D7, was tested in Beijing, China. The other systems were tested in house.

The main improvements achieved in the course of this work were the design of a new easier to tune and manufacture filter, the redesigned of the vacuum maintenance system for all the CRFE and an IR radiation shielding which has been added to reduce the required cooling power. Also a more sophisticated control system was proposed to enable remote monitoring of system performance. Details of these novel engineering solutions and the new series of CRFE developed are described below.

7.1 CRYOGENIC RECEIVER FRONT ENDS

The series of CRFE developed as part of this thesis fulfilled specific shortcomings of the D6 system. The first of these new systems was D7, which was based very closely on the successfully tested D6 except for the addition of a new six channel obelisk and Dewar. This enabled feed throughs for 6 RF channels for the main and diversity antenna in each sector of a three sector base station. The cryostat was also modified to use N-type connectors rather than SMA, to make it easier for telecom operators to connect cables to the front end. D8 was developed using the new obelisk with the goal of making the systems completely mountable into a 19 inch rack. This required orienting the cold head and Dewar horizontally rather than vertically and supporting the weight of each effectively. While not a huge technological step it was very important from the point of view of installation. This also led to the redevelopment of the housing of several components in order to minimise the weight placed on the cold head.

Figure 7.1. Pictures of D7 front and back showing the new N-type connectors for RF input (top of cryostat) and output (back panel)

Figure 7.2. Pictures of D7 with removed cryostat enclosure to display the new obelisk with a hexagonal cross section for the mounting of 6 Filter-LNA assemblies to be used with a 3 sector CDMA base station

Figure 7.3. Pictures of 19" Rack Mountable D8 Front and Back

M1 was the first mast mountable system developed and was designed to eliminate the noise introduced by the length of cable between the antenna and the front end. After amplification of the signals at the top of the tower this noise was no longer an issue, therefore mast mounting the CRFE was a logical evolutionary step. Once again the six channel setup was used with this system to cater for a full three sector base station.

Figure 7.4. Picture of the Mast Mountable System M1 with the Dewar Open and a Full Complement of Filters

D9, the newest of all the systems, was developed when Laybold stopped production of their Stirling coolers which have been used in all the previous systems. D9 is the first system to use the new Ricor Stirling cooler. The new cooler meant once again redesigning the placement of components in the new system, which was also to be horizontally mounted. Another immediately obvious issue was the control software packaged with the new cooler. This control system lacked the controllability and data logging features of the Laybold software. This led the author to develop a new electronic control system which improved communications, control, data logging, test facilities and additional programming flexibility to add new functionality should the need arise. Details of the improvements made to individual components are discussed in Chapters 7.2 and 7.3.

Figure 7.5. Picture of the Latest System, D9, Featuring a Ricor Stirling Cooler

7.2   CRYOGENIC COMPONENTS

The cryogenic components included all components which are cooled or connected to the cooling in some way, such as the HTS filter, LNA, Obelisk, radiation shielding and RF cables. All these systems have been redesigned or improved compared with CRFE D6 to improve the systems usability and performance based on the experiences gained from designing D6 and its field test.

7.2.1 HTS FILTER

The goal of this project was a new HTS filter which meets or exceeds base station requirements and, unlike the D6 filters, required little or no trimming or tuning before it is implemented into a CRFE. This is a very important aspect for the mass production of CRFE should the technology ever become truly commercial. As mentioned earlier, it currently can take up to several days to fully tune a filter and LNA combination which is problematic from time and cost points of view.

Two HTS filter designs have been developed in the course of this work: A 12 pole filter, shown in Figure 7.6, which was a substitute for the Tsinghua design used in D6 and a 20 pole filter (Figure 7.7) for situations where enhanced selectivity would be necessary. Both filters have been based on the same resonator design and exhibited improvements in most of the important aspects of the original filter characteristic. Using a very compact resonator design it was possible to place the same number of resonators as used in the Tsinghua filter on the same sized substrate, but with double the line width. The wider lines resulted in the resonators having a higher unloaded Q-factor and nonlinearity threshold. Consequently the losses of the newly designed filter were reduced and the IP3 point increased.

A capacitive distributed external coupling with a relatively wide gap to the first and last resonators was designed in order to avoid current crowding at the point of galvanic coupling, unlike in the Tsignhua design. This has further increased the IP3 point of the filter and improved its manufacturing tolerances, and as a result, made it more reliable. Shortening slightly of the length of the first and last resonators to shift them to a higher frequency (pre-detuning) compensated for resonator detuning due to the external loading and ultimately reduced the time required to tune the filter using tuning screws. The full design procedure for this filter is not given in this thesis as HTS filter design now well documented in literature including the author's honours thesis [30].
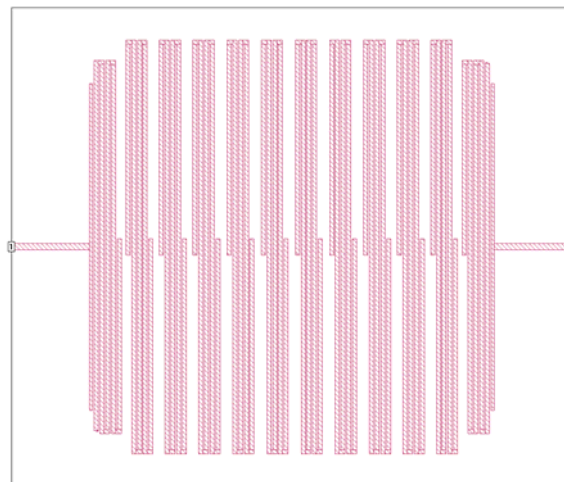
Figure 7.6. New Generation 12 Pole CDMA Filter Design
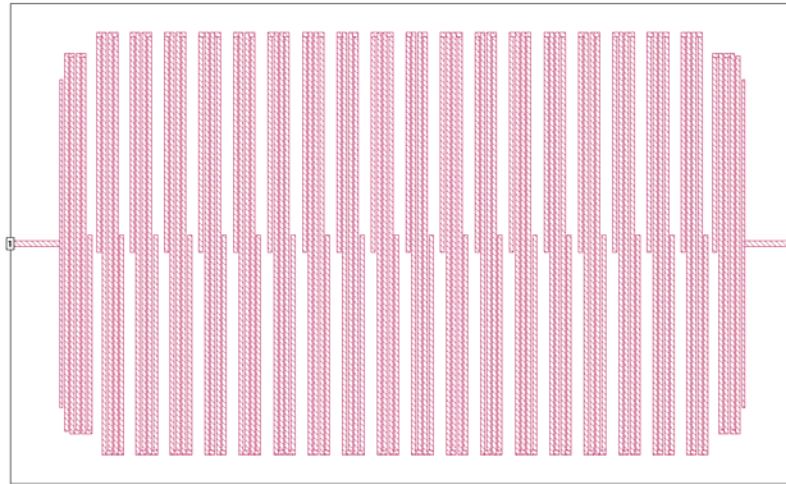
Figure 7.7. New Generation 20 Pole CDMA Filter Design

The individual resonators have a shape of a meandered line, but in contrast to well known designs, the coupling arms of the resonators start and finish somewhere close to the centre line of the filter, not at edges of the resonator structure. This enabled a very short separation between the adjacent resonators. Additionally it produced a filter characteristic with a symmetric pair of transmission zeros close to the passband. By adjusting the overlap of the coupling arms it was possible control the position of the transmission zeros. The full wave simulated characteristic of the 12 and 20 pole filters are shown in Figure 7.8 and Figure 7.9 respectively. The 20 pole characteristic exhibits less than 0.6dB insertion loss in the passband and pair of symmetric transmission zeros at the level of -70dB 1MHz from the edge of the passband.
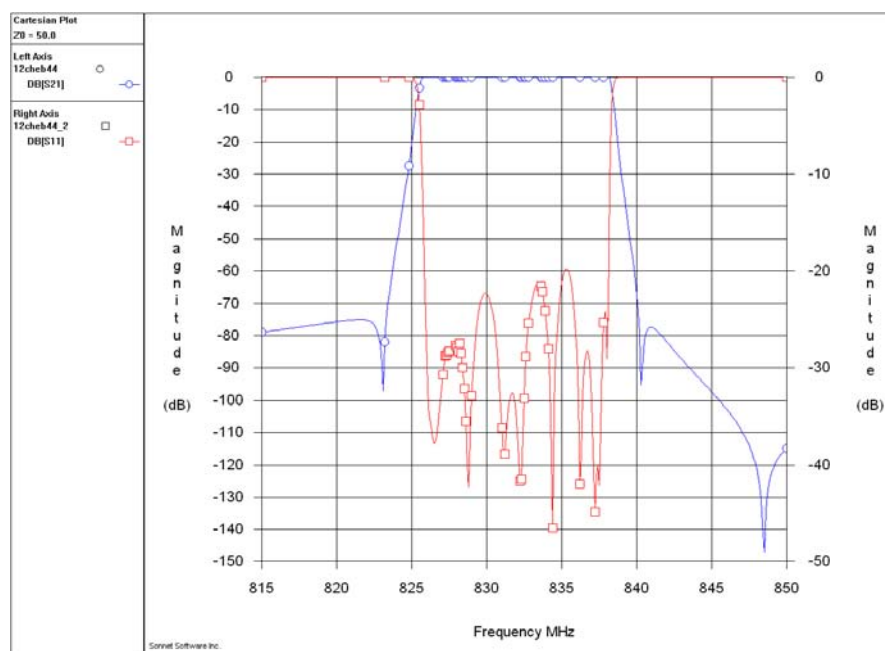
Figure 7.8. Full Wave Simulated Response of the New Generation 12 Pole CDMA Filter
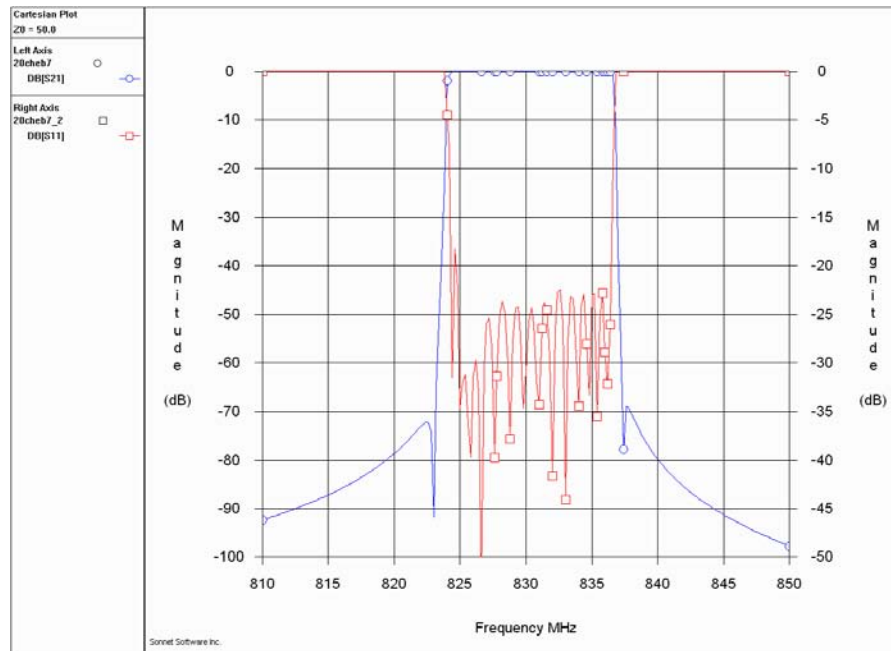
Figure 7.9. Full Wave Simulated Response of the New Generation 20 Pole CDMA Filter

7.2.1.1 HTS FILTER DESIGN FOR UMTS

Since the CDMA filters described above exhibited excellent performance, an UMTS filter was designed as a replacement to for the 17 pole elliptic filter design by Chaloupka (see Chapter 3.4.2) to be used either in an UMTS CRFE or for a multi-operator combiner (discussed in Chapter 8). The layout of a 20-pole UMTS filter is shown in Figure 7.10.
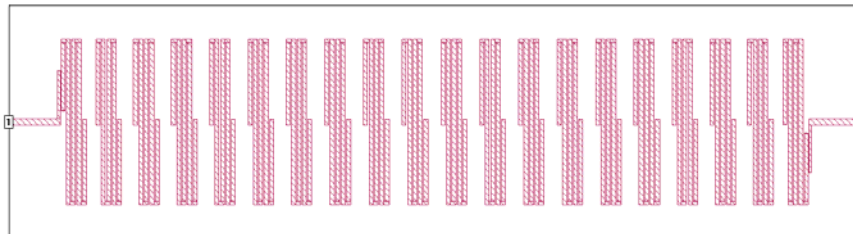
Figure 7.10. Layout of the new 20-pole UMTS Filter

As seen from the Figure 7.10 the distance between the adjacent resonators was made larger as compared to the CDMA filters. This was due to the stronger coupling between the resonators at frequencies more than twice as high as the CDMA frequency. In fact the magnetic coupling turned out to be dominant and as a result the filter characteristic does not look as attractive as that of the CDMA filters (Figure 7.11). Unfortunately even varying the overlapping the coupling arms of the adjacent resonators could not fully correct the balance of filter characteristic as the separation been the resonators was too large to have sufficiently strong electrical coupling to create the symmetric transmission zeros seen in the CDMA filter characteristic.
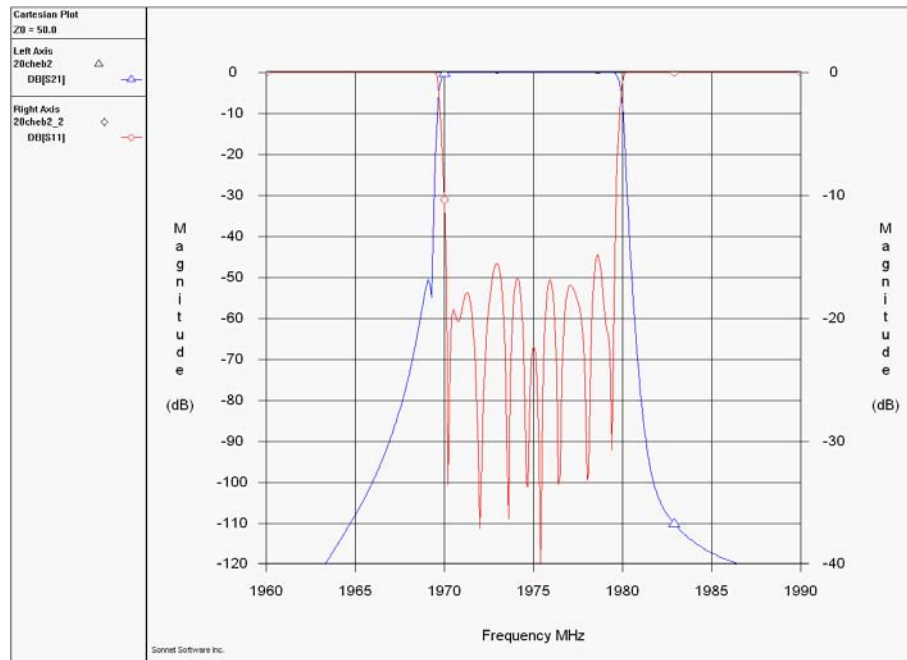
Figure 7.11. Full Wave Simulated Response of the New Generation 20 Pole UMTS Filter

Neither the CDMA nor the UMTS filter designs have been manufactured at the time of writing this thesis. The filters are planed to be manufactured when the Cryogenic Receiver Front End sparks more commercial interest.

7.2.2 LOW NOISE AMPLIFIER

The performance of the LNA manufactured by Cryoelectra for Demonstrator D6 (shown in Chapter 5.2.3) was very good and no immediate improvement was required. The housing of the LNA however, was brass, which is relatively heavy. Given the need to mount the filter LNA combinations in D8 horizontally, keeping the weight carried by the cold head (which is not a load bearing structure) to a minimum was important to maintain the life of the cooler. As such a new box made of aluminium (Figure 7.12) was developed and tested to ensure it performed as well as the brass housing. The first test was to determine whether the carrier that the LNA was mounted on could maintain its bond to the aluminium housing in the changing thermal conditions. Silver loaded two component epoxy adhesive was used to fix the carrier to the housing. The structure was then placed in liquid nitrogen to cool and then removed, to test the bond under these extreme conditions. The experiment proved successful and the aluminium LNA housing was developed.
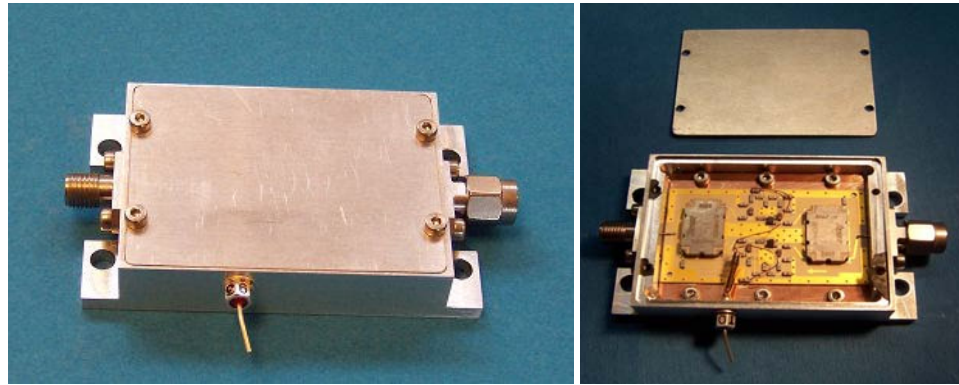
Figure 7.12. Aluminium Housed LNA

A further extension of this was the idea to mount the filter and the LNA in the one housing, thereby reducing the noise created by the connection between the SMA connectors between the two separate units. However this idea was never realised in practice.

7.2.3 THE FILTER & LNA MOUNTING STRUCTURE

To cool the HTS filter and LNA, both components are mounted on an obelisk attached to the cold head of the cryocooler inside the vacuum chamber. In previous designs the obelisk allowed for mounting 3 Filter LNA combinations. However the typical base station has 6 channels; a main and a diversity antenna for each of the three sectors. So an obelisk which carried 6 Filter LNA combinations was needed as one CRFE could service an entire base station and its sectors.
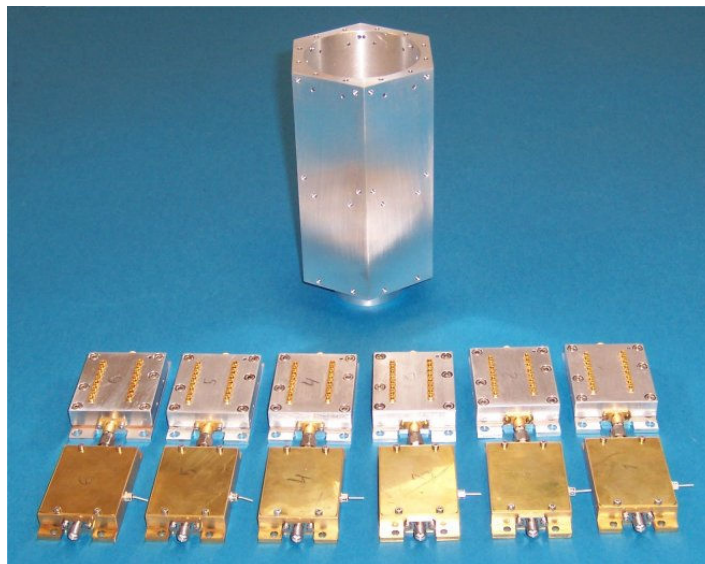
Figure 7.13. 6 Channel Obelisk with CDMA Filter LNA Combinations

The drawback of this solution was in the weight of the load being placed on the cold head. The cold head of the cryogenic cooler is fed by two thin stainless steel tubes which contain a moving piston arrangement. A very slight bending of these tubes due to the weight placed upon the cold head will cause additional friction between the piston and the walls which will damage the seal formed between the piston

and the stainless steel tube. This can lead to increased cooling power requirements and shortening the life of the cooler. It was not anticipated that the weight will have a great effect on the system in the vertical position, however it was possible the tubes may bend outward (Figure 7.14).
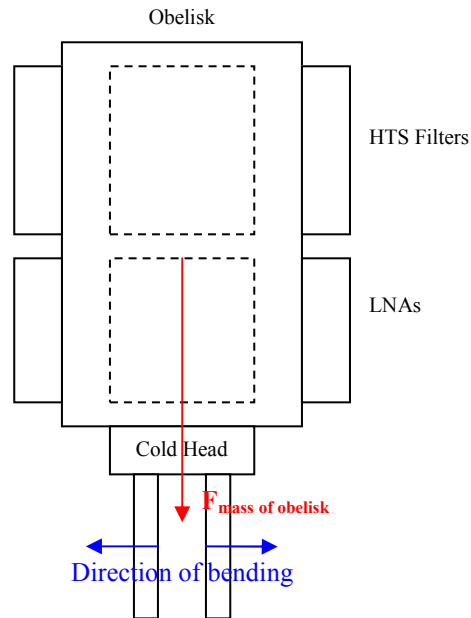
Figure 7.14 - Weight on the Cold Head (Vertical)

For the rack mountable system D8 the Dewar and therefore the cold head and the obelisk were mounted horizontally which meant that a torque was created on the cold head due to gravity acting on the loaded obelisk. Because the structural strength of the feed tubes was vertical, the force acting on the cold head could be damaging (Figure 7.15).
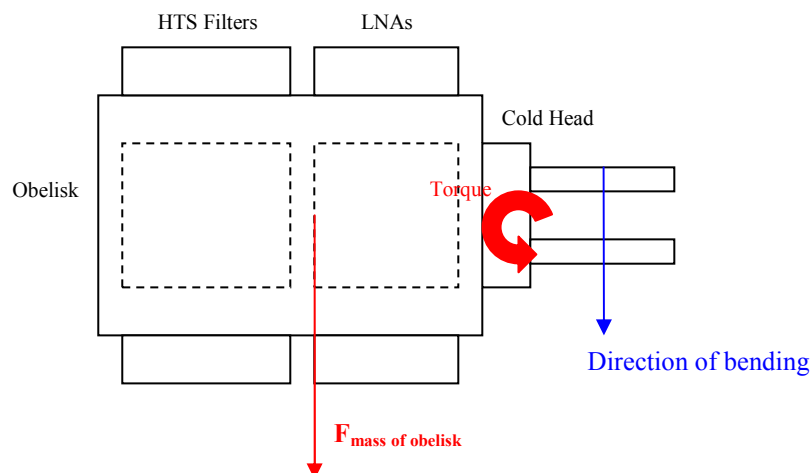
Figure 7.15 - Weight on the Cold Head (Horizontal)

To combat this torque being generated on the cold head a "spider" support system had been developed. This system attached to the top of the obelisk and distributed the weight to the base of the vacuum

chamber to reduce the torque. The drawback of the system was that it added another source of heat via conduction. To minimise the heat transfer to the cold head the cross-sectional size of the connection between the cold head and the base of the Dewar was made as small as possible and the distance maximised (Figure 7.16).
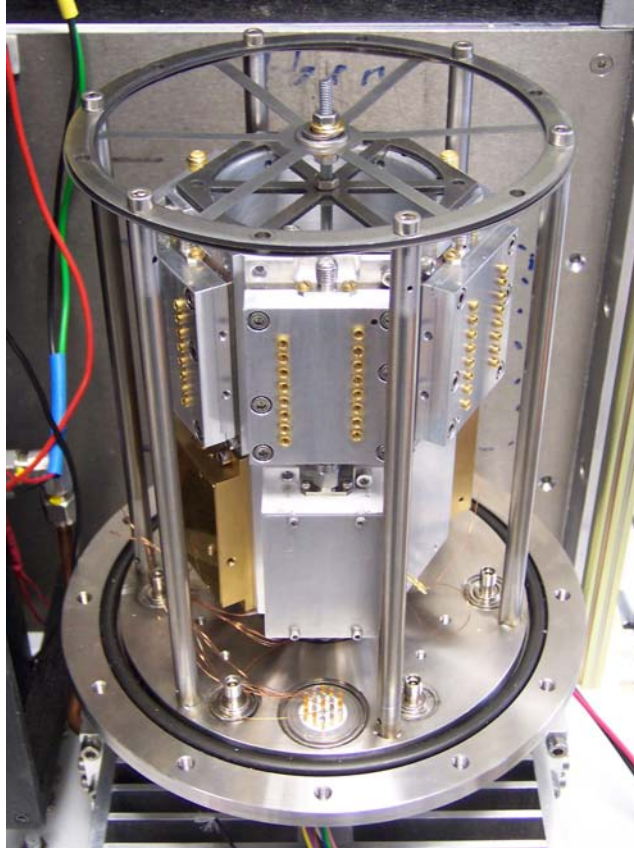
Figure 7.16 – CRFE D8 with Spider Support System Installed

To verify its usefulness the "spider" support system was tested using Demonstrator 8. The tests with the radiation shield suggested that the weight in the vertical position had no significant effect on the power usage of the system. Therefore the tests in the vertical position were considered a benchmark for the horizontal position. While these experiments did not contribute substantially to the body of knowledge they were important technological difficulties which had to be overcome in order to build a fully operational and viable CRFE.

All the tests were performed under vacuum and at 68K with the spider support system attached. Measurements were taken when the systems stabilised and reached equilibrium. The system was warmed up again after changing its orientation in order to get accurate results and avoid inaccuracies being introduced from the ice forming on the cold finger being shifted when the orientation was changed.

Table 7.1. Vertical and Horizontal Testing

#	Test (Vertical and Horizontal)
1	6 Filter/LNA Obelisk Weight = 880g
2	6 Filter/LNA Obelisk 3 Filter/LNA Combinations Weight = 1.693kg
3	6 Filter/LNA Obelisk 6 Filter/LNA Combinations Weight = 2.45kg

Results were recoded for D8 operating in the horizontal and vertical positions for approximately 24 hours for each test. The lowest power required to maintain the operating temperature of 68K was recorded immediately after the system reached equilibrium. The required power increased after a few hours of operation, possibly due to ice built up on parts of the cold finger. Ice seemed to have the effect of increasing the surface area which is affected by IR radiation, which increases the heat input into the system, which in turn requires the cryocooler to increase its power to compensate and maintain the operating temperature of 68K. The test results are presented in the Table below.

Table 7.2. Vertical and Horizontal Mounting Test Results of D8

Test Number	Vertical		Horizontal	
	Lowest Power	Highest Power	Lowest Power	Highest Power
1	71	76	72	77
2	85	87	86	88
3	98	101	98	102

Test Number	Vertical Average Power	Horizontal Average Power
1	73.5	74.5
2	86.0	87.0
3	99.5	100.0

The spider support system removed the problems associated with weight causing damage to the input to the cold finger. No significant change in the cooling power required by the CRFE was detected when the CRFE was operated in the horizontal position. This suggested that the CRFE could be successfully rack mounted without a significant reduction in the life of the cryocooler or impacting its performance.

It is interesting to note however that that addition of the spider support system appeared to increase the build up of ice after several hours, seen by the increase of power after the system reached equilibrium. Further investigation into this phenomenon suggested that the problem was due to air being trapped under the screws which fixed the spider to the obelisk. This has since been corrected by cross drilling ventilation holes into the screw holes to allow them to be evacuated.

7.2.4 RADIATION SHIELDING AND HEAT SOURCES

To avoid heat transfer to the cold head via gas conduction or convection, gas in the Dewar needs to be evacuated. This however does not stop radiation from entering the system. The addition of a radiation shield, not present on the D6 system, attempted to minimise the heat introduced to the system via hot body infrared radiation, to reduce the required cooler power and improve the cost of operating the system (in this case the hot body is the outer walls of the vacuum chamber). The radiation shield itself should be a uniformly smooth, shiny (ideally gold) surface in order to reflect as much of the radiation as possible. Heat shields can be wrapped in several layers; some kind of insulation is typically inserted between the layers to isolate them from one another. In this way the inner heat shields have reduced radiation from the outer heat shields incident on its surface, as the temperature of the shields is reduced from that of the original hot body (Figure 7.17).
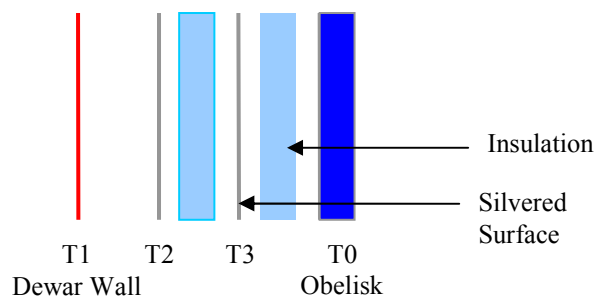
Figure 7.17 – Conceptual Block Diagram of Radiation Shield and Insulation

An expression for the variation of infrared radiation emission with temperature is given by the Stefan-Boltzmann Law [95],

$$Radiation \quad = \sigma \, \varepsilon \, A \, (T_1^4 - T_0^4) \qquad\qquad (7.1)$$

where A is the surface area which is radiated against, σ is Stefan's constant, 5.67×10^{-8} Wm^{-2}K^{-4}, and ε is the emissive efficiency, which is close to 1 for a blackened surface and very small for a silvered surface. The experimental radiation shield was designed using fibreglass insulation and an aluminium foil outer cover. The aluminium foil was chosen because it has a low emissive efficiency and was easy to shape. It was important to achieve a uniform surface for the radiation shield which the radiation would be incident on. The radiation shield would also effectively reduce the surface area, A, which the IR radiation will incident on; without the radiation shield the non-uniform surface of the obelisk and mounted filter-LNA appears very large and traps radiation, particularly in the hole at the top of the obelisk which acts as a black body. A series of experiments were performed on D8 and M1 to test the IR shield and the contribution from other heat sources. The details of these experiments are described in Appendix C.

The results of the experiments conducted showed that the developed CRFE required greater that 31W of additional power in order to maintain an operating temperature of 68K when there was an obelisk attached to the cold head due specifically to infrared radiation. This power requirement increased further if filter/LNA channels were added to the obelisk (because the surface area is increased). A simple

radiation shield could reduce the power increase due to infrared radiation by approximately 42% with additional layers being added to further reduce the radiation.

7.3 SUPPORTING SYSTEMS

7.3.1 VACUUM SYSTEMS

A constant pumping mechanism is required in CRFE to remove gases expelled from the surface of objects within the vacuum such as the obelisk, filters, LNA and the walls of the Dewar. While heat treating the walls of the Dewar before sealing removes much of the water and hence reduces the amount of gases expelled into the vacuum after the Dewar is sealed, the need for vacuum maintenance still exists. The CRFE D6 used an external ION Getter pump in order to maintain the vacuum inside the Dewar. The drawback of the ION Getter Pump was the requirement for a high voltage power supply (as illustrated in Figure 5.26) and its size making it sit outside the Dewar. Other solutions, such as Non-Evaporable Getter (NEG) Pump and Zeolite, offered potentially more elegant solutions to the problems of vacuum maintenance. NEG pumps work on a similar principle to the ION Getter pumps, however the active material is not evaporated or sputtered on the pumping surface but instead remains in a specially prepared inter-metallic compound. The pumping action of NEG pumps involves adsorption of gases followed by their diffusion inside the material. The diffusion process once again requires heating (200°C) but it can be delivered by a variable DC source (up to 3A). Because of the progressive saturation of the exposed surfaces the Getter must be reactivated by heating (900°C using a 10A DC source) to clean the surface.
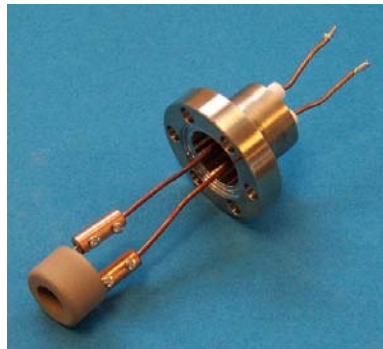
Figure 7.18. NEG Pump with Vacuum Feed Through for Heating Wires

Utilising Zeolite is a passive solution, which does not require power to operate, and only requires heating for the initial activation or out-gassing of the material. Zeolite is an inorganic porous material with a highly regular structure of pores and chambers that allow some molecules to pass through and other to be excluded or trapped and broken down. The specific Zeolite selected for a task depends upon the Zeolite's shape, size and charge distribution in the lattice structure [96].

Figure 7.19. Zeolite

While the ION Getter Pump works well in maintaining the vacuum a more elegant solution which did not require a physically large and expensive external pump was selected for the advanced CRFE D8, D9 and M1, namely a NEG pump system was selected to pump will pump H_2 and CO from the vacuum chamber [97].

The NEG pump used in D8 experiments was a St 127 Getter from SAES. It is activated at approximately 900°C with a current of 8A and was typically operated with a current of 3.1A at 200°C. The NEG pump was mounted above the obelisk in D8 using the vertical supports and the ring used in the spider support system (the spider support system was not used in the NEG pump experiments). The CRFE was then pumped using the turbo vacuum pump (TVP) and cooled to its operating temperature of 68K. The NEG pump was then activated at 900°C (8A), which expelled any gasses contained in the NEG pump leaving a clean surface for pumping once the vacuum chamber was sealed. Once the NEG pump had been activated it was operated at 3.1 Amps. The TVP was removed and the chamber is sealed once the cooler returned to the 68K operating temperature (note that due to the NEG pump acting as a new heat source the temperature of the system will increase until the control system increases the power of the cooler to compensate).

The important experiment was to determine if the pumping speed of the NEG pump was sufficient to maintain a satisfactory vacuum (better than 1×10^{-4} mbar). Because the vacuum pressure could not be measured directly in this case, the power required by the cooler was taken as in indicator of vacuum. In a system with a poor vacuum more heat is transferred to the cold head via convection, therefore more power is required from the cooler in order to maintain the operating temperature.
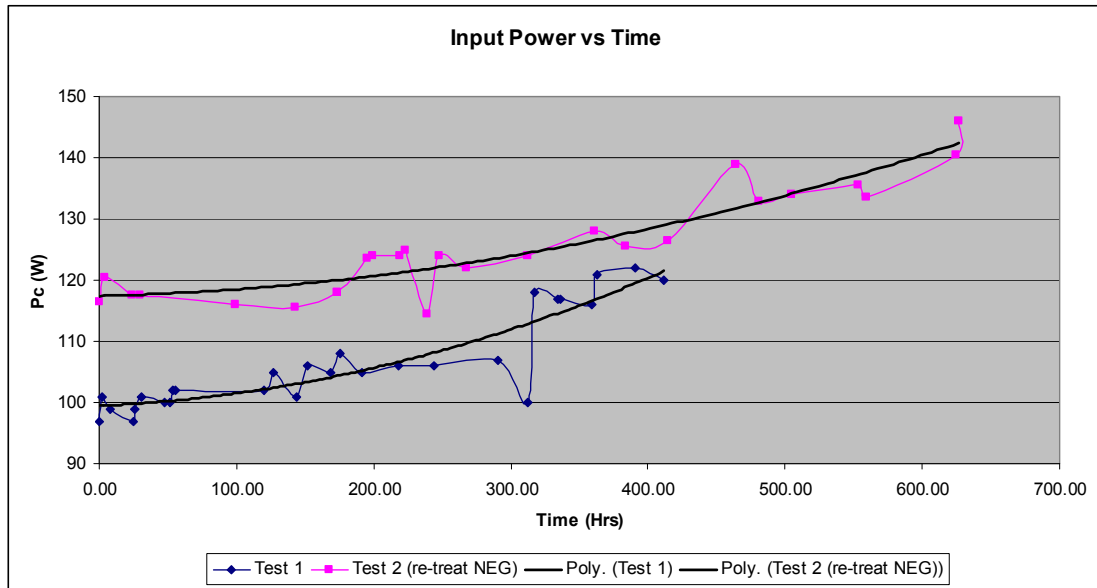
Figure 7.20. NEG Pump Tests – Cooler Input Power vs. Time

It can be seen in both tests shown in Figure 7.20 that the input power increases over time. The power required to maintain a temperature of 68K has increased by about 50W from 97W to 146W over 1 month, implying that the vacuum is spoiling. This meant that using one NEG pump was not adequate to maintain the vacuum under the condition when the Dewar has not been heat treated.

Given the findings found it is reasonable to assume that two NEG pumps need to be implemented in the system to approximately double the effective pumping speed. It remains to be seen whether two NEG pumps will be sufficient to maintain the vacuum through 5 years of continual operation. But this is also true for the reliability of other components as the test of D6 has only been running since March 2004, 2.5 years. Alternatively the same test could be performed using a system which has been heat treated to remove water vapour from the Dewar and therefore reduce the number of gaseous molecules entering the vacuum. Based on the data gathered a conservative decision was made to use ION Getter Pumps for all the field trials to minimise any chance of failure in during testing.

7.3.2 ELECTRONIC CRFE CONTROLLER

It was essential to develop a diagnostic and control system that reliably controls all critical functions of the CRFE. This was caused by the termination of the production of stirling cryocoolers by Laybold, which meant D9 was forced to use a new cryocooler by RICOR, a company in Israel. The Monitoring, Diagnostic and Control System (MDCS) had to be designed in order to measure electrical characteristics of the CRFE to be installed into Base Transceiver Stations for routine operation and field experiments with a single or multi-mast infrastructure.

The MDCS needed to have two basic simultaneous operating functions:

- CRFE transfer function monitoring and diagnostic with bypass switch control
- Cold finger temperature monitoring and cryocooler motor control.

with the possibility of increasing number of functions if a requirement exists.

The block-diagram of the MDCS designed in the course of this work is shown in Figure 7.21. The main component of the MDCS is a FPGA and digital signal processor (DSP) board. This board is equipped with a number of ADCs, DACs and digital inputs/outputs and can communicate with a local host computer via Ethernet, RS232, LPT or fibre-optic interface. The operation of the MDCS system is described below.

CRFE Transfer Function Monitoring, Diagnostic and Bypass Switch Control: This mode can be automatically activated by the program stored in the DSP board or by an operator from the local host computer any time. When the mode is enabled, the microwave switches route the signal from the antenna to the bypass line. By the same action the CRFE is connected to the measuring channel. The MDCS performs measurements of the transfer function of the CFE similar to those which could be done by a network analyser. The input signal is generated by a voltage controlled oscillator (VCO) which is phase-locked to a stable temperature compensated crystal oscillator (TCXO) of 1 MHz. By changing the programmable divider factor N from 20 to 80 the VCO generates frequencies from 1920 MHz to 1980 MHz with 1 MHz step. The transmitted signal at the CRFE output (RF) is down-converted to the intermediate frequency (IF) of 10 MHz by a double-balanced mixer. The local oscillator signal (LO) is derived by mixing the input signal with the 10 MHz signal from the TCXO. By doing this the LO signal is always 10 MHz higher then the RF signal. The IF signal is digitised by an analogue-to-digital converter (ADC) before being read by the central processor. The ADC is clocked with 40 MHz so that it samples the IF signal four times each period, allowing for digital I/Q detection. The insertion gain and insertion phase of the CRFE is calculated by comparison with stored I&Q values of the VCO signal at each frequency. The measured characteristics are sent to the local host computer and stored there. This data is compared with the previous measurements and if some degradation is found the alarm message is displayed. When the measurements are finished the microwave switches rout the signal from antenna back to the CRFE and to the BTS.

Cold Finger Temperature Monitoring and Cryocooler Motor Control: This function is perpetually active; the temperature of the cold finger is continually measured by a resistive thermometer (Pt 100) and the signal form the thermometer is digitised by an ADC and compared with the set value stored in the DSP. A pulse width modulated (PWM) signal is generated by the DSP according to the deviation of the measured and set temperatures. The PWM signal is used to generate an AC signal which controls the cryocooler's motor displacement, and consequently the cooling power of the cryocooler. As a result a constant cold finger temperature is maintained. If the required power exceeds the maximum allowed for a given cryocooler an alarm message is displayed at the host PC.

Soft-start and rapid warm-up functions are easily realisable using the same control processor and DSP board.
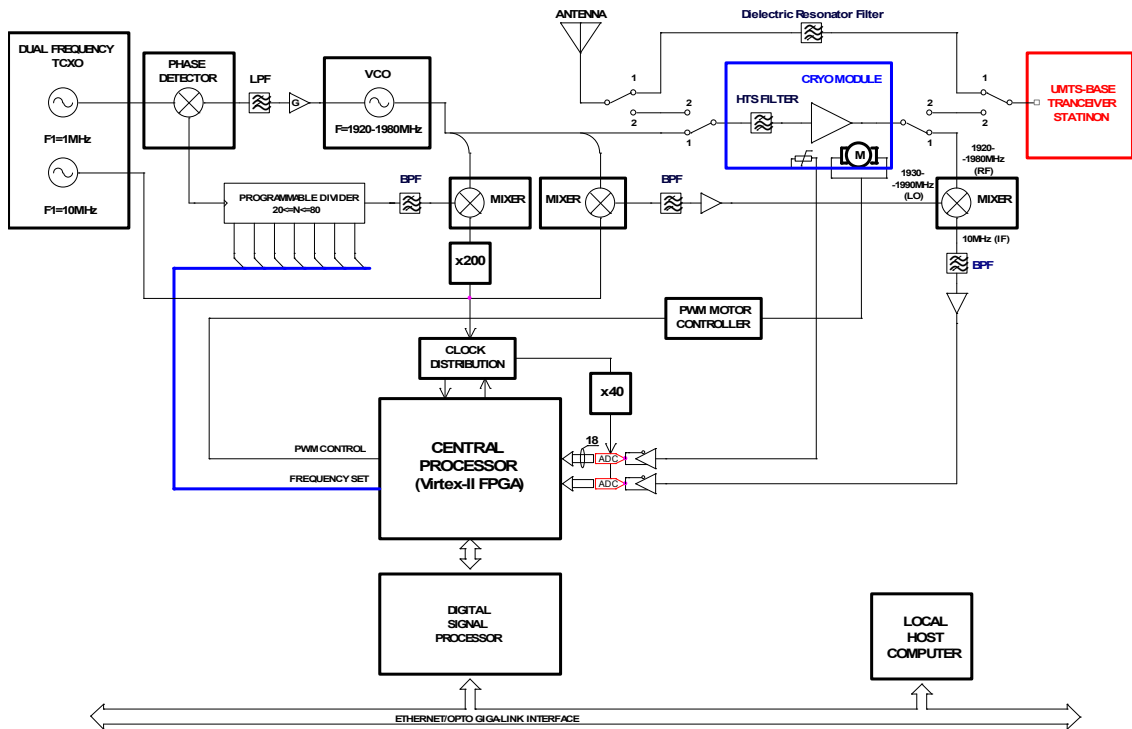
Figure 7.21 – Block-diagram of the built-in cryogenic front-end monitoring, diagnostic and control system

7.4 THE BEIJING FIELD TRIALS

The three and five mast field trials were held in Beijing's Haidian District in December 2005 using the same CRFE setup shown in Figure A.2. Some of the new hardware designed in the course of this work, such as the six channel setup and aluminium housed LNA (described in Chapter 7) was tested in this field trial using copies of the original system manufactured in China by Tsinghua University. This time, as well as the 'drive test' being performed, a 'statistics of service report' was produced based on quality of service (QoS) statistics generated during the field tests. The trials were expected to show the benefits of the CRFE by demonstrating a quantifiable:

- decrease in the average handset transmit power,
- reduction in the lost call rate,
- reduction in the access failure rate,
- and an increase in the Walsh code hours.

A cluster of five adjacent base stations in a high population and heavy traffic area were selected for the trials in order to evaluate the performance of the CRFE. Two different sets of data were analysed, first data from the drive tests and then the statistical data obtained in the quality of service report. Details of the test procedures and the results obtained are given in Appendix B.

7.4.1   ANALYSIS OF THE BEIJING FIELD TRIALS

As in the first field trial there was in this field trial in 2004 a significant decrease of 2.35dB in the handset transmit power in the CRFE enabled region in Beijing. This equates to a 72% improvement in coverage assuming that user numbers remain unchanged. Such an improvement in capacity, reduction in the frame error rate and a minimisation of cell breathing, which reduced the number of soft handoffs and therefore pilot pollution, and improved the Quality of Service metrics. The lost call rate was reduced by 16% in comparison to the trial region and 6.4% when compared to the district average (lost calls typically result from either a poor handoff to another base station or coverage black spots where building are degrading signal propagation).

The access failure rate with the CRFE installed was reduced by 41% and 21% when compared to the trial region and the district average respectively (access failures are a result of an incomplete setup handshake, which usually occurs in areas of poor and variable coverage such as in or near buildings or busy roads). The increased sensitivity of the CRFE meant that weaker signals from the handset were still distinguishable from noise and therefore previous black spots were covered effectively. As a result the quality of service provided by these CRFE fitted base stations has been improved. More users can successfully connect to and maintain communications with the base station.

On the basis of the field trials performance when fitted with the advanced CRFE it can be seen that the CRFE significantly improves CDMA BTS performance as compared to that with a conventional front end, in either urban or rural operating environments. However, in the author's opinion it was not possible to determine from these trials the extent of the improvement generated by each of the critical components.

7.5   FINAL COMMENTS ON THE CRFE FIELD TESTS

Both sets of field trials (Wunongchang and Beijing) demonstrated that the CRFEs, described in Chapter 5 and Chapter 7, which utilised the HTS filter and cooled LNA reduced the average handset transmission power by between 2.35dB and 3.114dB. The effect of the reduction in required average handset transmit power improved coverage and capacity, reduced cell breathing, lost calls and access failures. Additionally users should have experienced longer battery life in their handsets and better voice quality, although these metrics were never measured. The results are particular impressive given that the system has been operating as an "intruder", which, due to the presence of the standard operating equipment, has marginally reduced performance. Theoretically the developed CRFEs would operate at even higher performance if not operated as intruder systems, but as integrated parts of the base station.

The performed tests have shown that the manufactured CRFEs provided a significant performance advantage over the conventional technology, confirming that this technology is technically superior and applicable. Demonstrator D6 has been operational in Wunongchang base station for more than 2 years, demonstrating not only improved system performance but also the reliability of all the system components. However, it was more difficult to determine its economic viability; whether the performance increase is significant enough to justify the added expense of manufacturing, installing and maintaining a

suitable CRFE. In order to optimise the performance versus investment ratio it is important to know exactly how each of the improved front end parameters (insertion loss, selectivity and the linearity of the LNA) were responsible for the improvement seen in the results.

It is suspected that the improvements seen in the field trails were primarily due to the presence of the highly linear LNA, rather than the HTS filter. Because the CDMA channels are only 1.25MHz wide, the highly selective HTS filter still selects multiple channels close to channel of interest, which means there will be a level of inter-modulation distortion produced in non-linear components which the filter can not eliminate. The improved linearity of the LNA, can significantly reduce the IM products that could degrade system performance and is the most likely source of the improvements in these field trials. The advantage of the low insertion loss and noise of the HTS filter was largely unrealised due to the presence of the old duplexer after the main antenna in the tested base stations. Additionally the advantages of the selectivity are difficult to judge accurately due to the lack of available data about the Chinese spectrum from 800MHz to 900MHz.

In order to fully assess the necessity and importance of using HTS filters in advanced wireless front end technology it seemed logical to consider using alternative filter types with the same LNA. Specifically modern dielectric resonator filters were chosen to be investigated as an alternative high performance filter technology for wireless base stations.

CHAPTER 8

NOVEL DIELECTRIC RESONATOR FILTER

TECHNOLOGY FOR WIRELESS FRONT ENDS

Based on the simulations done using the CDMA Uplink model presented in Chapter 6 analysing the coverage and capacity of various systems in different situations and the results of the field trials of the developed CRFEs, several important front end parameters were identified as critical to improve wireless base station performance; namely

- Low system noise,
- Low noise amplifier of high dynamic range, and
- High filter selectivity

Achieving these parameters does not necessarily require the use of a costly CRFE utilising HTS filters and cooled low noise amplifiers. System noise comparable to that of a ground base CRFE can be achieved by tower mounting the conventional front end (providing weight allows for it). Installing the same modern LNA of high dynamic range as designed by Cryoelectra in the base station improved the system specifications such that they are close to those of the CRFE enable base station. The high selectivity and low insertion loss exhibited by HTS filters can also be achieved in a compact package by dielectric resonator filters operating at room temperature. The advantage of using HTS filters in a CRFE is that the entire front end, including the LNA, is cooled to cryogenic temperatures and therefore has a lower thermal noise figure, meaning that it is the optimum solution from a technical stand point. From an economic point of view, a solution that can provide similar performance with only slightly reduced coverage and capacity, at a significantly reduced cost is preferred.

As mention in Chapter 3, dielectric resonator filters have long been used as satellite communications filters operating in the L-Band and C-Band, with notable advanced design research by Mansour [98] and Klien [99]. More recently low loss DR filter have become of interest in terrestrial wireless applications [100]. This chapter investigates the practical suitability and engineering design complexity of DR filters. Two DR filters have successfully been designed by the author of this thesis at UMTS receive and transmit frequencies because of the high power handling capabilities of dielectric resonators and are the focus of the discussion. Although only the major design points are considered in this thesis the complete design procedure is available from two reports published internally at Cryolectra GmbH [101, 102].

The success of the DR filter designs at 1900MHz (UMTS receive) and 2100MHz (UMTS transmit) lead to two new concepts incorporating DR technology alone or combined with HTS technology, namely:

1. A DR duplexer to replace the cavity duplexers used on the main antennas in today's base stations. As is explained further in Section 8.2, the DR duplexer can be used either as a direct

replacement for the existing duplexer or combined with a CRFE to give the highest possible base station performance achievable today.

2. A very high performance multi-operator combiner utilising DR and HTS technology that allows service providers to share the same antenna on one base station without a significant impact on system performance compared to a single operator base station is also presented in Section 8.3.

8.1   DIELECTRIC RESONATOR FILTERS FOR UMTS SYSTEMS

The UMTS band was selected for the dielectric resonator filter designs due to the high interest in UMTS systems in Europe. A dielectric puck purchased from Kyocera and enclosed in a quadratic cavity, as shown in Figure 8.1, was designed to have a base frequency at 1920MHz and be tuneable to each channel in the UMTS receive band (1920MHz – 1980MHz). A circular cavity would have the more obvious solution, but to facilitate the manufacturing and easy coupling of resonators the quadratic design was selected. The resonant frequency tuning of the dielectric resonator was achieved by using a metallic plunger of slightly larger radius than the dielectric puck inserted into the roof of the cavity (Figure 8.1 right). To minimise the conductive losses and maintain an acceptable cost the hosing and tuning elements were made from silver coated brass.
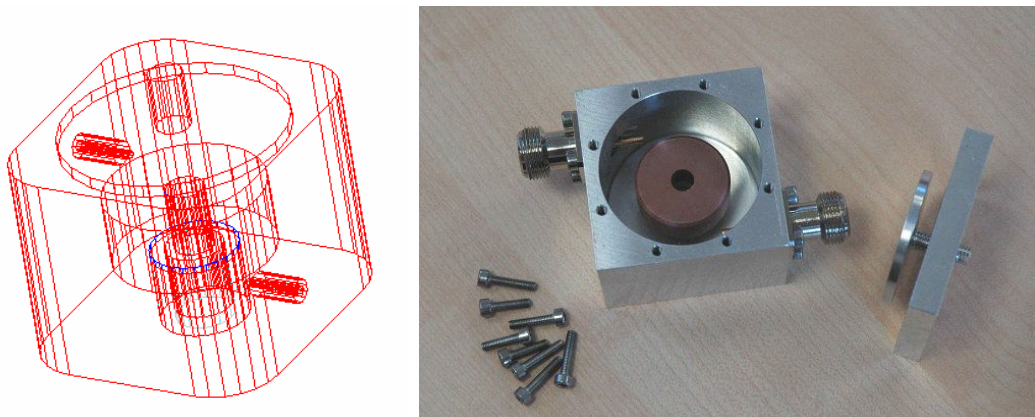
Figure 8.1. Dielectric Resonator (Left: HFSS Final Design, Right: Manufactured Initial Design)

In order for the manufactured DR filter characteristic to be as close as possible to the simulated characteristics it was necessary to measure precisely the relative permittivity, stated by the manufacture to be between 39 and 42, and unloaded quality factor, of approximately 50000, of the dielectric pucks. A simple circular cavity of a radius much larger than that of the dielectrics was used for the measurement of the Q-factor. It is well known that using a cavity with a very large radius minimises loess in the housing. The measured value of Q_0 of the dielectric puck was 28800 at 1.8888GHz and the relative permittivity (ε_r) was obtained as 40.42. The measured Q_0 implied that impurities may have developed on the surface of the dielectric puck and ultrasonic bath cleaning may be required or the housing losses were influencing the result more than expected in the manufactured resonator. Measurements of the unloaded Q-factor of the manufactured DR as it was tuned to higher frequencies in the UMTS range are presented in Figure 8.2. The results show that the DR maintains a respectable Q_0 of over 19000 at 1.98GHz which confirmed that this resonator was suitable for the entire UMTS receive range.
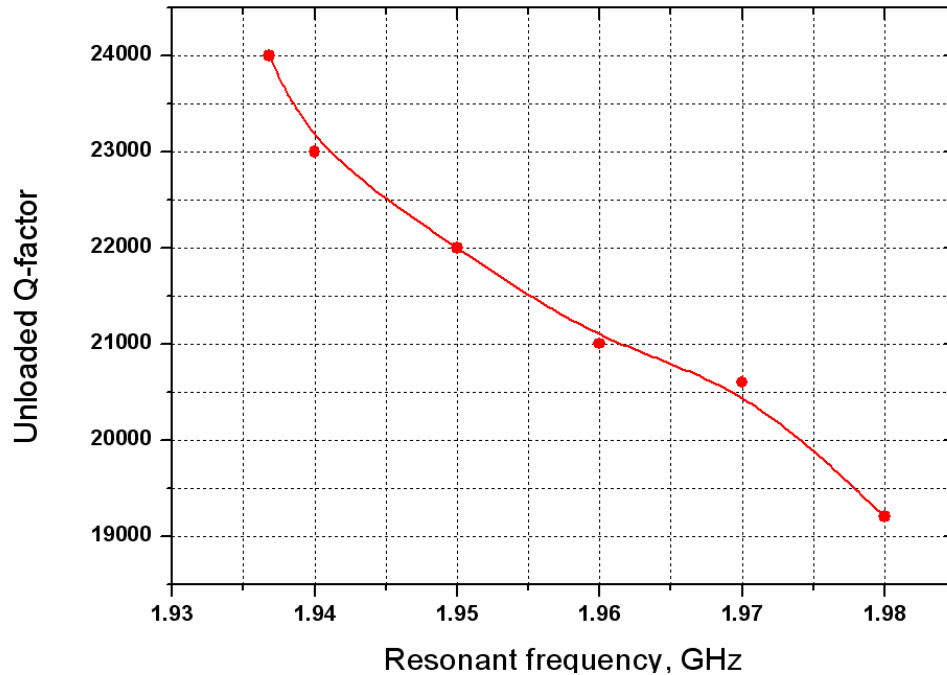
Figure 8.2. Measured Q-factor vs. Resonant Frequency of the Dielectric Resonator

Two DR filters have been designed and manufactured, namely a four pole filter and a nine pole filter, using the 1900MHz pucks described above. A CAD drawing of the 4 pole filter is shown in Figure 8.3 and the simulated performance is presented in Figure 8.5. Adjustable trim rods were used to trim the coupling between resonators and port coupling was achieved through antennas which followed the curve of the puck. The trim rods are specially made silver plated brass screws with a 0.5mm thread which are used to open and close the openings between the resonators and adjust the coupling. Tuning of the individual resonators was achieved using silver plated brass screws which had a large lid on one end. This lid could be moved closer to the dielectric thereby reducing the cavity size and increasing the resonators frequency (and losses too). Once again the filter cavities were manufactured using silver plated brass housing. The manufactured 4 pole DR filter shown in Figure 8.4 yielded the measured response after tuning given in Figure 8.6. A close up of the simulated and measured passband responses is shown in Figure 8.7 and Figure 8.8 respectively.
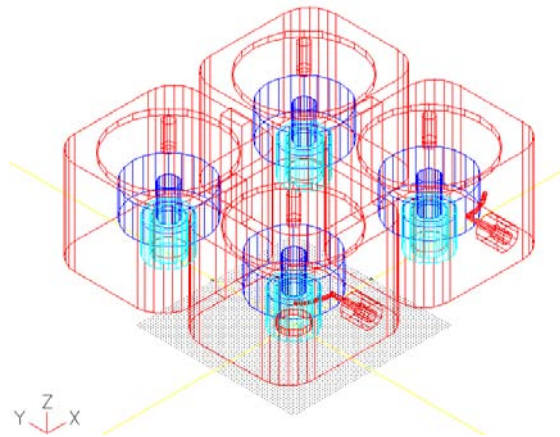
Figure 8.3. CAD drawing of 4 Pole DR Filter as seen in HFSS
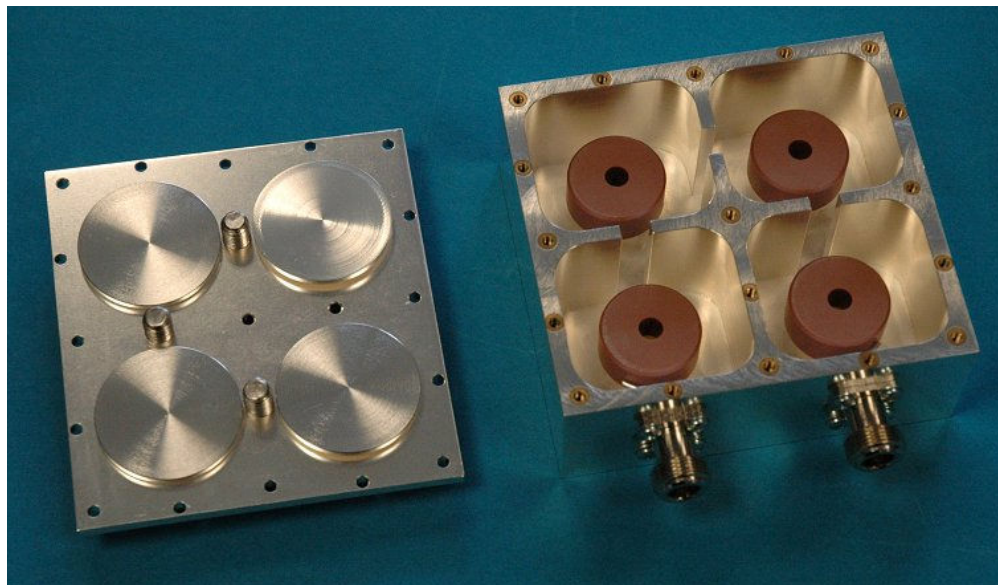
Figure 8.4. Manufactured 4 Pole Rx DR Filter (Note: Coupling Windows between Resonators and Corresponding Adjustable Trim Rods and Tuning Plates in the Lid)
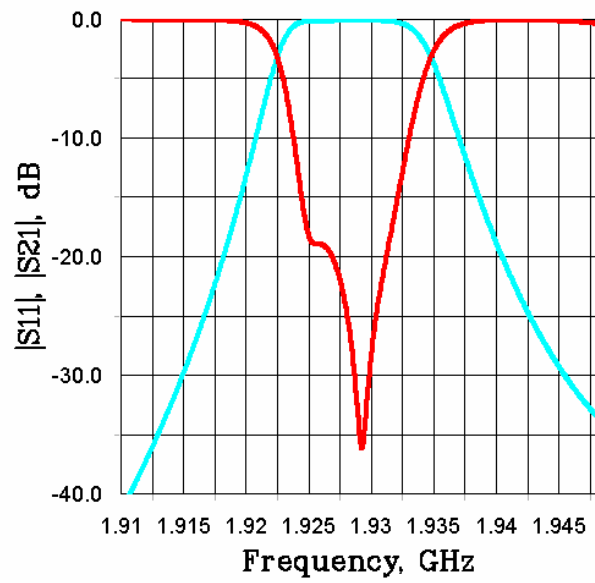
Figure 8.5. Simulated Frequency Response of 4 Pole Rx DR Filter using HTSS (S_{21} – Blue, S_{11} – Red)
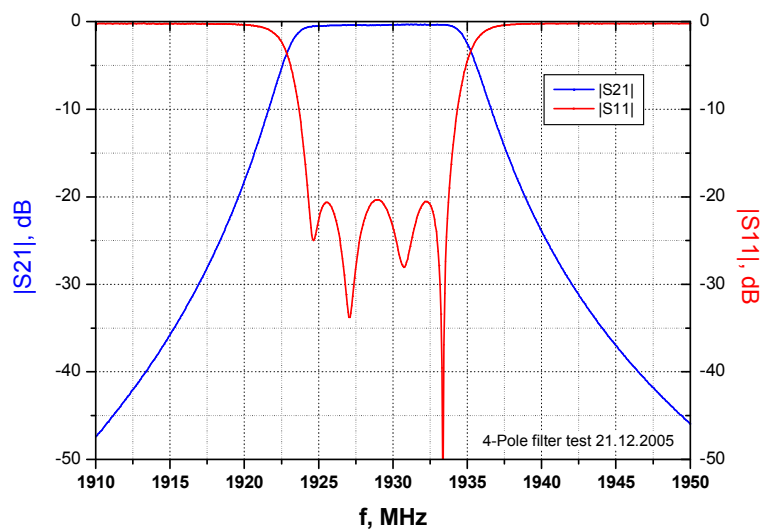
Figure 8.6. Measured 4 Pole Rx DR Filter Response
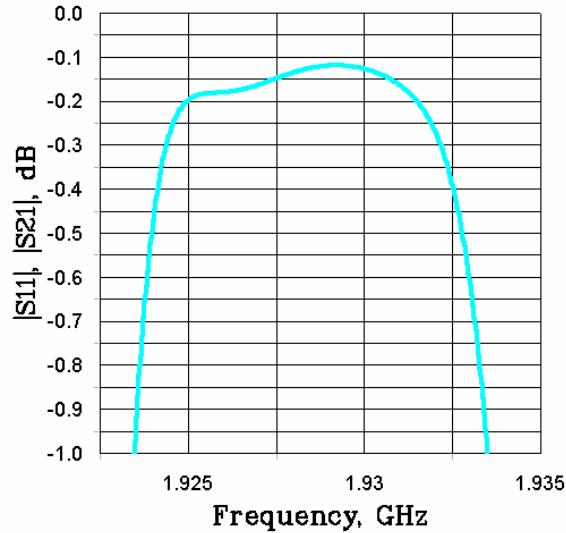
Figure 8.7. Simulated 4 Pole Rx DR Filter Passband Response ($Q_0 \approx 40000$)
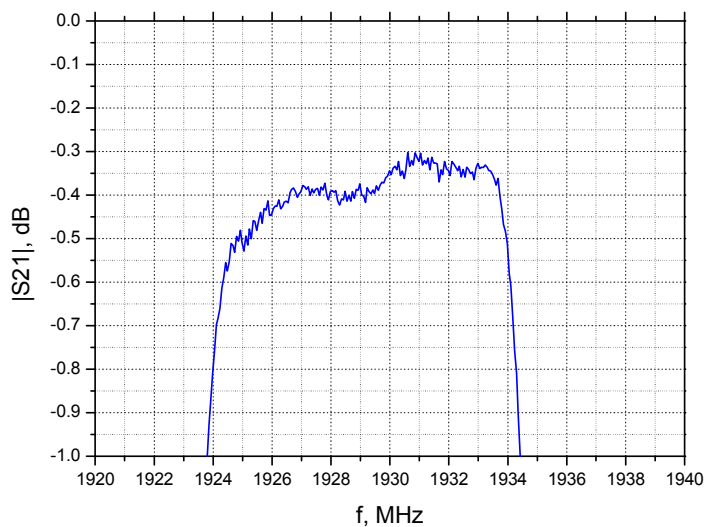
Figure 8.8. Measured 4 Pole Rx DR Filter Passband Response ($Q_0 \approx 20000$)

Because the cavity was simulated as made of an ideal conductor (to reduce simulation times) the unloaded Q-factor of the manufactured filter is significantly lower than the simulated Q_0 values. The losses in the simulation are due to the loss tangent of the measured dielectric puck only. Despite this simplification to the simulation the measured and simulated responses look very similar, but the measured one has a lower Q_0.

In order to be applied to the European UMTS systems the final DR filter required an operational bandwidth of 9.15MHz (to cover two neighbouring channels owned by one service provider) and an

insertion loss of less than 1dB. The attenuation was to be at least than -40dB, 1MHz from the passband edge, to achieve the 30dB isolation required between UMTS channels. Using a Chebyshev filter characteristic it was possible to achieve a selectivity of 17.9dB/MHz with an 8-pole, 23.3dB/MHz with a 9-pole and 28.6dB/MHz with a 10 pole, none of which satisfied the requirements. A design with more than 10 poles would be physically large and parasitic losses in the resonators would have made it difficult to achieve the desired 1dB insertion loss. Introducing a cross coupling to create a quasi-elliptic filter meant that an 8-pole filter with 1 cross-coupling produced a roll-off of 34.9dB/MHz, 2 cross-couplings produced 56dB/MHz but this solution was not selected because of the undesirable need to cross-couple using the port resonators in order to create the quadruplets (Figure 8.9). The final filter design was selected to have nine poles with one cross-coupling to give a 51.1dB/MHz roll-off.
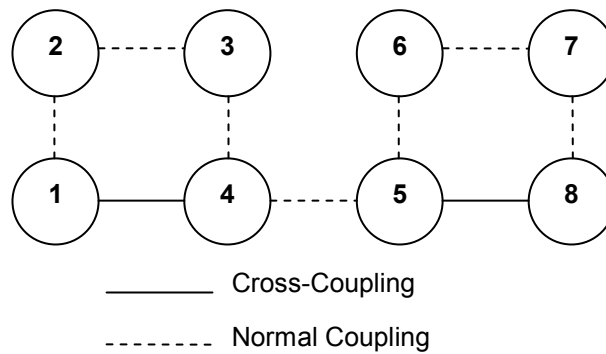
Figure 8.9. Eight Pole Filter Design with 2 Cross-Couplings

The 9-pole DR filter CAD drawing is shown in Figure 8.10. The design has had the couplings pre-tuned to the lowest frequency channel in the UMTS receive band (Figure 8.11) allowing tuning to higher frequency channels to take place using tuning plungers.
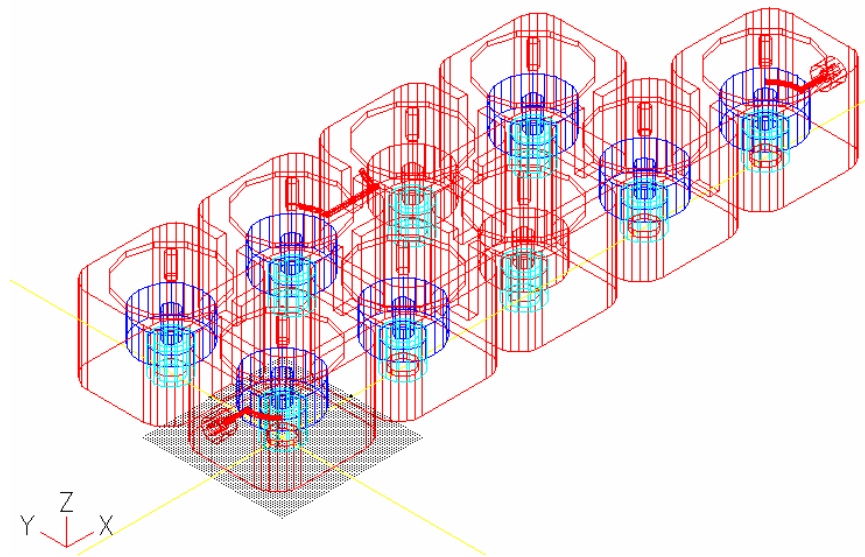
Figure 8.10. CAD drawing of 9 Pole DR Filter as seen in HFSS
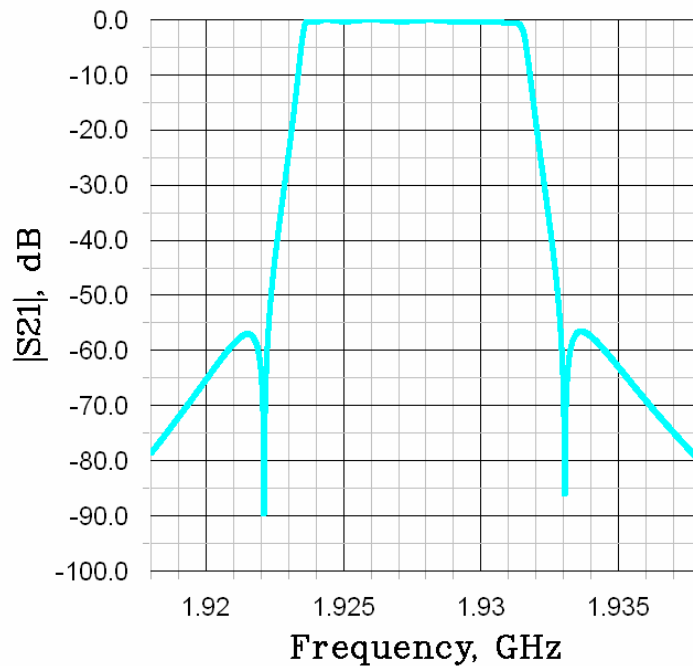
Figure 8.11. Simulated Frequency Response of 9 Pole Rx DR Filter

The UMTS transmit band frequencies (2110 – 2170MHz) were achieved using a set of dielectric pucks manufactured for 2.1GHz. The manufactured transmit filter (Figure 8.12) was tuned to give a Chebyshev response which exhibited approximately 20dB matching across the passband. The prototype filter characteristic centred at 2115MHz with a 6MHz bandwidth and better than 21dB matching across the passband (Figure 8.13). The insertion loss of 1dB and the steepness in the transition region suggested a Q-factor of higher than 20000. The bandwidth was narrower than the target of 10MHz due to the coupling being too weak between the resonators. The weak coupling was caused by the coupling windows between resonators 1 and 2, 2 and 3, 7 and 8, and 8 and 9 not being large enough to achieve the target 10MHz bandwidth. However, this allowed for the opportunity to test a more exciting prospect of using this filter for channel selection of 5MHz bandwidth, not just for operator selection (10MHz bandwidth).
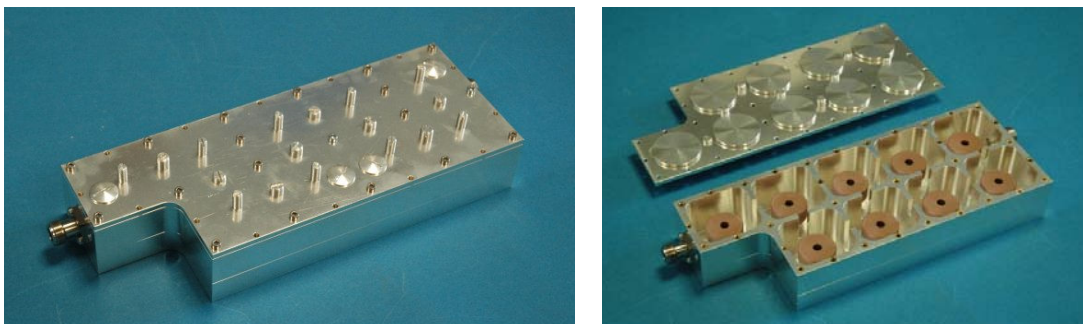
Figure 8.12 Photograph of the 9-Pole DR Filter for the UMTS Uplink (left: complete package, right: open lid)
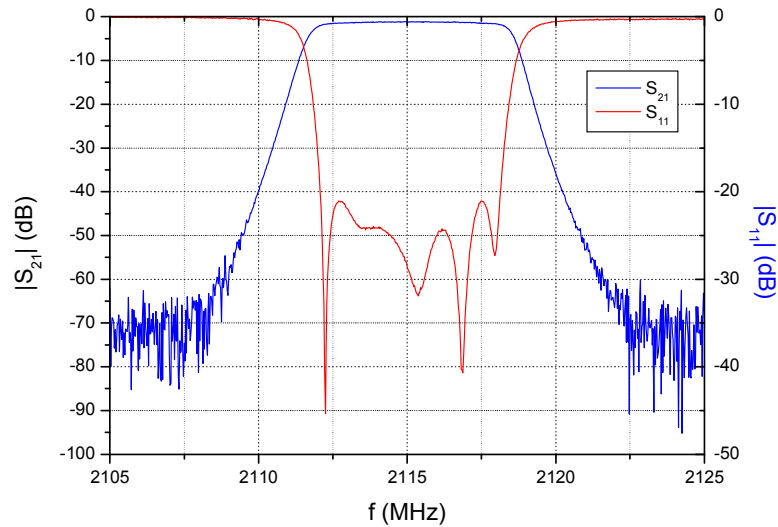
Figure 8.13. Measured Chebyshev Response of the 9-Pole Tx DR Filter Showing -21dB matching at 2115MHz with 6MHz Bandwidth

The cross coupling was added to the housing (Figure 8.14) to obtain a quasi-elliptic response (Figure 8.15). With cross couplings the filter characteristic exhibited better than 21dB matching across a 5MHz passband with a centre frequency of 2116MHz. The measured skirt steepness of the Tx filter was 40dB/MHz with two symmetric transmission zeros at the band edges. Compared to the calculated ideal response of a Chebyshev filter described by Matthaei, Young and Jones [52] it is estimated that the insertion loss of 1.076dB (Figure 8.16) and rounding of the passband equates to a Q-factor of approximately 25000.
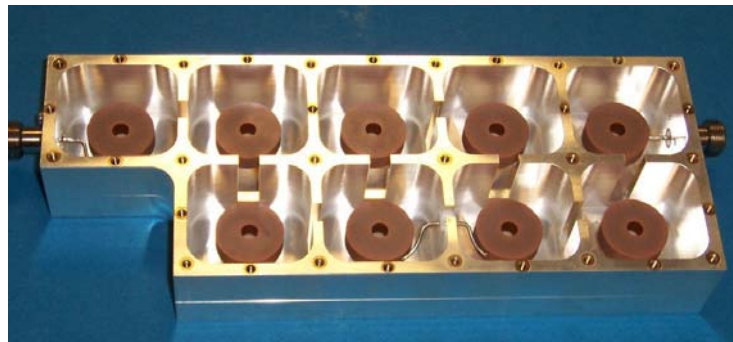
Figure 8.14. Photograph of the 9-Pole-Uplink UMTS-Filter with Cross Coupling (Open Lid)
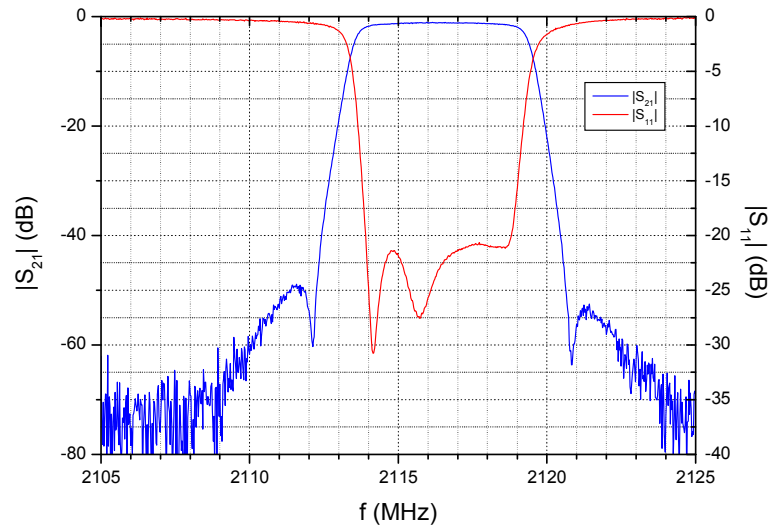
Figure 8.15. Measured Quasi-Elliptic Response of the 9-Pole Tx DR Filter Showing -21dB matching at 2116MHz with 5MHz Bandwidth
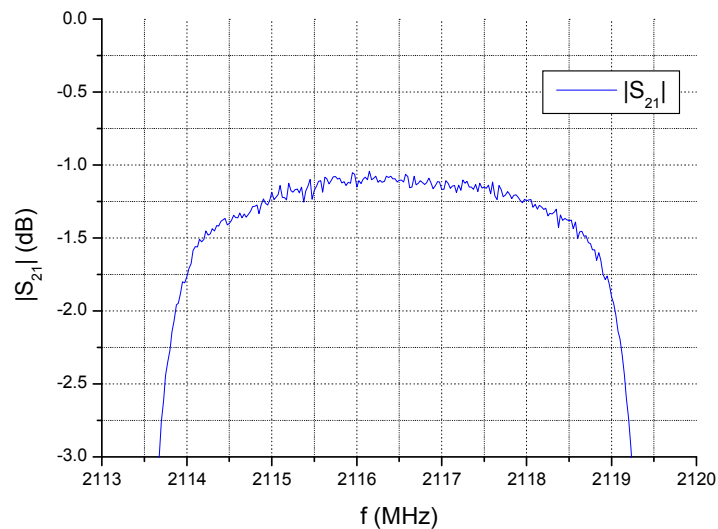
Figure 8.16. Measured Quasi-Elliptic Response in the Passband of the 9-Pole Tx DR Filter

The success achieved with the 9-pole DR filters at 1925MHz and 2115MHz paved the way for the conceptual design of a DR duplexer. A DR duplexer that exhibits lower loss and higher selectivity than the cavity duplexers currently used on the main antennas of conventional cellular base stations can offer performance improvements as suggested by simulations using the CDMA Uplink model. Two novel duplexers have been designed in the course of this work; the first to be used as an economical solution to replace the conventional cavity filters. The second is using the DR duplexer in combination with the CRFE to provide the ultimate in front end performance. Both duplexers are described below in Section 8.2. Additionally the DR filters can also be applied to an advanced Multi-operator Combiner (MoC), to

utilise the increased selection and low losses of DR filters and HTS filters to produce a greatly improved system when compared to currently available MoCs. The concept of this novel MoC is presented and compared to a current state MoCs in Section 8.3.

8.2 NOVEL CONCEPT OF DIELECTRIC RESONATOR DUPLEXERS

A dielectric resonator duplexer could be a suitable upgrade from conventional cavity duplexers, providing improved signal selection, protection and reduced noise. As mentioned earlier in this chapter the success of the DR filter designs for both receive and transmit bands of UMTS networks lead to the conceptualisation and development of a DR duplexer. It is proposed by the author of this thesis that two DR filters (transmit and receive) are joined and separate antennas split from the main antenna are inserted into the last resonator of the transmit filter and the first resonator of the receiver filter to create a DR duplexer for main antenna of a UMTS base station. Care has to be taken to ensure the two filters do not couple, although this is not too difficult due to the frequency spacing of the UMTS Tx and Rx bands. A DR duplexer for CDMA is also possible, however the modifications to the port resonators to prevent coupling may be more significant than those required for the UMTS duplexer, due to the proximity of the CDMA transmit and receive bands.

As mentioned in Chapter 2 the duplexers are used to protect the sensitive receiver section on the main antenna from the substantially more powerful transmitted signals. If these duplexer are to be used with CRFE it is important that this duplexer attenuates sufficiently the transmit signal (which would cause non-linearities and even destroy the superconductivity). At the same time the duplexer must minimise the noise it introduces to the received signal as any noise introduced before the LNA would contribute negatively to the SNR of the system. Two possible options to achieve the highest levels of base station performance using DR duplexers investigated in this thesis are;

Option 1: Dielectric Resonator Receiver Front End (Figure 8.17)

- A DR duplexer at the main antenna serves as Rx-filter and Tx-filter.
- A DR Rx-filter at the diversity antenna.
- Rx- and Tx-filters are 5 or 10MHz bandwidth (depending on the channel allocations to providers and the usage of those channels).
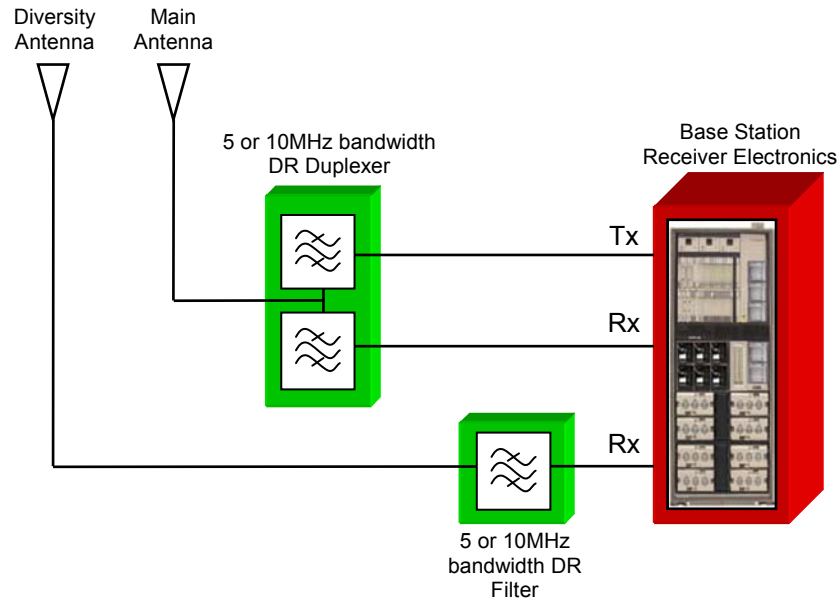
Figure 8.17. Option 1 – DR Duplexer Front End

The proposed Option 1 is a non-cryogenic solution where the filtering of transmit and receive channels (5MHz) or provider blocks (10MHz in Europe) will be done using the DR duplexer on the main antenna and a DR filter on the diversity antenna (Figure 8.17). Traditional cavity duplexers select the entire 60MHz receive band and rely on base band and digital filtering to perform the channel selection. The drawback of this approach is the inter-modulation distortion created in nonlinear components (such as the low noise amplifier) due to the existence of adjacent UMTS channel signals. With an ideal amplifier inter-modulation distortion would not exist to degrade the systems performance, but this is not the case with current technology. Hence a pre-selection filtering of the channels using either 5MHz or 10MHz bandwidth DR filters (depending on the required setup) is a good way to reduce or eliminate this source of interference. On the transmit side, filtering specific UMTS channels before they are transmitted (again either 5MHz of 10MHz bandwidth depending on the channel allocations and usage) will reduce channel leakage created by non-linear components spreading the transmission signal.

Option 2: Cryogenic Receiver Front End with Wideband DR Duplexer (Figure 8.18)

- A DR duplexer at the main antenna serves as the Tx-filter and a wideband Rx-filter protects the HTS Rx-filters in the CRFE.
- HTS Rx-filter at the diversity antenna.
- 5 or 10MHz bandwidth DR Tx-filter (bandwidth dependant on the channel allocations to providers and the usage of those channels).
- 60MHz DR Rx-filter with low insertion loss to cover the entire UMTS band to protect the pre-selection receiver HTS filters of 5MHz or 10MHz bandwidth.
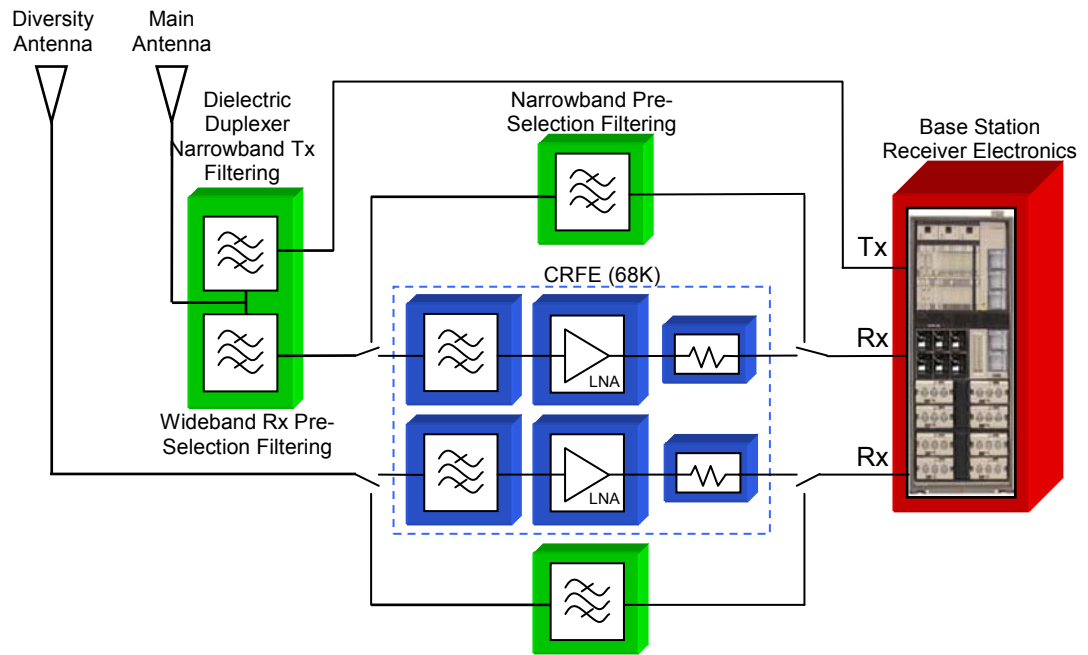
Figure 8.18. Option 2 – Wideband DR Duplexer and CRFE

The proposed Option 2 utilises the developed CRFE for filtering the receiver side signal in the main and diversity antennas (Figure 8.18). The receive side of the duplexer is 60MHz with a low number of poles to minimise insertion loss. This is because the CRFE is responsible for the channel selection while the receive side of the DR duplexer is only used to protect the HTS filters in the CRFE from the high power transmit signals. The transmit side filter is the same transmit filter as in the DR duplexer discussed in Option 1. This setup is predicted to have the highest selectivity and sensitivity of any front end available today, resulting in the best cellular base station performance.

Simulations to verify the proposed duplexers were done using Agilent Advance Design System (ADS). Due to the frequency spacing of the UMTS transmit and receive channels, designing the duplexer only required coupling the input from the antenna to the two correct lumped element filters in ADS. The Option 2 duplexer shown below in Figure 8.19 has a 60MHz four pole one cross coupling DR filter on the receive side and an 5MHz, eight pole, one cross coupling filter at the first transmit band (2110 – 2115MHz) on the transmit side. It was calculated that to obtain the specified -45dBc minimum channel isolation in the transmit band, the unloaded quality factor of the filter needed to be greater than 28000. Although the required Q_0 is slightly greater than what was achieved with the DR filter prototype, refinement of the housing and tuning plates would probably result in an improvement to meet the specification. The simulated characteristic of the DR duplexer showing the 5MHz bandwidth transmission response (S_{31}), 60MHz reception response (S_{21}) and the reflection (S_{11}) is given in Figure 8.20. A close up of the transmission response at 2110MHz is presented in Figure 8.21.
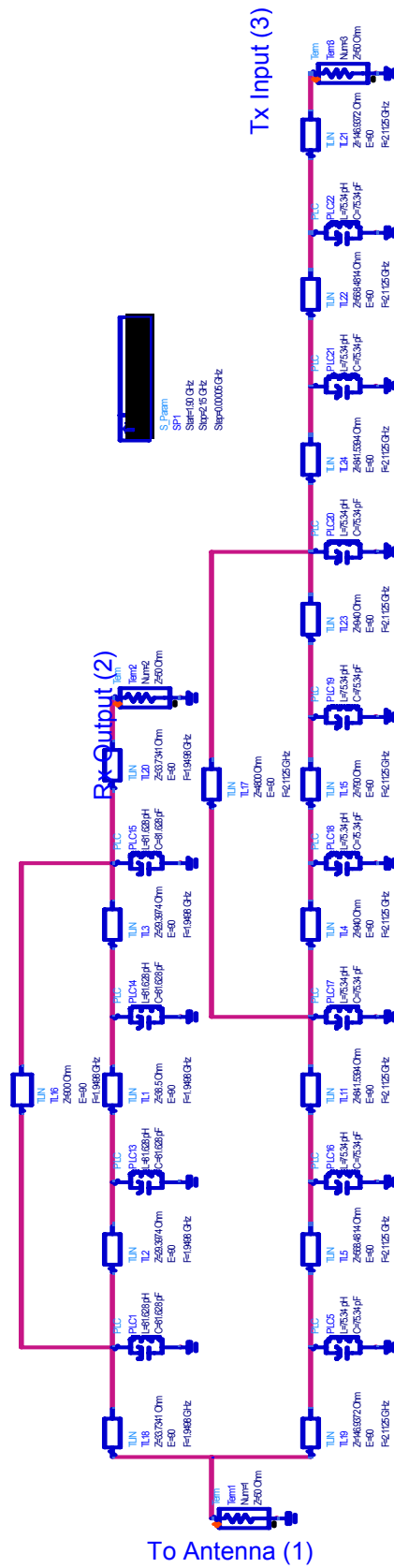
Figure 8.19. DR Duplexer Lumped Element Circuit Model
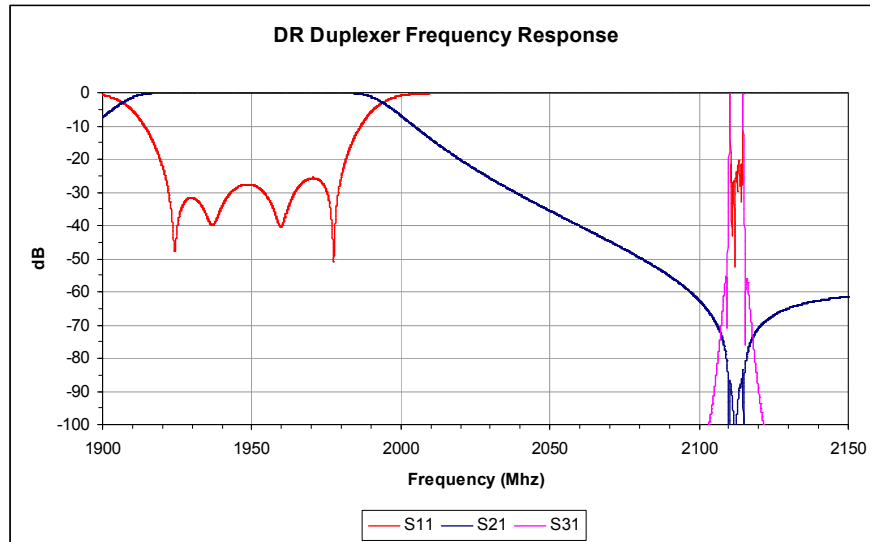
Figure 8.20. DR Duplexer Response of Transmit and Receive Channels
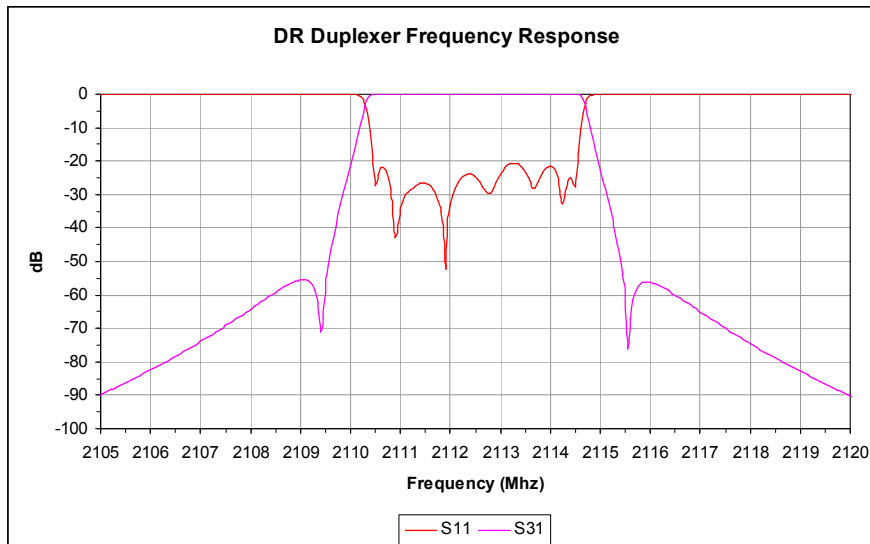
Figure 8.21. DR Duplexer Close Up of Transmit Channel Response

While current cellular systems may benefit from the improved front end performance by using one of, or the combination of, DR and HTS technology, an even more significant effect of very high performance filter technology could be in Multi-operator Combiners.

8.3 NOVEL CONCEPT OF ADVANCED MULTI-OPERATOR COMBINERS

As described before, the two advantages offered by HTS filters over existing cavity filters are:
1. Reduced insertion loss (noise)
2. Improved selectivity

The present wireless standards and frequency allocations in most regions are designed based on metallic cavity filters (briefly described in Chapter 3.2). Improving the selectivity of the filters is only necessary in

situations where another wireless service is operating very close to the cellular band, such as in some parts of the USA where another wireless service is placed in the middle of the mobile phone spectrum [103]. In Europe and most other parts of the world, due to the good radio spectrum management, there is currently no necessity for very high selectivity and the noise reduction is the only benefit (as was demonstrated in Chapter 6 and Chapter 7). However it is the author's opinion that even in this situation it is possible to take advantage of the high selectivity of HTS and DR filters by implementing them in a Multi-operator Combiner (MoC).

A Multi-operator Combiner (MoC) allows a number of operators (up to 6 in the case of Europe) to use the same antennas and mast to operate their portion of the mobile spectrum. The MoCs have great potential for use with indoor antennas such as those in subways, large tunnels, airports, large shopping malls, stadiums, and office buildings, where it is not feasible for each operator to deploy its own antennas. There is a potential for using the MoC outdoors too, in order to reduce the number of antennas erected in metropolitan and dense suburban areas and curb people's growing animosity towards them.

A conventional MoC splits the received UMTS signal into two, such that the 10MHz channels can be isolated using conventional cavity filters, as illustrated in Figure 8.22. Unfortunately this process causes each half of the signal to have only 50% of the original power, meaning that there is 3dB of attenuation caused by the splitting process. Examples of conventional MoCs currently available can be found in references [104-107]. A MoC which implements highly selective HTS or even DR filters would not require the incoming signal to be divided because the HTS filters can achieve the desired channel isolation of over 35dB. Due to the significantly smaller losses in both dielectric resonator and cryogenically cooled HTS filters the proposed MoC will have appreciably better operator band isolation and a reduced noise figure. Additionally by using DR filters on the transmitted signals from each operator the transmission spectrum could be "cleaned up" too.
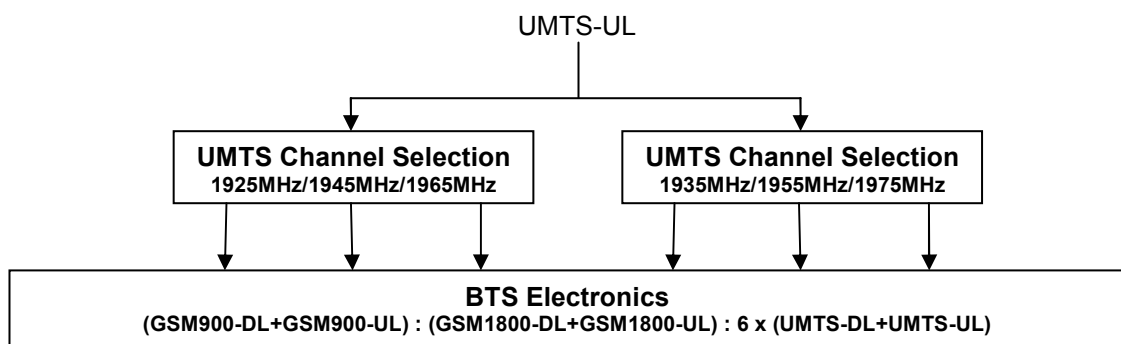
Figure 8.22. Block Diagram of a Traditional MoC Splitting the UMTS Signal for Filtering with Cavity Filters

Figure 8.23 shows a block diagram of how the transmit and receive signals would be distributed in the MoC proposed in this thesis for the European spectrum allocation. Elements shown in green represent dielectric resonator filter elements. A single wideband antenna will be used to receive GSM900,

GSM1800 and UMTS. A basic LC-duplexer will be used to isolate the low frequency GSM900 signal from the high frequency GSM1800 and UMTS signals. A Combline duplexer connected directly to the BTS electronics will then be used to isolate the GSM900 downlink and uplink signals. On the high frequency side a combline quadruplexer will be used to separate the GSM1800 and UMTS downlink and uplink signals like in a conventional BTS, except that only the GSM1800 signals connect directly to the BTS electronics. The UMTS signals will be connected to a pair of DR hexaplexers which isolate the 10MHz operator blocks.
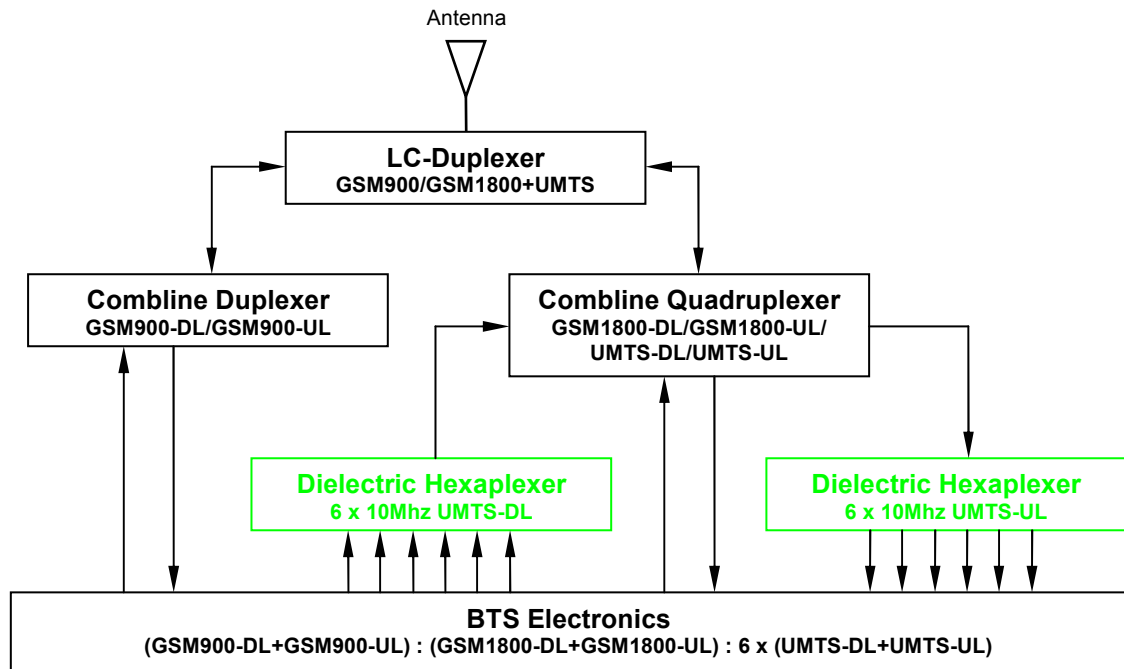
Figure 8.23. Block Diagram of a Dielectric Resonator MoC

Figure 8.24 presents a higher performance MoC with the HTS filter and LNA combination from the CRFE on the receive side (shown as the blue element). The same dielectric hexaplexer is used on the transmit side as with the first MoC design due to the high power handling requirements on transmission filters.
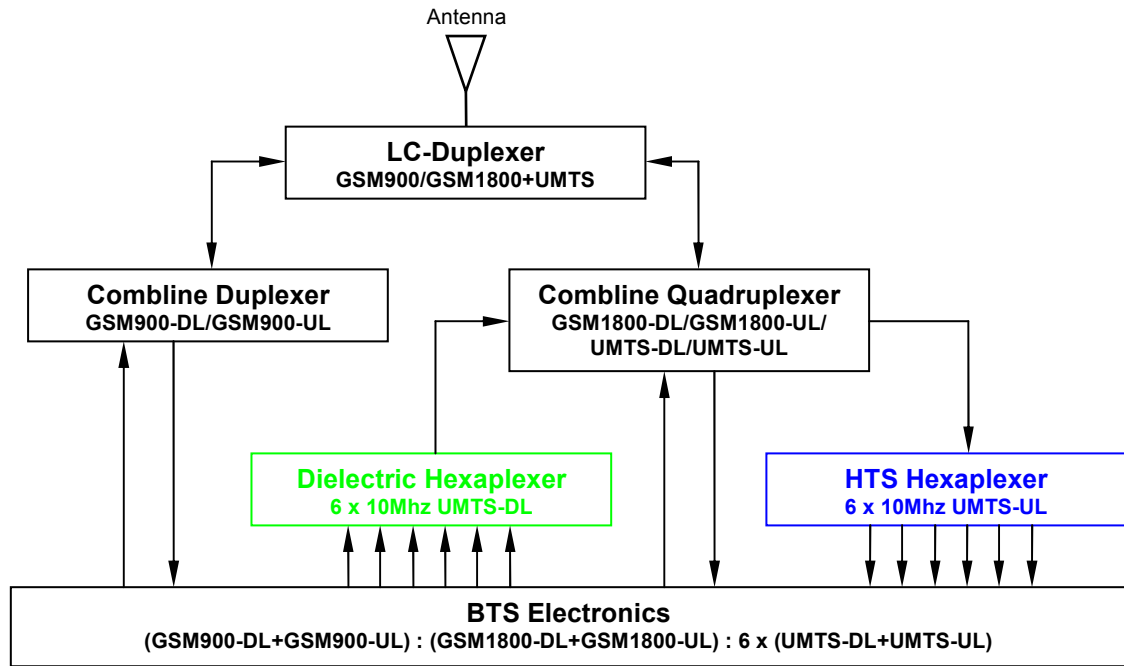
Figure 8.24. Block Diagram of the DR and HTS MoC

The second proposed MoC shown in Figure 8.24 utilises all the same subsystems for the HTS hexaplexer as the developed CRFE discussed in Chapter 7 plus some additional signal distribution manifolds. One of the complexities of designing such a MoC will be in the design and tuning of a suitable manifold to distribute the incoming signal to the six pre-selection filters. If the manifold is mistuned then reflections from the different channels will increase the noise on incoming signal significantly. Simulations suggest that the concept will work and designing the manifold is possible; however a hardware implementation has not been done in the course of this thesis. The simulated frequency response required for successful implementation of the receiver HTS hexaplexer used in this MoC is shown in Figure 8.25. Table 8.1 shows the possible improvement due to the proposed DR and combination DR and HTS MoC over one of the conventional MoC currently in use in Europe.
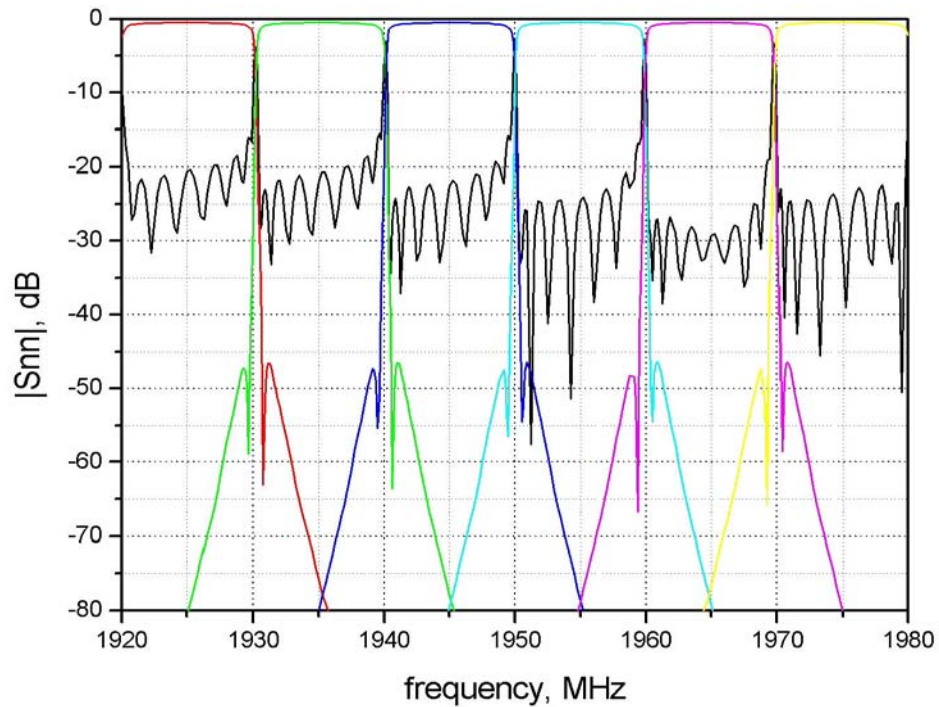
Figure 8.25. HTS Hexaplexer Simulated Frequency Response

Table 8.1. Comparison of Important Parameters of Proposed and Conventional MoC

Front End Parameter	Frequency Range	Conventional Cavity Multi-Operator Combiner	Proposed Dielectric Multi-Operator Combiner	Proposed Cryogenic Multi-Operator Combiner
Attenuation (dB)	1920-1980	4.8	1.8	0.4
	2110-2170	4.8	1.8	1.8
Noise Figure (dB)	1920-1980	6.6	2.7	0.9
	2110-2170	6.6	2.7	2.7
Maximum Transmission Power (W)	2110-2170	50	50	50
Isolation between channels (dB)	1920-1980	25	35	50
	2110-2170	25	35	35

While the MoC proposed in this thesis has not been implemented, the possibility of its implementation to improve cellular communication is clear. Aside from the performance benefits mentioned in Table 8.1, cost sharing between operators makes the MoC economical to deploy in a shared base station when compared to the cost of each operator building their own base station. Additionally the reduction of the number and density of base stations due to the antenna sharing have environmental benefits. For these reasons the MoC presented which utilises HTS and DR technology is considered to be a significant item of future development in wireless telecommunications.

CHAPTER 9

DISCUSSIONS AND CONCLUSIONS

Since the early 1990s HTS RF filters have demonstrated the highest unload Q-factors in the smallest packages of any modern day filter. The expense incurred in overcoming difficulties, such as cooling, coupled with current wireless communications standards, which do not require very highly selective filters, resulted in this technology being largely dismissed by the telecommunications industry, leaving it firmly in the realm of academia. But the early dismissal of HTS RF filters by industry does not necessarily imply that the technology can not be an important technological contribution to wireless communications, only that the market was not ready for what was being offered or what was being offered was not ready for the market.

Through the course of this thesis various tools have been developed to show whether HTS filters can already be reliably used in the market and if their benefits are quantifiable and significant.

1. The first of these tools was the development of a fully operational cryogenic receiver front end (Chapter 7). The CRFE housed six specifically designed CDMA filters made from YBCO thin films on a sapphire substrate, each connected to a high dynamic range LNA. These elements were supported by a either a Laybold or Ricor Stirling cooler, a ION Getter or NEG pump and suitable electronic controls which could be operated from either a terminal PC or directly from the front panel of the unit after the internal software had been setup. This CRFE can service all the main and diversity antennas in a three sector base station. Because the system is modular, UMTS and other wireless services are catered for by simply exchanging the Filter-LNA combination for ones at the correct frequency. All of these improvements increased the performance and reduced the size, weight and cost of the CRFE significantly which improves its chances of acceptability in the market.

2. The developed CRFE designs were trialled in the field first at China's Wonongchang base station and then at 5 base stations in Beijing (5.3 & 7.4). The CRFEs when placed in previously underperforming base stations yielded impressive results; A 3dB or 50% reduction in the required handset uplink power as well as a 41% drop in access failures and 21% drop in lost calls. This indicated that the new CRFE provided a significant technical advantage over the old front end. Over two years of continual operation in Wunongchang base station at the request of China Unicom has demonstrated the reliability of the system up until now. In contrast STI, who operate their systems in the USA where another service operates in the middle of the middle of phone spectrum, demonstrated a 7 times reduction in the required mobile handset transmission power [108]. This result shows the advantages of steep filters in situations where close out-of-band interferers generate a large amounts of inter-modulation distortion in the receiver. While

technically superior, the cost of such a system, even if it were to be mass produced, means that for the moment it's most prominent use would be in areas where the current BTS are delivering below average performance.

3. Witnessing the technical superiority of a system that most people in the field of HTS filter research believed would be superior, while validating their beliefs, would not be enough to convince sceptics and the market of the worth of HTS filters. A full understanding of the improvements was necessary in order to further improve each of the components in the CRFE and convince the market of its applicability in certain situations. The tool to achieve this is the CDMA uplink model (Chapter 6) which can be used to analyse the coverage and capacity of a CDMA using different Filter-LNA combinations under different noise and interference conditions. The low RF losses exhibited in HTS allow for low insertion loss, narrow bandwidth and a sharp roll-off in the transition band. The CDMA uplink model suggests that the improved insertion loss, which would improve the sensitivity of the front end, was not significant in increasing the coverage of the BTS but rather enhanced its capacity. The narrow bandwidth and sharp roll-off was only significant in the presence of out-of-band interference, which caused inter-modulation distortion due to nonlinear components in the system. However, because the CDMA channels are only 1.25MHz wide there are still many channels present in the filters passband and in most systems the interferers are not present due to network and frequency spectrum planning. This means that the results from the field trials were most probably due the improved dynamic range and the reduced noise figure of the LNA rather than the selectivity of the filter removing adjacent channels and interferers. This would leave HTS filters being primarily used to attenuate very near out-of-band interferers which are causing unacceptable inter-modulation products inside the CDMA channels.

4. It was the idea the LNA could be completely responsible for results seen in the field trails which spurred the development of the DR filter (Chapter 8), which would be used to compare HTS and Dielectrics in a future set of field trials. The success of developing a 5MHz bandwidth DR filter with a Q_0 of more than 25000 combined with its large tuneable range lead directly to the design of DR duplexer. The DR duplexer is designed to replace the old metallic duplexer on the main antenna of the BTS and increase the front end sensitivity. Coupled with HTS filters which can select individual channels in the UMTS network the combination would yield the best performance front end currently available. The low losses would ensure the highest sensitivity the individual channel selectivity would eliminate inter-modulation distortion which may be generated from neighbouring channels and services.

5. The same features which make HTS filters useful for UMTS also make HTS filters ideal for use in a Multi Operator Combiner (MoC). The very high unload Q-factors and sharp roll-off of the filters mean that the UMTS receive channels do not require splitting before filtering, which creates a greater than 4dB reduction in the incoming signal attenuation. The improved filtering

also eliminates inter-modulation distortion which may be generated from neighbouring channels. Due to the antenna sharing and therefore cost sharing which a MoC enables from a operator acceptance point of view this may be the best option for entering HTS filters into the market at this stage.

9.1 RECOMMENDATIONS

As with any form of research answering one question typically generates many more unanswered questions. The development work that goes into answering the original question is, in the view of the developer, never finished and can always be improved upon. To that end the continued development of the CRFE is imperative to the success of HTS filters in the wireless communication industry. The reduction of cost especially of the cryogenic cooler, reduction of heat input to the cold parts of CRFE and the perfection of a vacuum maintenance system are issues which need attention if CRFEs are to become economically viable. The proposed control system (Chapter 7.3.2) will also be an important factor in the market acceptance of CRFEs, particularly if operators can monitor front end performance metrics remotely. While DR filters are probably the next step for wireless communications after cavity filters, designers and operators alike should be aware that a higher performance system is available so that they can be incorporated into future system and network designs.

The development of DR duplexers and advanced MoCs using the developed DR filters and CRFE as a solid building platform, hold the greatest potential for the immediate uptake by the telecommunications industry of the technologies discussed in this thesis. While these systems are only conceptual designs the implementation is realisable in light of the simulated results for both the DR duplexers and MoCs.

9.2 CONCLUSIONS

The problem that HTS filters face currently is that while they can provide some benefits for current wireless systems the full potential can not be realised. The current systems were designed around older, more established and less expensive filtering technology and therefore the interference from adjacent channels and services is dealt with using wide enough guard bands such that metallic filters can be used effectively. Even though an improvement was seen in the performance of the CDMA base stations in all the field trials the CRFE is still being used as an intruder system and not fully integrated into the base station. In this intruder setup the overall performance of the base station is still being blunted somewhat by losses in the old technology.

Although a mature technology now, the solution to increasing capacity of the system is still to increase the density of base stations. As the spectrum becomes more crowded, user numbers increase and data services are expanded, network operators will need to maximise their use of the available spectrum in order to achieve the highest data rates, voice quality and user numbers. This will possibly happen several cellular communication generations into the future. These new generation systems will require reduced guard bands to maximise usable channel bandwidth and therefore need to utilise the best available filtering technology. However, this would appear to be some way into the future and the DR filters

combined with a LNA of high dynamic range would appear to be the immediate next step between the current metallic filter technology and HTS filter technology. Meaning that while today HTS filters may not be widely accepted outside very special circumstances where traditional filters do not perform adequately, it is distinctly possible that in the future HTS filter technology will become a part of everyday life.

9.3   THESIS RELATED PUBLICATIONS

During the course of this thesis the following papers have been published in conjunction with other researchers in the field.

[1] Jacob MV, Mazierska J, Knack AP,   "Narrowband Superconducting Filters for mobile communication", *Transactions of the Materials Research Society of Japan*, vol 29, No. 4, pp. 1273 – 1276, 2004.

[2] Jacob MV, Mazierska J, Knack AP, Takeuchi S, "Miniaturized 10-pole superconducting filter on MgO substrate for mobile communication", *Proceedings of TENCON 2004, IEEE Region 10 Technical Conference on Analog and Digital Techniques in Electrical Engineering*, 21-24 November 2004, Chiang Mai, Thailand, IEEE Press, ISBN: 0-7803-8561-6, pp. 554 – 557, 2004.

[3] Piel H, Aminov B, Chaloupka H, Getta M, Kolesov S, Wehler D, Mazierska J, Sinclair MW, Knack AP, Jacob MV, "High temperature superconducting elliptic filters for UMTS Cryogenic Receiver", *Proceedings of Asia Pacific Microwave Conference 2004 (APMC 2004)*, 15-18 December 2004, Allied Publishers Private Limited, ISBN: 81-7764-722-9, pp. 563-567, 2004.

[4] Piel H, Aminov B, Aminova F, Bisong C, Getta M, Kolesov S, Knack A.P, Mazierska J, Pupeter N, Bin Wei, Wehler D, Xiaoping Z, "A Cryogenic Front End for CDMA and UMTS Wireless Base Stations", *Journal of Physics: Conference Series (7th European Conference on Applied Superconductivity)*, vol. 43, pp. 1354-1357, 2006.

[5] Knack A.P, Kolesov S, Mazierska J, "CDMA Coverage Capacity Uplink Model: An Assessment of Implementing Superconducting Technology in CDMA Cellular Networks", Proceedings of *Asia Pacific Microwave Conference APMC 2005*, Suzhou, China, 4-7 December 2005, IEEE Press, ISBN: 0-7803-9434-8. pp. 1692-1695, 2005.

REFERENCES

[1]   G. Bednorz and A. Müller, "Perovskite-Type Oxides - The New Approach To High-Tc Superconductivity," *Nobel Prize Lecture*, 1987.

[2]   M. K. Wu, et al., "Superconductivity at 93K in a New Mixed Phase Y-Ba-Cu-O Compound System at Ambient Pressure," *Physics Review Letters*, vol. 58, pp. 908, 1987.

[3]   J. Eck, "Superconductors.org," Web Site, http://superconductors.org, 2004.

[4]   M. Hagen, et al., "Observation of RF superconductivity in $Y_1Ba_2Cu_3O_{9-\delta}$ at 3 GHz," *Journal of Magnetism and Magnetic Materials*, vol. 68, pp. L1-L5, 1987.

[5]   N. Klein, et al., *Applied Physics Letters*, vol. 54, pp. 757, 1989.

[6]   N. Klein, et al., *Journal of Applied Physics*, vol. 67, pp. 6940, 1990.

[7]   P. Berberich, et al., *Physica C*, vol. 219, pp. 497-504, 1994.

[8]   W. C. Y. Lee, "Lee's Essentials of Wireless Communications", *McGraw-Hill*, 2001.

[9]   L. Garfield, "Mobile phone usage doubles since 2000, but growth to slow," InfoSync World, Web Page, http://www.infosyncworld.com/news/n/5636.html, 2004.

[10]   J. Mazierska and M. Jacob, "High Temperature Superconducting Planar Filters for Wireless Communication," in *Novel Technologies For Microwave And Millimeter-Wave Applications*, P. J.-F. Kiang, Ed.: Kluver Academic Publishers, pp. 123 - 151, 2003.

[11]   A. P. Knack, S. Kolesov, and J. Mazierska, "CDMA Coverage Capacity Uplink Model: An Assessment of Implementing Superconducting Technology in CDMA Cellular Networks," *Proceedings of Asia Pasific Microwave Conference*, pp. 1692-1695, 2005.

[12]   M. I. Salkola and D. J. Scalapino, "Benefits of Superconducting Technology to Wireless CDMA Networks," Report for STI, May 9, 2003.

[13]   A. Miceli and B. Spann, "Maximizing CDMA Capacity with Antenna and Infrastructure Improvements," Report for Antenna Systems & Technology, May/June 2002, 2002.

[14]   H. Piel, et al., "A Cryogenic Front End for CDMA and UMTS Wireless Base Stations," *Journal of Physics: Conference Series (7th European Conference on Applied Superconductivity)*, vol. 43, pp. 1354-1357, 2006.

[15]   D. Guha, "Broadband Deisgn of Microstrip Antennas: Recent Trends and Developments," *Mechanics, Automatic Control and Robotics*, vol. 3, pp. 1083 - 1088, 2003.

[16]   Antenova, "New Generation Technology," Webpage, http://www.antenova.com/technology.htm, 2005.

[17]   T. Farley and T. van der Hoek, "Cell Phone Basics," Farley, Tom, Website and PDF, http://www.privateline.com/Cellbasics/Cellbasics.html, 2006.

[18]   W. C. Y. Lee, "Overview of Cellular CDMA," *Vehicular Technology, IEEE Transactions on*, vol. 40, pp. 291-302, 1991.

[19]   B. Sklar, "Rayleigh Fading Channels in Mobile Digital Communication Systems Part I: Characterization," *IEEE Communications Magazine*, pp. 90 - 100, 1997.

[20]   E. Drucker, "Downlink Receive Diversity: Something for (Almost) Nothing?," in *Wireless Week*, 2006.

[21]   J. Scourias, "Overview of the Global System for Mobile," Webpage, http://ccnga.uwaterloo.ca/~jscouria/GSM/gsmreport.html, 1997.

[22]   Answers.com, "GSM Frequency Rages," Webpage, http://www.answers.com/topic/gsm-frequency-ranges, 2006.

[23]   K. S. Gilhousen, et al., "On the Capacity of a Cellular CDMA System," *Vehicular Technology, IEEE Transactions on*, vol. 40, pp. 303-312, 1991.

[24]   N. J. Muller, "Spread Spectrum," in *Bluetooth Demystified*: McGraw-Hill Professional Publishing, pp. 60-66, 2000.

[25]   P. Bedell, "Code Division multiple Access," in *Cellular/PCs Management*: McGraw-Hill Professional Publishing, pp. 225-229, 1999.

[26]   S. Forum, "3G Overview," Webpage, http://www.smarthomeforum.com/start/3g.asp?ID=1, 2006.

[27]   C. D. Group, "CDMA Development Group White Paper: 3G Systems," Report for, 1999.

[28]   U. World, "WCDMA (UMTS)," http://www.umtsworld.com/technology/wcdma.htm, 2006.

[29]   J. Mazierska, et al., "High Temperature Superconducting Elliptic Filters for UMTS Cryogenic Receiver," proceedings of Asia Pacific Microwave Conference 2004, New Delhi, 15-18 December, 2004.

[30]   A. Knack, "Superconducting Bandpass Filters For 3rd Generation Cellular Phone Communication Base Stations," Honours Thesis in *Bachelor of Computer Systems Engineering*, James Cook University, Townsville, 2003.

[31]   G. Tsuzuki, M. Suzuki, and N. Sakakibara, "Superconducting filter for IMT-2000 band," *Microwave Theory and Techniques, IEEE Transactions on*, vol. 48, pp. 2519 - 2525, 2000.

[32]   G. Tsuzuki, S. Ye, and S. Berkowitz, "Ultra-selective 22-pole 10-transmission zero superconducting bandpass filter surpasses 50-pole Chebyshev filter," *Microwave Theory and Techniques, IEEE Transactions on*, vol. 50, pp. 2924 - 2929, 2002.

[33]   G. Tsuzuki, S. Ye, and S. Berkowitz, "Ultra selective HTS bandpass filter for 3G wireless application," *Applied Superconductivity, IEEE Transactions on*, vol. 13, pp. 261-264, 2003.

[34]   H. Padamsee, J. Knobloch, and T. Hays, "RF Superconductivity for Accelerators", *John Wiley & Sons, Inc.*, New York, 1998.

[35]   H. Chaloupka, "Microwave applications of high-temperature superconductors," *Applications of Superconductivity*, pp. 295-383, 2000.

[36]   H. Piel, "Superconducting Cavities." Wuppertal, West Germany: Fachbereich Physik der Bergischen Universität, 1989.

[37]   J. D. Jackson, "Classical Electrodynamics", Second Edition ed, *John Wiley & Sons*, New York, 1962.

[38]   DESY, "X-Ray Free Electron Laser," DESY, Web Page, http://xfel.desy.de/, 2006.

[39]   ACCEL, "ACCEL Homepage," www.accel.de, 2006.

[40]   W. C. Tang, et al., "Dielectric Resonator Output Multiplexer for C-Band Satellite Applications," *IEEE MTT-S Digest*, vol. 85, pp. 343-345, 1985.

[41]   S. Jerry Fiedziuszko, et al., "Dielectric Materials, Devices and Circuits," *IEEE Transactions on Microwave Therory and Techniques*, vol. 50, pp. 706-720, 2002.

[42]   J. Krupka, et al., "A dielectric resonator for measurements of complex permittivity of low loss dielectric materials as a function of temperature," *Measurements in Science and Technolology*, vol. 9, pp. 1751-1756, 1998.

[43]   R. Grabovickic, "Accurate Calculations of Geometrical Factors of Hakki-Coleman Shielded Dielectric Resonators," *IEEE Transactions on Applied Superconductivity*, vol. 9, pp. 4607-4612, 1999.

[44]   J.-F. Liang and W. D. Blair, "High-Q TE01 Mode DR Filters for PCS Wireless Base Stations," *IEEE Transactions on Microwave Therory and Techniques*, vol. 46, pp. 2493-2505, 1998.

[45]   R. J. Cameron, A. R. Harish, and C. J. Radcliffe, "Synthesis of Advanced Microwave Filters Without Diagonal Cross-Couplings," *IEEE MTT-S CDROM*, pp. 1437-1440, 2002.

[46]   A. V. Velichko, M. J. Lancaster, and A. Porch, "Nonlinear microwave properties of high Tc thin films," *Superconductor Science and Technology*, vol. 18, pp. 24-49, 2005.

[47]   K. F. Raihan, et al., "Highly selective HTS band pass filter with multiple resonator cross-couplings," proceedings of IEEE MTT-S International Microwave Symposium Digest, 2000.

[48]   H. Kanaya, et al., "Design method of miniaturized HTS coplanar waveguide bandpass filters using cross coupling," *Applied Superconductivity, IEEE Transactions on*, vol. 13, pp. 265-268, 2003.

[49]   M. Barra, et al., "Hilbert fractal curves for HTS miniaturized filters," *IEEE MTT-S Intenational Microwave Symposium Digest*, vol. 1, pp. 123-126, 2004.

[50]   H. T. Kim, et al., "A compact narrowband HTS microstrip filter for PCS applications," *Applied Superconductivity, IEEE Transactions on*, vol. 9, pp. 3909-3912, 1999.

[51]   Private Communication H. Piel, 2004.

[52]   G. L. Matthaei, J. Young, and E. M. T. Jones, "Microwave Filters, Impedance-Matching Networks, and Coupling Structures", *McGraw-Hill*, 1980.

[53]   Private Communication H. Piel, 2006.

[54]   H. Chaloupka, "High-Frequency Bandpass Filter Arrangement having Damping Poles," Patent in Germany, 1998.

[55]   Z. M. Hejazi, P. S. Excell, and Z. Jiang, "Compact dual-mode filters for HTS satellite communication systems," *Microwave and Guided Wave Letters, IEEE [see also IEEE Microwave and Wireless Components Letters]*, vol. 8, pp. 275-277, 1998.

[56]   M. J. Lancaster, "Prof. MJ Lancaster - Publications," University of Birmingham, Web Page, http://www.edt.bham.ac.uk/mjpubs.htm, 2005.

[57]   H. Chaloupka and T. Kaesser, "HTS Microwave Filters: Properties, design and system applications," in *High Temperature Superconductivity 2 Engineering Applications*, A. V. Narlikar, Ed. Berlin: Springer, pp. 411 - 476, 2004.

[58]   H. Chaloupka, "Microwave Engineering: Publications," University of Wuppertal, Web Page, http://www.hft.uni-wuppertal.de/187.0.html, 2005.

[59]   H. Chaloupka and S. Kolesov, "Design of Lumped-Element 2D RF Devices," in *Microwave Superconductivity*, H. Weinstock and M. Nisenoff, Eds. Netherlands: Kluwer Academic Publishers, pp. 205-238, 2001.

[60]   E. B. D. E. 2004, "BSC Theory," CD Edition, 2004.

[61]   H. K. Onnes, *Commun. Phys. Lab.12,120*, 1911.

[62]   R. P. Feynman, "The Feyman Lectures on Physics Vol III", *Addison Wesley Publ. Comp.*, 1965.

[63]   W. Meissner and R. Oschenfeld, *Naturwiss*, vol. 21, pp. 787, 1933.

[64]   W. Buckel, "Supraleitung", *VCH Verlagsgesellschaft mbH*, 1972.

[65]   D. E. Oates, et al., "Microwave power dependence of YBa$_2$Cu$_3$O$_7$ thin-film Josephson edge junctions," *Applied Physics Letters*, vol. 68, pp. 705-707, 1996.

[66]   M. Jacob and J. Mazierska, "Microwave characterisation of YBCO films on Sapphire and LAO substrates," *Journal of Low Temperature Physics*, vol. 131, pp. 647-651, 2003.

[67]   M. J. Lancaster, "5.5 Non-linear effects and power handling," in *Passive Microwave Device Applications of High-Temperature Superconductors*. Cambridge: Cambridge University Press, pp. 161-166, 1997.

[68]   A. V. Velichko and M. J. Lancaster, "Nonlinear Microwave Properties of HTS Think Films," proceedings of MSMW'04, Kharkov, Ukraine, June 21-26, 2004.

[69]   C. Wilker, et al., "Nonlinear Effects in High Temperature Superconductors: 3rd Order Intercept from Harmonic Generation," *IEEE Transactions on Applied Superconductivity*, vol. 5, pp. 1665-1670, 1995.

[70]   P. P. Nguyen, *Physical Review B*, vol. 48, pp. 6400-6412, 1993.

[71]   A. V. Velichko, "Origin of the deviation of intermodulation distortion in high-Tc thin films from the classical 3:1 scaling," *Superconductor Science and Technology*, vol. 16, pp. 1-7, 2003.

[72]   D. E. Oates, et al., "Nonlinear Surface Resistance in YBa$_2$Cu$_3$O$_{7-x}$ in Thin Films," *IEEE Transactions on Applied Superconductivity*, vol. 3, pp. 1114-1119, 1993.

[73]   A. V. Velichko, et al., "Anomalous Features in Surface Imedance of Y-Ba-Cu-O Thin Films: Dependence on Frequency, RF and DC Fields," *IEEE Transactions on Applied Superconductivity*, vol. 11, pp. 3497-3500, 2001.

[74]   J. Wosik, et al., "Power Handling Capabilities of Superconducting YBCO Thin Films: Thermally Induced Nonlinearity Effects," *Journal of Superconductivity*, vol. 10, pp. 97-103, 1997.

[75]   J. Mazierska, "Superconducting Cryogenic Front End Receivers for Cellular Phone Base Stations," *MIKON, 15th Int. Conference on Microwaves, Radar and Wireless Communications*, pp. 351-354, 2004.

[76]   Xilinx, "Block Diagram for Wireless Base Station," Xilinx, Web page, http://www.xilinx.com/esp/popups/basestation.htm, 2005.

[77]   Toshiba, "Base Station System Block Diagram," Toshiba, Web Page, http://www.toshiba.com/taec/applications/basestation.shtml, 2005.

[78]   PMC-Sierra, "3G Wireless Base Transceiver Station," PMC-Sierra, Web Page, http://www.pmc-sierra.com/products/diagrams/WirelessBaseTransceiverStation.html, 2005.

[79]   J. Mazierska and M. V. Jacob, "High Temperature Superconducting Filters for Mobile Communciation," *Proceedings of the International Symposium on Recent Advances in Microwave Technology, ISRAMT'99*, 1999.

[80]   STI, "A Band 850MHz Systems - SuperLink RX850," STI

[81]   S. Kolesov, "A Cryogenic Amplifier with High Dynamic Range," Report for Cryoelectra, Wuppertal, 2002.

[82]   B. Aminov, et al., "A Cryogenic Front End for UMTS Base Stations," Report for Cryoelectra GmbH, 2002.

[83]   E. S. Technologies, "What is Vacuum Insulation?," Energy Storage Technologies, Web Site, http://www.estglobal.com/tech-vip.html,

[84]   V. I. Panels, "What is Vacuum Insulation and a Vacuum Insulation Panel?," Vacuum Insulation Panels, Web Site, http://www.dupontteijinfilms.com/cntMarketsVIPLearnAbout.htm,

[85]   Grayce, T. Mooney, and R. Barrans, "How does a Thermos Work?," Ask A Scientist, Web Site, http://www.newton.dep.anl.gov/askasci/phy99/phy99x81.htm,

[86]   M. Hablanian, "Gettering and Ion Pumping," Web Page, http://www.aiv.it/ita/pubblicazioni/articolo.php?articolo=art4,

[87]   S. C. Bundy, "Quantifying the Benefits of Enhanced Filter Selectivity," in *IEEE Microwave Magazine*, vol. 4, pp. 48-59, 2003.

[88]   B. Aminov, "Superconducting Receiver Front-End: Performance Evaluation for CDMA Base Stations," Report for Cryoelectra, Wuppertal, Internal Report, 2001.

[89]   R. Padovani, "Reverse Link Performance of IS-95 Based Cellular Systems," *IEEE Personal Communications*, pp. 28-34, 1994.

[90]   K. Heiska, et al., "Capacity Reduction of WCDMA Downlink in the Presence of Interference From Adjacent Narrow-Band System," *Vehicular Technology, IEEE Transactions on*, vol. 51, pp. 37-51, 2002.

[91]   AWE-Communications, "Propagation Model of Hata-Okumura," AWE Communications, Web Page, http://www.awe-communications.com/Propagation/hata_oku/hatoku.htm, 2004.

[92]   AWE-Communications, "AWE Communications," AWE Communications, http://www.awe-communications.com, 2004.

[93]   Narda, "Components, Networks, and Instruments For the 21st Century," Narda, 2000.

[94]   J. Lucek and R. Damen, "LNA Design for CDMA Front End," Report for Philips.

[95]   C. N. Booth, "Thermal Physics - Transfer of Heat - Radiation," Web Site, http://www.shef.ac.uk/physics/teaching/phy001/unit7.html,

[96]   MCS, "The MCS Zeolite Page," Web Page, http://www.mall-net.com/mcs/zeolite.html,

[97]   SAES-Getters, "st171 and st172 Sintered and Porous Getters," SAES Getters

[98]   R. R. Mansour, "Dual-mode dielectric resonator filters with improved spurious performance," *Proceedings of IEEE MTT-S International Microwave Symposium Digest, 1993*, pp. 439-442, 1993.

[99]   N. Klien and H. Yi, "DIELECTRIC RESONATOR FILTERS," Homepage, http://www.fz-juelich.de/isg/Klein/diel_filter.htm, 2006.

[100]   Trilithic, "Trilithic RF and Microwave Components Home Page," Webpage, http://www.trilithic.com/, 2006.

[101]   A. P. Knack, "Dielectric Resonator Filter Report March 2006," Report for Cryolectra, Wuppertal, 2006.

[102]   A. P. Knack, S. Kolesov, and H. Piel, "Advances in Cryogenic Front Ends 2005," Report for Cryoelectra, Wuppertal, 2006.

[103]   "United States Frequency Allocations (The Radio Spectrum)," National Telecommunications and Information Administration Office of Spectrum Management, 2006.

[104]   Aerial, "Antenna Sharing Solutions for Multi-Band, Multi-Operator Base Station Installations," http://www.aerial.co.uk/, 2004.

[105]   Aerial, "Multi-Operator and Multi-System Combining for Common Antenna Sharing," http://www.aerial.co.uk/, 2004.

[106]   REMEC, "Multi-Operator Dual Band GSM900/1800 Passive Combiner Unit (4-input) - High Power," REMEC, http://www.remec.com/, 2004.

[107]   Quintel, "QVT3000 Combiner Base Unit," http://www.quintel.co.uk/, 2004.

[108]   B. A. Willemsen, "Low Cost, High Reliability HTS Cryogenic Receiver Front Ends for Commercial Wireless," proceedings of HTSHFF 2006, Cardiff, Wales, 2006.

[109]   S. McGarrity, "Gaining Control of CDMA Power," Webpage, http://www.commsdesign.com/main/2000/09/0009feat3.htm, 2006.

[110]   J. A. Clark, "Heat Transfer," in *Cryogenic Technology*, R. W. Vance, Ed. New York, London: John Wiley & Sons Inc., pp. 121 - 195, 1963.

APPENDIX A – WUNONGCHANG FIELD TRIAL

EXPERIMENTAL PROCEDURE

The test conducted in this field trial is known as a "drive test". In this test the transmit power of the mobile station required for an active uplink to the base station is measured as the mobile station moved along a predetermined route at a constant speed (approx. 25-30km/h). This tests relies on power control algorithms inherent in CDMA systems which reduce the mobile handset transmit power to the minimum value required in order to maintain a successful link with the host base transceiver station [109]. This process is described in Chapter 2.2.2 on CDMA wireless communication technology. The test was performed in two stages, first with China Unicom's original BTS configuration as shown in Figure A.1 and then the second stage was with the CRFE and bypass network (in case of cooler failure) installed as shown in Figure A.2.
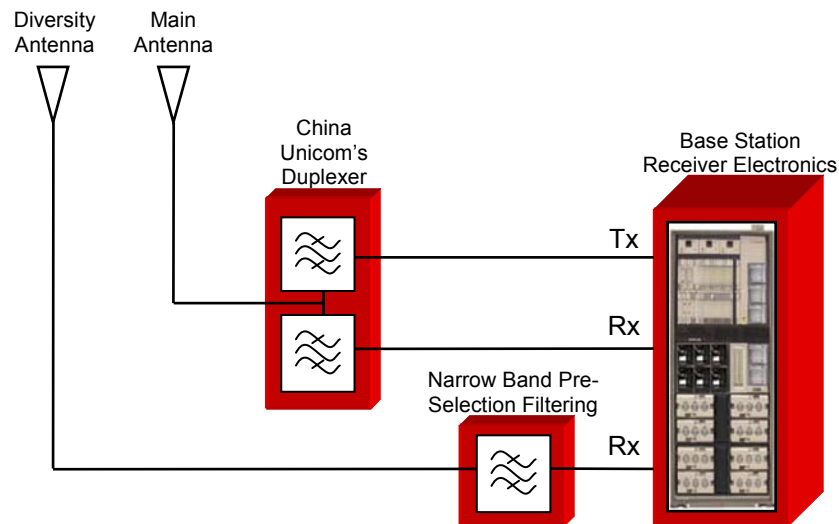
Figure A.1. Traditional BTS subsystem
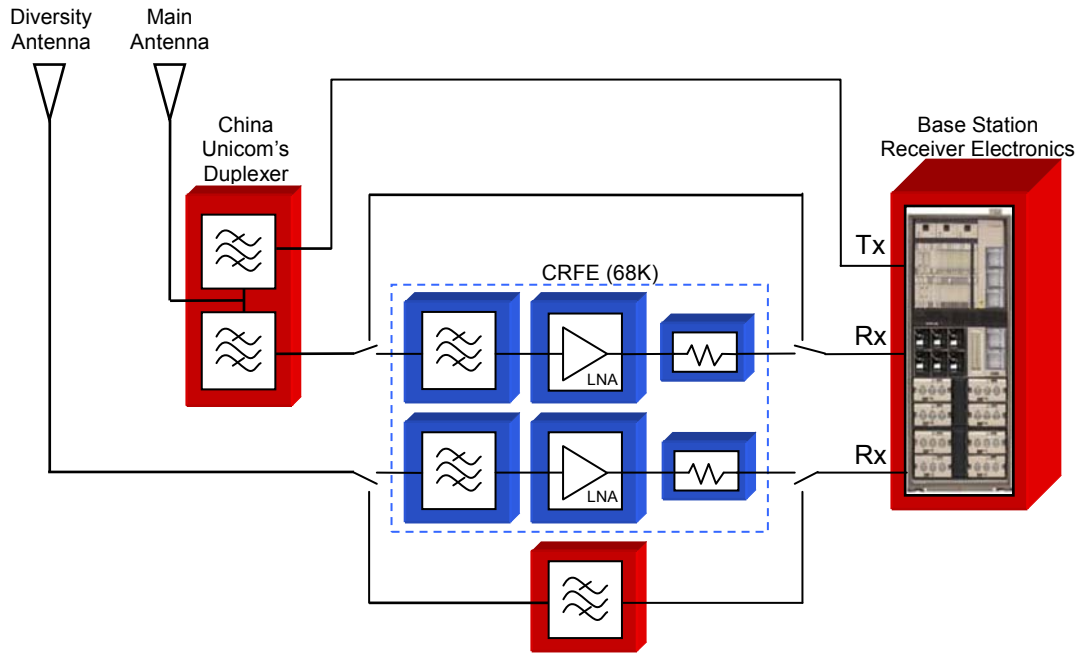
Figure A.2. Implementation of CRFE for Field Trial into BTS Subsystem

Wunongchang BTS, denoted by the large red dot in Figure A.3, is a three sector base station located in a rural part of China. The red line is the drive test path and the BTS sectors are shown by the blue dashed lines. Cryoelectra's D6 CRFE was installed on the main and diversity antennas in the third sector (PN 460).
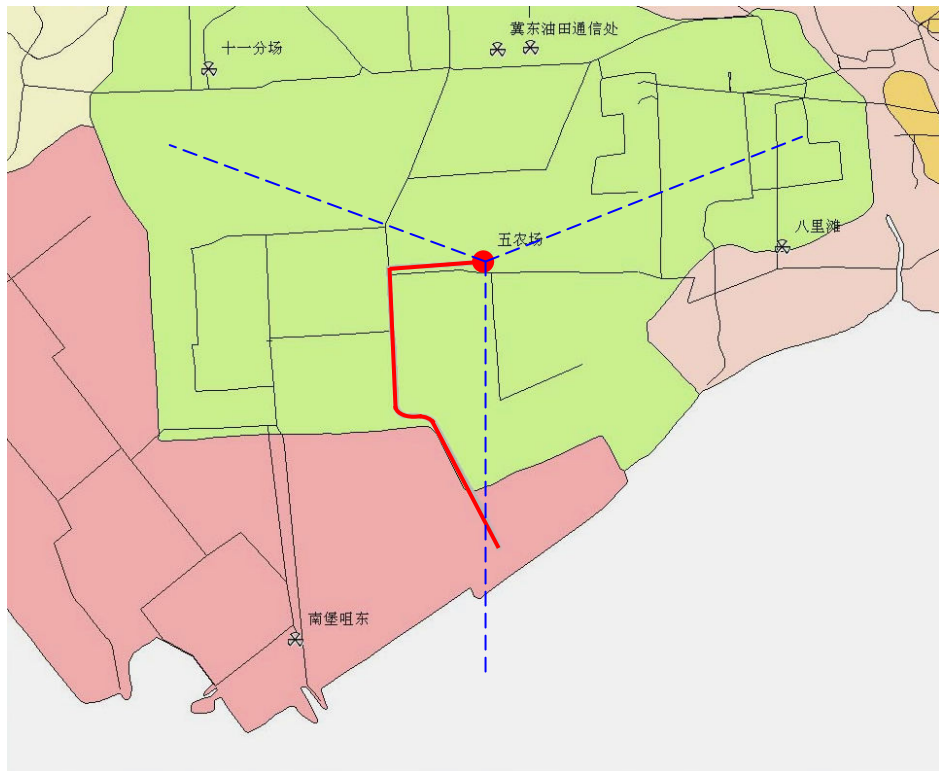
Figure A.3. Wunongchang BTS - Drive Test Path (Red), Sectors (Blue)

RESULTS

Three drive tests were performed with each system setup. Table A.1 shows a break down of all the measured transmit powers for each of the drive tests and the average number of times that each transmit power was recorded over all the tests.

Table A.1. Mobile Transmit Power Statistics of Drive Test

Transmit Power	China Unicom				CRFE			
	1A	2A	3A	Average	1A	3A	5A	Average
-100 to -30	1	13	8	0.39%	47	31	30	1.68%
-30 to -20	43	56	50	2.67%	110	99	98	4.78%
-20 to -10	68	92	75	4.21%	200	142	186	8.22%
-10 to 0	400	740	546	30.20%	725	823	799	36.54%
0 to 5	510	477	610	28.61%	662	464	553	26.14%
5 to 10	482	368	383	22.09%	471	308	226	15.65%
10 to 20	270	152	210	11.32%	209	162	59	6.68%
20 to 100	13	8	7	0.50%	4	12	3	0.30%
Total Points	1787	1906	1889		2428	2041	1954	

Figure A.4 shows graphically the average number of times that each transmit power was recorded over all the tests. These columns have been highlighted in Table A.1 for easy reference to the raw data.
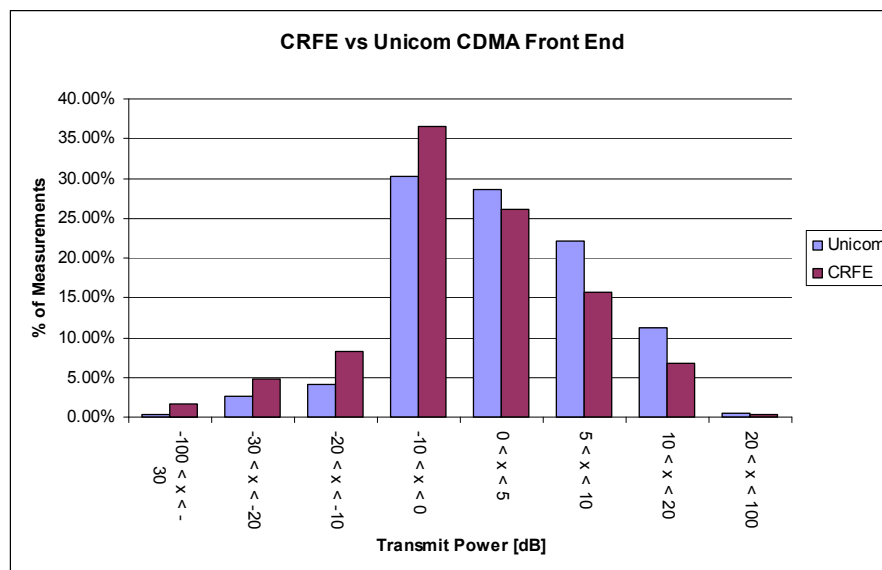
Figure A.4. Average Number of Measurements at Specified Transmit Power for 1 Mast Field Test

Results for two drive tests are also shown on the maps in Figure A.5 for the China Unicom setup test 1A and in Figure A.6 for the CRFE setup test 3A. Green and blue colours on the maps represent areas of low mobile unit transmission power while yellow and red areas require higher transmit power. The results show that most regions which required high transmit powers with the China Unicom system require significantly less with the CRFE installed.

Figure A.5. Wunongchang Field Test Result China Unicom Setup (1A)

Figure A.6. Wunongchang Field Test Result CRFE Setup (3A)

Table A.2 shows the sum of all the results obtained during the three tests. The average mobile transmit power for each system is calculated by dividing the total power (sum of all the measured powers) for each system by the total number of test points for each system.

Table A.2. Average Mobile Transmit Power

	Total Power [dB]	Total Test Points	Average Power [dB]
Unicom	7283.36	5582	1.305
HTS	-11616.63	6423	-1.809
Difference in Average Transmit Power due to CRFE [dB]			**3.114**

APPENDIX B – BEIJING FIELD TRIAL

EXPERIMENTAL PROCEDURE

Even with all the CDMA BTS operating with the same hardware configurations the QoS is typically quite different in an urban environment as a result of large user numbers, high electromagnetic interference and shadowing from buildings. A cluster of adjacent BTS were selected for the field trial in order to demonstrate the performance of the CRFE conditions where there is high population and heavy traffic.

A QoS figure of merit was calculated for each of the nearly 100 BTS in the Beijing Haidian district using statistics from service reports taken over several weeks just before the field tests were scheduled. The QoS figure of merit was calculated using five weighted indexes; Walsh code hours, lost call rate, number of lost calls, failed connection attempt rate and number of fail connection attempts. The weight of each index is described in Table B.1.

Table B.1. BTS QoS Weighted Indexes

Walsh Code Hours	Wt.	Lost Calls	Wt.	Lost Call Rate (%)	Wt.
<200	0	<50	0	<0.50	0
200 – 300	1	50 – 75	1	0.50 – 0.75	1
300 – 400	2	75 – 100	3	0.75 – 1.00	2
>400	3	100 – 125	5	1.00 – 1.25	3
		>125	7	>1.25	4

Failed Connection Attempts	Wt.	Failed Connection Attempts Rate (%)	Wt.
<100	1	<1.5	0
100 – 200	2	1.5 – 2.5	1
200 – 300	3	2.5 – 3.5	3
300 – 400	4	>3.5	5
>400	5		

The five selected worst performing base stations, 'LianXiangQiao', 'ZhiChunLi', 'ZaoJunMiao', 'XiWuDaoKou' and 'ShouDuTiYuXueYuan', cover a highly populated area and several heavy traffic roads (Figure B.1). For the three station trials 14 FLNA channels were installed into 'LianXiangQiao', 'ZhiChunLi' and 'ZaoJunMiao' BTS. An additional 16 FLNA combinators were installed in the remaining sectors of the first three BTS as well as 'XiWuDaoKou' and 'ShouDuTiYuXueYuan' to enable the five mast field test to cover the full 15 sectors.
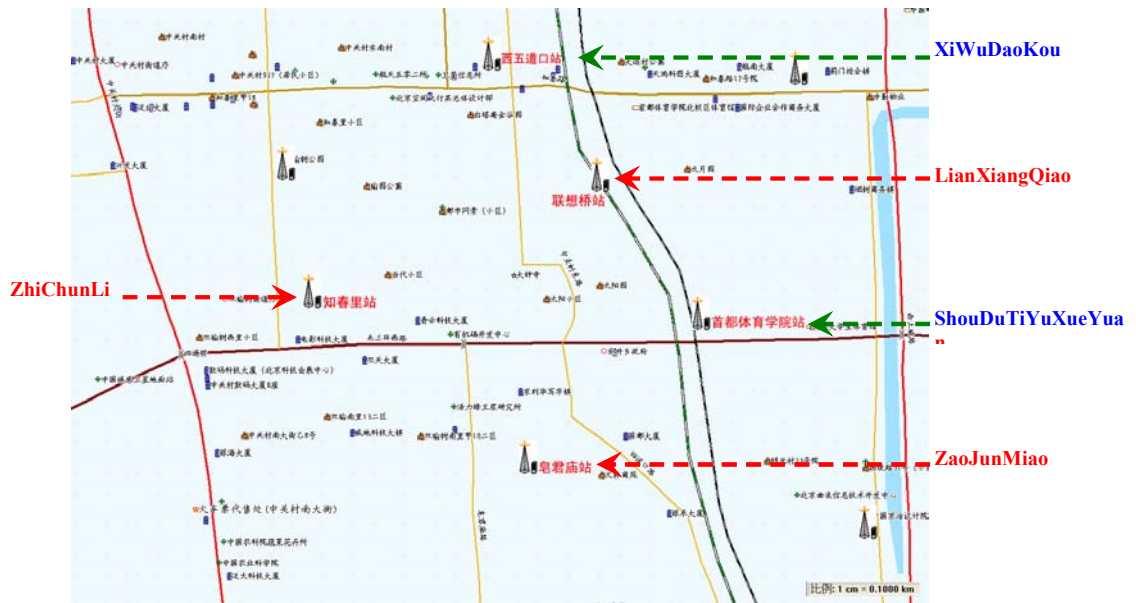
Figure B.1. Map Showing the 5 BTS used in the Field Trials in Beijing's Haidin District, China

For these field trials two different sets of data were analysed; from the drive tests and the statistical data obtained in the service report.

DRIVE TESTS

Two drive tests were conducted using all 15 sectors of the five BTS first under normal service conditions using all original BTS equipment and then repeated under CRFE enabled service, which utilised the HTS filter and cooled LNA. During each drive test the handset transmit power (Tx), receive power (Rx), frame error rate (FER) and signal to noise ration (E_c/I_o) were recorded. The test route started from 'XiWuDaoKou' and covered the main and surrounding roads in the trial region (Figure B.2) before returning to 'XiWuDaoKou'.
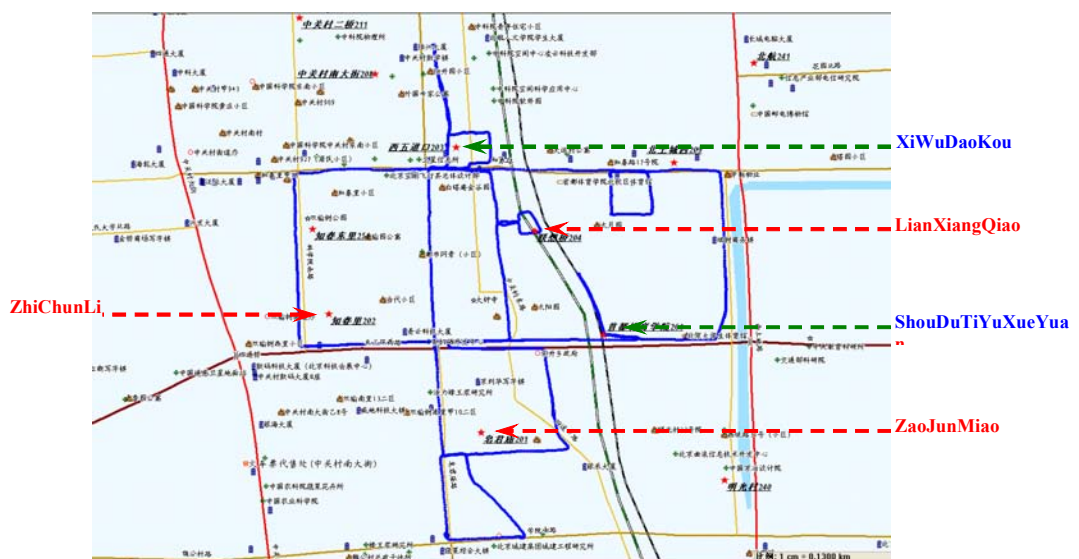
Figure B.2. Map Showing the Drive Test Route

SERVICE REPORT

The statistical data for Walsh code hours, lost call rate and access failure rate was collected over two weeks for the normal service and the CRFE enabled service respectively. The time period of the trials, two weeks, accounts for periodic fluctuations in traffic to ensure accurate statistical data. The comparison of the data from normal and CRFE enabled services shows the improvement in the QoS of the base station due to the presence of the CRFE. A comparison to the surrounding base stations shows how the QoS has improved with respect to the district average BTS performance.

DRIVE TEST RESULTS

The drive tests were performed on the 20th of December 2005 starting with the normal service at 10:03 from 'XiWuDaoKou' and returning at 11:28. At 11:38 the five BTS were switched to the CRFE and the drive test took place up to 12:40. The measured handset transmit power for each test is shown in Figure B.3 and Figure B.4.

Figure B.3. Drive Test Data for Normal Service

Figure B.4. Drive Test Data for CRFE Enabled Service

The recorded QoS data is presented in Figure B.5 - Figure B.7. The average handset transmit power was decreased by 2.35dB in the trial region when the CRFE was installed compared to the normal situation. As expected the SNR, FER and received power were all relatively unchanged due to CDMA power control operating in the BTS. Figure B.8 shows a detailed distribution of the transmit power during the drive tests and the probability that each power level was obtained. A Gaussian distribution curve has bee fitted to the data and clearly shows the reduction in the required handset transmission power.
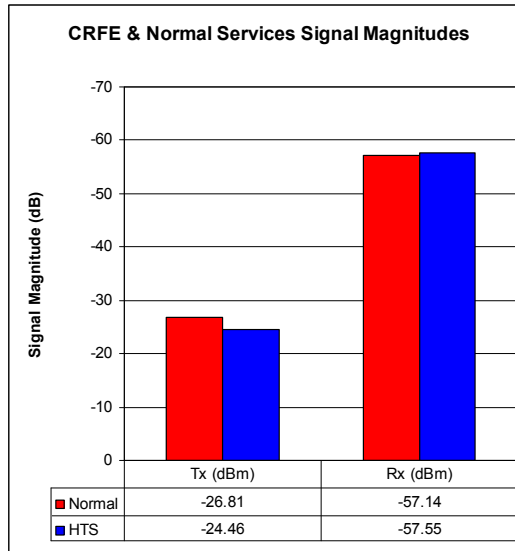
Figure B.5. CRFE & Normal Services Signal Magnitudes
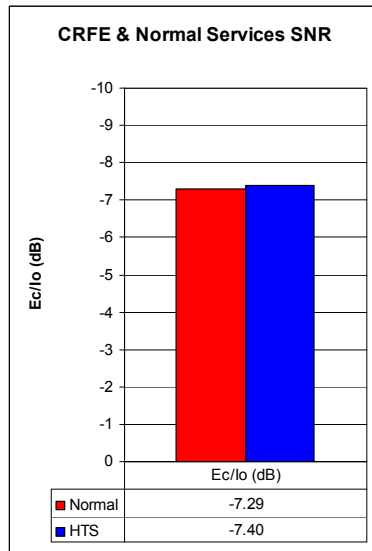
Figure B.6. CRFE & Normal Services SNR
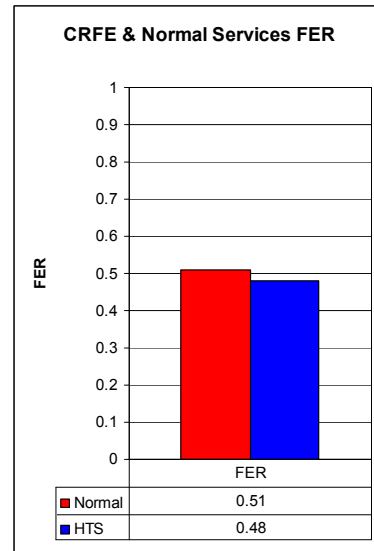
Figure B.7. CRFE & Normal Services FER
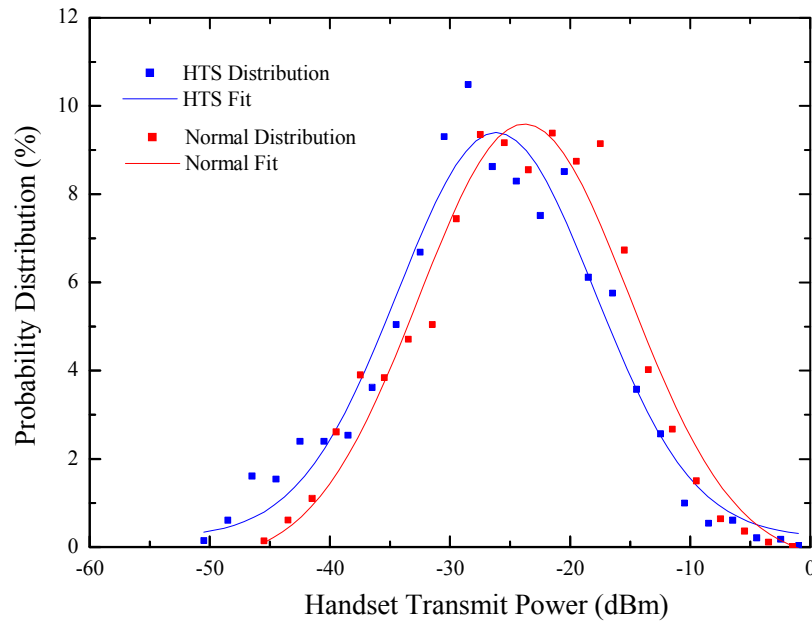
Figure B.8. Probability Distribution of Handset Transmit Power for Drive Tests

SERVICE REPORT RESULTS

The three base station service report gathered data between the 28th of July and the 10th of August, 2005 using the normal service. CRFE enabled service data was collected between the 12th and 23rd of August, 2005. The results are displayed in Figure B.9 to Figure B.11.

	Mon	Tues	Wed	Thurs	Fri	Sat	Sun	Average
Normal	478.5	470.5	471.1	476.7	474.2	395.1	375.3	448.8
HTS	476.4	475.9	481.7	494.7	479.8	400.1	377.5	455.1
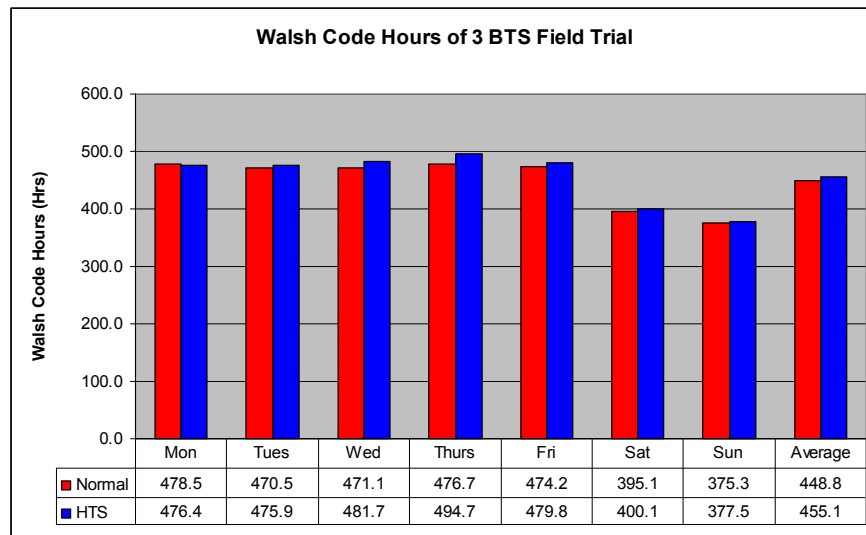
Figure B.9. Walsh Code Hours for the 3 BTS Field Trial

Lost Call Rate

	Mon	Tues	Wed	Thurs	Fri	Sat	Sun	Average
■ Normal	0.833	0.706	0.545	0.564	0.504	0.623	0.664	0.634
■ HTS	0.531	0.553	0.537	0.502	0.551	0.521	0.523	0.532
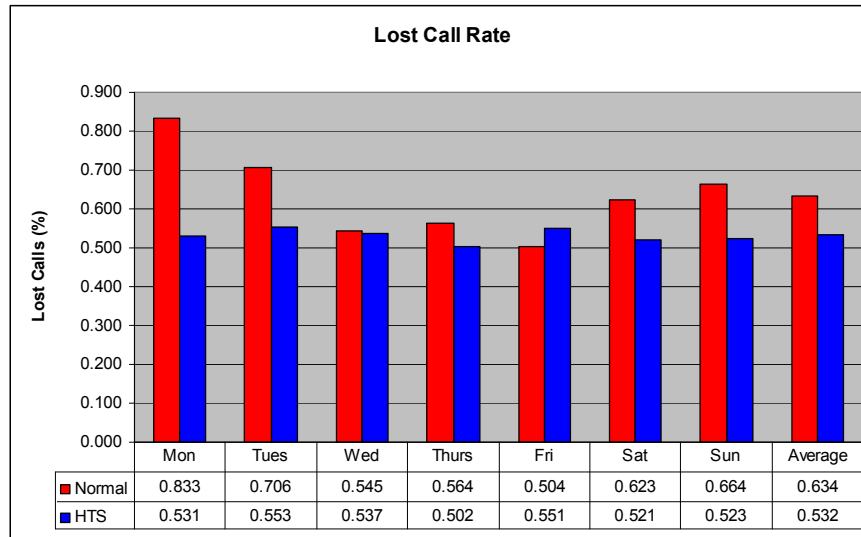
Figure B.10. Lost Call Rate for the 3 BTS Field Trial

Access Failure Rate

	Mon	Tues	Wed	Thurs	Fri	Sat	Sun	Average
■ Normal	3.11	2.47	1.93	1.25	1.78	3.29	3.70	2.45
■ HTS	1.48	1.76	1.26	1.25	1.29	1.44	1.61	1.45
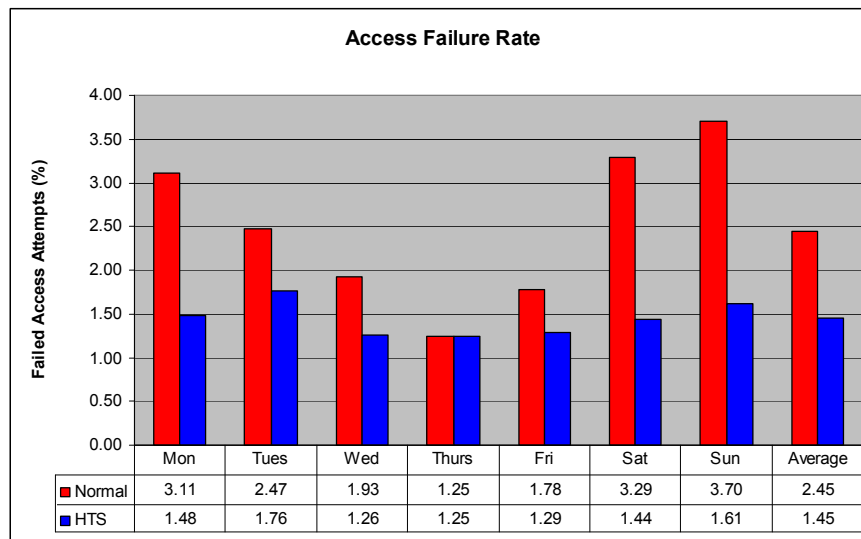
Figure B.11. Access Failure Rate for the 3 BTS Field Trial

Table B.2. Summary of 3 BTS Field Trial Results

	Walsh Code Hours (Hours)	Lost Call Rate (%)	Access Failure Rate (%)
Normal	448.8	0.634	2.452
CRFE	455.1	0.532	1.438
Δ	1.4%	-16%	-41%

The results show an improvement in the lost call rate by 16% and a reduction in the access failure rate by 41% due to the presence of the CRFE. There has been a slight increase in the Walsh Code hours as a result of the improved connectivity.

The results compared to the surrounding base stations; "Zhong guan chun station", "Hai dian yin yuan station", "li gong da sha station", "Xi wu dao kou station", "Bei tu cheng xi station", "Ming guang chun station", "Zhi chun li dong station", "Zao jun xi li station", "Shou du ti yu xue yuan station" are presented in Figure B.12 to Figure B.14.

Walsh Code Hours of 3 BTS and Surrounding BTS

	Mon	Tues	Wed	Thurs	Fri	Sat	Sun	Average
Normal	397.1	391.4	392.2	391.5	386.4	313.2	297.4	367.0
HTS	399.4	398.7	399.6	405.3	393.4	322.5	304.2	455.1
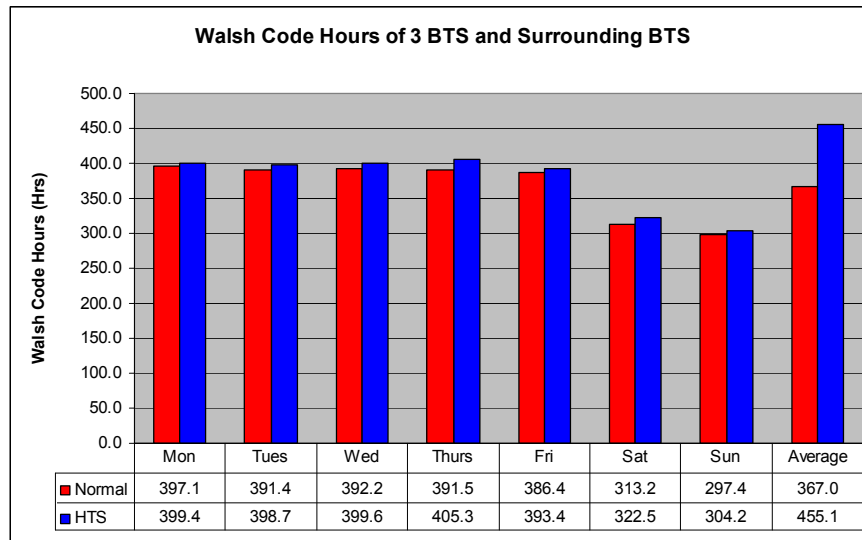
Figure B.12. Walsh Code Hours for the 3 BTS Field Trial and Surrounds

Lost Call Rate

	Mon	Tues	Wed	Thurs	Fri	Sat	Sun	Average
Normal	0.620	0.562	0.500	0.539	0.508	0.547	0.564	0.548
HTS	0.490	0.524	0.564	0.536	0.502	0.486	0.473	0.513
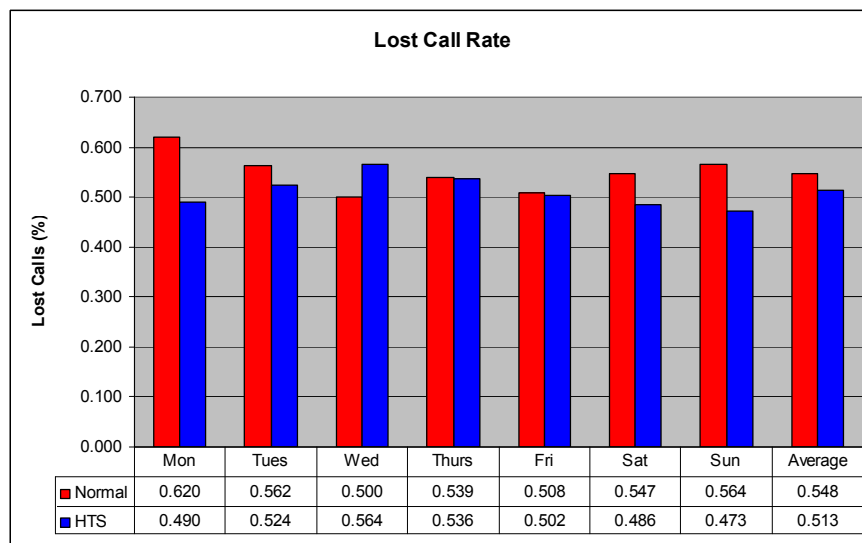
Figure B.13. Lost Call Rate for the 3 BTS Field Trial and Surrounds
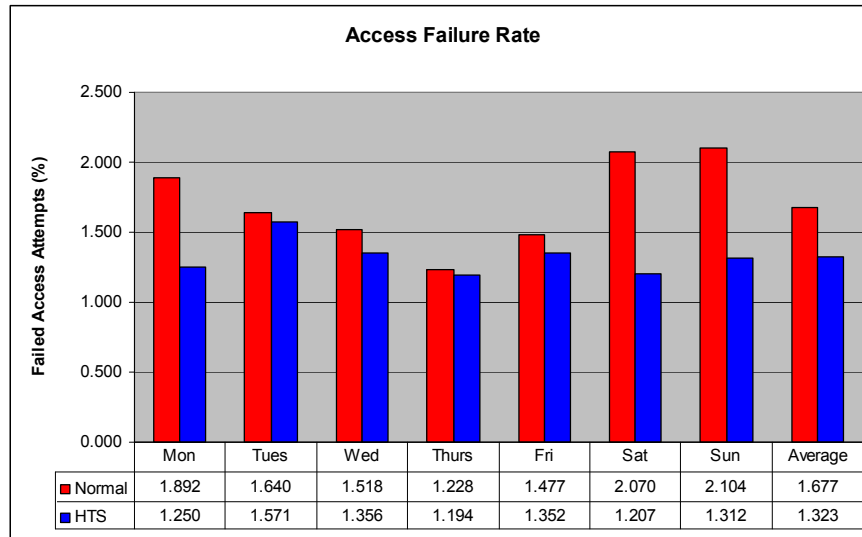
Figure B.14. Access Failure Rate for the 3 BTS Field Trial and Surrounds

Table B.3. Summary of 3 BTS & Surrounding BTS Results

	Walsh Code Hours (Hours)	Lost Call Rate (%)	Access Failure Rate (%)
Normal	367	0.548	1.677
CRFE	374.7	0.513	1.323
Δ	**2.1%**	**-6.4%**	**-21%**

The results again show an improvement in the lost call rate, but only by 6.4%, and a reduction in the access failure rate by just 21% due to the presence of the CRFE when compared to the surrounding situation. Once again there has been a slight increase in the Walsh Code hours as a result of the improved connectivity. These results are quite impressive when it is considered that prior to enabling the CRFE at the selected base stations they all exhibited significantly worse performance characteristics than their district counterparts. With the CRFE enabled the performance of these BTS becomes significantly better than the district average.

APPENDIX C – IR SHIELD AND HEAT SOURCES

The testing of the radiation shield was performed in normal operating conditions (a vacuum at 68K) and the measurements we performed when the system had reached equilibrium. The following tests were performed to assess the performance of the radiation shield and analyse possible sources of heat transfer into the system.

1. System without the obelisk.
2. System with the obelisk.
    The change in the cooling power, P_c, between these first two tests gave the amount of heat radiation absorbed by the obelisk.
3. System with the obelisk and the heat shield.
    The change in the cooling power, Pc, between the second and third tests gave the reduction in heat radiation due to the addition of the heat radiation shield.
4. System with the obelisk and 1 Filter/LNA combination.
    Shows additional radiation absorbed by the addition of Filter/LNA combinations.
5. System with the obelisk, 1 Filter/LNA combination and the heat radiation shield.
    Should yield similar a result to 3.
6. System with the obelisk plus 1.15Kg weight and heat radiation shield.
    Examined how the weight of the system influenced P_c.
7. System with the obelisk, 4 Filter/LNA combinations, heat radiation shield and fibreglass insulation.
    Investigated the effect of the fibreglass insulation. (Note: 4 Filter/LNA combinations weigh about 1.15Kg).
8. System with the obelisk, 4 Filter/LNA combinations, heat radiation shield, fibreglass insulation and 1 stainless steel RF cable connection.
    Investigated the additional heat introduced via RF cables.
9. System with the obelisk, 4 Filter/LNA combinations, heat radiation shield, fibreglass insulation and 4 stainless steel RF cable connection.
    Investigated the additional heat introduced via RF cables.

A second series of experiments were performed on D8 using the 6 pole obelisk and appropriate numbers of filter/LNA combinations. These experiments were used to identify heat sources in the system and the effects of various radiation shields. The procedure was as follows.

1. Calculate theoretical radiation input ($\varepsilon_{Polished\ Stainless\ Steel\ Dewar}$ = 0.03).
2. Experimental power requirements tests
    a. No obelisk.
    b. No obelisk + aluminium cap (ε = 0.03) on the cold head test.
    c. Obelisk (ε = 0.09).
    d. Obelisk + aluminium foil wrap (ε = 0.03).
    e. Obelisk + weight equivalent of 4 filter/LNA combinations + aluminium foil wrap (ε = 0.03).
    f. Obelisk + aluminium foil and fibreglass radiation shield (ε = 0.03).
    g. Obelisk + 6 Filter LNA Combinations (larger surface area A).
    h. Obelisk + 6 Filter/LNA Combinations + aluminium foil wrap (ε = 0.03).

The results from the preceding experiments are displayed in Table C.1. Unless otherwise stated all the tests were performed with a 6 Filter/LNA obelisk, and cooled to 68K using a Laybold Stirling cryocooler.

Table C.1. Results of Heat Transfer Experiments

Experiment	Description	P_0
1	No Obelisk	40 W
2	Obelisk	71 W
3	Obelisk Heat Radiation Shield	58 W
4	Obelisk (3 Filter/LNA) 1 Filter/LNA	64 W
5	Obelisk (3 Filter/LNA) 1 Filter/LNA Heat Radiation Shield	54 W
6	Obelisk 1.15Kg Weight	66 W
7	Obelisk 4 Filter/LNA Heat Radiation Shield Fibre Glass Insulation	62 W
8	Obelisk 4 Filter/LNA Heat Radiation Shield Fibre Glass Insulation 1 RF Cable Connection	75 W
9	Obelisk 4 Filter/LNA Heat Radiation Shield Fibre Glass Insulation 4 RF Cable Connection	95 W

From experiments 1 and 2 it can be seen that the addition of the obelisk has increased the cooling power, P_0, from 40W to 71W. Given that no input or output RF cables were connected to the system and assuming that the weight of the obelisk was not causing additional friction inside feed tubes to the cold head, by Equation (A.1) the increase in P_0 must be due to radiation. Therefore there was approximately 31W of infrared radiation being added to the system.

$$P_0 = \text{Heat flow through RF cables}$$
$$+ \text{ Heat flow through the cold head (1.2 Watts)} \qquad (A.1)$$
$$+ \text{ Radiation}$$

Experiment 3 showed that adding a radiation shield to the system decreases the power, P_0, to 58W. This corresponds to a 13W (71 - 58 = 13) or 41.94% (13 ÷ 31 = 0.4194) decrease in radiation. This is a substantial decrease keeping in mind that no insulation has been used and the foil is not gold or perfectly shaped.

Experiment 4 was performed with the much smaller 3 filter/LNA obelisk and one filter/LNA channel. P_0 is 64W, meaning approximately 24W of radiation is present in the system. The addition of the aluminium radiation shield in experiment 5 reduces P_0 to 54W. This is a 10W or 41.66% decrease in power due to infrared radiation. This result corresponds with the findings of experiments 2 and 3 which also yielded a reduction in radiation of approximately 42%.

Experiment 6 examined the effect of weight on the system by adding a 1.15Kg mass (this weight is approximately equivalent to 4 filter/LNA channels) to the centre of the obelisk. P_0 is found to be 66W. When comparing this result with the result in experiment 2 without the mass added it could be seen that there has been a 5W decrease in P_0. This was likely due to the 1.15Kg mass covering the hole at the top of the obelisk, therefore reducing the surface area A and hence the radiation. Testing with a radiation shield in experiment d showed that the additional weight produced no significant increase in power. Hence weight had no effect on the system in the vertical position.

The next three experiments were used to determine the heat input due to the stainless steel RF input/output cables. All the tests are performed with the 6 filter/LNA obelisk with 4 filter/LNA channels, the radiation shield and insulation. The insulation is included primarily to prevent the LNA inputs from sorting against the radiation shield.

Experiment 7 was the control and shows that with no input/output connections that P_0 is 62W (22W due to radiation). Experiment 8 added one stainless steel RF cable connection to both the input and the output of one filter/LNA channel. The result was the power, P_0, increased by 13W to 75W. Experiment 9 added another 3 connections (both input and output) taking the total to 4 channels fully connected. This was significant because this was to be the number of channels used in some of front ends in the three mast field tests in China. The result was 95W of cooling required, meaning approximately 8.25W of extra cooling is required per channel.

The second series of experiments on D8 involved first calculating the approximate radiation power input into the system and converting this to additional power input required from the cooler. This was done using equation (7.1) [110]:

Where,

$\sigma = 5.67 \times 10^{-8}$

ε_1 = emissivity of the inside of the stainless steel Dewar ≈ 0.14

ε_2 = emissivity of cold surface

T_0 = temperature of the cold surface = 68 K

T_1 = room temperature = 300 K

A = area of the cold surface

The theoretical radiation was calculated on the cryocooler assuming 2.5% efficiency at 68 Kelvin.

$$\textit{Theoretical Radiation = Radiation Power} \div \textit{Cooler Efficiency} \qquad \text{(A.2)}$$

Results are presented in Table C.2. The experimental radiation was defined to be the difference between the experimental power of the current experiment and the experimental power of experiment b.

Table C.2. Theoretical and Experimental Results for Radiation Shielding

Experiment	Theoretical Radiation (W)	Experimental Power (W)	Experimental Radiation (W)
a	0	35	0
b	0	35	0
c	28.55	63	28
d	5.46	48	13
e	5.46	51	16
f	0 (ideally)	44	9
g	-	85	50
h	-	52	17

In all the tests the theoretical radiation was lower than the experimental. This was expected because the emissivity of the surfaces is calculated based on a perfectly smooth surface, which neither the obelisk nor the inside of the Dewar was.

The results of the experiments conducted showed that the developed CRFE required greater that 31W of additional power in order to maintain an operating temperature of 68K when there was an obelisk attached to the cold head due specifically to infrared radiation. This power requirement increased further if filter/LNA channels were added to the obelisk (because the surface area is increased). A simple radiation shield could reduce the power increase due to infrared radiation by approximately 42% with additional layers being added to further reduce the radiation.

Trials to determine the effect of weight on the required cooling power of the CRFE found that the cold finger could operate with the projected 2.5kg mass introduced by the 6 filter/LNA combinations and the obelisk without a significant increase in required cooling power.

The semi-ridged stainless steel RF cables require approximately 8.25W of extra cooling for each input output pair. For a total of 6 filter/LNA channels this equates to 49.5W of additional cooling.

Assuming only one layer of radiation shielding is used a Cryogenic Front End equipped with 6 filter/LNA channels for a 3 sector base station would require approximately 112W of cooling, providing the vacuum is maintained well and the warm end of the cold head is adequately cooled.

GLOSSARY

0-9

2G: The second generation of cellular communication which marked the change from analogue to digital systems such as GSM and CDMA. Limited data capabilities were included such as Short Message Service (SMS) and Wireless Application Protocol (WAP).

2.5G: Current systems (as at 2004) extending data services of the 2G systems. The new services included Multimedia Messaging Service (MMS), removal on character limit of SMS services and higher speed data transfer with GPRS.

3G: The third generation systems are designed to allow for high speed data rates using packet transport (packets are used in many common networking protocols such as TCP/IP). These packets are transmitted over a larger bandwidth channel, which supports more simultaneous voice and data calls. There are currently three systems proposed Wideband CDMA (W-CDMA also known as UMTS in Europe), CDMA2000 and EDGE which is the only TDMA system of the three.

A

Adaptive Power Control: The power of a radio transmitter is adjusted adaptively to the needs of the link between the base station and the mobile subscriber. The received power reduced to its minimum necessary value in order to maintain a link of given quality.

Al_2O_3: Sapphire, commonly used as a substrate for deposition of HTS films (*see Substrate*). Suffers from anisotropy of the dielectric constant (*see Anisotropy*).

Anisotropy: Different values of ε_r when measured along axes with different directions.

B

BCCH: Broadcast Control Channel, operates on the downlink and continuously sends out identifying information about its cell site.

BCS Theory: The first theory to explain superconductivity in most metals in the framework of accepted field theory of solids put forth in 1957 by John Bardeen, Leon Cooper and John Schreiffer. Awarded with a Nobel Prize in 1972.

Bit Error Rate: The number of erroneous bits divided by the total number of bits transmitted, received, or processed over some stipulated period. The errors are usually caused by noise in the system making the bit read as the wrong value.

BSIC: Base Station Identity Code, identifies the cellular carrier and the base station the mobile is connecting to.

Butterworth Approximation: A Butterworth filter approximation is used for filter design of flat magnitude response across the pass band for a given rate of fall into the stop band. To achieve this, the transfer function contains only poles and no zeros.

C

Capacity: Refers to the number of users which can concurrently use a cellular communication system. Typically this is limited by the uplink signal (*see uplink*).

CDMA: Code Division Multiple Access, a spread spectrum technique that splits the voice or data over the entire channel in a pseudo-random fashion. The receiver "must know" how to decode this pseudo-random spectrum to recreate the initial message. Uses a 1.25kHz wide carrier signal.

CDMA2000: A 3rd Generation solution based on IS-95 CDMA (a modification of the original cdmaOne standard) providing an evolutionary path to a 3G network for existing CDMA operators.

CFE: Cryogenic Front End, consists of a cryocooled filter/LNA combination place between the antennas (main and diversity) and the receiver to improve the sensitivity and selectivity of the receiver.

Chebyshev Approximation: A Chebyshev filter approximation allows for filter designs with ripples in the passband in order to realise a narrower transition region.

Cold Finger: Refers to the cold part of the cryocooler.

Cold Head: *See Cold Finger.*

Cooper Pair: Two electrons that appear to bond, in accordance with the BCS theory, despite the fact that they both have negative charges and would normally repel each other. The pair of electrons then travels without colliding with the crystal structure.

Coupling: There are primarily two forms of coupling between resonators used for filter design, capacitive and inductive. As these terms suggest they are closely related to the process that is undergone by capacitors and inductors in discrete circuit technology. Capacitive coupling is achieved by placing resonators side by side. The current in the first resonator will charge the adjacent resonator as if it were a capacitor, causing current to flow in it and charge resonators that are adjacent to it. Inductive coupling occurs within a resonator.

Coverage: Refers to the area over which a base station can provide quality unlink and downlink to a mobile unit. Typically this is limited by the uplink signal.

CRFE: Cryogenic Receiver Front End, *see CFE*.

Cryocooler: A cooler which works similar to a refrigerator but cools to very low temperatures (<-50°C). In the context of this project they are used to cool the filters/LNA to their operating temperature (*see T_c*).

Cryoelectra GmbH: Company based in Germany, established in 1992 and devoted to the research and development of high technology electronics. See www.cryoelectra.de

Cut-off Frequency: or 3dB cut-off, specify the bandwidth of the filter, frequencies between the cut-off frequencies in a band pass filter are the pass band. Beyond the cut-off frequencies lay the transition region and stop bands.

D

Diamagnetism: The ability to exclude a magnetic field. Superconductors exhibit perfect diamagnetism.

Dielectric: A dielectric material is an insulator (does not conduct electricity), but can be polarised by an electric field and therefore stores energy in the form of an electric field.

Discontinuous Transmission (DTX): The transmitter is only powered on when the subscriber is actively speaking. At all other times nothing is transmitted except some signalling traffic to maintain the link.

Downlink: Refers to the link from the base station to the mobile unit.

Dropped Calls: Refers to a mobile call being disconnected. Usually occurs when the signal is interrupted by an object such as a building, when the signal is transferred from one base station to another, when the capacity is reached or when a region of no coverage is entered.

Dual Mode Resonator: A resonator which supports two resonant frequencies.

E

EDGE: Enhanced Data GSM Environment, a faster version of the TDMA based GSM system for 3G cellular communications. Using existing cell arrangements it will enable the delivery of multimedia and other broadband applications by providing data rates up to 384Kbps once the network has been upgraded to a full IP based system.

Elliptical Approximation: By allowing a controlled amount of ripple in both pass and stop bands elliptical filter designs produce the fastest transition rate when compared to other designs approximations.

EM field: Electromagnetic field, is generated when charged particles, such as electrons, are accelerated. All electrically charged particles are surrounded by electric fields. Charged particles in motion produce magnetic fields. When the velocity of a charged particle changes, an EM field is produced.

F

FCB: Frequency Control Bits**.**

FDMA: Frequency Division Multiple Access, is the division of the frequency band into channels, each of which can carry either voice or digital data. Each channel can be assigned to only one user at a time. This system was used in the original analogue mobile phone service (AMPS – Advanced Mobile Phone Service).

Filter Approximations: When designing a filter there are a number of approximations that are used in order to achieve a result which is as close to the ideal magnitude and phase response as possible. These approximations focus on achieving a particular aspect of the phase or magnitude response rather than trying to produce an ideal filter. Also see *Butterworth, Chebyshev* and *Elliptical Approximations*.

Frequency Hopping: The frequency a subscriber is using is changed according to a frequency hopping algorithm to average the influence of interference in FDMA and TDMA systems.

G

Gain: Usually refers to the ratio of output power divided by input power in an amplifier. Can also refer to the gain of an entire system using the same ratio, however in this case the gain is dependent on an amplifier and the other components in the system that reduce the strength of the output signal.

Ginzburg-Landau Theory: In physics, Ginzburg-Landau theory is a mathematical theory used to model superconductivity. It does not claim to explain the microscopic mechanisms giving rise to superconductivity. Instead, it examines the macroscopic properties of a superconductor with the aid of general thermodynamic arguments.

GPRS: Global Packet Radio Service, is an enhancement to the GSM network that introduces packet data transmission allowing for a permanent connection to online services and the internet but do not pay for these services unless they are actively using them. GPRS can be views as a 2.5G service since basically only packet data nodes have been added to the existing 3G network.

Group Delay: Describes the phase delay (usually in milliseconds) at a particular frequency due to the presence of the filter.

GSM: Global System for Mobile communication, is a digital mobile telephone system which uses a variation of the TDMA scheme. GSM digitises and compresses the data and sends it over a channel with two other streams of data, each in its own time slot. Typical operating frequencies are either in the 900MHz or 1800MHz bands.

H

Handoff: In a cellular network a handoff is the transition of a user's signal from one base station to a geographically adjacent base station as the user moves around. Theoretically the cells in a network overlap, hence the subscriber's mobile is within range of more than one base station at any given time. The network is responsible for determining which base station will handle the signals for the subscriber. Ideally the handoff occurs with out gaps in communication or dropped calls.

HTS: High Temperature Superconductor/Superconductivity, There is no widely accepted temperature that separates HTS from low temperature superconductivity. The first HTS material had a T_c of 30K. Any superconductors with a Tc above the boiling point of liquid nitrogen (77K) such as those used in filters are certainly considered as HTS materials (*also see Superconductivity*).

I

Insertion Loss: This is the loss within the pass band introduced by the filter presence in the system. In practice, due to resistive losses in any filter system, it is not possible to achieve an ideal insertion loss of 0 dB.

Inter-modulation Distortion: Nonlinear distortion characterised by the appearance, at the output of a device, of frequencies that are linear combinations of the fundamental frequencies and all harmonics present in the input signals.

J

K

Kelvin: K, A temperature scale that is an extension of the Celsius scale down to absolute zero, a hypothetical temperature characterised by the complete absence of heat energy.

L

LaAlO$_3$: Lanthanum Aluminate, a previously commonly used dielectric substrate with YBCO thin films for the production of very compact HTS filters. This substrate is not so popular now due to twinning boundaries that can be present (*also see MgO and Al$_2$O$_3$*)

LNA: Low Noise Amplifier, a specially design amplifier which produces as little noise as possible. The noise can be improved further by cooling the LNA to cryogenic temperatures such as is done in a CFE.

London Penetration Depth: A superconductor placed in a uniform external magnetic field smaller than the critical magnetic field, H_c, completely expellees the magnetic field. The interior of the superconductor is screened by currents which flow in a very thin skin layer on the surface. The external magnetic field exponentially decays in the surface layer and its decay length is called the London penetration depth, λ.

London Theory: Following the discovery of the Meissner effect, F. and H. London developed appropriate electrodynamics for the expression for the rate of change of the lossless component of current.

Loss Tangent: *tan δ*, also know as the dissipation factor, a measure of the loss of power which takes place in all dielectric materials. It is expressed as the ratio of the resistive loss component of the current to the capacitive component of the current and is equal to the tangent of the loss angle.

Lumped Element Model: a simplified model of electronic circuits making the assumption that each element is an point in space and that wires connecting elements are perfect conductors. This is reasonable for many circuits but breaks down when circuit impedances are very low or when the lengths of wire approach the wavelength of the circuit's operating frequency. In this situation non-ideal characteristics need to be accounted for, such as leakage in capacitors and inductive resistances in wires. This model can aid in designing planar filters.

M

MCPA: Multi-Channel Power Amplifier.

Meissner Effect: When a superconducting material actively excludes magnetic fields from its interior; this is called the Meissner effect. This is distinct from perfect diamagnetism.

MgO: Magnesium Oxide, a commonly used dielectric substrate to realise HTS filters because it allows for the deposition of thicker films and hence lower losses. The MgO also does not suffer from twinning or anisotropy such as other substrates like $LaAlO_3$ or Sapphire might. YBCO coated MgO substrates are more expensive than either YBCO coated Sapphire or LaAlO3 substrates.

Microwave Frequencies: Typically refers to frequencies between 1GHz (30cm) and 300GHz (1mm). Common applications are usually between 1GHz and 40GHz.

MoC: Multi-operator Combiner, allows a number of operators (up to 6) to all use the same antennas and mast to operate their portion of the mobile spectrum.

N

Noise: The receiver noise is created in the electrical components. Electrical current is carried by the movement of electrons. Even if there is no signal at the input of the receiver there is an irregular thermal motion of these so called conduction electrons in the electrical components of the receiver. They perform a "trembling motion" around their equilibrium position in wires and resistors as well as other electrical components of the receiver. This thermal movement creates an irregular jitter of the output voltage of the receiver.

O

Out-of-band Rejection: Also known as *out-of-band attenuation*, measured in dB it is a measure of how much signals outside the pass band are attenuated due to the filter.

P

Packets: Although data can be sent one character at a time, it is more efficient to send larger blocks of characters called *data packets*. Typically these blocks contain protocol information so they can be reassembled into the original message and error checking.

Parasitic Coupling: Refers to the coupling of non-adjacent resonators. This degrades the response of the filter and if the parasitic coupling is of opposite sign to the intended coupling an uncontrollable transmission zero can be created.

Pass band: The range of frequencies that is passed through the filter without attenuation.

Planar filter: Planar designs are produced by etching half or quarter wavelength resonators into a conductive film on a dielectric layer rather than using discrete components.

PLMN: Public Land Mobile Network, otherwise known as a cellular wireless carrier, mobile phone carrier or operator.

Protocol: A set of characteristics at the beginning and end of a message that enables a computer (or a machine) to communicate with another.

Q

Q-factor: The unloaded Q-factor is a quality metric for a resonator given by the ratio of the total energy stored in a resonator divided by the energy dissipated per cycle,

$$Q_0 = \omega_0 \frac{\text{total energy stored}}{\text{energy disipated per cycle}} = \frac{\omega_0 W}{P} .$$

Quasi-Elliptic Response: A quasi-elliptic filter response is similar to an elliptical filter response except that the number of finite transmission zeros is less than N-1, where N is the number of poles. This means that the roll off will not be as steep as in a truly elliptical filter. Typically filters using these responses are built by starting with a Chebyshev design and introducing controlled cross-couplings between non-adjacent resonators.

R

Relative Permittivity: ε_r, Ratio of electric field strength in a given medium to that in a vacuum. It was formally known as the dielectric constant.

Resistance: R, the opposition that a substance offers to the flow of electric current give by the ratio of DC voltage to the current, R = V/I. Measured in ohms (Ω).

Resonant Frequency: f_0, is a natural frequency of vibration determined by the physical parameters of the vibrating object.

Resonator: An object that resonates at a given frequency (determined by its physical properties), allowing the resonant frequency to be transmitted and others to be rejected.

Roll off: The rate at which the filter starts to attenuate the signal in the transition region. Usually given in dB/MHz.

S

Selectivity: A measure of how selective of frequency a filter is. Usually given by the ratio of the bandwidth to the resonant frequency.

Signal to Noise Ratio: S/N or SNR, the ratio of the strength of the received signal to the background noise. Measured in decibels (dB)

Skirt Steepness: *see Roll off*.

STI: Superconductor Technologies Inc., a company bases in California, USA specialising in using superconducting technology in cellular communications, see www.suptech.com.

Stop band: The frequencies beyond the cut-off frequencies where the signal is attenuated beyond a specified amount.

Superconductor: An element, inter-metallic alloy or compound that will conduct DC electricity without resistance below the critical temperature, T_c. All know superconductors require extreme cold in order to enter a superconductive state. Superconductors do exhibit some resistance to AC current flows.

Surface resistance: *see Resistance.*

Surface resistivity: ρ, defined for electric current flowing across a surface as the ratio of DC voltage drop per unit length to the surface current per unit width. The physical unit is Ω, however it is often expressed in Ω/unit-length^2.

T

T_c: The scientific notation representing the critical temperature below which a material begins to exhibit no resistance to DC current flows.

TCP/IP: Two protocols developed by the U.S. military to allow computers to communicate with each other over long distance networks. IP is responsible for moving packets of data between nodes. TCP is responsible for verifying delivery from the client to the server. TCP/IP forms the basis for the internet and most local area networks.

TDMA: Time Division Multiple Access, a technology used in cellular communication which allocates time slots to each user in a round robin fashion. A version of TDMA is used in the popular GSM system.

Thin films deposition: a technique for controlled deposition of thin films (30Å to 0.45mm) of material on to a substrate used in the manufacture of superconducting filters (as well as other electronic components).

Time slot: The small amount of time allocated to each user within a channel, the time slots are cycled in a round robin fashion in a similar way to a computer processing multiple tasks.

Transition region: The region between the cut-off frequency and stop band of a filter response.

Trimming: The complicated process of using dielectric tuning screws to modify the coupling between resonators and obtain a good match across the pass band of a filter response.

Tuning: The process of adjusting dielectric tuning screws to modify the coupling between resonators and obtain the correct centre frequency for the filter response.

Two fluid model: A model of normal and superconducting electrons that accounts for the thermal properties of superconductors developed by Gorter and Casimir.

U

UMTS: Universal Mobile Telecommunications Service, a third generation broadband, packet-based transmission of text, digitised voice, video and multimedia at data rates up to 2Mbps that offers a

consistent set of services to mobile computer and phone users no matter where they are located in the world. UMTS is also known as WCDMA in parts of the world outside Europe.

Uplink: The link from the mobile unit to the base station. This is the limiting factor in the range, capacity and data rates of systems because the signal from the mobile unit is very low and therefore prone to noise interference. Hence work is being done to increase the sensitivity of the receiver such that it can determine even very weak signals from a mobile unit.

V

W

WAP: Wireless Application Protocol, an application environment and set of communication protocols for wireless devices, such as mobile phones and personal digital assistants (PDA's), designed to enable technology-independent access to the Internet and other advance telephony services.

WCDMA: Wideband Code Division Multiple Access, an ITU standard derived from CDMA. WCDMA is a 3G mobile wireless technology that provides mobile voice, images, data and video communications at up to 2Mbps. A 5MHz wide carrier is used compared to the 1.25 kHz wide carrier for standard CDMA. In Europe WCDMA is also known as UMTS.

X

Y

YBCO: $YBa_2Cu_3O_{7-x}$, Yttrium Barium Copper Oxide, a commonly used thin film superconductor in HTS filter design.

Z